

2012

Chemical and biological evaluation of antibiotic-based ionic liquids and GUMBOS against pathogenic bacteria

Marsha Rae Cole

Louisiana State University and Agricultural and Mechanical College, mcole3@tigers.lsu.edu

Follow this and additional works at: https://digitalcommons.lsu.edu/gradschool_dissertations



Part of the [Chemistry Commons](#)

Recommended Citation

Cole, Marsha Rae, "Chemical and biological evaluation of antibiotic-based ionic liquids and GUMBOS against pathogenic bacteria" (2012). *LSU Doctoral Dissertations*. 487.

https://digitalcommons.lsu.edu/gradschool_dissertations/487

This Dissertation is brought to you for free and open access by the Graduate School at LSU Digital Commons. It has been accepted for inclusion in LSU Doctoral Dissertations by an authorized graduate school editor of LSU Digital Commons. For more information, please contact gradetd@lsu.edu.

CHEMICAL AND BIOLOGICAL EVALUATION OF ANTIBIOTIC-BASED IONIC
LIQUIDS AND GUMBOS AGAINST PATHOGENIC BACTERIA

A Dissertation
Submitted to the Graduate Faculty of the
Louisiana State University and
Agricultural and Mechanical College
in partial fulfillment of the
requirements for the degree of
Doctor of Philosophy
in
The Department of Chemistry

by
Marsha Cole
B.S., Grambling State University, 2007
August 2012

To the legacy of Williams and Coles...past, present, and future

ACKNOWLEDGEMENTS

“Trust in the Lord with all thine heart and lean not unto thine own understanding, in all thy ways acknowledge Him and He will make your paths straight.”

King James Bible, Proverbs 3:5-6

First and foremost, I would like to thank Jesus Christ, my Lord and Savior, for keeping me while directing my path through the tumultuous journeys and painful experiences that I have tread in my life. I understand that this accolade would be completely unattainable if it were not for Him. So I humbly submit my gratitude for His continual direction from the start of this journey through the beginning of my next. All glory is to Him.

Secondly, I would like to thank my advisor, Dr. Isiah M. Warner, for allowing me the opportunity to conduct research in his laboratory. I am especially grateful to him for allowing me to pursue my own ideas and experiments in the lab, thus molding me into the independent and resourceful research chemist that I am. Although the numerous group meetings, journal revisions, seminars, and research colloquia that we were required to attend each week sometimes seemed like cruel and unusual punishment, I am appreciative for them since they have helped me to continue learning even after my formal coursework was complete. I cannot thank both you and Mrs. Warner enough for your support, encouragement, and kind gestures. I will miss the laughs and the hugs. Thank you for being my extended family.

Thirdly, I would like to thank all of the graduate students, postdocs, and undergraduate students that I have worked with over the years while matriculating as a Ph.D. student. I will miss you all dearly. Many of you have grown to be more like brothers and sisters than friends and I hope like family are bonds that will be forever. I thank you all for the laughter in times I wanted to

cry, for reading scripture and fellowshiping when I've missed church, singing badly along to the radio with, shopping and bargain hunting for clothes and shoes, for providing insight and comfort during demanding and stressful times, falling victim to prank calls, and in general for making time spent in and out of the lab much more enjoyable. All of you have contributed something so special and endearing to me and have made this Ph.D. journey an invaluable experience. Likewise, I appreciate you for always being there to help with experiments and presentations and never being reluctant to help answer my thousands of questions.

I thank the members of my committee: Dr. Daniel Hayes, Dr. Robert Cook, Dr. Marlene Janes, and Dr. James Moroney for taking the time out of each of their schedules to serve on my committee and for always perpetuating my boundless curiosity with their insightful questions. I also thank Dr. Jeffrey Hobden and Dr. George Stanley, although not formal committee members, for being resourceful and honest when I sought guidance. Last but not least, I thank Dr. Sandra McGuire, an angel in disguise, a wizard of academic success, and a doctor of educational crises. You have selflessly listened and contributed encouragement while reinforcing confidence when I thought the Ph.D. was too difficult to obtain. I thank you for getting me through many of the road bumps that are evident in this journey, and I think God couldn't have placed a woman any better than you to serve as a mentor and comforter to me. Most importantly, I thank you for your countless encouragement, recommendations, and support as I tried to collect my abstract approach to science and mount it into something bigger than I could have ever imagined. Thank you for understanding that honesty, hardwork, and serendipitous ambition are my best attributes.

As I conclude this chapter of my life, I cannot help but acknowledge the other people who have also helped get me to this point. These people will always hold a special place in my heart and will never be forgotten. Thank you to my undergraduate chemistry professors: Dr. Danny

Hubbard, Dr. Allen Miles, Dr. Bobby Burkes, Dr. Frank Ohene amongst other “Grambling” friends and family. You all have been instrumental in my future and I truly believe that each of you have helped lay the foundation that was necessary for me to make it to this point. Special thanks to my friends from home and at Grambling for the fun times that helped me relieve stress during study hours, whether it was giggles over “Rotel Nachos”, free styling amateur rap lyrics, playing beauty shop, running midnight “fat-attacks” to TCBY and Popeyes or simple sisterly relations eating “skee-wee cakes” and taunting BB the cat, each moment shared is memorable and always helped me enjoy my journey through each phase of this academic career.

Lastly, I give a very special acknowledgement to my own personal support system: Mark and Patti Cole (my parents) and Marcus Cole (my brother) for without them I would have never been encouraged to pursue something so daring, foreign, and pressing. I love you all with every ounce of my breath and drop of my blood. I want you to know that I am proud to represent our family and our name. I am eternally grateful for your love and support because this accolade was not only for me, but it was for us. Thank you Daddy for teaching me the “6 P’s” and that the only security in life is the one that I create for myself. Because of your wisdom, I have secured my future as a trailblazer and not as a statistic. Papa Bear, consider yourself a success as a parent. Mommy, I appreciate you for being my best friend during my loneliest times and my mother during the hardest times. You are the hardest working woman that I have ever known, and I’m glad to know that I have inherited such diligence and perseverance from you. It is because of your strength that I have learned to push through the seeming insanities that accompany the Ph.D. program. Most importantly, you have taught me to smile and stay kind through it all. Marcus, thank you for keeping me focused on the meaningful things in life. You have been my silent knight and I thank you for always protecting and encouraging me when others would belittle me because I

was “smart”. Since you have stood guard over your kid sister, I have finally become who you knew I could be. I also thank Aunt Paula Ross and Uncle Joseph Williams for always looking out for me whenever my parents weren’t able. You two were always there for me both academically and socially and I am grateful for the time that you have contributed to help make the final steps of my education less intense. From teaching me how to read to building kinetic machines, you have impacted me immensely and I will always cherish those memories. I will never forget how you have nurtured my love for education and science. Because of our family, I have become a trailblazer and no other first means more than logging this moment into our family history. Last and definitely not least, I would like to thank Kevin Roberson for your infinite encouragement, continuous friendship, and enthusiasm during this journey which has given me the motivation to realize this achievement. From the first week of school, we have grown closer and I am thankful to God that he has placed such an awesome man by my side to travel this journey together with. Your cupcakes, cards, and conversation has been a priceless investment to me accomplishing this journey and I want express my gratitude for all you have done for me during this process. I love you all more than time could measure and my gratitude to you extends infinitely beyond the measures of this world.

Thank you....

XOXO

Rae

TABLE OF CONTENTS

DEDICATION.....	ii
ACKNOWLEDGEMENTS.....	iii
LIST OF TABLES.....	xi
LIST OF FIGURES.....	xiii
ABSTRACT.....	xvii
CHAPTER 1 INTRODUCTION.....	1
1.1 Bacteriology and Infectious Disease.....	1
1.1.1 Bacteria.....	1
1.1.2 Morphology and Cellular Structure.....	2
1.1.3 Growth and Reproduction.....	3
1.1.4 Associations with Other Organisms.....	4
1.1.5 Pathogenic Bacteria and Infectious Disease.....	5
1.2 Introduction to Antibacterial Drugs.....	7
1.2.1 History of Antibiotic Development.....	7
1.2.2 Types of Antibacterial Drugs by Class.....	10
1.2.3 Mechanisms of Antibiotic Action and Resistance.....	17
1.3 Introduction to Antiseptics and Disinfectants.....	18
1.3.1 Quaternary Ammonium Compounds.....	21
1.3.2 Chlorhexidine and Bisbiguanidines.....	23
1.3.3 Structural Differences between QACs and Chlorhexidine and Their Antibacterial Mechanism of Activity.....	25
1.4 Combination Antibacterial Drug Therapy (CAT).....	27
1.4.1 Hybrid Antibiotics.....	32
1.4.2 Loewe's Additivity Model.....	35
1.5 Ionic Liquids.....	38
1.5.1 Groups of Uniform Materials Based on Organic Salts (GUMBOS).....	41
1.5.2 Antibacterial Ionic Liquids.....	42
1.5.3 Active Pharmaceutical Ingredient Based Ionic Liquids.....	44
1.6 References.....	47

CHAPTER 2 ANALYTICAL TECHNIQUES, MECHANISM OF ACTION VALIDATION, AND ANTIMICROBIAL CHARACTERIZATION	54
2.1 Pharmacological Techniques and Characterization	54
2.1.1 Rate of Dissolution	54
2.1.2 Predictive Intestinal Permeability.....	55
2.2 Antimicrobial Testing and Preparation	57
2.2.1 Turbidity Standards for Inoculum Preparation	57
2.2.2 Broth Dilution Tests	58
2.2.3 Kirby-Bauer Disk Diffusion Test	60
2.2.4 Mechanism of Action Studies.....	62
2.3 Absorbance-based Techniques.....	62
2.3.1 Michaelis-Menten Kinetics.....	65
2.3.2 Mammalian Cell Cytotoxicity	67
2.4 Fluorescent-based Techniques	70
2.4.1 1-N-Phenyl naphthylamine (NPN) Permeability Assay	74
2.4.2 BacLight Live/Dead Assay.....	75
2.4.3 BacLight Membrane Potential Assay	76
2.4.4 Lipopolysaccharide (LPS) Endotoxin Sequestration.....	80
2.5 Scanning Electron Microscopy	81
2.6 References.....	83
 CHAPTER 3 DESIGN, SYNTHESIS, AND BIOLOGICAL EVALUATION OF BETA (β)- LACTAM ANTIBIOTIC-BASED IMIDAZOLIUM- AND PYRIDINIUM-TYPE IONIC LIQUIDS	85
3.1 Introduction.....	85
3.2 Experimental	86
3.2.1 Materials and Methods	86
3.3 Results and Discussion	89
3.3.1 Physical Characterization of Amp-ILs	89
3.3.2 Antibacterial MIC of ILs	97
3.3.3 Critical Micelle Concentration and Antibacterial Activity Relationship	104
3.3.4 Effect of Ampicillin-content in ILs	107
3.3.5 Antibacterial Activity of Combinations	109
3.3.6 Loewe's Additivity Model.....	110
3.4 Conclusion	112
3.5 References.....	114

CHAPTER 4 SYNTHESIS, CHARACTERIZATION, AND BIOLOGICAL EVALUATION OF BETA (β)-LACTAM BASED CHLORHEXIDINE GUMBOS AGAINST ENTEROHEMORRHAGIC ESCHERICHIA COLI

117	117	119	119	120	120	121	122	122	124	125	125	131	139	146	152	152	158	162	166	167	168																						
4.1	Introduction.....	4.2	Materials and Methods.....	4.2.1	Synthesis of Chlorhexidine di-ampicillin GUMBOS.....	4.2.2	Dissolution Profile Measurement	4.2.3	<i>In Vivo</i> Prediction of Intestinal Permeability and Absorption.....	4.2.4	Antimicrobial Activity.....	4.2.5	GUMBOS Interaction Indices	4.2.6	Time-Kill Kinetics of Chlorhexidine di-ampicillin	4.2.7	Mechanism of Action Studies.....	4.2.8	HeLa, NIH/3T3, and EOMA Cell Viability Tests.....	4.3	Results.....	4.3.1	Representative GUMBOS Structural Analysis: Chlorhexidine di-Ampicillin.....	4.3.2	Pharmacokinetic Properties and Bioavailability of β -lactam-based Chlorhexidine GUMBOS	4.3.3	Anti-EHEC Activity	4.3.4	Interaction Indices	4.3.5	Time-kill Activity of Chlorhexidine di-ampicillin on <i>E. coli</i> O157:H7 43895.....	4.3.6	Mechanism of Action Studies.....	4.3.7	Cytotoxicity	4.4	Discussion	4.5	Conclusions.....	4.6	Acknowledgements.....	4.7	References.....

CHAPTER 5 ANTIBACTERIAL EFFECTS OF BETA (β)-LACTAM ANTIBIOTIC-CHLORHEXIDINE HYBRID SALTS ON ANTIBIOTIC RESISTANT MICROORGANISMS

172	172	174	174	176	176				
5.1	Introduction.....	5.2	Materials and Methods.....	5.2.1	Antimicrobial Activity.....	5.2.2	Lipopolysaccharide (LPS) Sequestration	5.3	Results and Discussion

5.3.1	Representative Antibacterial activities of Chlorhexidine diacetate and β -lactam Antibiotics against <i>S. aureus</i> 29523 and <i>K. pneumoniae</i> 10031	176
5.3.2	Comparative Antibacterial Activities of Chlorhexidine and β -lactam Antibiotics in Combination and as GUMBOS	177
5.3.3	Antibacterial Activities of β -lactam-based Chlorhexidine GUMBOS	178
5.3.4	Interaction Indices	185
5.3.5	Antibacterial activity in 10% Human Serum Albumin	185
5.3.6	Therapeutic Indices Chlorhexidine and Antibiotics in Combination and as GUMBOS	186
5.3.7	Lipopolysaccharide (LPS) Sequestration	187
5.4	Michaelis-Menten Kinetics using CENTA as a Substrate against Type I Penicillinase	192
5.4.1	CENTA and Chlorhexidine	192
5.4.2	CENTA and Chlorhexidine di-Ampicillin	195
5.5	Conclusion	197
5.6	References	199
CHAPTER 6 CONCLUSIONS AND FUTURE STUDIES		201
6.1	Concluding Remarks	201
6.2	Future Studies	202
APPENDIX: LETTERS OF PERMISSION		205
VITA		211

LIST OF TABLES

Table 1.1. Examples of adhesin-receptors per adhesion site by various bacteria. ²	6
Table 1.2. Summary of antibiotic classes, activities, and current mechanisms of action, and resistances.	19
Table 1.3. Chemical structures and use of select antiseptics and disinfectants against non-sporulating bacteria (Adapted from G. McDonnell and A. D. Russell (1999), with permission from the American Society for Microbiology).	20
Table 3.1. Synthesis and structures of five ampicillin-based ionic liquids by anion-exchange reactions.	96
Table 3.2. Diffusion zone ranges based on NCCLs diameter criterion for sodium ampicillin disks against Gram-negative and Gram-positive bacteria.	97
Table 3.3. Minimum inhibitory concentrations (MIC, μM) of ammonium-, imidazolium-, and pyridinium-type ampicillin ionic liquids. MIC values and minimum bactericidal concentrations were equivalent in this study.	106
Table 3.4. Interaction indices for ammonium-, imidazolium-, and pyridinium-type ampicillin ionic liquids.*	106
Table 4.1. List of ions with structures detected in positive-ion and negative-ion mode.	137
Table 4.2. Diffusion rates and predicted intestinal permeability acquired using PAMPA GenTest assay.	131
Table 4.3. <i>Escherichia coli</i> Strains.	140
Table 4.4. Minimum inhibitory concentrations (μM) of antibacterial agents. Standard deviations are from three measurements.	147
Table 4.5. Average minimum inhibitory concentrations (μM) of β -lactam-based chlorhexidine GUMBOS against <i>E. coli</i> 43895. Standard deviations are from six measurements.	148
Table 4.6. Calculated interaction indices (classification denoted in parentheses, where A = Antagonism, N = Neutral, and S = Synergy) for chlorhexidine di-ampicillin GUMBOS and the combined parent salts according a modified Loewe's Additivity Model.	149
Table 4.7. Calculated interaction indices (classification denoted in parentheses, where A = Antagonism, N = Neutral, and S = Synergy) for β -lactam based chlorhexidine GUMBOS according a modified Loewe's Additivity Model.	150
Table 4.8. Acute cytotoxicity (LD_{50}) of chlorhexidine di-ampicillin, chlorhexidine diacetate, sodium ampicillin, and the stoichiometric equivalent on HeLa cells. Standard deviations from four measurements.	161

Table 5.1. Sources and characteristics of drug-susceptible and drug-resistant bacterial strains 175

Table 5.2. Antibacterial activities (MIC, μM) of chlorhexidine diacetate, sodium ampicillin, disodium carbenicillin, sodium cephalothin, and sodium oxacillin against representative microorganisms *S. aureus* 29523 and *K. pneumoniae* 10031..... 177

Table 5.3. Antibacterial activities (MIC, μM) of chlorhexidine diacetate, chlorhexidine di-ampicillin, chlorhexidine carbenicillin, chlorhexidine di- cephalothin, and chlorhexidine di-oxacillin against representative microorganism *E. coli* 43895 in the presence of 10% human serum albumin. 186

Table 5.4. Average kinetic parameters between Type 1 penicillinase and CENTA substrate in the presence of sodium ampicillin, chlorhexidine diacetate, and chlorhexidine di-ampicillin secondary substrates. The Michaelis-Menten constants were calculated using linear regions from the different rate saturation curves. Apparent values are an average with standard deviations from all kinetic parameters acquired for each inhibitor concentration from four measurements. 193

LIST OF FIGURES

Figure 1.1. Types of bacteria by shape.	1
Figure 1.2. Basic components of a bacterial cell.	2
Figure 1.3. General structure of the five classes of β -lactam antibiotics.	11
Figure 1.4. Two examples of glycopeptide antibiotics.	12
Figure 1.5. Examples of three types of antibiotics that inhibit protein and nucleic acid syntheses.	13
Figure 1.6. Examples of DNA- and RNA-targeting antibiotics.	14
Figure 1.7. Structures of Tigecycline and Fosfomycin antibiotics.	15
Figure 1.8. Structure of cetyltrimethylammonium bromide as a representative cationic quaternary ammonium compound.	21
Figure 1.9. Hypothesized mechanism of action for quaternary ammonium biocides where a-f show progressive adsorption of the quaternary headgroup to acidic phospholipids in the membrane with increasing QAC exposure/concentration. A decreased fluidity of the bilayers and the creation of hydrophilic voids are formed in the membrane causing protein activity to be disrupted, cell lysis, and solubilization of membrane components into micelles (Adapted from P. Gilbert and L.E. Moore (2005), with permission from John Wiley and Sons).	22
Figure 1.10. Structure of chlorhexidine base.	24
Figure 1.11. Hypothesized mechanism of action for the interaction of chlorhexidine with the bacterial cytoplasmic membrane. Diagram shows progressive decreases in fluidity of the outer leaflet with increasing exposure to the bisbiguanide (Adapted from P. Gilbert and L.E. Moore (2005), with permission from John Wiley and Sons).	26
Figure 1.12. Schematic representing the differences between conventional combination antibiotic therapy and hybrid antibiotic therapy.	35
Figure 1.13. Representative concentration-response isobologram attributed to the activity of two drugs in combination, where (a) is the line of additivity, (b & c) indicate synergistic combinations and (d & e) indicate antagonistic mixtures.	37
Figure 1.14. Representative cations and anions that compose first-, second-, and third generation ionic liquids (ILs) and groups of uniform materials based on organic salts (GUMBOS).	40
Figure 1.15. Schematic representing the activity of pharmaceutically active ionic liquids and GUMBOS.	46
Figure 2.1. Example of broth dilution susceptibility testing and determination of minimum inhibitory and minimum bactericidal concentrations.	60

Figure 2.2. Kirby-Bauer disk diffusion assay showing various zones of inhibition.....	62
Figure 2.3. Schematic of the instrumental configuration of conventional absorbance spectrophotometers.	64
Figure 2.4. Instrumental configuration of a 96-well plate absorbance and emission plate reader. ²	65
Figure 2.5. Representative rate versus substrate concentration plot obtained from Michaelis-Menten kinetic experiments.....	67
Figure 2.6. Conversion of MTS to soluble formazan by cellular dehydrogenase enzymes present in viable cells. ⁵	70
Figure 2.7. Jablonski diagram illustrating photophysical transitions of an excited molecule.	72
Figure 2.8. Instrumental configuration of a fluorescence spectrophotometer.	73
Figure 2.9. Structure of 1-N-phenyl naphthylamine (NPN) fluorophore used in membrane permeability studies.	75
Figure 2.10. Structure of propidium iodide (A), SYTO 9 (B), and the spectra representing percentages of live and dead cells (C).	76
Figure 2.11. Direction of ion flux and their differences in intracellular and extracellular ionicity, where the abundance of potassium K^+ (red), sodium Na^+ (yellow), and calcium Ca^{+2} (blue) are highlighted and presented in an embedded table.	78
Figure 2.12. Chemical structure of DIOC ₂ membrane potential probe.	79
Figure 2.13. Instrumental configuration of a scanning electron microscope.....	83
Figure 3.1. Stacked proton nuclear magnetic spectra of various Amp-ILs synthesized in this study, where A=[CP][Amp]; B= [CTA][Amp]; C =[C16M2Im][Amp]; D = [C16M1Im][Amp]; E = [BmIm][Amp]; and F = [Na][Amp].....	92
Figure 3.2. Comparison between critical micelle concentrations of imidazolium and pyridinium halides and their corresponding Amp-ILs.....	95
Figure 3.3. Experimental zone diameters obtained using Kirby-Bauer disk diffusion assay. Top panel (A) demonstrate zones of inhibition results, and thresholds for resistance (R), intermediate (I), and susceptible (S) against <i>E. coli</i> O157:H7 and <i>S. typhimurium</i> . Bottom panel (B) demonstrates experimental inhibition zones acquired for <i>S. aureus</i> and <i>L. monocytogenes</i>	105
Figure 3.4. Bar graph depicting active concentrations of ampicillin content within Amp-ILs from MIC (μ M) for Gram-positive (A) and Gram-negative bacteria (B).	108
Figure 3.5. Interaction indices calculated for ampicillin-based ionic liquids. Each color correlates to a specific Amp-IL, where red = [CP][Amp] and its combinations, blue =	

[C₁₆M₁Im][Amp] and its combinations, and green = [C₁₆M₂Im][Amp] and its combinations. Darker colors are measured by the left axis indicative of *E. faecium* results and the right axis describes the interaction indices against *E. coli* O157:H7. 113

Figure 4.1 Molecular structures of dicationic chlorhexidine (top) and X counterions (from left to right) acetate, ampicillin, oxacillin, and cephalothin and Y counterion carbenicillin. GUMBOS consisting of chlorhexidine X consists of two anionic molecules electrostatically tethered to one chlorhexidine molecule, whereas chlorhexidine Y consist of one carbenicillin molecule ionically bound to chlorhexidine. 126

Figure 4.2. Proton (¹H)-NMR of chlorhexidine di-ampicillin. 132

Figure 4.3. Carbon (¹³C)-NMR of chlorhexidine di-ampicillin. The peaks indicative of either ion are labeled as CHX (chlorhexidine) and AMP (ampicillin) in addition to their color coated structural assignments in the embedded picture. 133

Figure 4.4. Mass spectra of chlorhexidine di-ampicillin GUMBOS in both negative-ion mode (top) and positive-ion mode (bottom). 134

Figure 4.5. Optical ellipticities of chlorhexidine di-ampicillin (solid) and sodium ampicillin (dashed) in PBS (100mM, pH 7.4). 135

Figure 4.6. Absorbance spectra of chlorhexidine di-ampicillin in methanol. 136

Figure 4.7. Release and first-order dissolution profiles of β-lactam based chlorhexidine GUMBOS in deionized water at 298 K. 138

Figure 4.8. Antibacterial activities of chlorhexidine diacetate and sodium ampicillin in combination against *E. coli* 25922 and EHEC isolates. 141

Figure 4.9. Antibacterial activities of three mixtures of chlorhexidine diacetate and sodium ampicillin against *E. coli* 25922 and EHEC isolates. 142

Figure 4.10. Interaction indices for mixtures of chlorhexidine diacetate and sodium ampicillin against *E. coli* 25922 and EHEC isolates. 143

Figure 4.11. Killing kinetics of *E. coli* O157:H7 ATCC 43895 at 7.3 μM chlorhexidine di-ampicillin (Δ) and chlorhexidine diacetate (□) as compared to the control (◇). Error bars represent standard deviations from three measurements. 151

Figure 4.12. Effect of GUMBOS on *E.coli* O157:H7 ATCC 43895 outer membranes in absence (top) and presence (bottom) of 5mM magnesium ions. Results normalized to NPN membrane fluorescence obtained by EDTA as negative control. 152

Figure 4.13. Changes in *Escherichia coli* O157:H7 ATCC 43895 membrane potentials using DIOC₂ stained cells treated with increasing concentrations of GUMBOS. The Panel (A) show the red/green ratiometric fluorescence obtained for different concentration of GUMBOS. Using

the Nernst equation, results in Panel (A) are converted to membrane potential values as shown in Panel (B). GUMBOS Error bars represent standard deviations from nine measurements. 155

Figure 4.14. Antibacterial activity of β -lactam based chlorhexidine GUMBOS against wild-type and imp4213 *E. coli* strains..... 156

Figure 4.15. SEM images of A) untreated and antibacterial treated *E. coli* O157:H7 ATCC 43895 with B) 50 μ M sodium ampicillin, C) 50 μ M chlorhexidine diacetate, D) 50 μ M chlorhexidine di-ampicillin, and E) 50 μ M stoichiometric mixture of parent salts..... 157

Figure 5.1. Interaction indices determined by fractional inhibitory concentrations (μ M) of chlorhexidine diacetate and A) sodium ampicillin, B) disodium carbenicillin, C) sodium cephalothin, or D) sodium oxacillin against *S. aureus* 25923. 180

Figure 5.2. Interaction indices determined by fractional inhibitory concentrations (μ M) of chlorhexidine diacetate and A) sodium ampicillin, B) disodium carbenicillin, C) sodium cephalothin, or D) sodium oxacillin against *K. pneumoniae* 10031. 181

Figure 5.3. Antibacterial activity of β -lactam-based chlorhexidine GUMBOS on drug-susceptible and drug-resistant Gram-positive bacteria. 182

Figure 5.4. Antibacterial activity of β -lactam-based Chlorhexidine GUMBOS on drug-susceptible and drug-resistant Gram-negative bacteria. 183

Figure 5.5. Interaction indices on MDR- and MDS bacteria for chlorhexidine di-ampicillin, chlorhexidine carbenicillin, chlorhexidine di-cephalothin, and chlorhexidine di-oxacillin. 188

Figure 5.6. Therapeutic Indices using mean inhibitory concentrations per bacteria drug susceptibilities for β -lactam-based chlorhexidine GUMBOS, where A = HeLa, B = NIH/3T3, and C = EOMA. 189

Figure 5.7. Determination of BODIPY-cadaverine (BC) displacement from LPS (left) and remaining LPS concentration (right) by chlorhexidine diacetate, chlorhexidine di-ampicillin, chlorhexidine di-cephalothin, chlorhexidine di-oxacillin, and chlorhexidine carbenicillin. BODIPY-cadaverine was mixed with LPS and various concentrations of GUMBOS added. Displacement of BODIPY-cadaverine from LPS was calculated as $[1-(F - F_0)/(F_{\max} - F_0)] * 100\%$, where F_0 is the fluorescence intensity at LPS saturation with BODIPY-cadaverine and F_{\max} is the fluorescence intensity without LPS. 190

Figure 5.8. Saturation curve with 0.5 units Type 1 penicillinase showing the relationship between CENTA (substrate) concentration and its degradation rates in the presence of increasing concentrations of chlorhexidine diacetate at 37°C..... 194

Figure 5.9. Saturation curves with 0.5 units Type 1 penicillinase showing the relationship between CENTA (substrate) concentration and its degradation rates in the presence of increasing concentrations of chlorhexidine di-ampicillin at 37°C. 196

ABSTRACT

Outbreaks of shiga-toxin producing *Escherichia coli* (STEC), namely *E. coli* O157:H7, with other multi-drug resistant bacteria (MDRB) alongside the unfortunate dearth in antibiotic drug development have helped to create a platform in which infections caused by pathogenic bacteria have become superior. This problem necessitates the development of novel antimicrobial agents with high potency and low toxicity.

The research presented in this dissertation explores a novel pragmatic therapeutic approach for control, prevention, and treatment of infectious disease using Active-Pharmaceutical Ingredient-based Ionic Liquids (API-ILs) and Groups of Uniform Materials Based on Organic Salts (GUMBOS). Accordingly, several antiseptic- and antibiotic-based API-ILs and GUMBOS were synthesized and characterized using a combination of analytical and microbiological techniques. Overall, this research presents an advanced alternative to combination antibiotic therapy by using a novel group of ionic antimicrobial materials that have controlled pharmacokinetics, improved bioavailabilities, reduced toxicities, multi-modal properties, and potent antimicrobial spectrum of activity as a viable alternative to combating bacterial infections.

The first part of this research provides the physical characterization and subsequent *in vitro* antimicrobial activity of ampicillin-based ILs consisting of several different quaternary ammonium compounds (QACs) on *Escherichia coli* O157:H7, *Klebsiella pneumoniae*, *Staphylococcus aureus*, and *Listeria monocytogenes*. The synthesized API-ILs were validated with proton nuclear magnetic resonance spectroscopy (NMR) and elemental analysis. Melting points, critical micelle concentrations, and solubility were among the other physical properties

investigated. Improved antibacterial activity was evaluated using Loewe's Additivity Mathematical Model and interaction indices were established and compared to mixtures of precursor QACs and ampicillin.

The second part of the dissertation research focuses on the synthesis and antibacterial activity of GUMBOS created from an antiseptic and several β -lactam antibiotics. Using anion metathesis, four β -lactam antibiotic-based chlorhexidine GUMBOS were synthesized prior to validation using proton and carbon NMR, mass spectrometry, elemental analysis, and absorbance spectroscopy. Several orders of improvement in *in vitro* antibacterial activities were obtained on isolates of *Escherichia coli* O157:H7, *Salmonella typhi*, *Acinetobacter baumannii*, *Enterbacter cloacae*, *Enterbacter aerogenes*, *Klebsiella pneumoniae*, *Pseudomonas aeruginosa*, *Serratia marscescens*, *Staphylococcus aureus*, *Streptococcus mutans* *Streptococcus faecalis*, *Micrococcus luteus*, *Bacillus cereus*, and Methicillin-resistant *Staphylococcus aureus*. Interaction indices show the GUMBOS to be synergetic ion-pairs despite additivity and antagonism observed by the mixtures of antiseptic and antibiotic precursor ions. Furthermore, the mechanisms of action studies for these materials were defined with emphasis on membrane permeability and membrane potential. Finally, acute cytotoxicity against fibroblast, endothelium, and cervical cellular lines in addition to an assessment of intestinal permeability and bioavailability were completed.

Specific target applications for this work include the reduction of STEC fecal shedding from ruminant sources, prevention of meningitis onset in neonates by the eradication of Group B. Streptococci, reduction in catheter-associated bacteremia, and extension of antibacterial efficacy and spectrum of activity of antibiotics against multi-drug-resistant microbes that colonize in wound beds.

CHAPTER 1 INTRODUCTION

1.1 Bacteriology and Infectious Disease

1.1.1 Bacteria

Originally called “animalcules”, bacteria were studied microscopically by Antonie van Leeuwenhoek during the mid- 17th century.¹ They were not known as bacteria until the 1830s when Christian Gottfried Ehrenbug defined the genus based on his scientific observations as “non-spore forming rod-shaped bacteria”.¹ However, bacteria are defined as single-celled, prokaryotic microorganisms.¹ Bacteria have several morphologies (*i.e.* spheres, rods, and spirals) and sizes which range on the scale of microns (Figure 1.1). Most bacteria are spherical, named cocci, or rod-shaped, called bacilli.¹ Slight differences in the morphology from spheres or rods have led to different classes of bacteria named by their shapes such as comma (*Vibrio*), spiral (*Spirilla*), or coiled (*Spirochaetes*). The shapes of bacteria are determined by the cell wall and its cytoskeleton.¹ Aside from morphology, bacteria arrange in ordered arrays that add to their diverse nomenclature. For example, *Streptococci* species form chains whereas *Staphylococci* species form clusters.

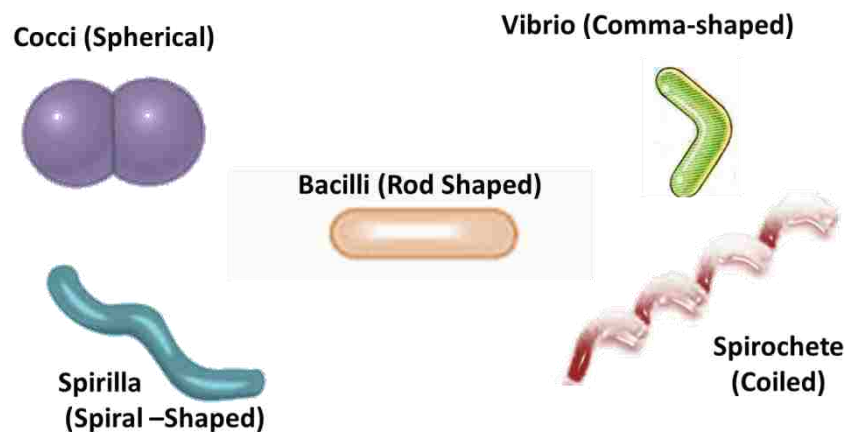


Figure 1.1. Types of bacteria by shape.

1.1.2 Morphology and Cellular Structure

Bacteria are visually distinguishable using Gram-staining (named after Christian Gram, Danish scientist and physician, 1853-1938).¹ This bacteriological method separates bacteria into two classes based on their abilities to retain dyes and the physical properties of their cellular walls. Additionally, this method allows for their morphologies and arrangements to be visualized microscopically. The principle of Gram-staining is premised on the notion that Gram-positive bacteria have a thicker cellular wall than Gram-negative.¹ Hence, Gram-positive bacteria retain both the crystal violet and safranin stains while Gram-negative bacteria only show the pink safranin dye. Examples of Gram-positive bacteria are *Staphylococcus* and *Enterococcus* and examples of Gram-negative bacteria are *Escherichia* and *Salmonella*.

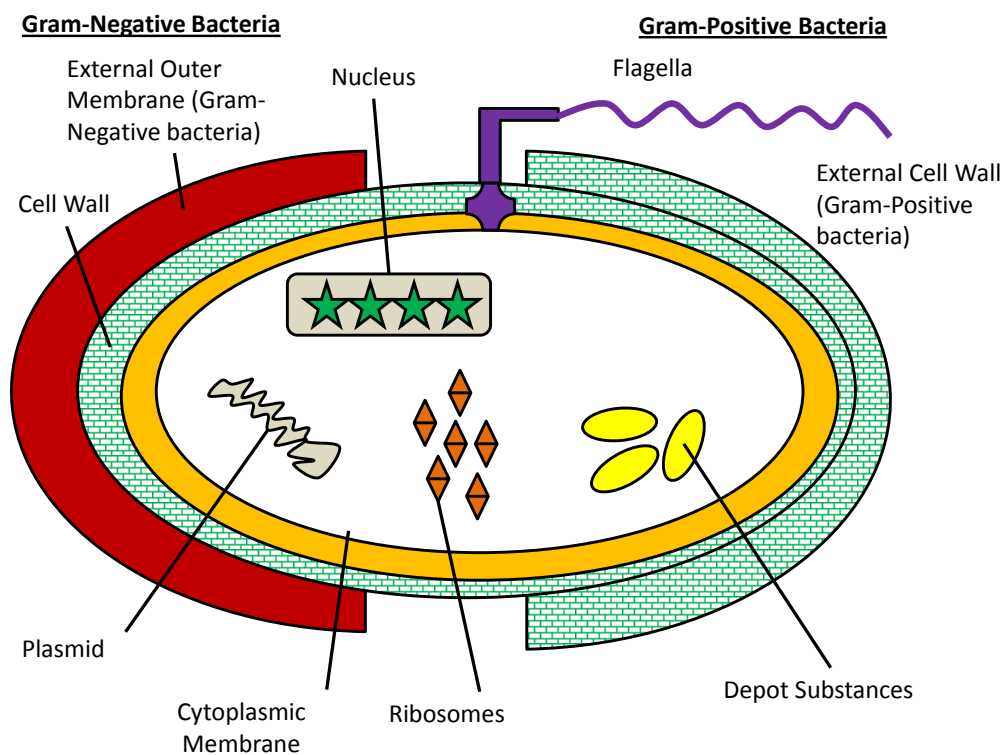


Figure 1.2. Basic components of a bacterial cell.

Bacteria are structurally composed of two major parts: intracellular and extracellular components (Figure 1.2). The intracellular components are enclosed by a hydrophobic cell membrane which envelopes its essential materials. Prokaryotes are structurally simple as compared to eukaryotic cells since they do not contain various membrane bound organelles.¹ Instead of mitochondria, bacteria use micro-compartments that maintain cellular metabolisms and membrane potentials which are generated via biochemical reactions across cellular membranes.¹ Bacteria have a nucleoid that stores its genetic material. The only common feature amongst all cells is the presence of ribosomes which helps to generate proteins and enzymes for routine function. The intracellular components are protected by a cellular wall composed of peptidoglycan, which is also the lethal target of beta (β)-lactam antibiotics.¹ As previously mentioned, Gram-staining reveals the structural differences in the extracellular components of Gram-positive and Gram-negative bacteria. Gram-positive bacteria have a thicker cell wall that is composed of both peptidoglycan and teichoic acid layers, which helps to retain Gram-stains.¹ However, Gram-negative bacteria have a thin layer of a peptidoglycan cell wall with a thick secondary cell membrane composed of lipopolysaccharides and lipoproteins.¹ Although the conventional structure of bacteria contains a cell membrane and cell wall, the thickness and assembly can vary affecting the bacterium's susceptibility to many antimicrobial agents. Additional components on the extracellular framework, can include flagella, fimbriae, and pili as well as the production of protective slime layers, but are not characteristic of the bacteria studied in this research and details about their roles are omitted.

1.1.3 Growth and Reproduction

Bacteria are asexual microorganisms that reproduce via binary fission. Cell growth are defined as occurring in three phases, i.e. lag phase, logarithmic phase, and stationary phase, prior to cell death.¹ The first phase, called the lag phase, allows the bacteria to adapt to its growth

environment. This is a slow growth process and has the highest protein synthesis rates prior to the logarithmic phase. In this phase, the bacteria have become well-adjusted to its environment and begin to multiply exponentially. The rate at which bacteria multiply is known as the growth rate which is dependent on the cells splitting rate known as generation time.¹ The rate limiting factor during this phase is the speed in which the key nutrients required for optimal growth are consumed. Once depleted, bacteria growth becomes static and cells enter into the stationary phase. This phase causes cells to adapt to the lack of nutrients as they try to survive in a stress response state.¹ Prior to cell death, bacteria express high amounts of genetic information relevant to DNA repair, antioxidant metabolism, and nutrient transport.

1.1.4 Associations with Other Organisms

Bacteria are highly adaptable and thus are found in a wide variety of environments. They are capable of forming complex associations with other organisms in which these associations can be categorized as parasitism, mutualism, and commensalism.¹ Within the scope of this dissertation, only associations based on commensalism and parasitism will be addressed. Bacteria that exercise commensalism are able to survive without harming or helping the host. Examples of commensalism lie in the types of bacteria that innocuously reside inside the mouth, nose, and intestinal tract of mammals.¹ In any type of benefit to the host, the colonization of these bacteria prevents the intrusion of harmful bacteria into that site. As a result, some are beneficial as part of the normal human flora while some bacteria can cause several diseases and infections. Bacteria that unilaterally deplete the host's health and detrimentally affect its immune system as an effort to survive are considered to be opportunistic and are parasitic.¹ These bacteria proliferate at the expense of the host causing its exposure to various secreted poisonous substances. Contact with such poisons (*i.e.* endotoxins and exotoxins) can result in the onset of

disease and infection.¹ Therefore antibacterial agents are used to prevent the effects of their parasitic intrusion that results in host morbidity and mortality.

1.1.5 Pathogenic Bacteria and Infectious Disease

Pathogenic bacteria are microorganisms that cause infection which sometimes result in disease. Their degree of pathogenicity or virulence is often the result of their genetic, biochemical, or structural features.¹ Since pathogenic bacteria are parasitic microorganisms, the degree of virulence is dependent on the strength of the host's immune system, the resilience or susceptibility of the bacteria, and the bacteria's virulence factors.¹ Pathogenic bacteria have two main methods of inflicting disease: 1) invading tissues and colonizing and/or 2) producing toxins.¹ Invasiveness allows the bacteria to initially adhere to the tissue surface, grow, and produce extracellular substances that debilitate host mechanisms.¹ This usually occurs at sites exposed to the external environment such as the urogenital tract, digestive tract, respiratory tract and the eye. Bacteria that prey on these sites have special adherence mechanisms which allow resistance to host defenses. There are two mechanisms (*i.e.* nonspecific adherence and specific adherence) that facilitate bacteria cell adhesion, in which examples of bacterium-specific adhesin-receptors per adhesion site are listed in Table 1.1.¹ Nonspecific adherence to eukaryotic cells uses various attractive forces and Brownian motion.¹ However, a bacteria's ability to specifically adhere to a site relies on a receptor and ligand relationship. Receptors are commonly peptides, proteins, or carbohydrates, on the surface of a eukaryotic cell.¹ However, the bacterial ligand is called an adhesin. Adhesins are polymeric cell surface proteins that control the complimentary interaction between the bacteria and host cell receptor site.¹ This is a property of the bacteria extracellular components, namely the pilli and fimbriae. More specifically, some bacteria choose particular cells and tissue sites in which to colonize. Examples of histotropic bacteria that use their invasiveness to inflict disease are *Pseudomonas aeruginosa*, *Acinetobacter*

baumanii, and *Enterbacter cloacae*, since they have an apparent tissue preference over others. The methods in which these bacteria and some others adhere to cell receptors sites and the resulting disease are highlighted in Table 1.1.

Table 1.1. Examples of adhesin-receptors per adhesion site by various bacteria.²

Bacterium	Adhesin	Receptor	Attachment site	Disease
<i>Streptococcus pneumoniae</i>	Cell-bound protein	N-acetylhexos-amine-galactose disaccharide	Mucosal epithelium	Pneumonia
		Amino terminus of fibronectin		
<i>Staphylococcus aureus</i>	Cell-bound protein	Species-specific carbohydrate(s)	Mucosal epithelium	Various
<i>Enterotoxigenic E. coli</i>	Type-I fimbriae	Complex carbohydrate	Intestinal epithelium	Diarrhea
<i>Uropathogenic E. coli</i>	Type I fimbriae	Globobiose linked to ceramide lipid	Urethral epithelium	Urethritis
<i>Pseudomonas aeruginosa</i>	Type-I V Pilli	Species-specific carbohydrate(s)	Upper respiratory tract	Pneumonia
<i>Klebsiella pneumoniae</i>	Type-I fimbriae	Species-specific carbohydrate(s)	Upper respiratory tract	Pneumonia
<i>Enterobacter cloacae</i>	Type – I fimbriae	Species-specific carbohydrate(s)	Mucosal epithelium	Pneumonia
<i>Acinetobacter baumannii</i>	Cell-bound protein	Species-specific carbohydrate(s)	Mucosal epithelium	Pneumonia

The other method, toxigenesis, is a method in which bacteria excretes either endotoxins or exotoxins which can adversely affect the host. Endotoxins are cell-associated molecules that are usually found within the outer membrane (*i.e.* lipopolysaccharide) of Gram-negative bacteria.¹ These toxins are not secreted by cells, but rather are released when lysed by antibiotic therapy or the host's immune defenses.¹ Bacteria that harvest endotoxins are Gram-negative pathogens such

as *Neisseria meningitides* that causes meningococcal disease and *Listeria monocytogenes* that causes listeriosis. By contrast, exotoxins are released from bacterial cells. Some exotoxins behave differently on target cells and can be categorized by: (1) identification of toxin-producing organism, (2) identification of organism susceptible to toxin, (3) target susceptibility to toxin, (4) chemical structure or morphology, (5) resistance to environmental stressors, and (6) chronological discovery-based nomenclature.² Many exotoxins can be identified by several of these categories. An example of an exotoxin is botulinum toxin produced by *Clostridium botulinum*. Both endotoxins and exotoxins can be transported in circulation and result in cytotoxic effects at localized and remote sites of invasion.¹

1.2 Introduction to Antibacterial Drugs

1.2.1 History of Antibiotic Development

The emergence of antibiotic drug resistance among bacteria has become an increasing health problem. Therefore, to better understand this dilemma it is useful to understand the history and development of antibacterial drugs or antimicrobial agents. Antimicrobial agents are generally classified into two categories: 1) antimicrobial drugs such as antibiotics amongst other systemic drugs for infection treatment, and 2) antiseptics and disinfectants, used to sterilize surfaces.¹ Several types of antimicrobial drugs exist. Naturally occurring drugs synthesized from microorganisms are defined as antibiotics.¹ Chemically synthesized drugs that do not resemble the pharmacophoric groups of antibiotics are called synthetic drugs.¹ The majority of antimicrobial drugs that have been developed are known as semi-synthetic drugs, which are chemical derivatives of antibiotics.¹

Prior to modern day medicine, society relied on plant products to treat disease even though their therapeutic properties were not clearly understood. These earlier medicines were most effective on protozoan disease rather than bacterial infections. Early records show that both

cinchona and ipecacuanha roots were effective treatments for malaria and dysentery, respectively.³ Bacterial infections (*i.e.* syphilis) caused by *Treponema pallidum* was treated with guaiacum and heartsease and sometimes systemic mercury.³

The use of synthetic materials as antimicrobial agents serendipitously began with Paul Ehrlich. He hypothesized that a “magic bullet” for the diagnosis and treatment of opportunistic bacterial infections could come about a combinatorial based staining treatment that consisted of a pathogen selective dye and a bactericidal toxin.⁴ In the midst of searching for a less toxic version of the sleeping sickness cure Atoxyl, Ehrlich with Sahachiro Hata discovered that the arsphenamine compound known as Salvarsan had anti-syphilitic activity.⁴ However, this compound required the body to metabolize it into its active form even though still exploiting patients to its idiosyncratic side effects. Sulfonamides or sulfa-drugs are credited to be the first class of synthetic drugs. The antibacterial property of the first sulfonamide, trademarked as Prontosil, was discovered by Gerhard Domagk.⁴ It had strong preferential antibacterial activity for hemolytic streptococci rather than other Gram-positive cocci. Unfortunately, Prontosil did not show antibacterial activity *in vitro*. Later it was revealed by Ernest Fourneau that when Protosil is administered *in vivo* it is metabolized into two portions, an inactive dye and a pharmacologically active sulfanilamide.⁴ This discovery led to the manipulation of the sulfanilamide molecule as an effort to identify more broadly active, potent antimicrobials with reduced cytotoxicity.

The idea to use microorganisms therapeutically is not new. Known formally as antibiotics, this approach was used to describe any substance produced by one microorganism that inhibited the growth of a secondary opportunistic microorganism.¹ This definition excludes naturally occurring substances lethal to microorganisms that were not produced by other

microorganisms or chemically synthesized substances such as in the case of sulfonamides.¹ Native Americans relied on antibiotic therapy for many years. Early Native American documents report the use of a “slimy” fungus to treat skin abscesses.³ In the 1890s, Rudolf Emmerich and Oscar Low Coghill at the United States Department of Agriculture's Northern Regional Research Laboratory in Illinois used mold from a cantaloupe to produce higher yields of penicillin.⁵ Throughout the 1940s and 1950s, substantial efforts were pursued to capitalize on the new found ability to extract high yields of penicillin. Dorothy Crowfoot Hodgkin elucidated the 6-aminopenicillanic acid (6-APA) chemical structure of penicillin in 1945.⁵

A variety of antibiotics surfaced after the discovery of penicillin, mostly those composed of the 6-APA backbone. In 1948, Giuseppe Brotzu isolated a similar drug to penicillin known as cephalosporin from *Cephalosporium acremonium*.⁵ It is documented to be one of the first antibiotics effective against *Salmonella typhi*, which was resistant to other penicillin analogs. Guy Newton, Edward Abraham, and Sir William Dunn isolated cephalosporin C, in which the 7-aminocephalosporanic acid (7-ACA) backbone was determined.⁵ Cephalothin was the first synthetic cephalosporin manufactured by Eli Lilly & Co. in 1964.¹ Other antibiotics were subsequently developed. For example, Selman Waksman and Albert Schatz are accredited for the discovery of streptomycin and neomycin, later part of the antibiotic class of aminoglycosides.⁶ Likewise, Rene Dubos discovered the polypeptide-type antibiotic gramicidin from *Bacillus brevis* in 1939.⁷ Shortly after, chlortetracycline and chloramphenicol were added to the growing antibiotic arsenal.^{4, 8} In 1962, the synthesis of nalidixic acid led to another antibiotic class known as fluoroquinolones.⁴

The drugs developed since the 1960s have been analogs of existing synthetic antibacterial drugs. Resulting in more than 12,000 different active agents, structural modifications to the

pharmacophoric skeletons of existing antibiotics have resulted in improved bactericidal potency, broadened spectrum of activity, reduced toxicity, and attenuated adverse side effects. Collectively, antibiotics have been the most important factor in extending the human lifespan.

1.2.2 Types of Antibacterial Drugs by Class

Infections caused by some bacteria pose a serious threat. Primarily, Gram-negative bacteria are quite efficient in acquiring resistance which can limit antibiotic therapy. Aside from deactivating various antibiotics, Gram-negative bacteria are able to release endotoxins from their outer membranes which also makes antibiotic therapy a contraindicated treatment option as well.

Traditional synthetic approaches have yet to make a substantial contribution to any new classes of antibacterial agents. Thus, clinicians have relied on a series of antibiotic analogs that have reduced toxicities with increase spectrum and potent antibacterial activities. Though not differing vastly in structural components, the pharmacophoric groups of these antibacterial agents still face deactivation mechanisms already utilized by both Gram-negative and Gram-positive bacteria. In this section, mechanisms of action for each antibiotic class and mechanisms of antibiotic resistance are outlined.

1.2.2.1 Inhibitors of Cell-wall Synthesis

Beta-(β)-lactam antibiotics and inhibitors are among the most commonly prescribed drugs, grouped together based upon the key pharmacophoric feature, the β -lactam ring, which inhibits the activity of transpeptidase and causing the cell wall to become defective.¹ The basic structure of β -lactams consists of three parts: 1) a fused β -lactam ring, 2) a free carboxylic acid group, and 3) a substituted amino acid group.¹ Structural variation around the β -lactam ring has yielded other drugs within this class such as penicillins, cephalosporins, carbapenems, and monobactams with added greater antimicrobial potency against broader spectra of microorganisms (Figure 1.3). Most advances in antibacterial therapy have been effective on

Gram-positive bacteria, but recently approved β -lactam antibiotics such as ertapenem and doripenem have shown useful against *Pseudomonas aeruginosa*. Since some β -lactam antibiotics have lost potency against various species of Gram-negative bacteria, they are often combined with β -lactamase inhibitors.¹ Inhibitors prevent enzymatic degradation of β -lactam drugs caused by β -lactamase (penicillinase) enzymes. Currently, there are three β -lactamase inhibitors available (*i.e.* sulbactam, tazobactam, and clavulanic acid).¹ Due to the emergence of resistance to both β -lactam drugs and β -lactamase inhibitors, particularly by Gram-negative bacteria, these agents are losing usefulness in treating nosocomial infections.

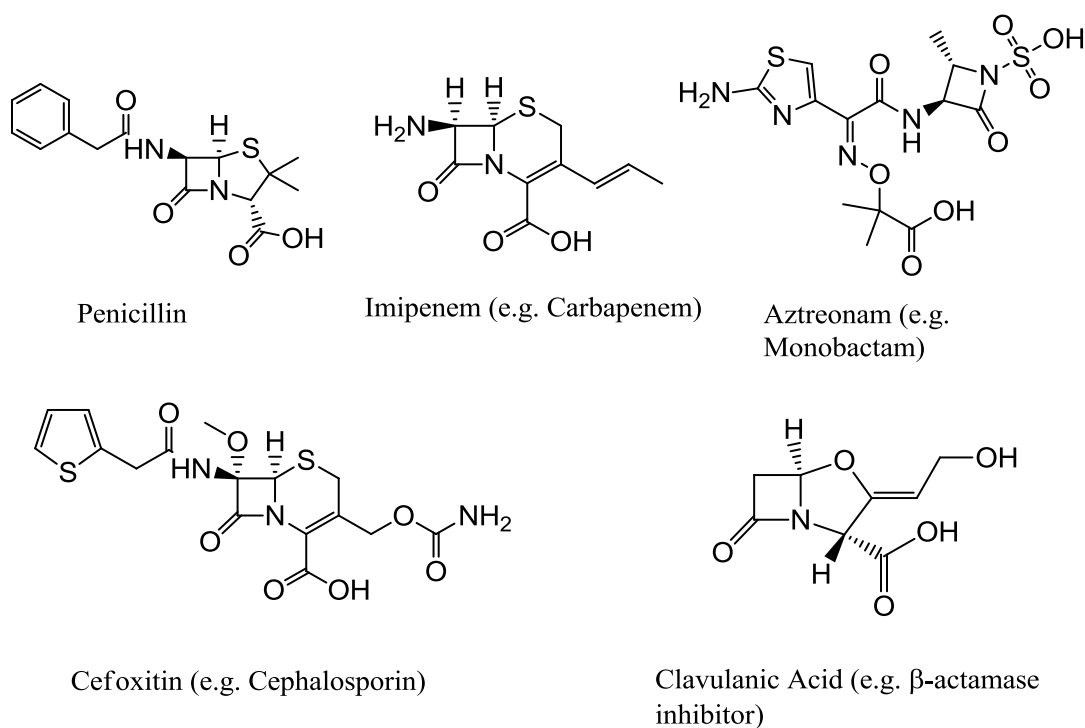


Figure 1.3. General structure of the five classes of β -lactam antibiotics.

Other examples of antibiotics that attack the cell wall are within the class of glycopeptides. Glycopeptides are composed of either a glycosylated cyclic or polycyclic nonribosomal peptide which makes these molecules very large compared to other cell wall inhibitors (Figure 1.4). These antibiotics deactivate Gram-positive bacteria by binding to the

acyl-D-alanyl-D-alanine units that prevents the formation of new additions to the peptidoglycan cell wall.¹ Due to their large sizes, these molecules are often excluded from Gram-negative bacteria and were commonly used to treat Gram-positive bacterial infections. Additionally, they are bacteriostatic against most species but are lethal to *Enterococci* species. However, vancomycin-resistance towards both *Staphylococci* and *Enterococci* species and toxicity has limited its clinical use.

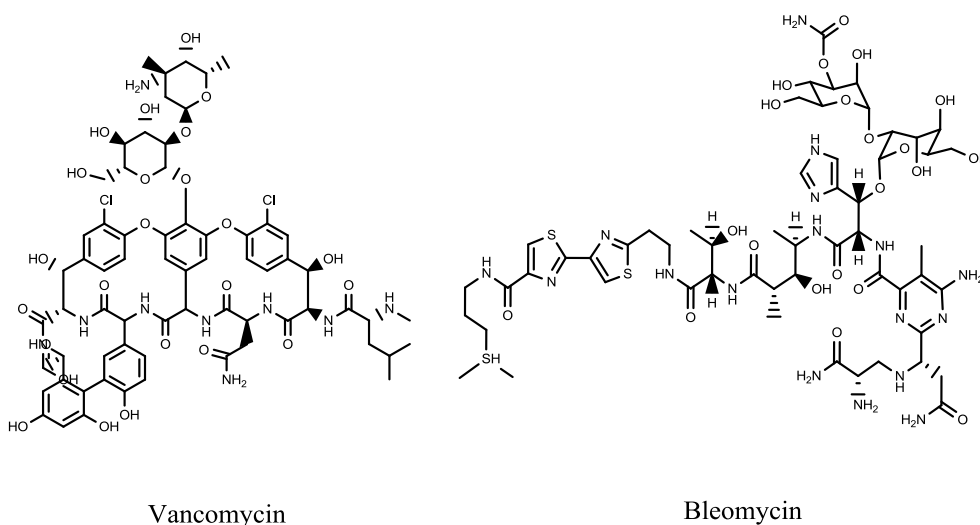


Figure 1.4. Two examples of glycopeptide antibiotics.

1.2.2.2 Inhibitors of Protein and Nucleic Acid Synthesis

Other conventional antibiotics belong to classes that attack protein synthesis or inhibit nucleic acid synthesis. Examples of these types of antibiotics are shown in Figure 1.5. Antibiotics that target the protein synthetic pathways selectively target bacterial ribosomes. Known as aminoglycosides, these molecules consist of amino-modified sugars and enter the bacterial cell through active transport to subsequently bind to the ribosomal subunit.¹ With over 14 analogs, these molecules selectively target different ribosomal subunits within the cell.¹ For instance, streptomycins target the 30S ribosomal subunit; whereas, kanamycins and neomycins bind to both 30S and 50S subunits but in different locations than streptomycins.¹ In addition to protein

inhibition, these molecules are also capable of disrupting the cell membrane by creating fissures and causing the intracellular components to leak. This antibiotic is typically administered to treat Gram-negative bacterial infections; however, modification to ribosomal proteins, alteration to cellular membranes or degradation of this antibiotic has led to increased bacterial resistance.¹

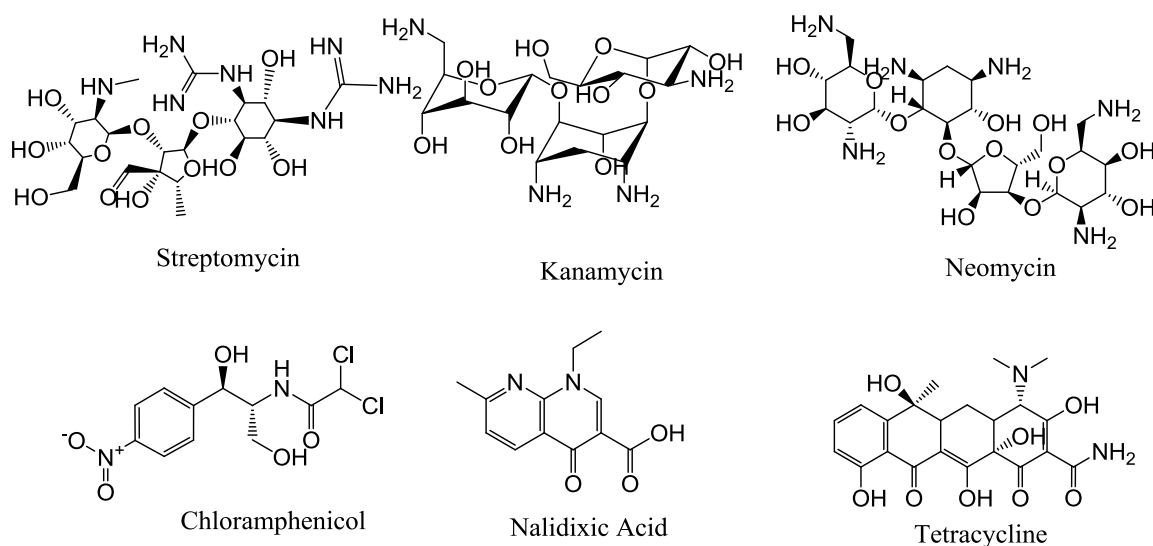


Figure 1.5. Examples of three types of antibiotics that inhibit protein and nucleic acid syntheses.

Chloramphenicol is a broad-spectrum antibiotic that also inhibits protein synthesis by targeting the 70S ribosomes.¹ This molecule is active against resistant Gram-positive bacteria and some Gram-negative bacteria. For example, this drug is not an effective treatment for infections caused by *Pseudomonas aeruginosa* or *Enterobacter* species. This antibiotic has been replaced by more recent, inexpensive alternatives but still remains the ideal treatment for meningitis and infections in those with penicillin allergy. Unfortunately, therapeutic use of this antibiotic has resulted in several adverse reactions such as aplastic anemia, leukemia, and Gray Baby Syndrome.¹ Resistance to chloramphenicol has also been reported. Enzymatic degradation of chloramphenicol by chloramphenicol acetyl-transferase prevents its binding to the bacterial ribosome.¹ Similar to other large molecules, changes in the outer membrane permeability in

Gram-negative bacteria also inhibits the entrance of the bacteriostatic drug. Lastly, tetracyclines target protein synthesis by binding to the 30S subunit and deactivating aminoacyl tRNA. Tetracyclines are cationic broad-spectrum antibiotics consisting of four fused rings.¹ Resistance also limits the clinical use of this type of antibiotic in that it is easily removed by efflux pumps, proteins have modified its target ribosomal binding subunit, or it is enzymatically inactivated.¹

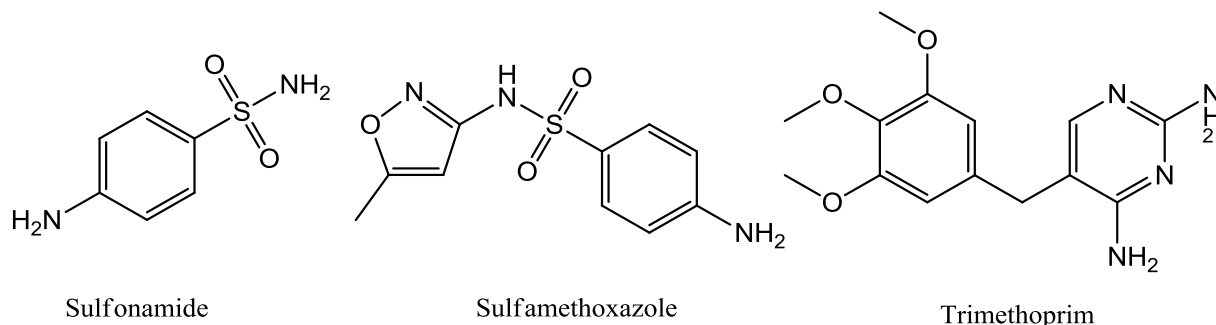


Figure 1.6. Examples of DNA- and RNA-targeting antibiotics.

Some antibiotics that inhibit nucleic acid synthesis also stop folate synthesis. Representative DNA and RNA targeting antibiotics are shown in Figure 1.6. Folate is a coenzyme used to produce DNA and RNA in bacteria and is the target of sulfonamides and diaminopyrimidines.¹ Limited to sulfur allergies, sulfonamides are commonly not used unless used in combination with a diaminopyrimidine as in the formulation of trimethoprim-sulfamethoxazole.¹ The inefficacy of sulfonamide drugs results from the over-production of p-aminobenzoic acid or production of dihydropteroate synthetase while the over-production of dihydrofolate reductase or production of a drug resistant version collectively limits the activity of diaminopyrimidines.¹ Quinolones also inhibit bacteria growth by acting on enzymes in DNA synthesis. Its broad spectrum activity results from its ability to target primary DNA in Gram-negative bacteria and topoisomerase IV in Gram-positive bacteria.¹ Quinolone resistance results from decreased expression of membrane porins which enables its activity on DNA.¹ However,

modifications in efflux pumps and alterations in target enzymes also prevent this antibiotic from being effective.

A new class of antibiotics, known as glycylicyclines, has broad-spectrum antibacterial action for both drug-susceptible and resistant Gram-positive and Gram-negative microorganisms (Figure 1.7). Similar to tetracycline and aminoglycoside antibiotics, glycylicyclines antibiotics block protein synthesis by binding to the 30S ribosomal unit in the bacterial cell.¹The most recent advancement, Tigecycline, was approved in 2005 by the United State Food and Drug Administration (FDA) as a treatment for skin and wound infections.¹ Unfortunately, this antibiotic's utility is limited due to its inability to overcome the resistant efflux pump mechanism, specifically MexXY, in *P. aeruginosa* bacterial cells.¹Another recently developed antibiotic that exhibits good antimicrobial activity against *Enterobacteriaceae* is fosfomycin tromethamine.¹ Although it has better pharmacokinetic properties, it also shows limited activity against *P. aeruginosa*. Both tigecycline and fosfomycin are the better antibiotic options available to treat infections caused by Gram-negative bacteria; however, concerns about resistance still prevail

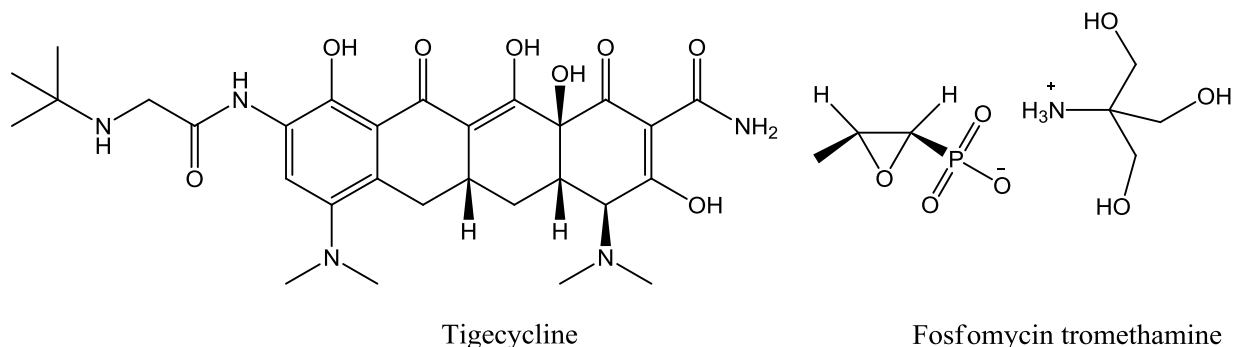


Figure 1.7. Structures of Tigecycline and Fosfomycin antibiotics.

1.2.2.3 Antimicrobial Peptides

Antimicrobial peptides are a unique and diverse class of biologically available molecules that have broad spectrum activity against a wide variety of microorganisms, including drug-resistant bacteria. Composed generally of 12 – 50 amino acids, these peptides consist mostly of positively charged amino acids (*i.e.* arginine, lysine, or histadine) and hydrophobic residues.¹ Similar to other proteins, these antimicrobial agents can possess α -helical, β -stranded, β -hairpin, or extended configurations.¹ Because of its amphipathicity, these agents are able to partition into biological membranes by folding and inserting through the lipid bilayers forming pores. Their major mechanism of action involves membrane permeation, but these agents are able to target various sites within the bacterial cell making them highly effective.¹ An example of a potent antimicrobial peptide is Polymyxin B, the most promising new additions to this class being ceragenins and the NAB-series of polymyxins.¹ Often considered as a last resort, these agents have suffered from induced cytotoxicity and narrow spectrum activity against Gram-positive bacteria.

1.2.2.4 Anti-Toxigenesis and Invasiveness Inhibitors

An indirect approach to treating infections caused by Gram-negative bacteria is to interfere with the virulence factors and efflux pump regulation in the cells instead of targeting bacteria viability.¹ This approach prevents the process of infection because the bacteria cell is unable to recognize host signals thereby limiting its pathogenic effect on the host. This results in limited colonization in histological morbidity and improved host immune response. Main anti-virulence target approaches include inhibitors of toxins and adhesins, organism specific virulence gene expression, and organisms specific cell-to-cell signaling.² Controlling the activity of efflux pumps is another viable method to improve the efficacy of antibiotics on these organisms. Since Gram-negative bacteria rely heavily on efflux pumps to prevent the intrusion of antibiotics, this

is a sensible target when using combination drug therapy. Though useful in improving activity against multi-drug resistant (MDR) bacteria, these agents are limited and few have been approved for clinical use.

1.2.3 Mechanisms of Antibiotic Action and Resistance

Antibiotics are often grouped by their antibacterial action and spectrum of activity against a range of microorganisms. Targeting different regions of the bacterial cell allow for a variety of antibiotics to be used alternatively to ineffective antibiotics. The inability for an antibiotic to detrimentally impact the survival of bacteria in which it once was effective is known as antibiotic resistance.¹ Sometimes an innate feature of a bacterial species, antibiotic resistance is often an adaptation in which the bacterium modifies its cellular structure to resist the treatment of a familiar class of antibiotics.

Antibiotic resistance can be categorized into two types, intrinsic or acquired. Intrinsic resistance is an inherited trait within a bacterial species that prevents the bacterium from being negatively affected by a class of antibiotics.¹ This particular type of resistance requires no alterations to the DNA of the microorganism. Usually, antibiotics are ineffective on this type of species because the microbe either lacks an antibiotic target or has a barrier in which the antibiotic is unable to permeate. A classic example is the intrinsic resistance of mycoplasmas to β -lactam antibiotics, since they lack the peptidoglycan cell wall that these drugs target.¹ The second example is the impermeable outer membrane present in *Enterobacteriaecae*.¹ Acquired resistance can also occur through genetic mutation.¹ This type of resistance happens when an organism that is slowly exposed to an antibiotic adapts so it can tolerate further exposure to a particular class of antibiotics. Bacteria with acquired resistance are also able to structurally modify and deactivate an antibiotic, alter a drug's accessibility to its target, or inhibit the drug's

uptake.¹ A summary regarding each class of antibiotic, mechanism of action, and mechanism of resistance is outlined in Table 1.2.

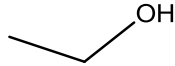
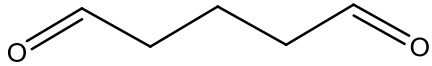
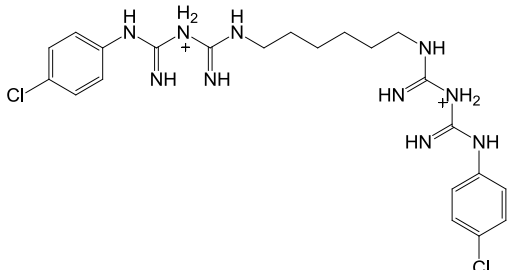
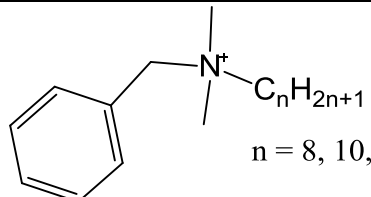
1.3 Introduction to Antiseptics and Disinfectants

Antiseptics and disinfectants have been indispensable in controlling infections in hospital settings and maintaining food safety and quality. Although the terms *antiseptic* and *disinfectant* are commonly used interchangeably, the two can be distinguished by their roles. By definition, antiseptics are defined as broad-spectrum antimicrobials that destroy or inhibit the growth of microorganisms on living tissues, while disinfectants inhibit bacterial existence on inanimate objects or surfaces.¹ Both agents have an essential role in controlling microbial growth as either an agent in sterilization or preservation.¹ Sterilization uses the chemical nature of an antimicrobial agent to remove the presence of microorganisms from a surface.¹ For instance, physicians sterilize their hands using surgical scrubs prior to surgery to eliminate the presence of any bacteria that could be transmitted or cause an infection. On the other hand, preservation uses the chemical nature of an antimicrobial to inhibit the growth of bacteria in a consumer product such as in food packaging or cosmetic applique.⁹ Whichever the type of antimicrobial agent or application, its mechanism of action can be summarized by four key functions: 1) its electrostatic attraction to the bacterium cell, 2) interaction of the agent with the cellular surface, 3) permeation of the cell structure, and 4) action at the target site⁹. In spite of the vast number and types of biocides available and their more detailed independent mechanisms of action, only quaternary ammonium and bisbiguanidinium compounds and their interactions with different types of bacteria will be discussed in further detail, as these are the biocides used in the research presented in this dissertation. However, Table 1.3 categorically lists other examples of anti-

Table 1.2. Summary of antibiotic classes, activities, and current mechanisms of action, and resistances.

Antibiotic Class	Mechanism of Action	Mechanism of Resistance
β-lactam	Binds to penicillin binding proteins (PBPs), inhibiting peptidoglycan cross-linking in the cell wall.	β -lactamase enzymes hydrolyze the β -lactam ring making it unable to inhibit peptidoglycan crosslinking
Glycopeptides	Binds to acyl-D-alanyl-D-alanine in the peptidoglycan cell wall	Enzymes use D-alanyl-D-lactate to construct peptidoglycan cell wall instead of acyl-D-alanyl-D-alanine
Aminoglycosides & Chloramphenicol	Binds to the 30S and/or 50S ribosomal subunit	Protein structure modification in the ribosome inhibits binding; Changes in cell membrane that causes a reduction in antibiotic active transport ; Antibiotic is enzymatically hydrolyzed causing structural modification
Tetracyclines	Inhibits protein synthesis by binding to 30S subunit in the ribosomal interfering with binding of aminoacyl tRNA.	Bacteria efflux pumps prevent drug from entering; “Protection” proteins prevent binding to the ribosome target; Antibiotic is enzymatically hydrolyzed causing structural modification
Macrolides	Promotes dissociation of tRNA from the ribosome inhibiting ribosome assembly and preventing protein elongation by inhibiting peptide bond formation	Bacteria efflux pumps prevent drug from entering; Site mutation of the ribosome allosterically prevents antibiotic binding
Sulfonamides	Interfere with nucleic acid synthesis by inhibiting folate synthesis	Overproduction in dihydrofolate reductase or alterations in dihydropteroate synthetase enzymes prevent antibiotic interference
Quinolones	Target DNA gyrase and topoisomerase IV	Decreased expression of membrane porins; Bacteria efflux pumps prevent drug from entering; Mutations in protein targets that reduce antibiotic binding affinity

Table 1.3. Chemical structures and use of select antiseptics and disinfectants against non-sporulating bacteria (Adapted from G. McDonnell and A. D. Russell (1999), with permission from the American Society for Microbiology).

Chemical Class	Example	Structure	Biocidal Class	Mechanism of Action
Alcohols	Ethanol		Sterilization Disinfection Preservation	Results in bacterial cell lysis via membrane damage, protein denaturation, and interference with metabolism
Aldehydes	Glutaraldehyde		Sterilization Disinfection Preservation	Binds strongly to unprotonated amines on cell surfaces inhibiting transport and enzymatic systems
Biguanides	Chlorhexidine		Antisepsis Antiplateque Deodorant Preservation	Results in cell lysis by acting on membrane, precipitating proteins, and leaking intracellular materials
Halogen-releasing Agents	Iodine	I_2	Disinfection Antisepsis Cleaning	Targets free-sulfur amino acids cysteine and methionine, nucleotides, and fatty acids
Heavy Metal	Silver	+ Ag	Disinfection Preservation Antisepsis	Inactivates enzymes and protein function
Peroxygens	Hydrogen Peroxide	H_2O_2	Disinfection Preservation	Produces active hydroxyl free radicals that attack lipids, proteins, and DNA
Quaternary Ammonium Compounds	Benzalkonium chloride	 $n = 8, 10, 12, 14, 16, \text{ and } 18$	Disinfection Antisepsis Preservation Cleaning	Distorts membrane integrity and results in intracellular material leakage

-septics and disinfectants by its application and chemical class to illustrate the similarities and differences between the types.

1.3.1 Quaternary Ammonium Compounds

Quaternary ammonium compounds (QAC)s represent a small fraction of surface-active agents that possess antibacterial properties widely used in disinfection. Other surface active agents with antimicrobial activities may lack a charge (*i.e.* nonionic) or have multiple charges (*i.e.* cationic, anionic, zwitterionic, or amphoteric). Most positively charged molecules with antimicrobial activity are QACs, although there are some molecules with negative charges. Structurally, these molecules consist of a charged “water-loving” head group and an aliphatic “water-fearing” tail group (Figure 1.8). This imbalance between its hydrophilic and hydrophobic regions helps its surface-active properties to be conducive in its antimicrobial activity.¹⁰

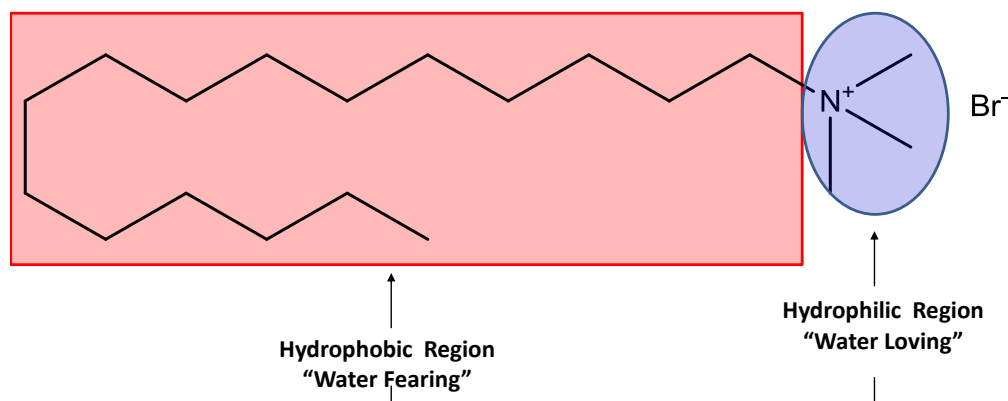


Figure 1.8. Structure of cetyltrimethylammonium bromide as a representative cationic quaternary ammonium compound.

The primary mechanism of action for QACs lies primarily in its membrane activity. Figure 1.9 illustrates the events that have been postulated to lead to bacteria cell death after exposure to a QAC: a) the QAC is adsorbed on to the cellular surface; b) the QAC penetrates the cellular wall in Gram-positive bacteria or the outer membrane in Gram-negative bacteria; c) the

inner membrane is imbalanced by the QAC perturbing the organization of the lipid bilayer; d) cellular structure begins to collapse allowing intracellular materials to leak; e) proteins and nucleic acids are degraded; and f) the cell wall is destroyed by autolytic enzymes.^{11, 12}

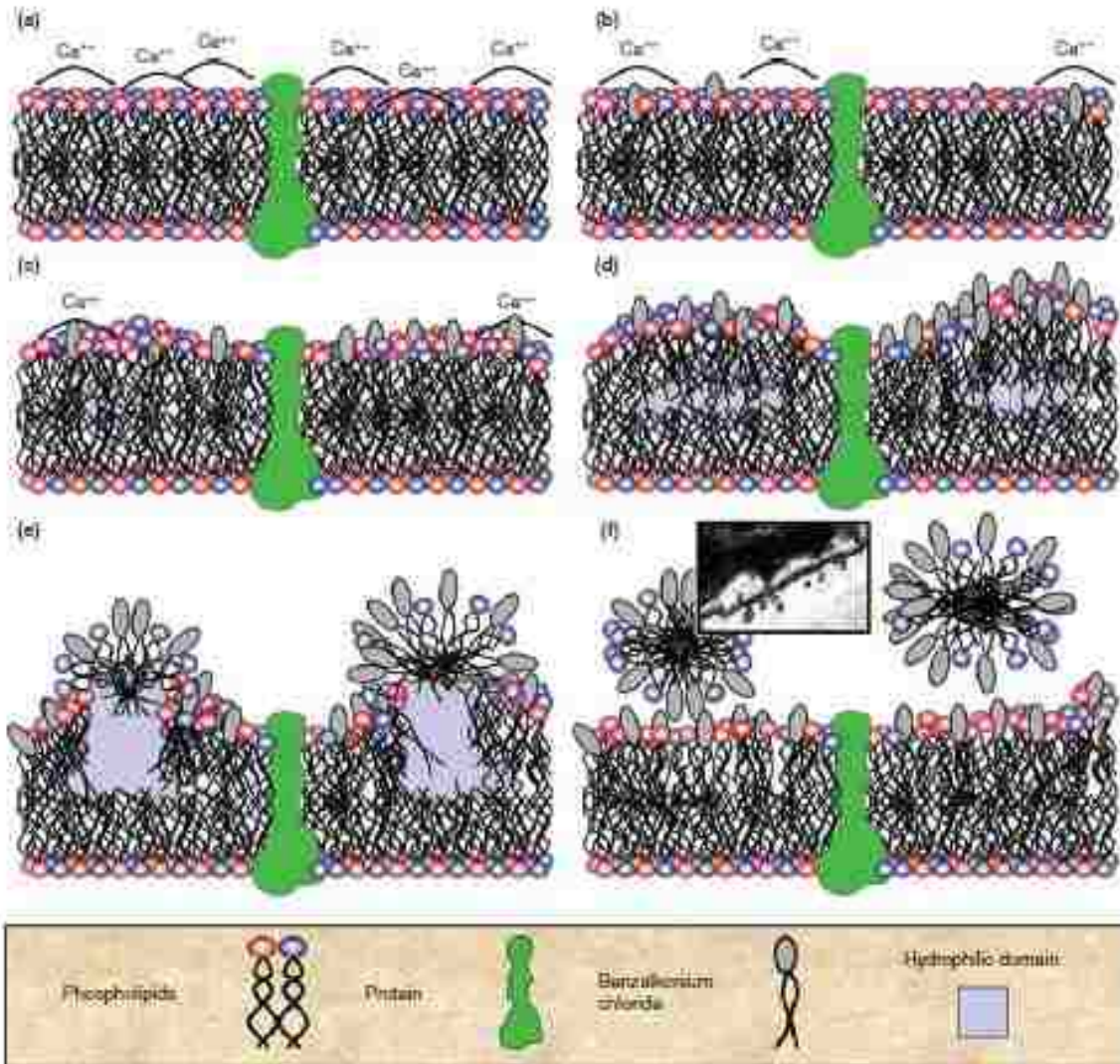
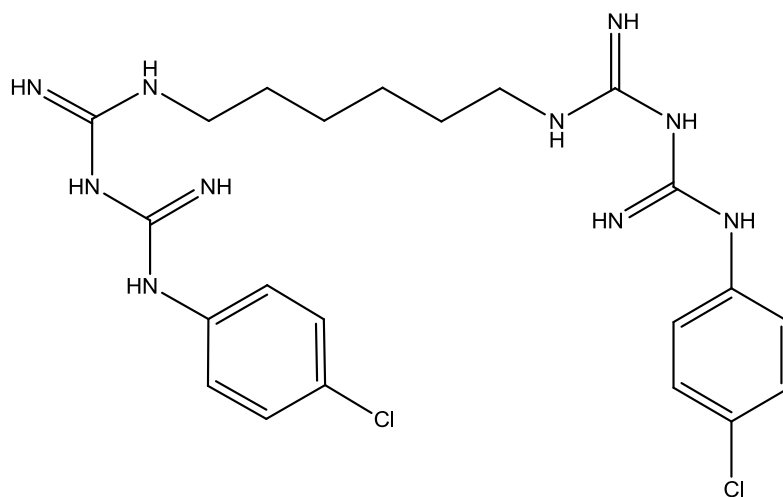


Figure 1.9. Hypothesized mechanism of action for quaternary ammonium biocides where a-f show progressive adsorption of the quaternary headgroup to acidic phospholipids in the membrane with increasing QAC exposure/concentration. A decreased fluidity of the bilayers and the creation of hydrophilic voids are formed in the membrane causing protein activity to be disrupted, cell lysis, and solubilization of membrane components into micelles (Adapted from P. Gilbert and L.E. Moore (2005), with permission from John Wiley and Sons).

In summary, examination of the literature suggests that QACs cause structural deformities and damage the cytoplasmic membrane within bacterial cells.^{12, 13}

1.3.2 Chlorhexidine and Bisbiguanidines

Molecules containing a bisbiguanide structure, e.g. polyhexamethylene biguanides (PHMB), are heavily used in antiseptic oral products and surgical scrubs. Originally synthesized in the early 20th century, these molecules have shown exceptional pharmacological activities. An example of a PHMB molecule with profound antimicrobial activity is the dicationic salt chlorhexidine (1,1'-hexamethylenebis(5-chlorophenyl)biguanide). This molecule is symmetrically balanced by two chlorophenyl moieties appended to a charged guanidine group linked together by a hexylmethylene-chain (Figure 1.10). Chlorhexidine is strongly basic and is stabilized when made into a salt.¹⁴ This structural modification effects the physical properties of chlorhexidine in that its relative hydrophobicity, solubility, and bioavailability is changed when dihydrochloride, diacetate, or digluconate are introduced to the chlorhexidine base.¹⁴ Regardless of the type of chlorhexidine formulated, the antibacterial activities remain unchanged.¹⁴ Collectively, bisbiguanide molecules have broad-spectrum activity as a membrane active agent against both sporulating and non-sporulating bacteria, mycobacteria, yeasts, protozoa, and lipid-enveloped viruses.⁹ Chlorhexidine antimicrobial activity is concentration dependent. At low concentrations, chlorhexidine predominantly affects membrane integrity; whereas at high concentrations it is capable of precipitating cytoplasmic materials.⁹ There are a few external factors that can diminish chlorhexidine antibacterial activity. Mainly, the presence of anionic substances (*i.e.* pus, lecithin, sodium dodecyl sulfate, and sodium carboxymethylcellulose), variable pH, or the high abundance of protein or sera has been reported to interfere with chlorhexidine antibacterial activity *in vivo*.^{9, 13, 14} On the other hand, chlorhexidine has shown compatibility with various anionic antibiotics like sulfonamides, β -lactams, tetracyclines, and chloramphenicol in which its antimicrobial efficacy is not suppressed.^{15, 16}



Chlorhexidine (base)

Figure 1.10. Structure of chlorhexidine base.

The potent antimicrobial activity of chlorhexidine salts made these molecules of particular interest in the medical field. Thus, a variety of consumer products were developed specifically for topical applications. Its potent activity against hemolytic streptococci made chlorhexidine optimal for treating wound infections and preventing sepsis.^{9, 13, 14} However, further evaluation of bisbiguanides was required to qualify its use to treat systemic infections or to use as an antiseptic. It was also shown that handwashing with chlorhexidine was able to reduce skin flora as much as 90%.⁹ Its post-antimicrobial activity (*i.e.* approximately 6 hours) on skin is another attractive feature for the prevention of skin sepsis and drug-resistant *S. aureus* or *Enterococci* outbreaks.¹⁷⁻¹⁹ Additionally, chlorhexidine provided in the nasal cavity in combination with mupirocin helped reduce the incidence of methicillin-resistant *S. aureus* among patients in intensive-care.²⁰ This bisbiguanide has also been effective in reducing catheter colonization and oropharynx infections.²¹

For decades, chlorhexidine has been widely approved as a skin and mucous membrane antiseptic. Its use intravenously was prohibited after *in vivo* testing in mice, calves, and rabbits revealed an 81-fold reduction in therapeutic index.²² As a result, chlorhexidine salts were

restricted to topical and oral applications where acute toxicity was less. Research suggests its nontoxicity in topical or oral applications to result from its poor absorption.²³ Although trace percutaneous absorption occurs, it was also noted that chlorhexidine was safe to use in obstetrics, ocular infections, and wound care since it did not induce birth defects, skin sensitivity (<2% w/v), or eye irritation (<0.2% w/v).¹⁴ It is not recommended for use in pre-operative sterility involving the central nervous system since it has occasionally shown ability to degenerate nerves.¹⁴ However, insufficient clinical data does not conclusively prohibit its use as a skin preparative before lumbar puncture, epidural catheter placement, or neurosurgical procedures. Since, chlorhexidine has been provided commercially at concentrations ranging between 0.5% - 4%, with and without co-solvents.

Chlorhexidine has been applied in both clinical and domestic settings for more than 50 years. Since that time few reports have indicated the development of resistance or significant loss in antimicrobial activity. Although a five-fold difference in antimicrobial activity was noted by Kropinski *et al.*, this difference was attributed to structural changes in the bacterial cell.²⁴ Of its broad spectrum antibacterial activity, chlorhexidine is particularly ineffective against some nonfermenting Gram-negative bacteria such as *Pseudomonas* species; however, if used with a chelating agent it has been shown to be effective against this bacterium.¹⁷ Few assumptions imply that current plasmid-mediated resistance, currently observed against QACs, will negatively alter chlorhexidine efficacy.

1.3.3 Structural Differences between QACs and Chlorhexidine and Their Antibacterial Mechanism of Activity

The differences between QAC and chlorhexidine structures directly explain their dissimilarity in antimicrobial activity. Typically, long alkyl chains between 12- 16 carbons are required for QACs to inflict damage on bacterial cells.^{9, 10, 13, 25} Still great difficulty arises in

achieving optimal chain lengths required to permeate the cell without becoming solubilized by the hydrophobic core of the bacteria.¹³ Since QACs interact fully with the membrane, they are susceptible to efflux pump resistance mechanisms.^{9, 13} This is not the case with chlorhexidine since the inflexible six-carbon chain length is fixed and does not result in the bacteria dissolving or inactivating it.¹³ This is because bisbiguanides interact solely with the surface of the lipid bilayer through cation displacement and head-group bridging via oblique insertion unlike QACs which interdigitates into the bilayer. Figure 1.11 describes chlorhexidine's mechanism of action.

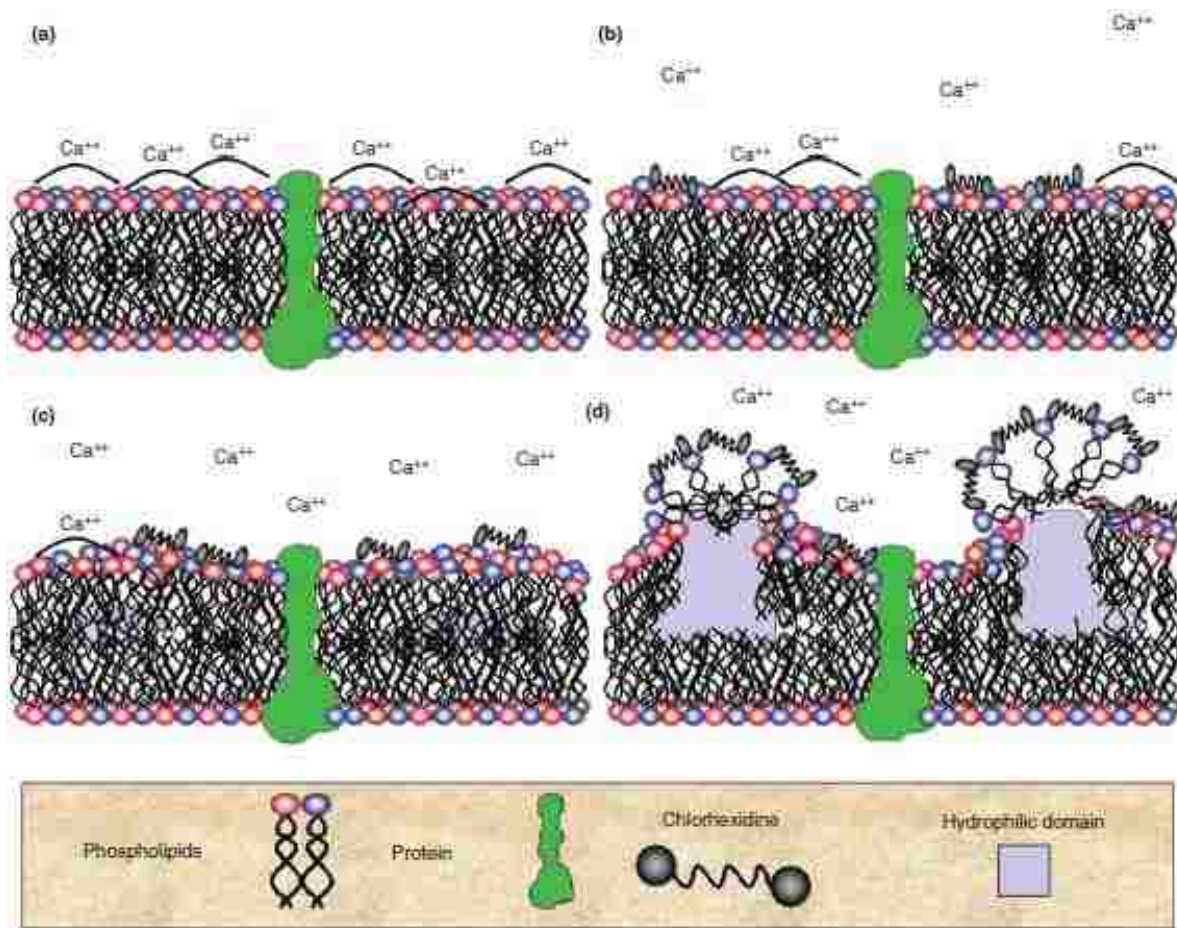


Figure 1.11. Hypothesized mechanism of action for the interaction of chlorhexidine with the bacterial cytoplasmic membrane. Diagram shows progressive decreases in fluidity of the outer leaflet with increasing exposure to the bisbiguanide (Adapted from P. Gilbert and L.E. Moore (2005), with permission from John Wiley and Sons).

The charged guanidinium groups present in chlorhexidine facilitates cell membrane adsorption which places it optimally at the cell surface so that chlorhexidine can bridge between bilayer phospholipids and displace its associated divalent cations.¹³ This results from the similar length of the hexamethylene linker to the distance between phospholipid head groups that aids in chlorhexidine binding, oblique insertion into lipid bilayer or cell wall, and antimicrobial activity.^{26, 27} Research indicates that increasing or decreasing the hexamethylene linker length detrimentally interferes with its binding ability and membrane disruption.^{13, 28} Chlorhexidine is able to overcome osmosregulation provided by multi-drug efflux pumps, detrimentally affecting many functions related to cell viability like inhibiting respiration, solubilizing membranes, or destroying metabolic function.^{13, 28} For the said reasons, there are more reports indicating resistance to QACs than to chlorhexidine salts.

1.4 Combination Antibacterial Drug Therapy (CAT)

Since antibiotic-resistant bacteria have dominated the arsenal of antimicrobial drugs currently available, there is a growing need to optimize the use of old and new antibiotics to treat infections. Combination antibiotic therapy (CAT) has been a promising strategy to combat bacterial resistance. Combination antibiotic therapy is a polytherapeutic approach that requires the use of more than one antibiotic to remove an infection, mainly resistant infections.²⁹ This approach relies on four principal modes of action for improved antibacterial activity to be observed using two or more compounds. Pokrovskaya and Baasov summarized the role of the second drug in the four methods as follows: i) its use to prevent the degradation or modification of the primary drug, ii) inhibits the efflux pumps so that Drug A can be retained until concentrations capable of bacteriolysis are accumulated, iii) impairs the tolerance mechanism of the microorganism, and iv) targets the pathway that drug A inhibited so that it could deactivate

the bacterium.³⁰ For CAT to be successful, the two drugs' mechanisms must differ and not interfere with each other and the target bacteria must be phenotypically susceptible to treatment.³¹ The overall goal of CAT is to achieve synergy, or a drug combination that results in better antibacterial activity than either antibiotic when used individually. Desirable synergistic combinations allow for lower concentrations of drugs within combination to be implemented and toxic dose-related responses to be reduced.³² Although a useful approach in treating MDR *Mycobacterium tuberculosis*, HIV, Alzheimer's disease, and a variety of different cancers among other chronic and infectious disease, only CAT applied to bacterial infections will be henceforth described.³³⁻³⁷

Preliminary successful antimicrobial combinations arose from the use of β -lactam drugs with beta-lactamase inhibitors or aminoglycoside antibiotics. Examples of current CAT containing β -lactam drugs with beta-lactamase inhibitors are Co-Amoxiclav (Amoxicillin + Clavulanate), Timentin (Ticarcillin + Clavulanate), Unasyn (Ampicillin + Sulbactam), and Zosyn (Piperacillin + Tazobactam).^{29, 31, 38} However, some antibiotic combinations do not result in improvement or affect the organisms' vitality (additivity) while other combinations interfere with the antibacterial activity of each antibiotic (antagonism). This has led to a number of combination drug therapies that have become the staple in treating resistant infections, while several pharmaceutical companies seek to discover improved dual-mode-of-action compounds. Therefore, the use of multiple drugs in tandem is gaining momentum as a systematic approach to treat infectious disease.

Many studies have evaluated the effects of combining multiple antibiotics *in vitro*; however, clinical studies often contradict superior *in vitro* antibacterial combinations. Since the late 1950s, creative CAT has expanded the types of antimicrobials used to treat arduous

infections but the optimization for CAT for a variety of bacterial infections has been a struggle. A direct result of the antibiotic susceptibility of bacteria and its unique dependence upon bacterial species, host tolerance, and dosing regimen often makes CAT a hit-or-miss approach.³¹ Therefore, correlating *in vitro* laboratory results with *in vivo* clinical treatments for bacterial infections has so far been challenging. Since some successful combinations have arisen in the past, scientists are still motivated to find better combined drug systems. Thus, the pursuit has been mainly focused on particular types of bacterial infections.

In recent years, experimental CAT has focused on Gram-negative bacterial infections since β -lactam/penicillinase inhibitor combinations have been very successful against resistant Gram-positive bacteria. Some CAT treatments included experiments using Gram-negative bacteria without complex resistant mechanisms. For example, synergetic antibacterial activity was observed in the treatment of pathogenic *E. coli* using combinations that consisted of aminocoumarin, novobiocin, and tetracycline; however antagonism was seen with novobiocin combinations with chloramphenicol, erythromycin, and lincomycin.³⁹ Successful antibiotic combinations were often subsequently investigated against difficult Gram-negative bacteria such as *Pseudomonas* species. Thus, the successful CAT consisting of novobiocin and tetracycline also show superior efficacy against six *Pseudomonas* species.⁴⁰ Other combinations containing β -lactam antibiotics with aminoglycosides have also been evaluated as a CAT treatment option for Gram-negative infections. Dalton *et al.* reported the mean susceptibility of thirty *Pseudomonas* isolates to *in vitro* carbenicillin and gentamicin combinations.⁴¹ However, clinical evaluation of 66 patients receiving gentamicin alone or in combination with penicillin, ampicillin, chloramphenicol, or streptomycin showed contradictory *in vitro* antibacterial activity.⁴² Only dual aminoglycoside + aminoglycoside CAT (*e.g.* kanamycin + gentamicin) were

synergetic in the treatment for the different *Pseudomonal* infections.⁴² Aminoglycoside antibiotics have also been effective in combination with select tetracyclines.⁴³ For instance, the ability of oxytetracycline to suppress the production of acid in combination with neomycin was synergetic against six enteropathogenic Gram-negative bacteria.⁴⁴ Although β -lactam + aminoglycoside CAT are effective against a broad panel of Gram-negative bacteria, they sometimes cause kidney failure or worsen the current condition of a patient.⁴⁵ For example, β -lactam + aminoglycosides CAT in febrile neutropenic patients is reported to be effective yet dangerous to the survival of these patients. DeJace *et al.* found that response rates of dual β -lactam + β -lactam CAT is similar to β -lactam + aminoglycosides CAT against most *Enterobacteriaceae*, excluding *Pseudomonas* species.³⁸ These results were contradicted *in vivo* after evaluating 7,600 patients and comparing the response observed for β -lactam monotherapy and β -lactam + aminoglycoside CAT diagnosed with *Pseudomonas aeruginosa* infections³⁸. Silbiger *et al.* concluded that the use of β -lactam + aminoglycoside CAT resulted in unchanged fatality rates and increased the incidence of nephrotoxicity.⁴⁶ More than 148 cases suggest that there is no clinical benefit for the use of β -lactam + aminoglycoside CAT for treating febrile neutropenia, pneumonia, abdominal/urinary tract infections, sepsis/bacteremia, endocarditis, or bronchitis.⁴⁵ As an alternative, hospitalized febrile neutropenic patients with *Pseudomonal* infections that were currently not receiving fluoroquinolone therapy was able to be administered β -lactam + ciprofloxacin CAT with a lower incidence of kidney failure.⁴⁷

Resistant Gram-negative rods harboring extended spectrum β -lactamases (ESBL), *Klebsiella pneumoniae* carbapenemases (KPC), and the New Delhi metallo- β -lactamases (NDM-1, NDM-2) have been the most recent targets for CAT. Still in its infancy, successful CAT against bacteria containing multiple-resistant mechanisms has only been performed *in vitro*. For

example, the use of polymyxins combined with fluoroquinolones or glycylicyclines have resulted in additive and synergetic interaction indices when used to treat NDM-1 producing *Enterobacteriaceae*.⁴⁸ Similarly, combined tigecycline and high-dose meropenem concentrations and colistin + meropenem CAT were effective against KPC isolates.^{49, 50} Combination studies with tigecycline + imipenem, tigecycline + amikacin, and tigecycline + ciprofloxacin yielded synergy against MDR *Klebsiella* species and *E. coli*.⁵¹ Ultimately, combinations under investigation include mixtures of all antibiotic classes to improve the efficacy of current antimicrobials against drug-resistant bacteria.^{52, 53} Mixtures of antibiotics with nonantibiotics have shown to be a useful approach to also extend therapy against MDR bacteria.⁵⁴

Since 1975, natural plant products have yielded synergetic responses with a variety of antibiotic classes against both Gram-positive and Gram-negative bacteria. Most of the research supports this CAT approach as an effective treatment against Methicillin-resistant *S. aureus* and Vancomycin-Resistant *Enterococcus* species. A review by Hemaiswarya *et al.* lists the following examples of effective natural products used with β -lactam drugs: carnosol epigallocatechin gallate (EGCg), tea catechin, green tea extract, Corilagin, Baicalin, Tellimagrandin I, Rugosin B, pomegranate extract, myricetin, sophoraflavanone, and novoimanin.⁵⁵ The use of green tea extract with levofloxacin, myricetin with β -lactam/ β -lactamase inhibitors, and butylatedhydroxyanisole with vancomycin was successful against *E. coli* O157:H7, ESBL-*K. pneumoniae*, and non-susceptible *E. coli*, respectively.⁵⁵ Although the most latest approach, Ejim *et al.* investigated the utility of 1,057 FDA approved nonantibiotic materials in potentiating the antibacterial activity of tetracycline drugs against opportunistic pathogens *P. aeruginosa* (PA01), *E. coli* (BW25113), and *S. aureus* (ATCC 29213). The most notable finding was the observed synergy in the use of nonantibiotic loperamide (trade name: Imodium) with antibiotic

minocycline both *in vitro* and *in vivo*.⁵⁴ These findings suggest the use of nonantibiotic + antibiotic CAT as potential treatments for MDR bacterial infections with minimal adverse effects on normal bacterial flora or host health.

Examination of recent literature clearly supports the use of CAT to treat difficult infections. Although this polytherapy can allow a patient the convenience of fewer dose regimens with potent antimicrobial activity and broadened activity spectrum, several problems associated with polytherapy still exist. Sometimes the selections of particular antibiotic mixtures are clinically contraindicated because either drug elicits unwanted side effects.^{32, 38, 39, 42} Aside from higher costs and uncontrollable drug responses with narrow therapeutic windows, each aforementioned CAT formulation is limited to the serendipitous chance that each drug will arrive and deactivate a bacterial cell at the same time without causing adverse or idiosyncratic reactions to the host or generating MDR organisms.⁵⁶

1.4.1 Hybrid Antibiotics

The development of hybrid antibiotics is a recent approach to CAT. More specifically, it consists of two covalently linked antibiotics, as opposed to consisting of two unreactive salts in a mixture, that inhibit dissimilar targets in a bacterial cell. This alternative to CAT was hypothesized to control the pharmacokinetic properties of antibiotics within combinations and prevent adverse host responses. However, hybrid antibiotics are not effective in treating bacterial infections caused by MDR strains. For that reason, most hybrid antibiotics consist of the drug classes that have the least antibiotic resistance mechanisms developed against them. In addition to the controlled pharmacokinetic properties, other advantages include improvements in antibacterial activity (potentiation), enhanced receptor binding affinity, increased spectrum of microorganisms' susceptibility against mono-resistant strains, and reduced host toxicity.

Hybrid antibiotics are a blend between conventional CAT and prodrug antibiotics. Their differences are illustrated in Figure 1.12. More specifically, this antibiotic combination consists of a linker between the antibiotic pair. This important feature is an adaptation from prodrug systems and is used to facilitate delivery of the two agents in tandem. Although not the main focus of the research presented in this dissertation, the mechanism behind prodrug activity is highlighted as it pertains to hybrid antibiotics. Most hybrid antibiotics are tethered together using a covalent bond. However, several sub-types of covalent links can be used to deliver the antimicrobial agents to the bacterial cell target. Covalent-bound hybrid antibiotics require the use of a labile covalent bond between the two antibiotic components so it can undergo chemical hydrolysis, enzymatic cleavage, or are environmentally responsive so that tethered-antibiotics can be released to the bacterial cell target synchronously. Similar to CAT, synergetic, antagonistic, and additive effects can be observed in hybrid antibiotic systems; this concept will be discussed in the next section titled “Loewe’s Additivity Model”. Therefore, the antibiotic components must be judiciously chosen to yield the greatest antimicrobial activity. Similarly, the most appropriate length and type of linker must be identified that will facilitate the best bactericidal behavior.

Most hybrid antibiotics reviewed to date consists of either fluoroquinolone or aminoglycoside antibiotics. An example lies in the potent fluoroquinolone-oxazolidinone hybrid known as MCB-3681 which contains a 4-hydroxy-piperidine linker. This patented antibiotic hybrid has shown antibacterial activity against *Bacillus anthracis* as well as other drug resistant Gram-positive and Gram-negative bacteria.⁵⁷ A phosphate ester derivative of the MCB-3681 prodrug has since progressed into human clinical trials.⁵⁸ Likewise, fluoroquinolone-anilinouracil hybrids have potent DNA polymerase and growth inhibitive properties. The best

representative of this antibiotic hybrid is the 251D fluoroquinolone-anilinouracil hybrid. This hybrid has shown enhanced antibacterial activities, as compared to its precursor antibiotics, when investigating its use on fluoroquinolone-resistant bacteria.⁵⁹ Yu and co-workers reported the development of aminoglycoside hybrids consisting of chloramphenicol or oxazolidinone to have broad-spectrum activity against Gram-positive and Gram-negative bacterial strains. These hybrids possess enhanced affinities to bind specifically to RNAs with lower dissociation constants than the neomycin B aminoglycoside antibiotic.^{57, 60-62} In spite of their improved binding affinities to RNA, their antimicrobial activities do not correlate well with their dissociation constants and have been reportedly lower than the neomycin B aminoglycoside when used alone.³⁰ Thus, this hybrid has not been investigated for use in human trials. In some instances the antibacterial activity of antibiotic hybrids are not greater than the precursor antibiotics. However, they have found use to treat resistant infections. Aminoglycoside-fluoroquinolone antibiotic hybrids were able to overcome some of the most prevalent aminoglycoside resistance enzymes while still effectively inhibiting bacterial protein synthesis, DNA gyrase, and topoisomerase IV activities.⁶³ In summary, most hybrid systems reported to date have been more effective in targeting active sites than the stoichiometric mixture of the antibiotic precursor components despite fickle *in vitro* antibacterial activities. As a result, it is a common hypothesis that there is a lower propensity to develop bacterial resistance to hybrid antibiotics. However, this type of antibiotic therapy is not the main focus of this dissertation and will not be described in great detail. Accordingly, an extensive review of the hybrid antibiotic systems can be found by Pokrovskaya and Baasov.³⁰

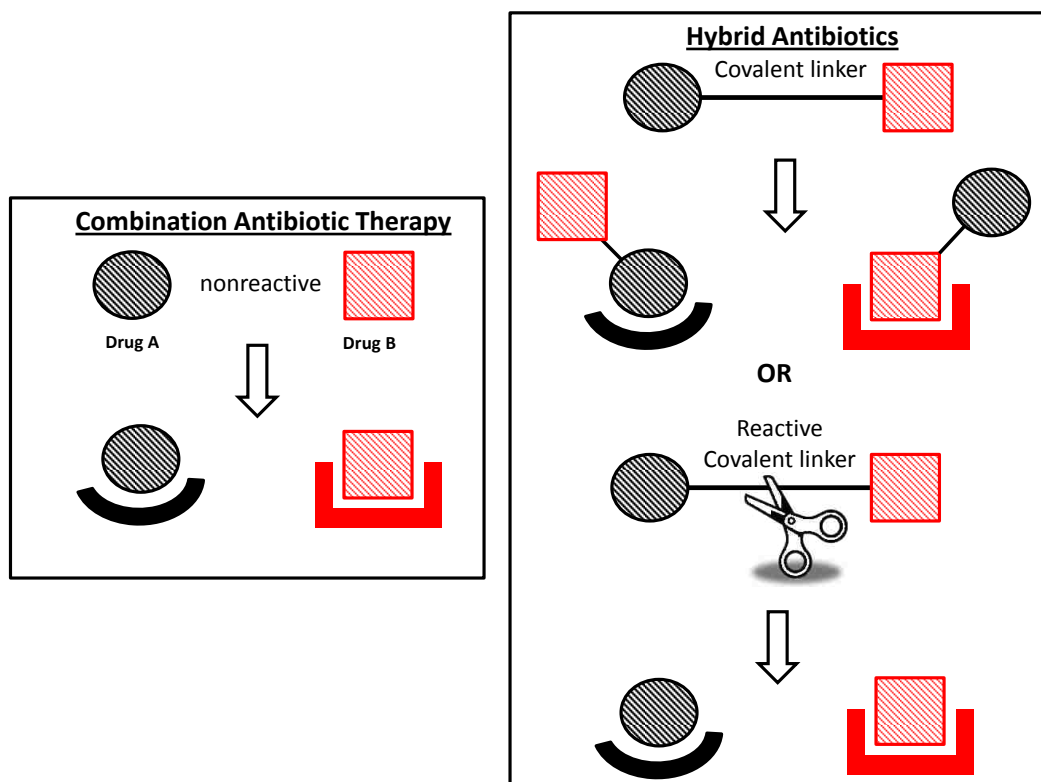


Figure 1.12. Schematic representing the differences between conventional combination antibiotic therapy and hybrid antibiotic therapy.

1.4.2 Loewe's Additivity Model

Studies at the forefront of pre-clinical drug development have continued to be a recent topic of frequent and growing interest among pharmacologists. For instance, the ability to quantify various interactions of drugs on the physiology of the body accurately is of utmost importance in the study of combination drug therapy. In conventional combination studies, interest centers on whether the drug combination creates an enhanced, worsened, or nullified effect as compared to that expected from the activities of the individual components.

Strategic and empirical models are necessary to premise the rationale of combination drug therapy and several have since been developed to calculate the “interaction index” between the components in a mixture. As a result, many statistical techniques have surfaced to assess

drug interactions when two or more compounds are mixed, namely Bliss Independence (1939),⁶⁴⁻⁶⁷ the Additivity Envelope (1979),⁶⁸ and Loewe's Additivity models (1926).^{31, 32, 38, 69-73} To be more specific, the Bliss independence model suggests that the interaction between two drugs is equal to the multiplication product of the activities of the agents when used individually. Accordingly, this implies that two drugs do not pharmacologically or physiologically interact with each other for the enhanced effect to be observed. The augmented therapeutic effect is often caused by independent modes and/or differing sites of activity for each compound in a mixture. Linear drug concentration-effect relationships are only supported by Bliss Independence model and not for nonlinear drug concentration-effect relationship such as the commonly observed sigmoidal curve seen in Loewe's Additivity model.⁷⁰ Hence, this model has limited applicability. Secondly, the additivity envelope model is used only to describe the log-linear cell survival relationship observed in radiation studies and cannot be applied to cytotoxic agents.⁷⁴ Therefore, the appropriate mathematical model used throughout this dissertation research is Loewe's Additivity Model which considers the commonly observed sigmoidal shape of the concentration-effect relationship for combination cytotoxic agents.⁷⁰

Loewe's Additivity Model is often illustrated graphically along a 3-dimensional surface with two horizontal lines that indicate the concentrations of the two drugs in combination and a vertical line that indicates the response respective to the fixed concentration of combined drugs.^{69, 70} This 3-dimensional iso-effect curve that represents the set of all drug combinations and their respective drug-like response is called an isobologram.⁷¹ Isobolograms were introduced by Fraser (c.a. 1870) as an area relationship between survival and drug combinations of toxic drug (atropine) and antidote (physostigmine) mixtures to illustrate interaction antagonisms.⁷⁴ Subsequently, Loewe used a similar relationship to define the synergetic reactions between two

drugs in a mixture and has since been refined by various investigators.⁷¹ Loewe used a straight line isobole to denote a zero (additive) interaction when the combined drugs caused in a similar dose-response relationship to the individual drugs as indicated in Figure 1.13. He also emphasized that the isobole would be curved concave upward or downward when the drug mixtures had dissimilar dose-response relationships from the parent drugs and this would denote either synergy or antagonism, respectively.

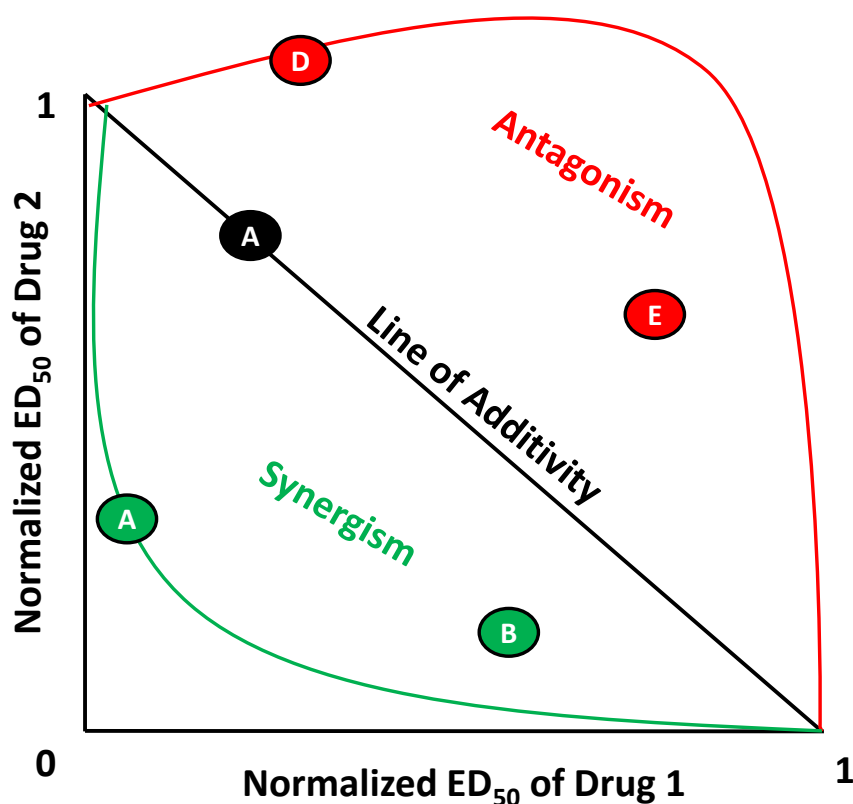


Figure 1.13. Representative concentration-response isobologram attributed to the activity of two drugs in combination, where (a) is the line of additivity, (b & c) indicate synergetic combinations and (d & e) indicate antagonistic mixtures.

Based on this model, the interaction index (I) between components in a mixture can be described numerically as either (1) synergetic, when their combined effects are greater than the

sum of their individual effects ($I < 1$), (2) additive or neutral, when the combined effect is equal to their individual activities ($1 \leq I \leq 3$), or (3) antagonistic, when the effect is smaller than one of the drugs itself or the presence of one drug nullifies the activity of the other ($I < 3$).⁷⁵⁻⁷⁷

The general equation (Eq. 1.1) of the Loewe additivity is defined as,

$$I = \frac{d_1}{D_1} + \frac{d_2}{D_2} \quad (\text{Eq. 1.1})$$

where d_1 and d_2 are doses of each drug in the mixture that yield an equal effect to drug 1 (D_1) and drug 2 (D_2) when used alone. This relationship was modified in this research to accommodate the interaction index of the novel API-ILs and GUMBOS as (Eq. 1.2.):

$$I_{\text{GUMBOS/API-ILs}} = \frac{[\% \text{ Cation} \times \text{IL}]_{100\%}}{[\text{Cation}]_{100\%}} + \frac{[\% \text{ Anion} \times \text{IL}]_{100\%}}{[\text{Anion}]_{100\%}} \quad (\text{Eq. 1.2})$$

Here, the concentration of drug 1 and 2 in the GUMBOS are calculated using the percent abundance of cation or anion responsible for the antibacterial activity within either GUMBOS or API-ILs and is multiplied by its minimum inhibitory concentrations (MIC) prior to dividing by the MIC of the precursor antibacterial agent when used alone. Interaction indices gauge how well the components in the GUMBOS interact as it compares to the stoichiometric mixture of the GUMBOS parent materials so the utility of these materials as potential pharmaceuticals can be compared to established combination antibiotic therapies. The standard checkerboard titration of multiple drugs tested against bacteria in tandem will be explained further in the Antibacterial Techniques and Characterization section.

1.5 Ionic Liquids

Ionic liquids (ILs) are a class of tunable ionic compounds that melt below 100 °C. These salts can be divided into two types (*i.e.* room-temperature ILs with $M_p < 25^\circ\text{C}$ and frozen IL

with Mp between 25 – 100°C) despite their similar chemical and physical properties.⁷⁸ These salts typically contain organic ions with differing sizes that allow changes in the usual physical properties observed in high-melting inorganic salts into the rare physical properties unique to ILs. Structurally, ILs have asymmetrical, bulky cations and anions that do not allow an ordered packing lattice structure which inhibits efficient crystallization and requires lower energy to melt these materials.⁷⁸ Other physical properties unique to ILs are its nonvolatile, negligible vapor pressure, nonflammable, and recyclable nature. In general, ILs are much more conductive, viscous, and dense than conventional organic solvents. Its high solvating power comes from its ability to behave as both a hydrogen bond acceptor (anion) and donor (cation) with molecules bearing both donor and acceptor sites.⁷⁸ As a result, two classes of ILs have been categorized based on their aqueous miscibility. In summary, all of the physical features explain their attractive thermal and chemical stability, and wide electrochemical window that attribute to their “green” identity.⁷⁹ To date, three generations of ILs have been reported in which first generation ILs have been applied to systems that would benefit from their physical and chemical property sets. Examples of cations and anions commonly used in first-generation ILs are shown in Figure 1.14. The cations usually consist of substituted heterocyclic amines and quaternary phosphonium groups, such as various alkylated imidazoliums, pyridinium, pyrrolidinium, and phosphonium ions. Typically, halides are the anions used in first-generation ILs. Applications that benefit from the customizable chemical and physical properties of first-generation ILs are often found in non-biologically related industries that do not require air stable, nontoxic low-melting materials.

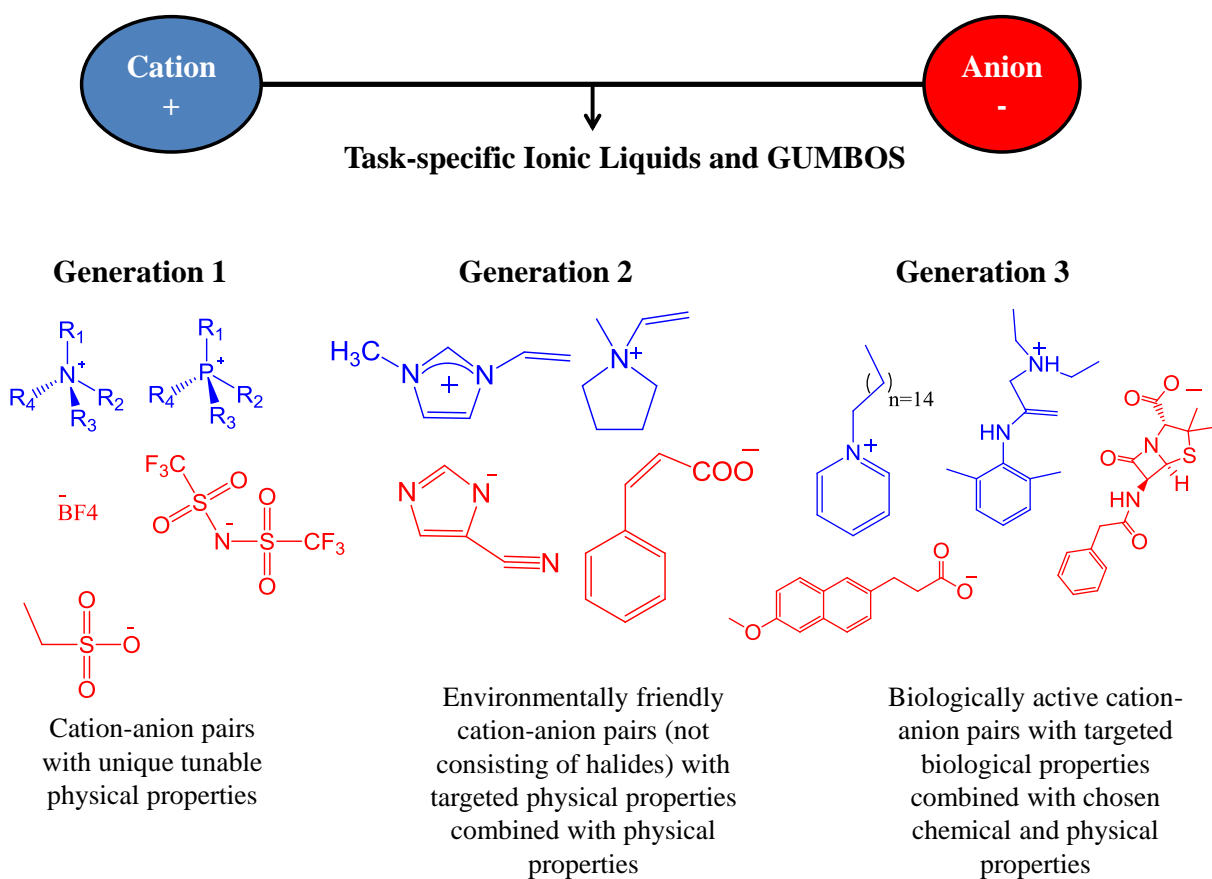


Figure 1.14. Representative cations and anions that compose first-, second-, and third generation ionic liquids (ILs) and groups of uniform materials based on organic salts (GUMBOS).

Since the most desirable feature of ILs is the ability to manipulate ion pairs to design task-specific molecules, researchers have begun investigating applied ILs by incorporating the applications into either ion. This has led to the development of second- and third generation ILs for applications that require more features than those related to its chemical and physical properties. In particular, second- and third-generation ILs take advantage of the limitless number of applied salts that melt below 100°C. Second-generation ILs, composed of halogen-free ions, were developed to provide environmentally-friendly and stable molten salts for use in energetic materials, synthesis, and chromatography. Most ILs consisting of tetrafluoroborate [BF₄], hexafluorophosphate [PF₆], bis (trifluoromethane)sulfonamide [NTf₂], and

bis(perfluoroethylsulfonyl)imide [BETI] are examples of second-generation ILs. Although a safer alternative and more stable, these salts still possessed the features of conventional ILs such as tunable solvent miscibility, ionic conductivity, selectivity, durability, resistance to thermal degradation, and negligible vapor pressure. Third-generation ILs are the most task-specific group of salts since they were especially synthesized to be application driven. For example, third-generation ILs consider all salts that in addition to having environmentally-friendly chemical and physical properties, they possess features that make them functional as primary active components in the desirable application. These salts have steadily emerged in to applications that once relied solely on organic or inorganic molecules. Although few in number, third-generation ILs have shown to have chirality, spectroscopy, antimicrobial, and medicinal uses. The diverse applications of ILs are numerous but can be limited by its defined thermal definition; thus, the emergence of a Group of Uniform Materials Based on Organic Salts (GUMBOS) redefines the useful limits of organic salts, thereby exponentially increasing the types of applied ions.

1.5.1 Groups of Uniform Materials Based on Organic Salts (GUMBOS)

The three generations of IL are not exclusive when the extended melting range provided by GUMBOS is considered. Previously, the definition of ILs was limited by the types of task-specific salts synthesized with melting points that exceeded 100°C. That is not the case with GUMBOS, which have melting points between 25°C and 250°C and still possesses the features of third-generation ILs. GUMBOS which are composed of organic and/or inorganic ions have a unique architectural platform in that multi-modal properties innate to the desired application can be incorporated into the salt via a judicious selection of the ions. To date, GUMBOS have exemplified the feasibility of architecturally modified amorphous nanomaterials (nanoGUMBOS) with multi-modal functionalities for application in energy conversion,

molecular sensing and extraction, biomolecular detection and imaging, and anticancer therapeutics.⁷⁸⁻⁸⁸ Although most of the GUMBOS research has been published on the nanoscale, the interesting properties observed in nanoGUMBOS remain expressed when used in the bulk form as well. This new field of multi-modal salts is being extensively investigated in the Warner Research Lab at Louisiana State University.

1.5.2 Antibacterial Ionic Liquids

Since ionic liquids (ILs) have offered promise as reagents that have the potential to replace many hazardous volatile organic solvents, interest in the use of ionic liquids in contamination control has reached a level sufficient to spur their commercialization as a green alternative to volatile sterilants. Many approaches have been used to achieve a nontoxic and biodegradable IL. More specifically, incorporating enzyme-hydrolyzing groups, short alkyl chain, and non-halide containing stable anions has been sought to maintain the “green” reputation of ILs in the ecosystem.⁸⁹⁻⁹² In 2007, Docherty et al. observed that alkyl chains between 6 and 10 carbons in pyridinium-based IL can be mineralized better than comparable imidazolium-based ILs.⁹³ Similarly, pyridinium-based ILs with pyridine or nicotinic acid side groups were exceptionally biodegradable under aerobic conditions implemented by Harjani *et al.*⁹⁴ However, it was reported that some ILs are poorly biodegradable and should not be considered “green” although it is suggested that these particular types of ILs may be useful in antimicrobial applications since an inherent toxicity to bacteria was evident.⁹⁵ Supported by the findings of Romero *et al.*, the IL bactericidal activity is said to have resulted from the inability of bacteria to use imidazolium salts as a carbon source. Quantitative-structure activity relationship (QSAR) findings show the alkyl length of the cationic substituents and type of halide anion detrimentally impact bacteria viability the most and govern the roles of IL in eco-toxicological

toxicity.^{90, 91} However, conflicting issues about their general safety and rates of biodegradation have been published.⁹⁶⁻⁹⁹ For instance, some IL cationic groups (*i.e.* imidazolium, pyridinium, and pyrrolidinium) were not lethal to Zebra fish, but ammonium-based ILs were more fatal than some organic solvents. Likewise, other IL eco-toxicological studies suggest significant toxicity to *Pseudokirchneriella supcapitata* (algae) and *Caenorhabditis elegans* (multi-cellular soil nematodes). Subsequent studies confirmed the “green”-prohibitive nature of these materials resulting in a shift in their application towards antiseptics and disinfectants.^{98, 99}

As previously mentioned, the potential to use ILs as antibacterial agents derived from concerns about their biodegradability and persistent environmental use. Over the last decade, most studies investigating the antimicrobial nature of ILs have been conducted on planktonic bacteria. In 2003, Pernak and Chwala introduced the broad spectrum antibacterial activity of five new groups of choline-derivative-based ILs.¹⁰⁰ A total of 63 choline-based ILs consisting of halides, non-nutritive sweeteners, and imides were synthesized and characterized for antimicrobial activity against Gram-positive and Gram-negative bacteria and fungi.^{100, 101} Other studies with structurally modified imidazolium IL revealed that the presence of a long alkyl chain led to superior antimicrobial activity.^{102, 103} Another quaternary amine, pyrrolidinium, was found to be effective against bacterial rods, cocci, and fungi. Similar to the findings of Pernak *et al.*, enhanced antimicrobial activity was present in pyrrolidinium IL with alkyl chain lengths ranging between 12- 16 carbons.¹⁰⁴ Introducing multiple alkyl chains to conventional IL cations, as that present in multi-geminal ILs, has led to improved antimicrobial activities as compared to geminal monomer, QACs, or typical ILs.¹⁰⁵ Additionally, QSAR studies reveal that undecane incorporated in chiral ammonium-based ILs sufficiently inhibited the viability of bacteria and fungi.^{106, 107} Biological properties of phosphonium-based ILs have also been evaluated.

Cieniecka-Rosionkiewicz *et al.* reported potent bactericidal activity against Gram-positive cocci with attenuated activity when the halide anion was replaced with a non-halide ion.¹⁰⁸ Long alkyl chain ILs consisting of azolate anions have also been reported to possess multi-functional antimicrobial activity.¹⁰⁹ However inconclusive findings suggest that the type of anion present in the IL system generally does not affect the antibacterial activity of the salt, and in fact that the cation is always responsible for IL antibacterial activity.¹¹⁰ Nevertheless three common findings that remain undisputed among present literature about the general features of ILs with antimicrobial activity are the presence of alkyl chain length, type of anion, and overall lipophilicity.^{10, 111, 112}

Few microbiological studies against nonplanktonic bacteria have been reported. The first report of IL activity in preventing the formation of biofilms occurred in 2009 by Carson *et al.* In this study, the antimicrobial activities a series of 1-alkyl-3-methylimidazolium chloride ILs have been evaluated against both planktonic and nonplanktonic clinical pathogens.¹¹³ Similar to the effects of ILs on planktonic bacteria, alkyl chain lengths greater than 10 carbons resulted in potent biofilm eradication.¹¹³ Overall, it is concluded that biofilms caused by Gram-positive bacteria and *Candida* species were more susceptible to 1-alkylmethylimidazolium ILs than Gram-negative bacterial biofilms.¹¹³ To date, 1-alkylquinolinium bromide ILs are considered to be the most potent antibiofilm ILs tested with superior toxicity to the previously synthesized antifouling IL, 1-alkyl-3-methylimidazolium ILs.¹¹⁴

1.5.3 Active Pharmaceutical Ingredient Based Ionic Liquids

First-generation ILs have been used extensively in organic chemistry for the synthesis of various biologically active compounds.¹¹⁵ However, the incorporation of active ingredients into the IL structure has recently led to another sector of third-generation ILs called Active

Pharmaceutical Ingredient-based ILs (API-ILs). Active Pharmaceutical Ingredient-based ILs are ionic salts that melt below 100°C in which either the cation or the anion contains a pharmaceutical ingredient in its structure (Figure 1.15).¹¹⁶ Although these materials have been coined API-ILs as of recently, literature shows that several existing pharmaceutical salts can also be classified as ILs.¹¹⁷ For instance, most therapeutic salts come in the form of a first-generation IL, even if the melting point exceeds 100°C. However, based on the definition of ILs, the API-ILs with melting points exceeding 100°C are appropriately considered to be API-GUMBOS in which most of the historical API-ILs fall into this category.

Conventional pharmaceutical salts typically contain an ion with a pharmacophoric group and an inert biocompatible counter-ion.¹¹⁷ Some pharmaceutical ingredient counter-ions that are generally regarded as safe by the Food and Drug Administration are sodium, potassium, sulfate, nitrate, chloride, or phosphate. Converting the acid/base form of different pharmaceuticals into a salt-form consisting of an inert counter-ion may provide desirable thermal stability, bioavailability, and biocompatibility to the API.¹¹⁷ In this way, crystalline active solids with approved mechanisms and properties can be monitored without interference from a secondary active ion.

Unfortunately, many APIs such as barbituates, sulfonamides, and steroids undergo polymorphic conversion and suffer from poor bioavailability which detrimentally affects their performance.¹¹⁵ The development of API-IL has shown to be a viable method to incorporate multiple functions into a salt while remedying pharmacological problems associated with API solids. This is represented in a couple of historical examples of structurally similar third-generation API-ILs, developed in 1951 and 1952, namely, phenazone gentisate (*i.e.* analgesic, anti-inflammatory, antipyretic, Mp = 87–88°C) and diphenhydrammonium 8-chlorotheophylline

or Dimenhydrinate (antihistaminic, anitvertigo, motion sickness treatment, Mp = 102-107°C), respectively.¹¹⁷ Rantidine docusate is a recent example of an API-ILs that eliminated drug polymorphism associated with Ranitidine hydrochloride.¹¹⁶ Additionally, API-ILs such as lidocaine docusate and didecyldimethylammonium Ibuprofen are other examples in which challenges associated with APIs are overcome. In these particular cases the biologically active ions within the API-IL structures are anionic and/or cationic, possess the properties of its precursor ion, and remedy solvation properties caused by API crystallinity.^{116, 118} The added control of the ion diffusion from the higher energetics within API-IL is another enhancement that these materials offer.

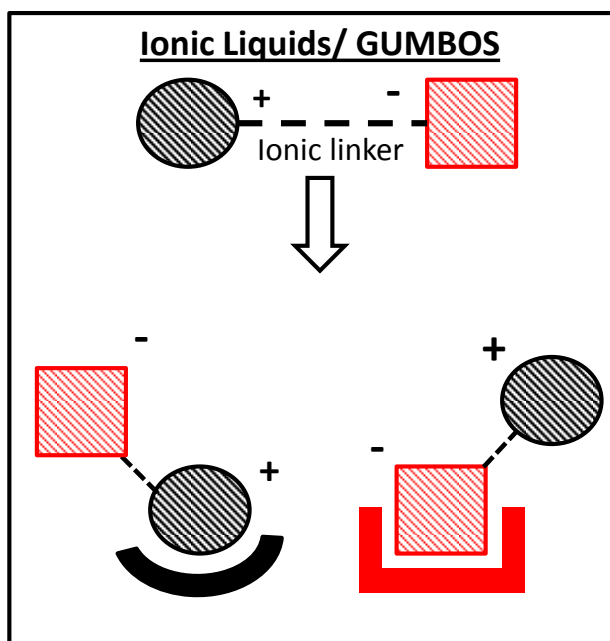


Figure 1.15. Schematic representing the activity of pharmaceutically active ionic liquids and GUMBOS.

Overall, API-ILs are designed to possess ionic-synergetic efficacy for the intended purpose, have controlled, yet tunable chemical, physical, and biological properties, improve bioavailability and pharmacokinetic properties, and reduce toxicity.^{115, 119} API-ILs possess the

advantages of both conventional combination antimicrobial therapy and hybrid antibiotic prodrug systems, although still vastly unique. With the exponential amount of possible active ion combinations, representative API-ILs or API-GUMBOS will be found in every sector of pharmaceuticals.

1.6 References

1. Mims, C.; Dockrell, H.M.; Goering, R.V.; Roitt, I.; Wakelin, D.; Zuckerman, M. *Medical Microbiology*. 3rd ed. Mosby: St. Louis, **2004**.
2. Wilson, J.W.; Schurr, M.J.; LeBlanc, C.L.; Ramamurthy, R.; Buchanan, K.L.; Nickerson, C.A., *Postgraduate Medical Journal*, **2002**, 78, (918), 216-224.
3. Mishra, B.B.; Tiwari, V.K., Eds. *Opportunity, Challenge, and Scope of Natural Products in Medicinal Chemistry*. Research Signpost: Kerala, India, **2011**.
4. Aminov, R.I., *Frontiers in Microbiology*, **2010**, 1, (134), 1-7.
5. Rolinson, G.N., *Journal of Antimicrobial Chemotherapy*, **1998**, 41, (6), 589-603.
6. Kingston, W., *Journal of the History of Medicine and Allied Sciences*, **2004**, 59, (3), 441-462.
7. Van Epps, H.L., *The Journal of Experimental Medicine*, **2006**, 203, (2), 259.
8. Jukes, T.H., *Reviews of Infectious Diseases*, **1985**, 7, (5), 702-707.
9. McDonnell, G.; Russell, A.D., *Clinical Microbiology Reviews*, **1999**, 12, (1), 147-179.
10. Pernak, J.; Skrzypczak, A., *European Journal of Medicinal Chemistry*, **1996**, 31, (11), 901-903.
11. Denyer, S.P.; Hugo, W.B., Eds. *Mechanisms of Action of Chemical Biocides: Their Study and Exploitation*. Blackwell Scientific Publications: Boston, **1991**.
12. Denyer, S.P.; Stewart, G.S.A.B., *International Biodeterioration and Biodegradation*, **1998**, 41, (3), 261-268.
13. Gilbert, P.; Moore, L.E., *Journal of Applied Microbiology*, **2005**, 99, (4), 703-715.
14. Beeuwkes, H., *Antonie van Leeuwenhoek*, **1958**, 24, (1), 49-62.
15. Barnham, M.; Kerby, J., *Journal of Hospital Infection*, **1980**, 1, (1), 77-81.

16. Barnham, M.; Husband, P., *Journal of Applied Microbiology*, **1980**, *49*, (2), 345-351.
17. Harper, W.E.; Epis, J.A., *Microbios*, **1987**, *51*, 107-112.
18. Brooks, S.E.P.; Walczak, M.A.R.N.; Hameed, R.M.D.; Coonan, P.E.; The University of Chicago Press on behalf of The Society for Healthcare Epidemiology of America, **2002**; Vol. *23*, pp 692-695.
19. Kawamura-Sato, K.; Wachino, J.-i.; Kondo, T.; Ito, H.; Arakawa, Y., *Journal of Antimicrobial Chemotherapy*, **2008**, *61*, (3), 568-576.
20. Bertrand, X.; Slekovec, C.; Talon, D., *Future Microbiology*, **2010**, *5*, (5), 701-703.
21. Panchabhai, T.S.; Dangayach, N.S.; Krishnan, A.; Kothari, V.M.; Karnad, D.R., *Chest*, **2009**, *135*, (5), 1150-1156.
22. Faria, G.; Celes, M.R.N.; De Rossi, A.; Silva, L.A.B.; Silva, J.S.; Rossi, M.A., *Journal of Endodontics*, **2007**, *33*, (6), 715-722.
23. Lboutounne, H.; Chaulet, J.-F.; Ploton, C.; Falson, F.; Pirot, F., *Journal of Controlled Release*, **2002**, *82*, (2-3), 319-334.
24. Kropinski, A.M.; Kuzio, J.; Angus, B.L.; Hancock, R.E., *Antimicrobial Agents and Chemotherapy*, **1982**, *21*, (2), 310-319.
25. Carmona-Ribeiro, A.M.; Vieira, D.B.; Lincopan, N., *Anti-Infective Agents in Medicinal Chemistry*, **2006**, *5*, 33-54.
26. David, S.A.; John Wiley & Sons, Ltd., **2001**; Vol. *14*, pp 370-387.
27. Burns, M.R.; Jenkins, S.A.; Wood, S.J.; Miller, K.; David, S.A., *Journal of Combinatorial Chemistry*, **2005**, *8*, (1), 32-43.
28. Broxton, P.; Woodcock, P.M.; Gilbert, P., *Journal of Applied Microbiology*, **1983**, *54*, (3), 345-353.
29. Cottarel, G.; Wierzbowski, J., *Trends in Biotechnology*, **2007**, *25*, (12), 547 - 555.
30. Pokrovskaya, V.; Baasov, T., *Expert Opin. Drug Discov.*, **2010**, *5*, (9), 883-902.
31. Fischbach, M.A., *Current Opinion in Microbiology*, **2011**, *14*, 519-523.
32. Moellering, R.C., *American Journal of Medicine*, **1983**, *75*, (2A), 4-8.
33. Xiong, G.L.; Doraiswamy, P.M., *Geriatrics*, **2005**, *60*, (6), 22-26.
34. Chesney, M.A.; Ickovics, J.R.; Hecht, F.M.; Sikipa, G.; Rabkin, J.G., *AIDS*, **1999**, *13*, (Suppl A), S271-S278.

35. Vorobeychik, Y.; Gordin, V.; Mao, J.; Chen, L., *CNS Drugs*, **2011**, *Epub ahead of print*.
36. Zhao, Q.; Zhang, H.; Li, Y.; Hu, X.; Fan, L., *Journal of Experimental Cancer Research*, **2010**, *29*, (1), 118.
37. Martinson, N.A.; Barnes, G.L.; Moulton, L.H.; Msandiwa, R.; Hausler, H.; Ram, M.; McIntyre, J.A.; Gray, G.E.; Chaisson, R.E., *New England Journal of Medicine*, *365*, (1), 11-20.
38. Pierre, D.; Klastersky, J., *American Journal of Medicine*, **1986**, *80*, (6B), 29-38.
39. Garrett, E.R.; Won, C.M., *Antimicrob. Agents Chemother.*, **1973**, *4*, (6), 626-633.
40. Calabi, O., *Journal of Medical Microbiology*, **1973**, *6*, (3), 293-306.
41. Dalton, A.C.; Plaut, M.E., *The American Journal of the Medical Sciences*, **1971**, *261*, (6), 335-340.
42. Smith, I.M., *Journal of Infectious Diseases*, **1971**, *124*, (Supplement 1), S198-S201.
43. Boulanger, L.L.; Etestad, P.; Fogarty, J.D.; Dennis, D.T.; Romig, D.; Mertz, G., *Clinical Infectious Diseases*, **2004**, *38*, (5), 663-669.
44. Williams, B.J., *Appl. Environ. Microbiol.*, **1971**, *21*, (4), 668-672.
45. Marcus, R.; Paul, M.; Elphick, H.; Leibovici, L., *International Journal of Antimicrobial Agents*, **2011**, *37*, 491-503.
46. Silbiger, P.M.; Grozinsky, S.; Soares-Weiser, K.; Leibovici, L., *Cochrane Database Syst. Rev.*, **2006**, *1*, (CD003344).
47. Biziotis, I.A.; Argyris, M.; Kasiakou, S.K.; Samonis, G.; Christodoulou, C.; Chrysanthopoulou, S.; Falagas, M.E., *Mayo Clinical Proceedings*, **2005**, *80*, (9), 1146-1156.
48. Bercot, B.; Poirel, L.; Dortet, L.; Nordmann, P., *Journal of Antimicrobial Chemotherapy*, *66*, (10), 2295-2297.
49. Wiskirchen, D.E.; Koomanachai, P.; Nicasio, A.M.; Nicolau, D.P.; Kuti, J.L., *Antimicrob. Agents Chemother.*, *55*, (4), 1420-1427.
50. Souli, M.; Galani, I.; Boukovalas, S.; Gourgoulis, M.G.; Chryssouli, Z.; Kanellakopoulou, K.; Panagea, T.; Giamarellou, H., *Antimicrob. Agents Chemother.*, *55*, (5), 2395-2397.
51. Yim, H.; Woo, H.; Song, W.; Park, M.-J.; Kim, H.S.; Lee, K.M.; Hur, J.; Park, M.-S., *Ann Clin Lab Sci*, *41*, (1), 39-43.

52. Clock, S.A.; Whittier, S.; Weisenberg, S.A.; Kubin, C.J.; Schuetz, A.N.; Tabibi, S.; Alba, L.; Jenkins, S.; Saiman, L. In *48th Annual Meeting of the Infectious Disease Society of America*: Vancouver, British Columbia, Canada, **2010**.
53. Bouza, E.; Cercenado, E., *Seminars in Respiratory Infections*, **2002**, *17*, (3), 215-230.
54. Ejim, L.; Farha, M.A.; Falconer, S.B.; Wildenhain, J.; Coombes, B.K.; Tyers, M.; Brown, E.D.; Wright, G.D., *Nat Chem Biol*, *7*, (6), 348-350.
55. Hemaiswarya, S.; Kruthiventi, A.K.; Doble, M., *Phytomedicine*, **2008**, *15*, 639 - 652.
56. Moellering, R.C., *American Journal of Medicine*, **1985**, *79*, (2A), 104-109.
57. Jaehoon Yu , J.L., Miyun Kwon , Kye-Jung Shin Heterodimeric conjugates of neomycin-oxazolidinone their preparation and their use. 2005.
58. Schiffman, R.M.L.B., CA, US), Graham, Richard (Irvine, CA, US), Rupp, David (San Pedro, CA, US), Johnson, Brent A. (Ladera Ranch, CA, US) Mixed antibiotic codrugs. 2006.
59. Butler, M.M.; LaMarr, W.A.; Foster, K.A.; Barnes, M.H.; Skow, D.J.; Lyden, P.T.; Kustigian, L.M.; Zhi, C.; Brown, N.C.; Wright, G.E.; Bowlin, T.L., *Antimicrobial Agents and Chemotherapy*, **2007**, *51*, (1), 119-127.
60. Miyun Kwon, H.-J.K., Jongkook Lee, Jaehoon Yu, *Bulletin of the Korean Chemical Society*, **2006**, *27*, (10), 1664-1666.
61. Jaehoon Yu , J.L., Miyun Kwon , Kye-Jung Shin Heterodimeric conjugates of neomycin-chloramphenicol having an enhanced specificity against RNA targets and its preparation. 2005.
62. Lee, J.; Kwon, M.; Lee, K.H.; Jeong, S.; Hyun, S.; Shin, K.J.; Yu, J., *Journal of the American Chemical Society*, **2004**, *126*, (7), 1956-1957.
63. Pokrovskaya, V.; Belakhov, V.; Hainrichson, M.; Yaron, S.; Baasov, T., *Journal of Medicinal Chemistry*, **2009**, *52*, (8), 2243-2254.
64. Webb, J.L. In *Enzymes and Metabolic Inhibitors*. Academic Press: New York, **1963**.
65. Valeriate, F.A.; Lin, H.S., *Cancer Chemotherapy Reports. Part 1*, **1975**, *59*, (5), 895-900.
66. Drewinko, B.; Loo, T.L.; Brown, B.; Gottlieb, J.A.; Freireich, E.J., *Cancer Biochemistry Biophysics*, **1976**, *1*, (4), 187-195.
67. Prichard, M.N.; Shipman Jr, C., *Antiviral Research*, **1990**, *14*, (4-5), 181-205.
68. Steel, G.; Peckham, M.J., *International journal of radiation oncology, biology, physics*, **1979**, *5*, (1), 85-91.

69. Boucher, A.N.; Tam, V.H., *Diagnostic Microbiology and Infectious Disease*, **2006**, *55*, (4), 319-325.
70. Goldoni, M.; Johansson, C., *Toxicology in Vitro*, **2007**, *21*, (5), 759-769.
71. Berenbaum, M.C., *Journal of Infectious Diseases*, **1978**, *137*, (2), 122-130.
72. Plummer, J.L., *Pain Reviews*, **1998**, *5*, (1), 16-31.
73. Zhao, L.; Wientjes, M.G.; Au, J.L.-S., *Clinical Cancer Research*, **2004**, *10*, (23), 7994-8004.
74. Fraser, T.R., *BMJ*, **1872**, *2*, (618), 485-487.
75. Tallarida, R.J., *Journal of Pharmacology and Experimental Therapeutics*, **2001** *298*, (3), 865-872.
76. Lee, J.J.; Kong, M.; Ayers, G.D.; Lotan, R., *Journal of Biopharmaceutical Statistics*, **2007**, *17*, (3), 461-480.
77. Straetemans, R.; O'Brien, T.; Wouters, L.; Van Dun, J.; Janicot, M.; Bijmens, L.; Burzykowski, T.; Aerts, M., *Biometrical Journal*, **2005**, *47*, 299-308.
78. Tesfai, A.; El-Zahab, B.; Bwambok, D.; Baker, G.; Fakayode, S.; Lowry, M.; Warner, I., *Nano Lett.*, **2008**, *8*, (3), 897-901.
79. Das, S.; Bwambok, D.; El-Zahab, B.; Monk, J.; de Rooy, S.L.; Challa, S.; Li, M.; Hung, F.R.; Baker, G.A.; Warner, I.M., *Langmuir*, **2010**, *26*, (15), 12867-12876.
80. Das, S.; de Rooy, S.L.; Jordan, A.N.; Chandler, L.; Negulescu, I.I.; El-Zahab, B.; Warner, I.M., *Langmuir*, **2011**, *28*, (1), 757-765.
81. de Rooy, S.L.; El-Zahab, B.; Li, M.; Das, S.; Broering, E.; Chandler, L.; Warner, I.M., *Chemical Communications*, **2011**, *47*, (31), 8916-8918.
82. De Rooy, S.L.; Li, M.; Bwambok, D.K.; El-Zahab, B.; Challa, S.; Warner, I.M., *Chirality*, **2011**, *23*, (1), 54-62.
83. Dumke, J.C.; El-Zahab, B.; Challa, S.; Das, S.; Chandler, L.; Tolocka, M.; Hayes, D.J.; Warner, I.M., *Langmuir*, **2010**, *26*, (19), 15599-15603.
84. Bwambok, D.K.; El-Zahab, B.; Challa, S.K.; Li, M.; Chandler, L.; Baker, G.A.; Warner, I.M., *ACS Nano*, **2009**, *3*, (12), 3854-3860.
85. Li, M.; De Rooy, S.L.; Bwambok, D.K.; El-Zahab, B.; DiTusa, J.F.; Warner, I.M., *Chemical Communications*, **2009**, (45), 6922-6924.
86. Li, M.; Gardella, J.; Bwambok, D.K.; El-Zahab, B.; de Rooy, S.; Cole, M.; Lowry, M.; Warner, I.M., *Journal of Combinatorial Chemistry*, **2009**, *11*, (6), 1105-1114.

87. Tesfai, A.; El-Zahab, B.; Kelley, A.T.; Li, M.; Garno, J.C.; Baker, G.A.; Warner, I.M., *ACS Nano*, **2009**, 3, (10), 3244-3250.
88. Cole, M.R.; Li, M.; El-Zahab, B.; Janes, M.E.; Hayes, D.; Warner, I.M., *Chemical Biology & Drug Design*, **2011**, 78, (1), 33-41.
89. Gathergood, N.; Scammells, P.J., *Australian Journal of Chemistry*, **2002**, 55, (9), 557-560.
90. Gathergood, N.; Garcia, M.T.; Scammells, P.J., *Green Chemistry*, **2004**, 6, (3), 166-175.
91. Garcia, M.T.; Gathergood, N.; Scammells, P.J., *Green Chemistry*, **2005**, 7, (1), 9-14.
92. Gathergood, N.; Scammells, P.J.; Garcia, M.T., *Green Chemistry*, **2006**, 8, (2), 156-160.
93. Docherty, K.; Dixon, J.; Kulpa Jr, C., *Biodegradation*, **2007**, 18, (4), 481-493.
94. Harjani, J.R.; Singer, R.D.; Garcia, M.T.; Scammells, P.J., *Green Chemistry*, **2008**, 10, (4), 436-438.
95. Romero, A.; Santos, A.; Tojo, J.; Rodriguez, A., *Journal of Hazardous Materials*, **2008**, 151, 268-273.
96. Stolte, S.; Abdulkarim, S.; Arning, J.; Blomeyer-Nienstedt, A.-K.; Bottin-Weber, U.; Matzke, M.; Ranke, J.; Jastorff, B.; Thoming, J., *Green Chemistry*, **2008**, 10, (2), 214-224.
97. Atefi, F.; Garcia, M.T.; Singer, R.D.; Scammells, P.J., *Green Chemistry*, **2009**, 11, (10), 1595-1604.
98. Thuy Pham, T.P.; Cho, C.-W.; Yun, Y.-S., *Water Research*, **2009**, 44, (2), 352-372.
99. Coleman, D.; Gathergood, N., *Chemical Society Reviews*, **2010**, 39, (2), 600-637.
100. Pernak, J.; Chwala, P.; *European Journal of Medicinal Chemistry*, 38, (11-12), 1035-1042.
101. Pernak, J.; Syguda, A.; Mirska, I.; Pernak, A.; Nawrot, J.; Prączyńska, A.; Griffin, S.T.; Rogers, R.D., *Chemistry – A European Journal*, **2007**, 13, (24), 6817-6827.
102. Pernak, J.; Kalewska, J.; Ksycinska, H.; Cybulski, J., *European Journal of Medicinal Chemistry*, **2001**, 36, (11-12), 899-907.
103. Pernak, J.; Sobaszekiewicz, K.; Mirska, I., *Green Chem.*, **2003**, 5, (1), 52-56.
104. Demberelnyamba, D.; Seung, P.; Huen, L.; Chang, K.; Ick-Dong, Y., *Bioorg.Med. Chem.*, **2004**, 12, 853-857.

105. Pernak, J.; Skrzypczak, A.; Lota, G.; Frackowiak, E., *Chemistry – A European Journal*, **2007**, *13*, (11), 3106-3112.
106. Pernak, J.; Feder-Kubis, J., *Tetrahedron: Asymmetry*, **2006**, *17*, (11), 1728-1737.
107. Cybulski, J.; Wisniewska, A.; Kulig-Adamiak, A.; Dabrowski, Z.; Praczyk, T.; Michalczyk, A.; Walkiewicz, F.; Materna, K.; Pernak, J., *Tetrahedron Letters*, **2011**, *52*, (12), 1325-1328.
108. Cieniecka-Roslonkiewicz, A.; Pernak, J.; Kubis-Feder, J.; Ramani, A.; Robertson, A.J.; Seddon, K.R., *Green Chemistry*, **2005**, *7*, (12), 855-862.
109. Walkiewicz, F.; Materna, K.; Kropacz, A.; Michalczyk, A.; Gwiazdowski, R.; Praczyk, T.; Pernak, J., *New Journal of Chemistry*, **2010**, *34*, (10), 2281-2289.
110. Docherty, K.M.; Kulpa, C.F., *Green Chem.*, **2005**, *7*, 185-189.
111. Skrzypczak, A.; Brycki, B.; Mirska, I.; Pernak, J., *European Journal of Medicinal Chemistry*, *32*, (7-8), 661-668.
112. Pernak, J.; Mirska, I.; Kmiecik, R., *European Journal of Medicinal Chemistry*, **1999**, *34*, (9), 765-771.
113. Carson, L.; Chau, P.K.W.; Earle, M.J.; Gilea, M.A.; Gilmore, B.F.; Gorman, S.P.; McCann, M.T.; Seddon, K.R., *Green Chemistry*, **2009**, *11*, (4), 492-497.
114. Busetti, A.; Crawford, D.E.; Earle, M.J.; Gilea, M.A.; Gilmore, B.F.; Gorman, S.P.; Lavery, G.; Lowry, A.F.; McLaughlin, M.; Seddon, K.R., *Green Chemistry*, *12*, (3), 420-425.
115. Hough, W.L., Rogers, Robin D. , *Bull. Chem. Soc. Jpn.*, **2007**, *80*, (12), 2262-2269.
116. Hough-Troutman, W.L.; Smiglak, M.; Rodriguez, H.; Swatloski, R.P.; Spear, S.K.; Daly, D.T.; Pernak, J.; Grisel, J.E.; Carliss, R.D.; Soutullo, M.D.; Davis, J.H.; Rogers, R.D., *New Journal of Chemistry*, **2007**, *31*, 1429-1436.
117. Kumar, V.; Malhotra, S.V. In *Ionic Liquid Applications: Pharmaceutical, Therapeutics, and Biotechnology*. Malhotra, S., Ed.; American Chemical Society: Washington D. C. , **2010**, p 12.
118. Bica, K.; Rijksen, C.; Nieuwenhuyzen, M.; Rogers, R.D., *Physical Chemistry Chemical Physics*, *12*, (8), 2011-2017.
119. Rodríguez, H., Bica, K., Rogers, R.D., *Tropical Journal of Pharmaceutical Research*, **2008**, *7*, (3), 1011-1012.

CHAPTER 2 ANALYTICAL TECHNIQUES, MECHANISM OF ACTION VALIDATION, AND ANTIMICROBIAL CHARACTERIZATION

The pharmacological techniques used to characterize the utility of ampicillin-based ionic liquids and β -lactam based chlorhexidine GUMBOS in biomedical application are highlighted in this section. More specifically, several studies that characterize the properties of the antimicrobial agents based on their physical and chemical features are described in addition to the absorbance and fluorescence methods used to validate their antimicrobial activity and mammalian cytotoxicity.

2.1 Pharmacological Techniques and Characterization

2.1.1 Rate of Dissolution

Drug dissolution is an analytical parameter that assesses the release profile of drugs into aqueous environments. By definition, dissolution involves the solubilization of the drug particles into the surrounding aqueous medium. This property is very important for systemic delivery of hydrophobic drugs. The kinetics of drug dissolution (DR) can be defined by the Noyes-Whitney equation (Equation 2.1), which correlates surface area (A), diffusion coefficient (D), boundary layer thickness (h), saturation solubility (C_s), and the amount of dissolved drug (X_d) in the volume of dissolution media (V).

$$DR = \frac{dx}{dt} = \frac{AD}{h} \left(C_s - \frac{X_d}{V} \right) \quad (\text{Eq. 2.1})$$

The dissolution rate (DR) or time required for drug to dissolve depends on the cohesive properties of the drug. More specifically, the physico-chemical properties of a drug and its physical form dictate how quickly a drug dissolves and will be absorbed. Therefore, many drugs are particularly formulated to control its rate of dissolution. Drugs are converted into a salt, free acid or base, or even pulverized to minimize the particle size and increase its dissolution rate. In

sum, more than 33% of drugs suffer from poor aqueous solubility and undergo chemical modifications to increase its systemic delivery. Hence, the onset of drug levels will be governed by the dissolution release kinetics of the drug.

2.1.2 Predictive Intestinal Permeability

Highly oral bioavailability is an attractive feature for novel antimicrobial drugs. It is defined as “the characteristics of a drug that affects the process by which unchanged drugs proceed from the site of administration to the site of measurement within the body”. Predominantly, its ability to provide convenience, patient compliance, and practicality as compared to conventional injections or suppositories makes this a valid characteristic for therapeutics. However, poor intestinal permeability (absorption) can label candidate molecules unsuitable regardless of their potent activity. This process can be affected by several physiological factors such as how well the drug was formulated or the contents of the gastrointestinal tract among other things. To overcome the potential physiological interferences inhibiting passive intestinal permeability, effective therapeutic agents have an optimal balance of lipophilicity/ hydrophilicity, hydrogen bonding, size, and charge since most drugs are passively absorbed through the lipid-aqueous interface of the cell membrane (transcellular transport) or water-filled tight junctions formed by the fusion of lipid membranes of adjacent cells (paracellular transport). Transcellular transport is the route commonly taken by molecules that are more lipophilic prior to becoming systemic. Thus, predicting drug oral bioavailability through intestinal permeability is vital to the success of candidate antimicrobial agents.

Various *in vitro* assays have been developed to quantify the relative lipophilicity and intestinal permeability of therapeutic agents. Yet, the Parallel Artificial Membrane Permeability Assay (BD Gentest pre-coated PAMPA Plate System; BD Biosciences, MA) and logarithmic

octanol-water partition coefficient assays were the techniques employed in this dissertation research. In the PAMPA technique, a diffusion cell consisting of a donor and acceptor compartment separated by a synthetic membrane was used to quantify the predictable intestinal permeability of the candidate molecules developed in this research. More specifically, this approach consists of a 96-well filter plate coated with a proprietary phospholipid membrane separating the donor and acceptor wells. Known concentrations of test solutions (*e.g.* 100 – 200 μM in buffer) are added to the donor plate while only buffer is placed in the acceptor well. Typically, rates of diffusion can be calculated by quantifying changes in drug concentrations in the acceptor well. However, the assay is developed to measure the final drug concentration after 5 hours of incubation using UV-vis spectroscopy. Effective permeability coefficients (P_e) are calculated based on initial millimolar concentration in donor well (C_o), millimolar concentration in donor well at 5 hours (C_D), millimolar concentration in acceptor well at 5 hours (C_A), volumes of donor (V_D) and acceptor wells (V_A), well filter area (A , 0.3 cm^2), and incubation time (t , 18000 s) as calculated using the relationship in Equation 2.2.

$$Pe \text{ (cm s}^{-1}\text{)} = \frac{-\ln\left[1 - \frac{C_A}{\frac{C_D \times V_D + C_A \times V_A}{V_D + V_A}}\right]}{A \times \left(\frac{1}{V_D} + \frac{1}{V_A}\right) \times t} \quad (\text{Eq. 2.2})$$

Pharmacologists can assess the drug-likeness of a given therapeutic agent based on its lipophilicity to various organic solvents or quantifying its partition coefficient. Specifically, the logarithmic octanol – water partition coefficient (Log P) is used extensively to describe a drug's lipophilic properties and its preferential affinity to either octanol or water. It is a ratiometric parameter based on the concentration of therapeutic in either phase of the two-phase system when at equilibrium (Equation 2.3). It logarithmic denotation is commonly used to characterize this value since it scales at least 12 orders of magnitude. Many studies have shown that Log P is

a valuable parameter in correlating a drug's transport process, its interactions with concomitant biological molecules, and its potential toxicity. Though the acquisition of Log P values can be logically simple, it can be irreproducible, time-consuming and expensive ultimately forging difficulty in its use at the screening level. Likewise, this method is not accurate for determining the partitioning nature of ionizable compounds because charged molecules do not partition into lipophilic environments regardless of its chemical features. However, the most reliable approach to date is the classical shake-flask method. To prevent minimal solvent miscibility, octanol is saturated with deionized water and allowed to separate for 24 hours prior to its use. Subsequently, a known concentration of candidate drug is added to the flask and allowed to mix for 2 hours minimal. The sample is then left undisturbed for 24 hours to allow the two solvents to separate and the analyte to partition into its desired phase. Both phases are quantified using absorbance spectroscopy and used to approximate the drugs lipophilic nature.

$$\text{Log } P = \text{Log} \frac{[\text{octanol}]}{[\text{water}]} \quad (\text{Eq. 2.3})$$

2.2 Antimicrobial Testing and Preparation

Antimicrobial susceptibility testing is important to identify levels of pathogen susceptibility to specific antimicrobial agents and/or to detect the development of resistance in individual bacterial isolates. Various techniques and methods are used to quantify the effects antimicrobial agents have on bacteria and those techniques are described in this section.

2.2.1 Turbidity Standards for Inoculum Preparation

Although there are many standards available to standardize the inoculum density for a susceptibility test, a BaSO₄ turbidity standard equivalent to a 0.5 McFarland standard was used. A 0.5 McFarland standard was prepared as outlined by the Center for the Disease Control and

Prevention where 500 μL of 1.175% $\text{BaCl}_2 \cdot 2\text{H}_2\text{O}$ is added to 99.5 mL of 1% v/v H_2SO_4 under gentle stirring. Frequent stirring is necessary to maintain the suspension. The density of the 0.5 MacFarland turbidity standard as verified using a spectrophotometer with a 1-cm light path at 625 nm should range between 0.08 to 0.10. To appropriately match the MacFarland standard to the bacterial inoculum, the standard is dispensed in to same size vials as the bacteria inoculum and sealed and stored in the dark. The standard should be replaced every month as their densities may change and large precipitate may form.

2.2.2 Broth Dilution Tests

National Committee for Clinical Laboratory Standards (NCCLS) criteria outline broth dilution tests as a quantitative measure of the drug-bacteria response.¹ In this method as depicted in Figure 2.1, two-fold dilutions of antibiotics are prepared in a liquid growth medium and dispensed in a 96-well microtiter plate. Stock concentrations of antimicrobial can be prepared in methanol, acetone, dimethylsulfoxide or in the testing solvent. Up to 2% organic solvent does not inhibit cell growth in aqueous medium. The antibiotic-containing wells are inoculated with a 0.5 MacFarland standardized bacterial suspension to match 10^7 - 10^8 CFU/mL. To prepare the concentration of bacteria for testing, the bacterial suspension must be diluted 100-fold in growth medium to a final concentration of 10^5 - 10^6 CFU/mL. Equivolume amounts of bacterial suspension are dispensed to the antibiotic dilutions for testing. This gives a final concentration testing range 5×10^4 - 5×10^5 CFU/mL. Following overnight incubation at 37°C , the wells are examined for visible bacterial growth as evidenced by turbidity. The lowest concentration of antibiotic that prevents growth is the minimal inhibitory concentration (MIC). This high-throughput method allows for as many as 12 antibiotics to be tested across eight concentrations. A high yield of precision within one or two dilutions from the MIC value, as typically caused by

deviations in antibiotic dilutions, is expected with this approach. The key advantage of this technique is that it quantifies the affect a range of antimicrobial agents have on the viability of a microorganism despite its tedious preparation. Thus, the same plates used for the MIC test can be used to identify the minimum bactericidal concentration (MBC). The MBC is the minimum concentration that kills the entire culture. To determine this value, each well that shows no turbidity is subcultured on to a fresh agar plate or sterile broth and incubated overnight at 37°C. The lowest concentration of antimicrobial agent that maintains no growth after inoculation on an agar plate or in broth is considered to be the MBC of the antimicrobial agent.

The checkerboard method, which is commonly used to measure the inhibitory properties of drugs used in combination, was incorporated in this study to evaluate the synergetic responses of precursor components at different concentrations. This approach combined with Loewe's Additivity Model (Section 1.8.2) allows the calculation of a fractional inhibitory concentration (FIC) index in which the antibacterial potencies of agents can be assessed against a particular microorganism. This approach is most suitable in identifying drug combinations that effectively inhibit the growth of drug resistant bacteria that are not susceptible to one or more of the agents used in combination. The experimental method to determine the FIC is similar to what one performs to identify the MIC value. More specifically, serial dilutions of one drug is performed traverse the 96-well microtiter plate from Columns 1 – 12 while another drug is serially diluted from Rows A – H. This allows each well in the microtiter plate to contain a different ratio of each drug and for multiple concentrations of Drug A to be tested with one concentration of Drug B, and vice versa. Subsequently, a known suspension of bacterial inocula is added to the wells in equivolume amounts and incubated for 18 – 24 hours at 37°C. Growth is identified by the turbidity of the bacterial suspension in each well or the use of a dye that is responsive to the

presence of viable cells. The lowest FIC values of both drugs used in combination identifies the best agent to inhibit the drug resistant microorganism.

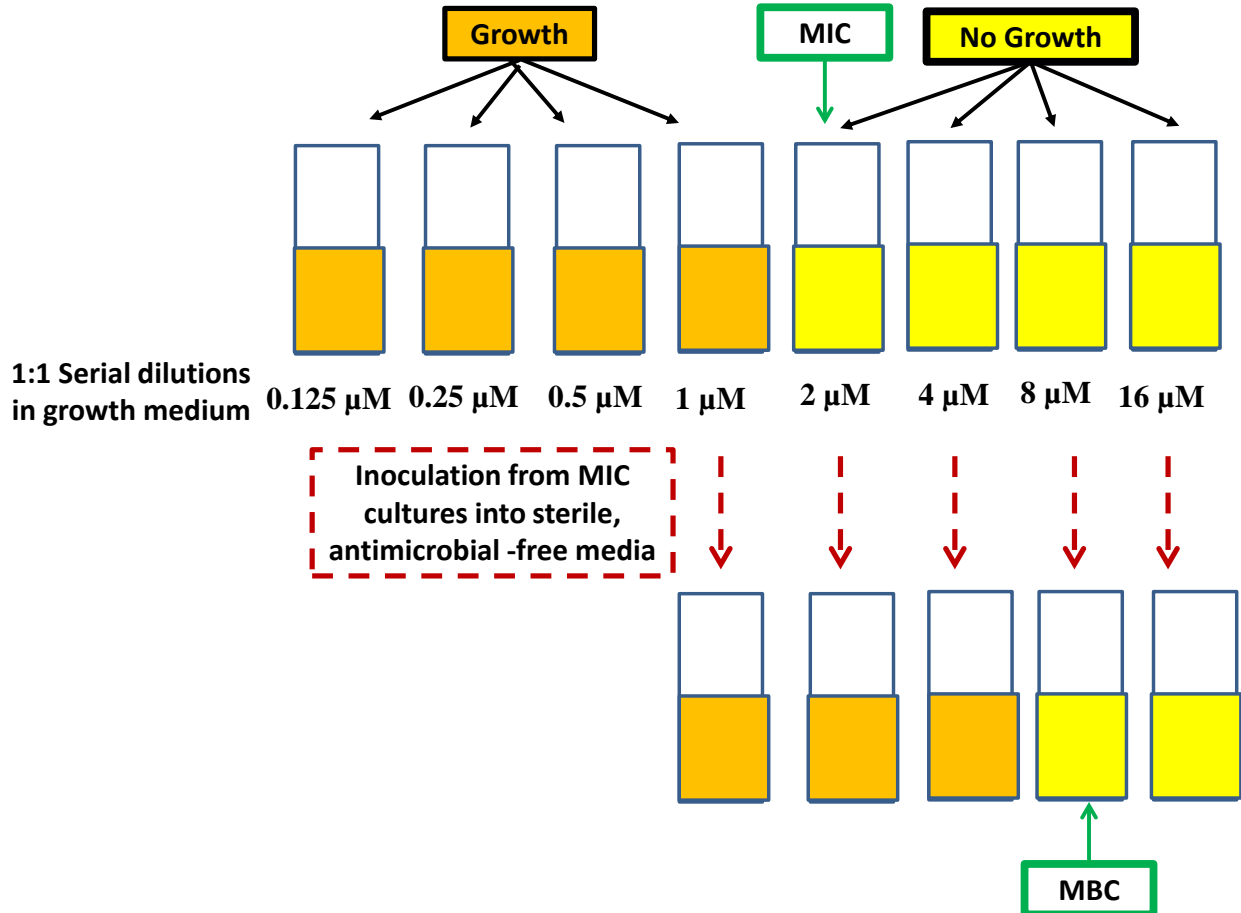


Figure 2.1. Example of broth dilution susceptibility testing and determination of minimum inhibitory and minimum bactericidal concentrations.

2.2.3 Kirby-Bauer Disk Diffusion Test

The Kirby-Bauer disk diffusion test is a qualitative susceptibility test that is often used to screen the efficacy of antimicrobial agents on specific microorganisms. This simple and practical test is performed by spreading a 10^8 CFU/mL bacterial inoculum on to the surface of a large Mueller-Hinton agar plate. Mueller-Hinton agar is prepared using a commercially available dehydrated base according to the manufacturer's instructions. Antibiotic solutions are pipetted on to sterile dry 10 mm paper disks and dried to remove the solvent. Paper disks containing

dehydrated antibiotic are placed on the inoculated agar surface and incubated overnight at 37°C to develop inhibition zones.

The growth of susceptible bacteria around the antibiotic disk is inhibited causing different size “halos” to be formed (Figure 2.2). More specifically, the zones are formed by the diffusing antimicrobial agent through the agar and its growth inhibitive properties on the microorganism. Thus, the concentration of antimicrobial agent is highest closest to the disk and decreases logarithmically towards the halo boundary. This rate of diffusion is governed by the physical and chemical properties of the antibiotic. Its relative hydrophobicity, aqueous solubility, and molecular weight dictate how rapidly it will diffuse through the agar. For instance, large molecules diffuse more slowly than smaller molecules and hydrophilic molecules diffuse more rapidly than hydrophobic molecules. This technique is not completely suitable for hydrophobic drugs and this test may result in hydrophobic molecules being categorized as poor antimicrobial agents. Overall, these factors contribute to the breakpoint zone that shows qualitatively how susceptible bacteria are to that compound.

The major disadvantage of this method is that the bacteriostatic (growth inhibitive) or bactericidal (lethal) concentrations cannot be quantified since a MIC value cannot be effectively determined. This is because the amount of antimicrobial agent that adheres to the disk cannot be quantitatively controlled. Likewise, the susceptibility of the drug as resistant, intermediate, or susceptible is categorized based on zone diameter limits fit within National Committee for Clinical Laboratory Standards (NCCLS) criteria.¹

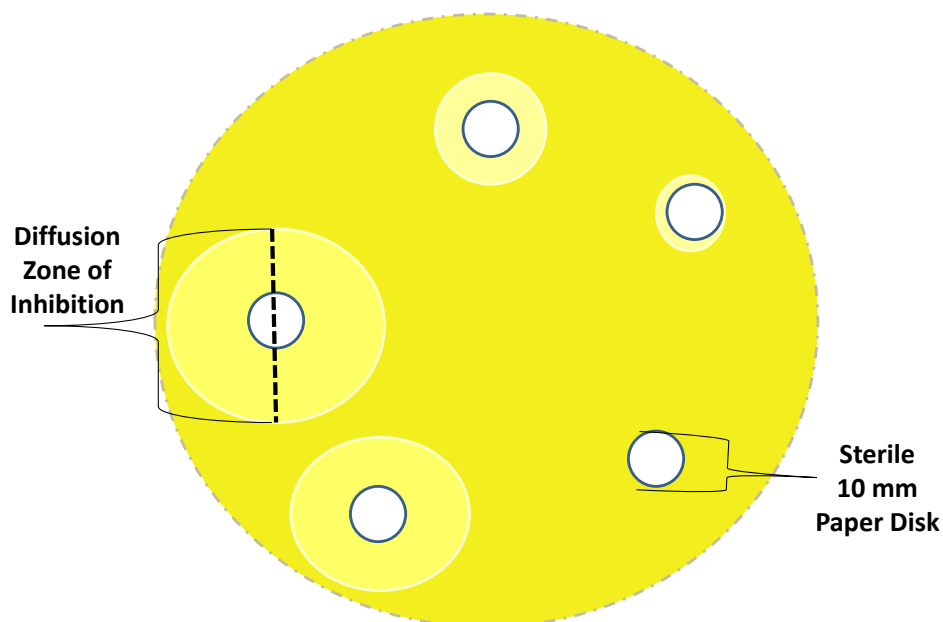


Figure 2.2. Kirby-Bauer disk diffusion assay showing various zones of inhibition.

2.2.4 Mechanism of Action Studies

Mechanism of action studies can reveal the detrimental role these agents have on viable organisms. Thus, lethal effects of the antimicrobial agents were evaluated in tandem using spectroscopic based assays. More specifically, fluorescence-based assays were employed to measure bactericidal rate, membrane permeation and depolarization, and ability to sequester lipopolysaccharide endotoxin. Absorbance spectroscopy was used to study the interaction between GUMBOS and penicillinase enzyme based on Michaelis-Menten kinetics using a β -lactam chromophore in competition. Lastly, scanning electron microscopy was used to visualize the detrimental effects the antimicrobial agents have on the bacterial cells.

2.3 Absorbance-based Techniques

Absorbance-based techniques have been used extensively in clinical experiments to evaluate the viability of microorganisms. Ultraviolet-visible absorption spectroscopy is the

formal name for the analytical technique that quantifies the amount of energy molecules absorb when exposed to light. More specifically, this technique quantifies the percent transmittance (%T) observed by the difference in incident light at a particular wavelength that was transmitted to the sample (I_T) and the remainder that passed through the sample (I_o) to the detector. Equations 2.4 and 2.5 show the relationship between %T and absorbance (A).

$$\%T = 100 \times \left(\frac{I_o}{I_T}\right) \quad (\text{Eq. 2.4})$$

$$A = \epsilon bC = \log\left(\frac{I_o}{I_T}\right) \quad (\text{Eq. 2.5})$$

Since many clinical samples are in an aqueous medium, it is necessary for absorbance detection to occur in electromagnetic regions where water is optically transparent. Water is optically transparent across the entire electromagnetic spectrum between 190 - 700 nm which makes this technique ideal.

A spectrophotometer consists of five linearly arranged basic components. The first component is a stable light source which can either be a continuum or line based. Continuum radiation sources provide a broad, featureless range of wavelengths. Depending on the wavelength of interest, xenon, deuterium, hydrogen, or tungsten lamps are used in spectrophotometers consisting of continuum light energy. In contrast, line-based sources produce narrow bands at specific wavelengths. Examples of line sources are hollow cathode lamps and lasers, and neither was used in the absorbance instrumentation employed in the dissertation research. Thus, a 75W tungsten-halogen continuum lamp source was used to irradiate the third component, the sample. The second component is a monochromator that selects the desired wavelength for the study. It is the monochromatic light that passes through the third component, the sample. To eliminate the loss of light, the sample is placed in an optically transparent sample

holder made of glass, quartz, or plastic depending on the requirements of the experiment. The transmitted light that passes through the sample is then detected by a photomultiplier tube or photodiode-array. Figure 2.3 shows the instrumental configuration of absorbance spectrophotometer.

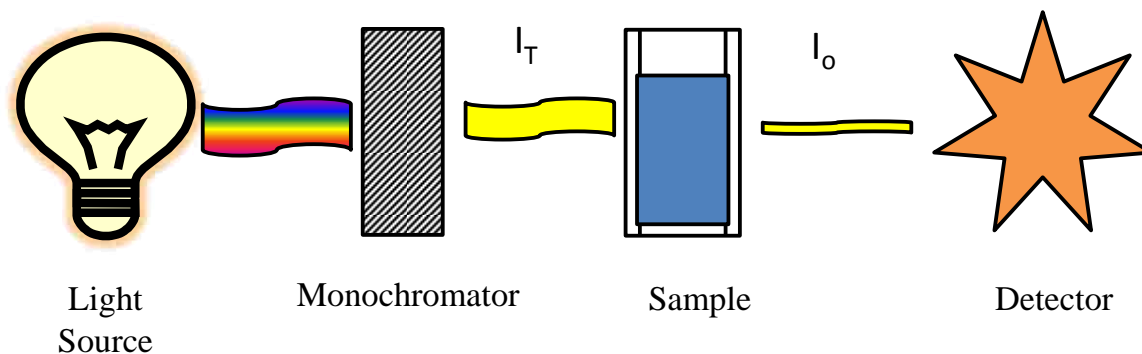


Figure 2.3. Schematic of the instrumental configuration of conventional absorbance spectrophotometers.

A 96-well microtiter plate reader was also used for absorbance measurements in this dissertation research. The major difference in absorbance-based plate readers and spectrophotometers is in the instrumental configuration (Figure 2.4). In this case, a specific wavelength of excited light passes through the sample well and strikes a secondary mirror that directs the transmitted light to the perpendicularly placed detector. Although conventional absorbance spectrophotometers are arranged linearly to permit the detection of all transmitted light, microplate readers achieve the same goal using mirrors. Likewise this optical arrangement promotes flexibility in the implementation of fluorescence experiments as well. The high-throughput nature of plate readers is based on the ability to measure responses from multiple sample wells incrementally. Instead of a cuvette as commonly used in spectrophotometers, an optically transparent flat-bottom 96-well microtiter plate is used to contain the sample.

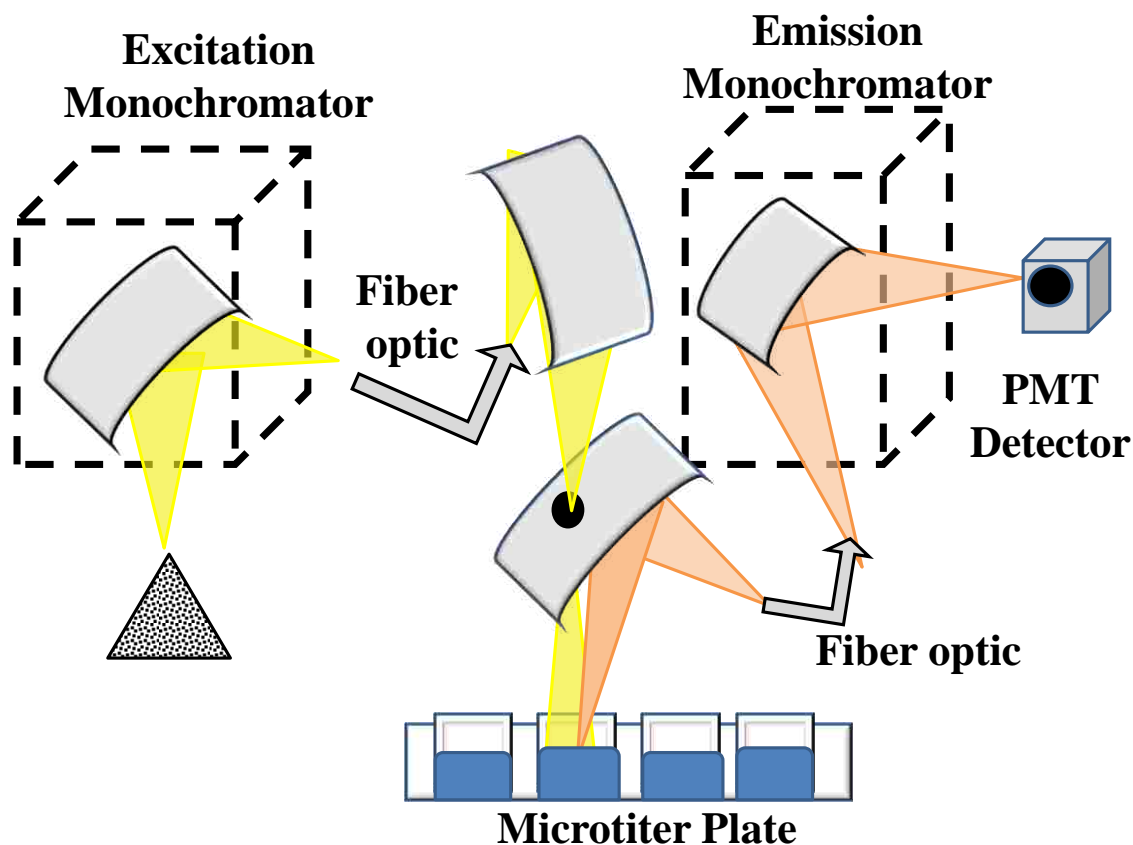


Figure 2.4. Instrumental configuration of a 96-well plate absorbance and emission plate reader.²

2.3.1 Michaelis-Menten Kinetics

Drug systems that monitor the activity between enzyme and substrates are best represented by Michaelis-Menten kinetic models. Specifically, it models the substrate conversion into product through a reversibly formed intermediate complex using an enzyme (Scheme 2.1). Symbolically enzyme kinetics can be denoted as S (substrate), E (enzyme), ES (complex), and P (product) using the following scheme:



Understanding this relationship, the interaction between a substrate and enzyme can be quantified. More precisely, several kinetic parameters can be investigated such as its rate of reaction (V_{max}), turnover number (K_{cat}), binding affinity (K_m), and catalytic efficiency

(K_{cat}/K_m). Figure 2.5 illustrates the typical rate versus substrate concentration curve in which the enzyme kinetic constants are elucidated. The rate of reaction is not necessarily important when it comes to quantifying the effects an enzyme has on a substrate. In fact, V_{max} is the value in which all enzyme active sites are consumed by substrate and changes in this rate of reaction can illustrate the types of substrate-enzyme interactions. The turnover number, K_{cat} , is a first-order rate constant that quantifies the number of molecules that the enzyme actively converts into product per unit of time. This comprehensive value considers all enzyme-substrate, enzyme-intermediate, and enzyme-product complexes. A less complicated value is the Michaelis-Menten constant, K_m . Experimentally, this value is determined as the substrate concentration at half the maximum velocity. This value mostly correlates the binding affinity between the substrate and enzyme. For example, a drug with a large K_m value is considered to bind poorly to the substrate active site. The specificity constant (K_{cat}/K_m) is the second-order rate constant that identifies how well the enzyme detaches from the complex and converts the complex into product. For some substrate-enzyme systems, the catalytic conversion from substrate to product might be instantaneous (*i.e.* $K_{cat}/K_m = 10^8 - 10^9 \text{ M}^{-1} \text{ s}^{-1}$).³ However, enzymes with poor catalytic efficiencies may have lower K_{cat}/K_m values indicative of poor complex-product conversion or irreversible substrate-enzyme binding.

In this research, Michaelis-Menten kinetics were used to monitor competition experiments between a β -lactam chromogenic substrate, candidate β -lactam GUMBOS, and penicillinase P-0389, type 1 (*B. cereus* 3/5/2/6) in an effort to identify the role the cation has in the degradation of the β -lactam antibiotics. In this way, indirect participation in the catalysis of the β -lactam anion in the GUMBOS can be investigated and changes in its specificity constant can be compared to the sodium antibiotic.

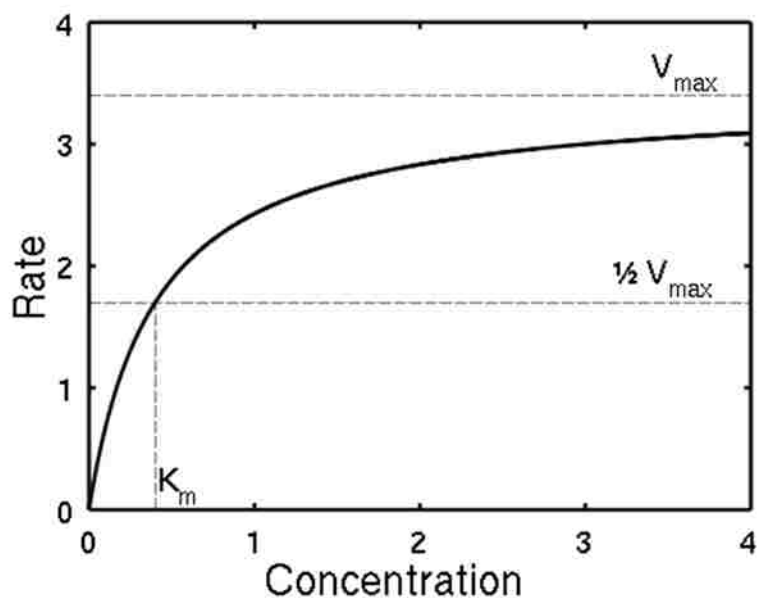


Figure 2.5. Representative rate versus substrate concentration plot obtained from Michaelis-Menten kinetic experiments.

The chromophore used in these experiments, CENTA, is a chromogenic analog to the β -lactam drug Cephalothin. Though not able to be used therapeutically, this agent has successfully exploited the kinetic properties of various penicillinase enzymes. Variations in its absorbance at either 260nm (decreasing; hydrolysis of the endocyclic amide bond) or 405 nm (increasing; appearance of the expelled chromophore) facilitates the monitoring of CENTA hydrolysis as reported by Bebrone *et al.*⁴ However, CENTA is incapable of displaying penicillinase presence and activity in agar colonies and therefore is limited to *in vitro* solution kinetic studies of viable penicillinase-containing bacteria or pure and crude enzyme extracts. Michaelis-Menten kinetic constants are interpreted using the aforementioned rate versus substrate concentration plot and mathematical relationships.

2.3.2 Mammalian Cell Cytotoxicity

In vitro cytotoxicity tests are necessary to assess cellular damage that is inflicted by the presence of different chemical agents. Likewise, the development of high throughput cell

viability assays has been propelled by the requisite to categorize potential therapeutics from poisons. This allows hypothetically toxic agents to be removed early in the drug discovery process. As such, cell viability assays premised on the absorbance of tetrazolium-converted formazan dyes has created the groundwork for many viability quantification studies.

There are several advantages to using *in vitro* cytotoxicity assays. Many assays have been developed to facilitate a quick and easy method to repetitiously assess drug toxicity. It relies on the sensitivity of an absorbance spectrophotometric plate reader and is able to be multiplexed to other systems. It also allows signal stability for flexible analysis time and minimal difference between sample plates. Sensitivity does depend on cell types, metabolic markers, incubation time, and cell quantity. Most importantly, it does not implement radioactive probes to assess cell viability. In contrast, it can be cost prohibitive and possible artifacts can come about that complicate the precise quantification of cell viability. For example, cell growth patterns among long term assay analysis studies can become problematic in that cells with high passage numbers may not convert dyes equally as younger cells. Similarly, some test compounds can interfere with the absorbance of the chromogenic probe.

The principle of tetrazolium-based assays relies upon the cellular metabolic activity of viable cells. In this case, mitochondrial reductases present in healthy, respirating cells are able to reduce the tetrazolium dye into formazan. When cellular damage has occurred by the presence of potential poisons, a reduction in the cell's metabolic activity occurs with a subsequent attenuation in the tetrazolium salt conversion to the formazan molecule. Dead cells are not able to reduce tetrazolium agents; thereby, creating a clear indicator of dead cells from living cells. To eliminate the confusion in dead and dying cells, most cytotoxicity measurements are performed either 24 hours or 48 hours after the addition of the novel therapeutic. That is because

apoptosis (programmed cell death) occurs within 30 minutes – 6 hours of drug exposure and robust cells may rehabilitate from toxicant exposure. More importantly, an absorbance measurement can be given by apoptotic cells (dying) and dying cells are not what is of interest in the early stages of drug discovery.

The first popular assay for measuring cell viability in a microtiter plate came from Mosmann in 1983, in which it was reported that viable cells reduce the yellow aqueous MTT (3-(4,5-dimethylthiazol-2-yl)-2,5-diphenyltetrazolium bromide) solution into a purple insoluble formazan crystal. Initially isopropanol was added as a cosolvent to dissolve the formazan solid. Nonetheless, dimethylsulfoxide, sodium dodecyl sulfate/dimethylformamide solutions, and other organic solvents have been used to also dissolve the formazan and make it readable using absorbance spectroscopy. This two-step assay creates a homogeneous solution with color intensity ($\lambda_{\text{abs}}=570\text{nm}$) that is directly related to cell population density. However, this assay has several chemical interferences that can distort the absorbance reading. Additionally, the judicious selection of a miscible co-solvent that will not destroy the microtiter plate is important as well. Therefore, the one-step MTS (3-(4,5-dimethylthiazol-2-yl)-5-(3-carboxymethoxyphenyl)-2-(4-sulfophenyl)-2H-tetrazolium) tetrazolium assay was developed to produce an aqueous soluble formazan product (Figure 2.6). A major difference in this assay and the MTT assay is that a co-solvent is not necessary due to the creation of the negatively charged formazan water-soluble molecule. Though less sensitive than MTT, this assay also has similar benefits to the MTT assay but absorbs differently at 490nm.

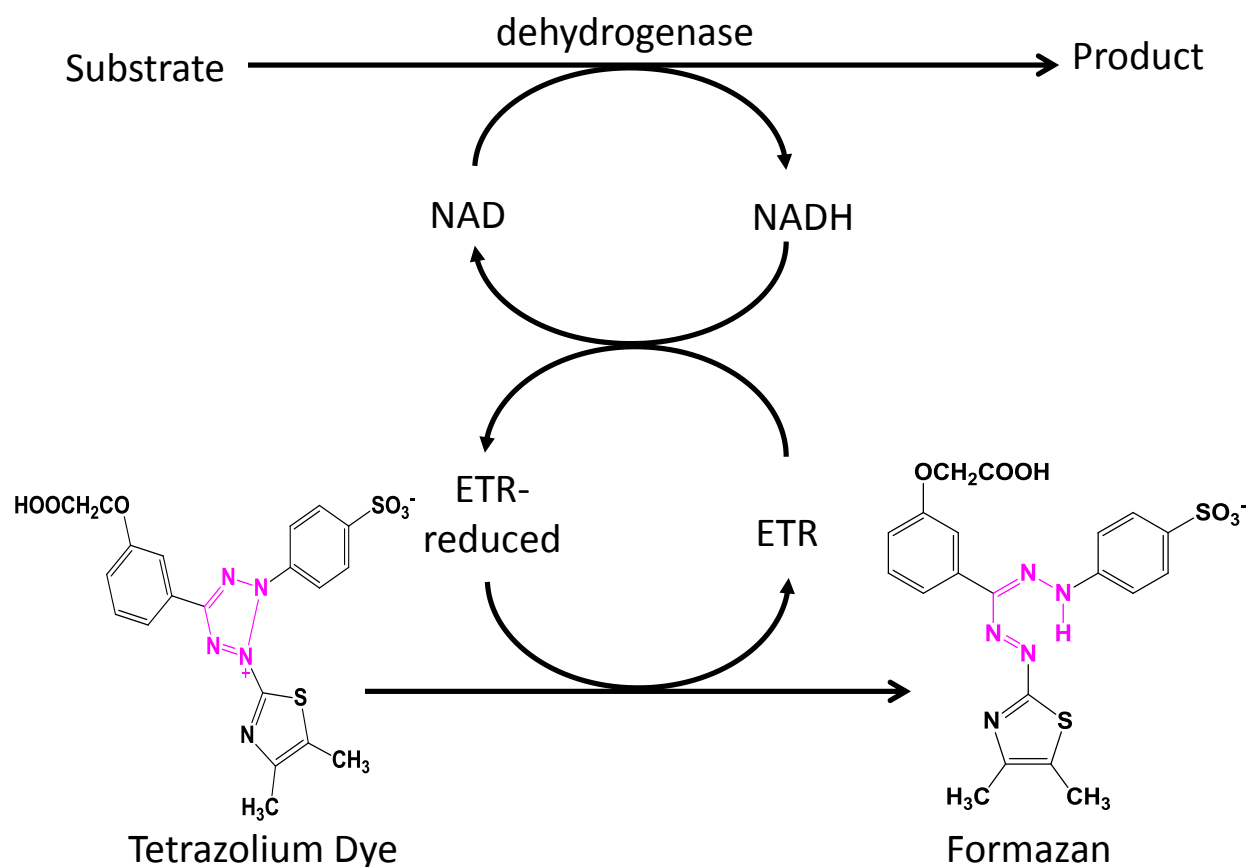


Figure 2.6. Conversion of MTS to soluble formazan by cellular dehydrogenase enzymes present in viable cells.⁵

2.4 Fluorescent-based Techniques

Biomedical research relies heavily on fluorescence-based techniques to reveal mechanisms at the cellular and molecular levels. The sensitivity and flexibility in fluorescence spectroscopy makes this approach suitable to investigate the intracellular and extracellular mechanisms of both eukaryotic and prokaryotic cells. Likewise, the ability to miniaturize this approach in microtiter plates yields minimal analyte consumption.

In fluorescence, a fluorophore absorbs a photon from an excitation source promoting it to a higher energy excited state in the same spin state. Highly absorbing fluorophores may become excited to higher electronic states above the first singlet excited state (S_1). In this case, the

photon will undergo a non-radiative decay via internal conversion to S_1 . Internal conversion may result from both vibrational and rotational losses such as collisions with solvent molecules or with other concomitants in the sample. Fluorescence emission from the first excited singlet state to ground state is a rapid process and occurs between 1×10^{-7} to 1×10^{-9} seconds.² A least probable radiative decay called phosphorescence occurs when an excited photon undergoes intersystem crossing to the excited triplet state and causes a phosphorescent emission as it decays to the ground triplet state. Phosphorescence has a longer radiative decay than fluorescence (*e.g.* 10^{-4} to 10 seconds) and as a result is usually the source used in glow-in-the-dark toys.² Often times a photon will decay to a higher vibrational level in the ground singlet state because it has emitted less energy than it absorbed. This causes a change, namely Stokes shift, in the emission spectrum to a longer wavelength (or lower energy state) relative to the excitation wavelength. Many factors can contribute to a Stokes shift such solvent effects, energy transfer, and the formation of complexes. The electronic transitions (*i.e.* non-radiative and radiative processes) of a molecule are illustrated using a Jablonski diagram (Figure 2.7).²

Steady-state fluorescence instrumentation consists of a light source, two monochromators (*i.e.* excitation and emission), a sample chamber, and a detector or photomultiplier tube (Figure 2.8). Many light sources are available for use in fluorescence spectroscopy, including lasers, photodiodes, and lamps. Two monochromators are used to filter transmitted light before and after passing through the sample. Differing from absorbance spectroscopy, the second monochromator is positioned orthogonally from the excitation light path to reduce the detection of incident radiation. Conventional fluorimeters use optically-transparent cuvettes (*e.g.* quartz, glass, polystyrene) to the wavelength ranges of interest to maximize the transmission and receipt of excited and emitted light, respectively.

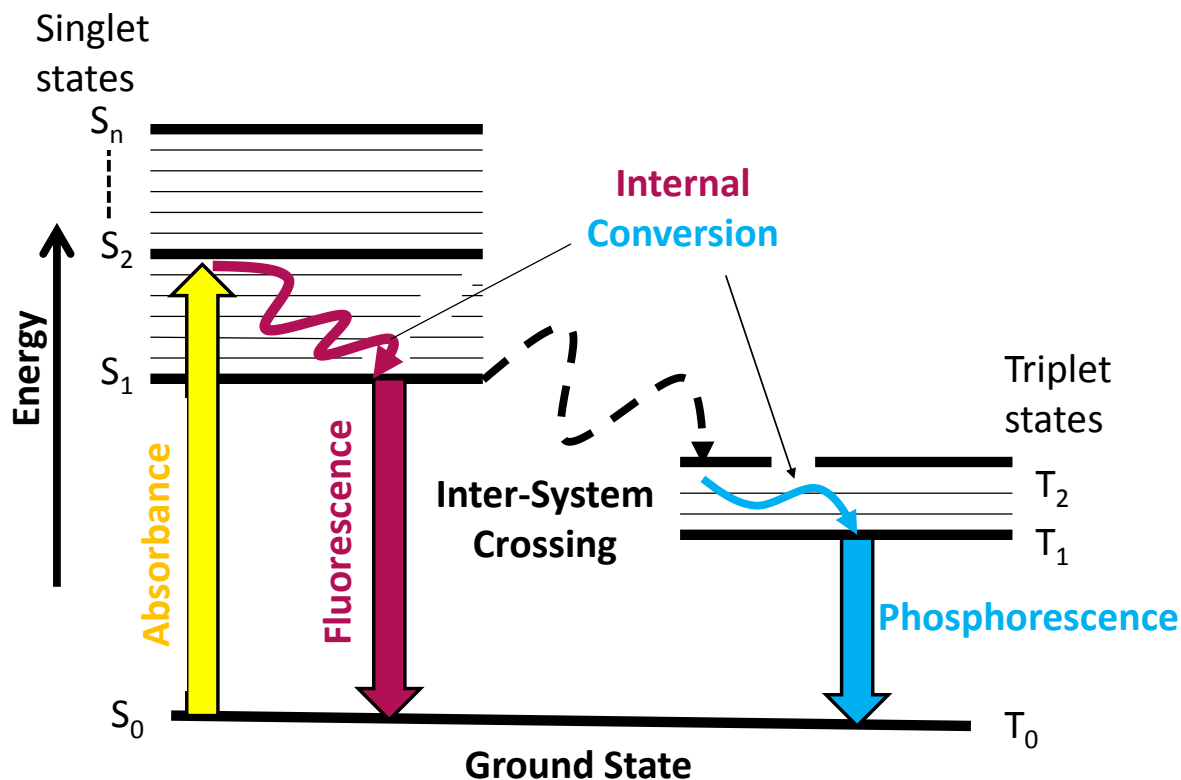


Figure 2.7. Jablonski diagram illustrating photophysical transitions of an excited molecule.

The optical pathway used in fluorescent plate readers is different than conventional steady state fluorimeters. Fluorescent microplate readers use special optics to guide the direction of the excited and emitted light to and from the sample well to the detector in an unconventional orthogonal manner. More specifically, excited light passes through the first monochromator to a mirror containing a hole that allows the excited light to be transmitted to the sample well.

Since the fluorescence occurs in all directions, the same mirror is used to direct the emitted light through the second monochromator to the detector. Opaque black-walled microtiter plates are used to minimize background fluorescence, scattering, and cross-talk between sample wells. Microplate readers also use various types of light sources; however, a 75W tungsten-halogen lamp was used as the light source for all fluorescence microtiter plate experiments

conducted in this dissertation. Tungsten-halogen lamps provide continuous light output from 250 to 700 nm making this approach useful for assaying fluorophores that emit from UV to near-IR wavelengths.² This high throughput approach uses an x-y scanning stage to continue automated measurements from well to well. A schematic of the optical pathway used in microplate reader was shown in Figure 2.4.

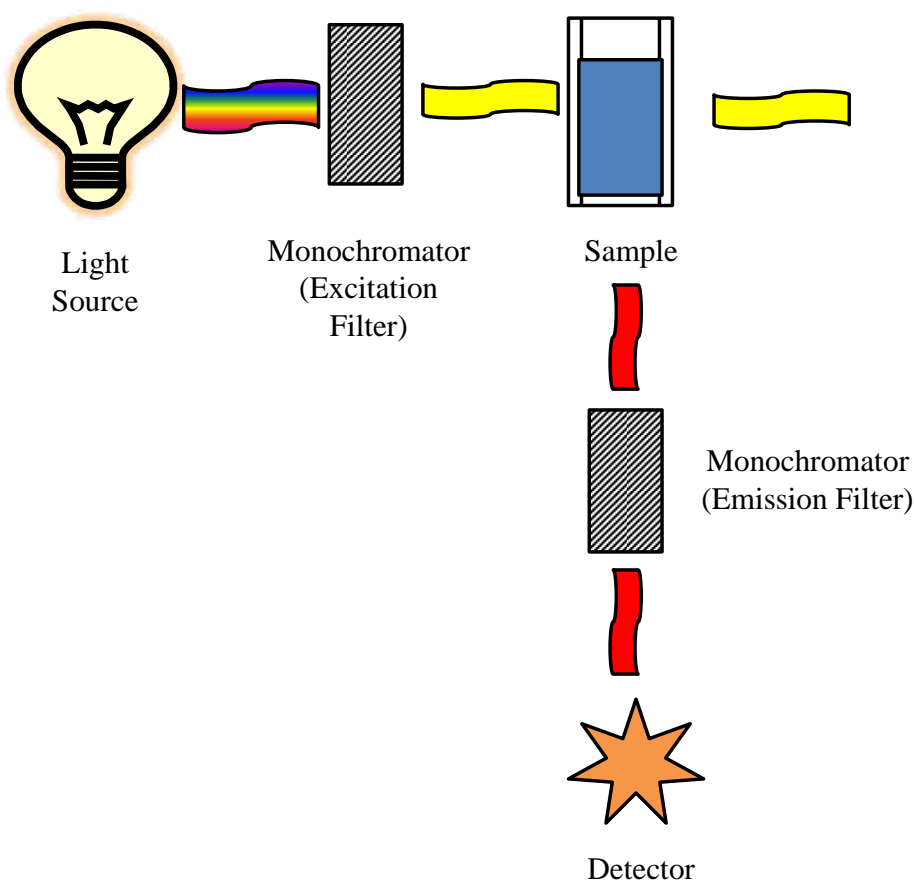


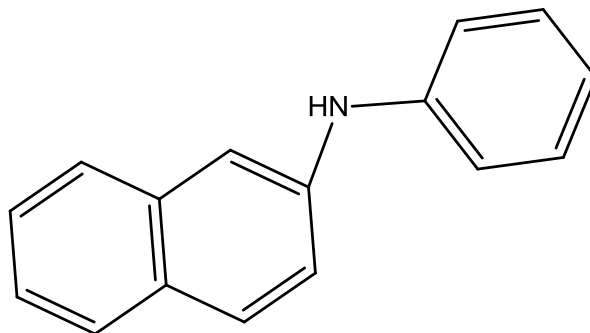
Figure 2.8. Instrumental configuration of a fluorescence spectrophotometer.

Both cuvette and microtiter plate steady-state fluorescence-based techniques were used in this dissertation to investigate the interactions the antimicrobial agents have with bacteria and to

elucidate their mechanisms of action. Several advantages and disadvantages are evident in the use of fluorescent techniques applied to *in vitro* bacterial research. For instance, fluorescent probes are able to be incorporated into intact cells without disrupting cellular membrane integrity. Likewise, they can be used at all phases throughout their maturation (*i.e.* lag, exponential, stationary, and death phases). Some probes can be used to distinguish viable and nonviable bacterial cells as well as specific cellular components and their activities. Thus, fluorescent probes were used in this research to examine the intracellular and extracellular changes within the microbe and their corresponding techniques and are briefly described below.

2.4.1 1-N-Phenylnaphthylamine (NPN) Permeability Assay

To investigate the membrane damage inflicted by the antimicrobial agents used in this research, an uncharged, lipophilic fluorophore called 1-N-Phenylnaphthylamine (NPN; $\lambda_{ex} = 350\text{nm}$, $\lambda_{em} = 420\text{ nm}$) was used Figure 2.9. Its drastic change in fluorescence emission from aqueous to lipophilic environments makes NPN a suitable probe to assess membrane damage. More specifically, NPN fluoresces weakly in aqueous environments but more strongly in hydrophobic environments similar to the interior of a bacterial membrane. NPN is not readily absorbed by viable bacteria cells and requires a membrane active antimicrobial agent to permeate the outer membrane for the fluorophore to interact with the lipophilic cellular constituents. Therefore, changes in the intensity of NPN steady-state fluorescence in membrane disrupted cells attributes this probe useful in elucidating antimicrobial agents and bacterial cell interactions. As such, NPN fluorescence has been used extensively to measure changes in outer membrane permeability of Gram-negative bacteria.⁶⁻¹⁷



1-N-Phenyl-naphthylamine (NPN)

Figure 2.9. Structure of 1-N-phenyl-naphthylamine (NPN) fluorophore used in membrane permeability studies.

2.4.2 BacLight Live/Dead Assay

BacLight Live/Dead assay uses two DNA intercalating dyes green fluorescent SYTO 9 and red fluorescent propidium iodide to investigate membrane integrity and cell viability. SYTO 9 penetrates all membranes in which green fluorescence is maintained by intact membranes. However propidium iodide, which can only penetrate permeabilized membranes due to its large size and negative charge, produces a red fluorescence in membrane-damaged cells by displacing SYTO 9 and quenching its fluorescence via Förster resonance energy transfer (FRET). FRET is a mechanism that describes the transfer of energy between two fluorophores when the emission band from a donor fluorophore overlaps with the excitation energy of an acceptor fluorophore.² This transfer of energy causes the acceptor fluorophore to become excited and emit energy. FRET efficiency is governed by the distance between acceptor and donor molecules, both SYTO 9 and propidium iodide must be in close proximity and the distance between donor – excitation and acceptor emission overlapping bands (<10nm).² The overlapping excitation/emission wavelengths between SYTO 9 (488 nm/533 nm) and propidium iodide (530 nm/635 nm) allow for propidium iodide to consume all of the emitted energy from SYTO 9 leading to its detection

being quenched and consequent quantification of living and dead cells to be performed. Representative spectra showing differences in percent live/dead cells are shown in Figure 2.10.

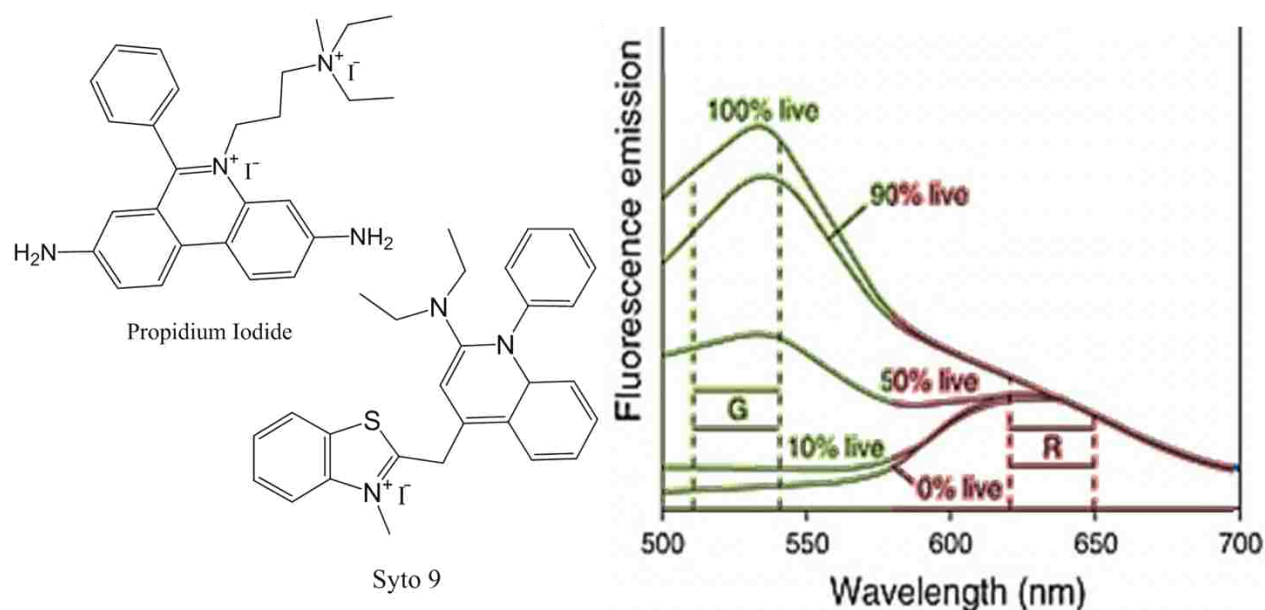


Figure 2.10. Structure of propidium iodide (A), SYTO 9 (B), and the spectra representing percentages of live and dead cells (C).

2.4.3 BacLight Membrane Potential Assay

Membrane potential is an important property of many functioning cells that governs the activity of biological processes. In theory, a voltage potential is generated when ions partition between the cells and the suspending medium thereby generating an electric charge. This difference in electrical potential between the interior and exterior of the cell can be quantified using the Nernst equation (Equation 2.6).

$$E = \frac{RT}{zF} \ln \frac{[X]_{out}}{[X]_{in}} \quad (\text{Eq. 2.6})$$

There are three factors that establish membrane potential: 1) intracellular and extracellular ion concentrations; 2) membrane permeability to ions by ion channels and their resulting ion conductance; and 3) the activity of electrogenic pumps that maintain the ion concentrations across the membrane.^{15, 17, 18} Therefore, an efflux or influx of certain ions (*e.g.*

potassium, sodium, chloride, hydrogen, magnesium, or calcium) into or from the cell in concentrations exceeding potential thresholds will cause detrimental effects on the viability of the organism or activity of the cellular process. The concentrations of select ions and the direction of flux are illustrated in Figure 2.11.

There are two extremes in membrane potential. Hyperpolarization occurs when a cell's membrane potential becomes more negative as caused by an efflux in potassium or influx of chloride. On the other hand, depolarization occurs when there is a net positive voltage in membrane potential. An influx in sodium ions or other cationic molecules can result in depolarization. When membrane active molecules permeate the cellular permeability barrier, ions contained extracellularly are able to distort membrane voltage as they travel inward. Thus, most membrane active molecules depolarize cells in addition to permeating the outer membrane. Studies on the neuronal networks, muscle contraction, and energy metabolism in both eukaryotes and prokaryotes have benefited from the use of voltage sensitive fluorescent probes. The ability of fluorescent probes to sense small incremental changes in membrane polarization and quantify differences in hyperpolarization or depolarization facilitates the impact various antibacterial agents have on bacterial cells. Much advancement in the development of voltage-sensitive probes and subsequent fluorescent based assays has been developed to overcome some challenges. More specifically, improvements in voltage sensitivity, absence of photodynamic damage, photobleaching, toxicity, and nonspecific binding have resulted in the success of rhodamine and carbocyanine dyes.

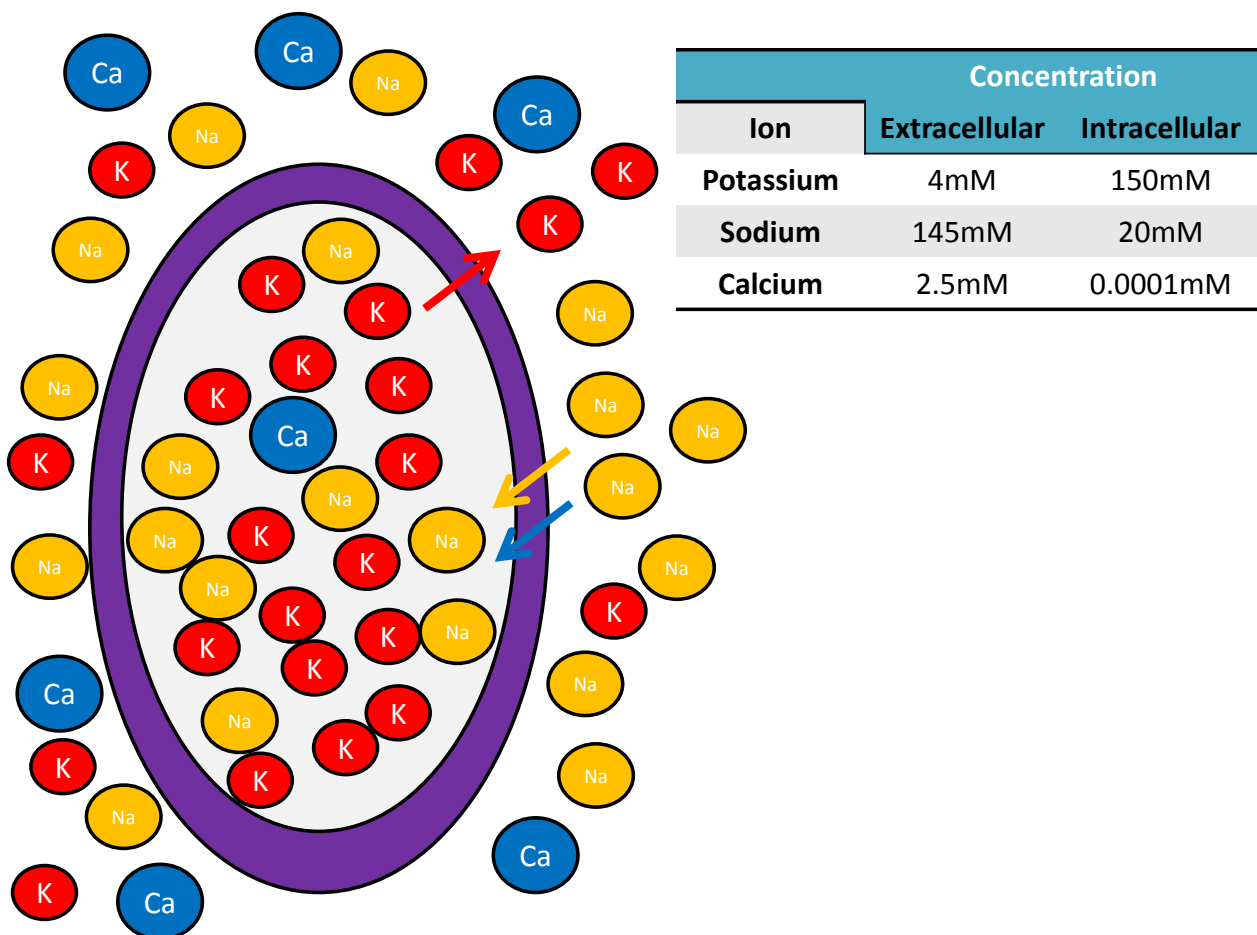


Figure 2.11. Direction of ion flux and their differences in intracellular and extracellular ionicity, where the abundance of potassium K^+ (red), sodium Na^+ (yellow), and calcium Ca^{+2} (blue) are highlighted and presented in an embedded table.

The fluorogenic dye used in this research is 3, 3'-diethylloxycarbocyanine iodide ($DiOC_2$) (Figure 2.12). This dye changes emission properties depending on the membrane potential environment of the cell. More specifically, $DiOC_2$ partitions into the cell and accumulates in the cytosolic regions. It becomes red when the cell is intact and can aggregate and the membrane potential is normal. However, red fluorescence (λ_{ex} 488nm, λ_{emRed} 612nm) decreases when the membrane potential is disrupted and the dye is released into the buffer medium. When the fluorophore is released into the aqueous medium as a result of depolarization, the strong fluorescence becomes green (λ_{ex} 488nm, $\lambda_{emGreen}$ 538nm).

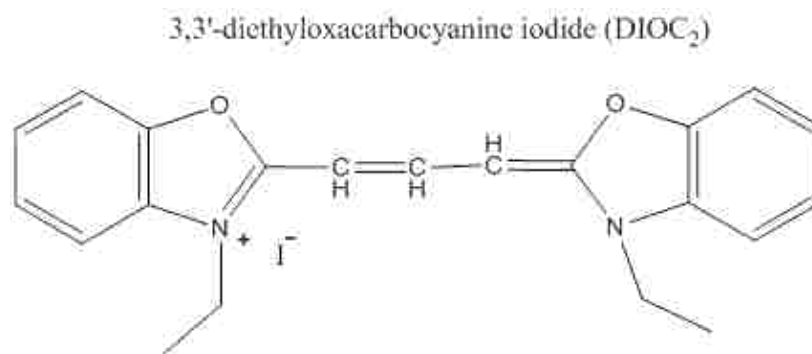


Figure 2.12. Chemical structure of DIOC₂ membrane potential probe.

To determine if the novel compounds affect the membrane potential of bacterial membranes, aliquots of log-phase inocula are treated with the antimicrobial agents as outlined in the BacLight™ Bacterial Membrane Potential assay kit. The proton ionophore that destroys membrane potential by eliminating the proton gradient but does not destroy membrane integrity, carbonyl cyanide 3-chlorophenylhydrazone (CCCP), is used as a positive control; whereas, the membrane permeant ethylenediaminetetraacetic acid (EDTA) was used as a negative control since it does not detrimentally effect membrane potential. Valinomycin, a potassium ionophore, helps to quantify the changes in membrane potential by translating fluorescence measurements into voltage so that the Nernst equation can be applied. Endpoint fluorescence red/green ratiometric values are used to quantify intracellular cytosolic potassium concentrations, its leakage, and corresponding changes in Nernst membrane potential. The red – to – green fluorescence ratio can distinguish the portion of bacteria with intact or hyperpolarized membranes (red fluorescence) and depolarized membranes (green fluorescence) since the DiOC₂ dye shifts from red – to – green emission upon changes in membrane potential and membrane integrity.

2.4.4 Lipopolysaccharide (LPS) Endotoxin Sequestration

Blood poisoning due to the release of lipopolysaccharides (LPS), or endotoxins, into the blood stream post-antibiotic therapy of Gram-negative bacterial infections is a common and serious problem. It plays a key role in the morbidity and mortality of critically ill patients since there are no present therapeutic options available to nullify its traumatic effects. LPS consists of two portions, a polysaccharide and a lipid (Lipid A). The polysaccharide moiety consists of repeating oligosaccharide units in which the number of units is uniquely associated to the species and genus among Gram-negative bacteria. The active and toxic portion of LPS is the hydrophilic negatively charged bisphosphorylated diglucosamine Lipid A. Although LPS is considered chemically inert, its systemic presence sets a cascade of exaggerated immune responses that lead to the implications associated with blood poisoning. For example, endotoxemia (endotoxins in blood) can seriously interfere with the proper function of the blood circulatory system and ultimately result in multiple organ failure.

To date, several macromolecules have been investigated for their potential in attenuating endotoxin-stimulated immunoinflammatory responses. More specifically, several polyclonal and monoclonal antibodies have been investigated for their ability to complex Lipid A. Unfortunately, both human and murine anti-Lipid A do not bind to LPS and thus show poor neutralization ability. Likewise, the use of non-antibody LPS complexants as an approach to prevent cellular recognition has been most recently pursued. Of this class, antimicrobial peptides (*i.e.* polymyxin B) have been recognized for their ability to sequester LPS but polymyxin B is too toxic for parenteral use. Hence, nontoxic analogs of polymyxin B with potent LPS sequestering abilities are in development. Since many potent drugs are not approved for parenteral use, structural-activity relationships have been sought to identify the pharmacophoric

regions within these molecules that allow successful binding and sequestration of LPS to further incorporate these features into nontoxic alternatives. Therefore, polycationic hydrophobic molecules with a clear demarcation of charged apolar regions are considered to be important. Similarly, the intermolecular distance between cationic groups is suggested to be $\sim 15\text{\AA}$ apart to match the distance between negative phosphate groups in the Lipid A structure.¹⁹⁻²¹ Several cationic amphiphilic molecules already approved for therapeutic use have been screened for their Lipid A binding and LPS neutralization activity. Among them were antimalarial, antipsychotic, and antiseptics. The strongest binders among those tested were chlorhexidine which was able to bind Lipid A with an affinity 80 times greater than monobiganidies. This confirmed that the inter-cationic distance and basicity of the cationic groups in dicationic molecules are important for strong LPS binding.

In this dissertation, chlorhexidine-based GUMBOS were investigated for their ability to sequester LPS endotoxins *in vitro* using the high-throughput BODIPY-cadaverine displacement assay.²² This assay uses the highly sensitive and robust BODIPY-TR Cadaverine (BC; $\lambda_{\text{ex}} = 580\text{nm}$, $\lambda_{\text{em}} = 620\text{nm}$) which has been shown to bind strongly to LPS. Using a displacement type of assay, the addition of a stronger binder than BC causes the fluorophore to be released and fluorescence emission to increase. This assay has been miniaturized and can be performed reproducibly using a cuvette or 96-well plate. Secondary properties of chlorhexidine can also be assessed when in the form of GUMBOS and the roles the various antibiotics have on its ability to successfully sequester LPS.

2.5 Scanning Electron Microscopy

Scanning electron microscopy (SEM) is a power microscopic technique used to characterize sub-micron materials and their morphologies. Its high spatial resolution capabilities

(*i.e.* <5nm) befits this technique to non-biological nanomaterials. However, SEM can also be used to characterize bacteria and visualize nanometer sized defects inflicted in its membrane. The instrumental configuration of a SEM is illustrated in Figure 2.13. A divergent electron gun is first used to generate a beam that is focused through condenser lenses to the sample. Scanning coils are used to move the electron beam across the sample that is focused using an objective lens. Electrons that collide with the sample become either backscattered or secondary electrons. Secondary electrons are collected into a photomultiplier tube which amplifies the electron signal and backscattered electrons are collected by a semiconductor array. Aberrations in the sample's surface deflect electrons with different intensities thereby causing the viewer to see an artificial three-dimensional image of the sample. For example, surfaces that are closer to the photomultiplier tube will result in the production of more backscattered electrons and a higher signal and surfaces that are further away appear darker. Since SEM measure sample deflected electrons, the sample must be prepared differently from that required of conventional microscopes. More specifically, SEM samples must be conductive in order for electrons to be deflected to the detector. If not, the sample will absorb the electrons and immediately become decomposed. Therefore, SEM sample are contained on a metal stub using conductive tape and are covered with a conductive coating (*e.g.* gold or platinum).

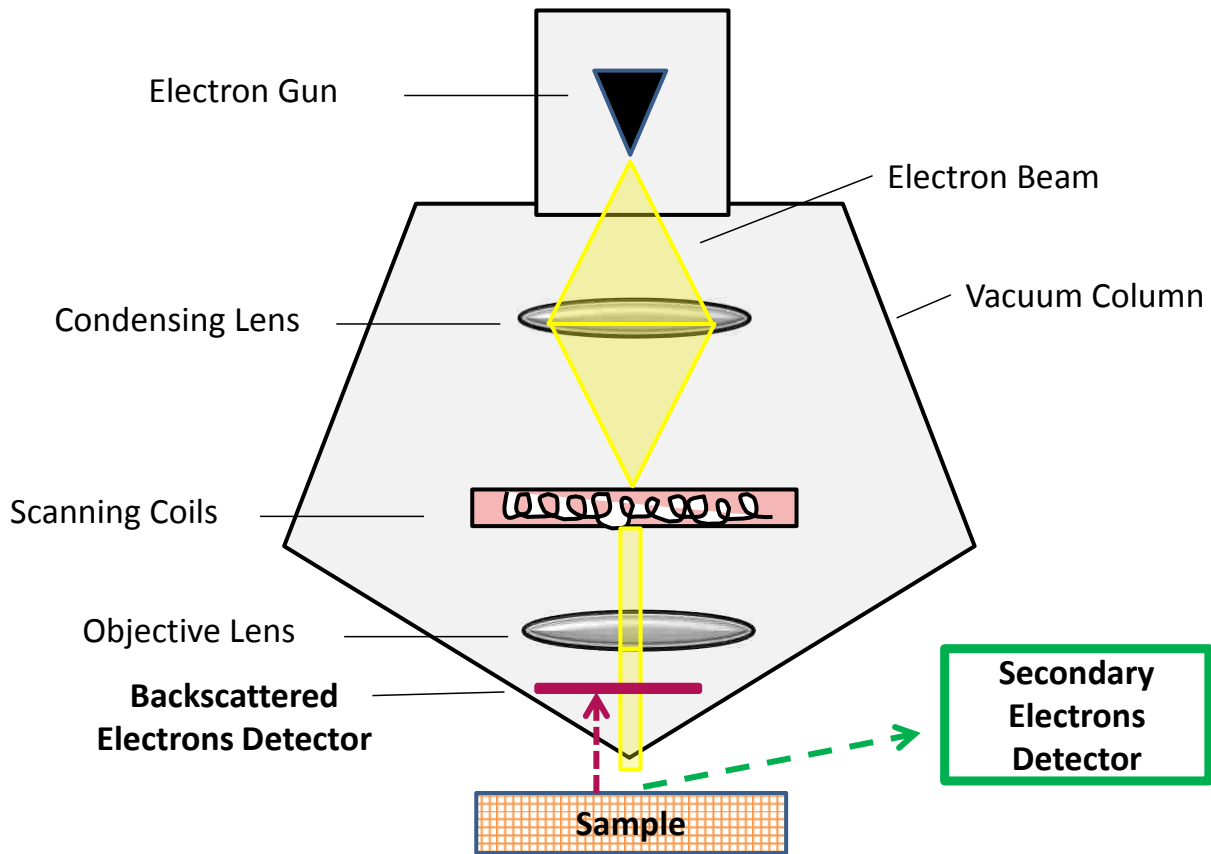


Figure 2.13. Instrumental configuration of a scanning electron microscope.

2.6 References

1. NCCLS. In *8th Informational Supplement*; National Committee for Clinical Laboratory Standards: Villanova, Pennsylvania, **2002**; Vol. *M100 S12*.
2. Lakowicz, J. *Principles of Fluorescence Spectroscopy*. 3rd ed. Springer Science: New York, **2006**.
3. Lehninger, A.L.; Nelson, D.L.; Cox, M.M., Eds. *Lehninger Principles of Biochemistry*. 4th ed. W H Freeman & Co: New York, **2004**.
4. Bebrone, C.; Moali, C.; Mahy, F.; Rival, S.; Docquier, J.D.; Rossolini, G.M.; Fastrez, J.; Pratt, R.F.; Frere, J.-M.; Galleni, M., *Antimicrobial Agents and Chemotherapy*, **2001**, *45*, (6), 1868-1871.
5. Riss, T.; Moravec, R., *Promega Notes Magazine*, **1996**, *59*, 19-23.

6. Broxton, P.; Woodcock, P.M.; Gilbert, P., *Journal of Applied Microbiology*, **1983**, *54*, (3), 345-353.
7. Hancock, R.E.; Wong, P.G., *Antimicrobial Agents and Chemotherapy*, **1984**, *26*, (1), 48-52.
8. Vaara, M., *Microbiological Reviews*, **1992**, *56*, (3), 395-411.
9. Ayres, H.; Furr, J.R.; Russell, A.D., *Letters in Applied Microbiology*, **1993**, *17*, (4), 149-151.
10. Cutter, C.N.; Siragusa, G.R., *Journal of Food Protection*, **1995**, *58*, (9), 977-983.
11. Helander, I.M.; Latva-Kala, K.; Lounatmaa, K., *Microbiology-Uk*, **1998**, *144*, 385-390.
12. Ayres, H.M.; Furr, J.R.; Russell, A.D., *Letters in Applied Microbiology*, **1999**, *28*, (1), 13-16.
13. Trauble, H.; Overath, P., *Biochimica Et Biophysica Acta*, **1973**, *307*, (3), 491-512.
14. Hancock, R.E.; Farmer, S.W.; Li, Z.S.; Poole, K., *Antimicrobial Agents and Chemotherapy*, **1991**, *35*, (7), 1309-1314.
15. Breeuwer, P.; Abee, T., *International Journal of Food Microbiology*, **2000**, *55*, (1-3), 193-200.
16. Helander, I.M.; Mattila-Sandholm, T., *Journal of Applied Microbiology*, **2000**, *88*, (2), 213-219.
17. Trevors, J.T., *Journal of Biochemical and Biophysical Methods*, **2003**, *57*, (2), 87-103.
18. Cao-Hoang, L.; Marechal, P.-A.; Lê-Thanh, M.; Gervais, P.; Waché, Y., *Biotechnology Journal*, **2008**, *3*, (7), 890-903.
19. David, S.A.; Sil, D.; Wang, X.; Quinn, P.J. Harris, J.R.; Biswas, B.B.; Quinn, P., Eds.; Springer Netherlands; Vol. 53, pp 255-283.
20. David, S.A.; Silverstein, R.; Amura, C.R.; Kielian, T.; Morrison, D.C., *Antimicrobial Agents and Chemotherapy*, **1999**, *43*, (4), 912-919.
21. David, S.A.; John Wiley & Sons, Ltd., **2001**; Vol. 14, pp 370-387.
22. Wood, S.J.; Miller, K.; David, S.A., *Combinatorial Chemistry & High Throughput Screening*, **2006**, *7*, (3), 239-249.

CHAPTER 3 DESIGN, SYNTHESIS, AND BIOLOGICAL EVALUATION OF BETA (β)-LACTAM ANTIBIOTIC-BASED IMIDAZOLIUM- AND PYRIDINIUM-TYPE IONIC LIQUIDS¹

3.1 Introduction

Data accumulated over the last decade show that there is an association between antimicrobial resistance in *Staphylococcus aureus*, *enterococci* and Gram-negative *bacilli* and increases in mortality, morbidity, length of hospitalization, and cost of healthcare.^{1, 2} Patients infected with antimicrobial-resistant organisms have higher associated treatment costs (US \$6,000–\$30,000) than do patients with infections of antimicrobial-susceptible organisms.³ Consequently, many antibiotics, particularly β -lactam drugs, are becoming less effective treatment options.^{1, 4-7} This challenge necessitates the development of more effective antibacterial agents. The development of ionic liquids (ILs) composed of antibiotics fortified with other antibacterial compounds was investigated in this study as a promising strategy to address antibiotic resistance.

Many strategies have been proposed to extend the efficacy and antibacterial spectrum of current antibiotics. As alternatives to *de novo* drug synthesis, methods that employ organized media as potential delivery agents to improve the absorption of various pharmaceutical agents have met with some clinical success.⁸⁻¹⁰ Examples include the use of QACs to improve the absorption, transport, and efficacy of various drugs. Specifically, dihydropyridinium salt delivery systems have successfully achieved targeted penicillin delivery to the central nervous system.¹¹ Other pyridinium salts have been used to selectively facilitate drug transport across the brain-blood barrier and dermis via enzymatic hydrolysis.¹²⁻¹⁵ Cetyltrimethylammonium bromide and related surfactants have enhanced drug absorption by various strains of Gram-negative and

¹ Reprinted by permission of Chemical Biology and Drug Design.

Gram-positive bacteria.¹⁶ These formulation strategies have been shown to facilitate the uptake of various antibiotics and improve their treatment properties.

In this study, a new set of ampicillin salts with quaternary ammonium cations, such as 1-butyl-3-methylimidazolium, 1-hexadecyl-3-methylimidazolium, 1-hexadecyl-2,3-dimethylimidazolium, cetyltrimethylammonium, and cetylpyridinium were synthesized and found effective on Gram-negative bacteria *Escherichia coli* O157:H7 and *Klebsiella pneumoniae*, as well as the Gram-positive *Staphylococcus aureus* and *Enterococcus faecium*. By taking advantage of the antibacterial nature of both the cationic and anionic components of the IL, we demonstrate the antibacterial utility of ILs for various biological and medical applications.

3.2 Experimental

3.2.1 Materials and Methods

3.2.1.1 Reagents

1-Methylimidazole and 1,2-dimethylimidazole, 1-bromohexadecane, cetylpyridinium bromide (CPB or [CP][Br]), cetyltrimethylammonium bromide (CTAB or [CTA][Br]), 1-butyl-3-methyl-imidazolium chloride ([BmIm][Cl]), sodium ampicillin ([Na][Amp]), sterile disks, brain heart infusion broth (BHI broth), Petri dishes (100 mm × 20 mm and 150 mm × 20 mm), 3-(4,5-dimethyl-2-thiazyl)-2,5-diphenyl-2H-tetrazolium bromide (MTT), chloroform, and diethyl ether were purchased from Sigma Aldrich (St. Louis, MO) and used without further purification; isopropanol and acetone were purchased from Mallinckrodt Chemicals (Phillipsburg, NJ), and ethanol was purchased from Pharmco-Aaper and Commercial Alcohols (Brookfield, CT). All solvents purchased were of analytical grade. Agar technical grade was purchased from Becton, Dickinson, and Company (Franklin Lakes, NJ).

3.2.1.2 Culture Preparation

Test organisms used in this study, *Escherichia coli* O157:H7 (ATCC 43895), *Escherichia coli* (ATCC 25922), *Staphylococcus aureus* (ATCC 6538), *Streptococcus mutans* (PCM 2502), *Enterococcus faecium* (ATCC 49474), *Listeria monocytogenes* (NCTC 7973), *Klebsiella pneumoniae* (ATCC 4352), *Salmonella enterica* serovar *typhimurium* (ATCC 14028) were received as a gift from collaborator Dr. Marlene Janes.¹⁷

3.2.1.3 General Procedure for Quaternization Reactions

Equimolar amounts of 1-methylimidazole or 1,2-dimethylimidazole and 1-bromoheptadecane were stirred in anhydrous ethanol under reflux for 48 h in an argon atmosphere. Ethanol was removed and the product was washed with diethyl ether. A white solid was obtained after filtration. The product was dried and purified in acetone using the recrystallization method.

3.2.1.4 General Procedure for Anion Metathesis

A typical anion-metathesis reaction procedure is as follows: [CP][Br] (1 equiv.) was dissolved in chloroform with the slow addition of aqueous [Na][Amp] (1.1 equiv.) into the solution. The chloroform-water mixture (4:1 v/v) was stirred for 48 h at room temperature. The upper aqueous solution was separated and washed with fresh chloroform to obtain all exchanged product. The removal of chloroform *in vacuo* yielded the white product, [CP][Amp], which was further freeze-dried on a lyophilizer. Other Amp-ILs (*i.e.* [Bmim][Amp], [C₁₆M₁Im][Amp], and [C₁₆M₂Im][Amp]) were synthesized in the same manner.

3.2.1.5 Ionic Liquid Characterization

These compounds were characterized using ¹H-NMR (Bruker Avance-250, 250MHz) with DMSO-d₆ as solvent. The elemental composition was determined using Leco 932 CHNS Analyzer (Atlantic Microlab, Inc. Norcross, GA). The thermal properties including melting

points were determined using a differential scanning calorimetry (DSC Q100, TA Instruments, Wilmington, DE).

3.2.1.6 Critical Micelle Concentration (CMC)

The critical micelle concentration of the Amp-ILs was determined by measuring the surface tension with a Sigma 703 tensiometer at 298K. Several half-fold dilutions were made from a 2mM stock solution of both QAC and Amp-ILs. This method used a DuNuoy ring with a circumference of 5.992 cm.

3.2.1.7 Solubility

The solubility of Amp-ILs was determined using a Shimadzu UV-3101 PC scanning spectrophotometer. Briefly, this included measuring the absorbance of half-fold dilution series ranging up to 2 mg/mL of sodium ampicillin in water. Since sodium ampicillin has three characteristic absorption bands (*i.e.* 257 nm, 262 nm, and 268 nm),¹⁸ these bands were used to confirm and quantify the solubilities of the Amp-ILs via the construction of a calibration curve (R=0.99). Two mg/mL of each Amp-IL was dissolved in water with one minute of high mixing and thirty minutes of sonication at room temperature. The suspension was filtered with a 0.45 μm and the filtrate was measured for solubility. The Amp-IL acquired absorbance was converted into concentration using a Beer's Law relationship from the sodium ampicillin slope. It was noted that the imidazolium bromide absorbs at lower energies and therefore does not interfere with the absorbance intensities of the ampicillin anion.¹⁹⁻²¹ Also, no absorption was detected for [CTA][Br] either. However, [CP][Br] does absorb within this same range. To compensate for the cross-absorbance in [CP][Amp], the absorbance of [CP][Br] at equal concentrations of [CP][Amp] were subtracted to only obtain the absorbance of the anionic portion of the Amp-IL.

3.2.1.8 Antibacterial activity - Minimum Inhibitory Concentration (MIC) and Minimum Bactericidal Concentration (MBC)

The minimal inhibitory concentration (MIC) values were determined in triplicate by the broth dilution method in a 96-well microtiter plate using Mueller-Hinton Broth.²² The test organisms were grown individually on brain heart infusion (BHI) agar for 24 h at 37°C prior to each antibacterial test. The growth was adjusted using colony plate counts. Bacteria of 10⁵ CFU/mL concentrations were exposed to an Amp-IL concentration range of 0.8 µM to 0.2 mM. The MIC for each Amp-IL was recorded as the lowest concentration that showed no turbidity after 24 h of incubation at 37°C. Turbidity is an indication of microbial growth and if present, the corresponding concentration of antibacterial agent is considered ineffective. To determine whether the Amp-ILs inhibited growth or killed the bacteria, twenty microliters of (3-[4,5-dimethylthiazol-2-yl]-2,5-diphenyl tetrazolium bromide) or MTT (1 mg/mL) was added to the non-turbid wells of the MIC assay plate and incubated for 2 h at 37 °C for the bacteriostatic/-cidal status determination.^{23, 24} In the case of viable cells with inhibited growth, the tetrazolium dye (*i.e.* yellow solution) would be metabolically reduced to aqueous soluble formazan crystals (*i.e.* purple solution); however, a solution containing dead bacterial cells would remain yellow.²⁴

3.3 Results and Discussion

3.3.1 Physical Characterization of Amp-ILs

3.3.1.1 Synthesis and Characterization

The synthesis of 1-alkyl-3-methylimidazolium ILs involved the quaternization of 1-methylimidazole or 1,2-dimethylimidazole with 1-bromohexadecane followed by anion-exchange. Quaternization was carried out for 48 h under reflux in anhydrous ethanol under argon atmosphere. Amp-ILs (Table 3.1) were synthesized by anion-exchange reactions between the synthesized imidazolium bromides [Im][Br] or commercially available QAC (*e.g.*

cetyltrimethylammonium [CTA][Br] and cetylpyridinium bromide [CP][Br]) and excess sodium ampicillin [Na][Amp] in a chloroform-water (4:1 v/v) mixture. The resulting products, 1-butyl-3-methylimidazolium ampicillin [BmIm][Amp], 1-hexadecyl-3-methylimidazolium ampicillin [C₁₆M₁Im][Amp], 1-hexadecyl-2,3-dimethylimidazolium ampicillin [C₁₆M₂Im][Amp], cetyltrimethylammonium ampicillin [CTA][Amp], and cetylpyridinium ampicillin [CP][Amp], were isolated as solids at room temperature and purified by washing with anhydrous diethyl ether. These salts have limited solubility in water, but are soluble in ethanol, isopropanol, dimethylsulfoxide, and chloroform.

3.3.1.2 Ampicillin – ILS NMR Characterization

Amp-ILs were characterized using ¹H-NMR (Figure 3.1) and elemental analysis. All Amp-ILs contained the chemical shifts of the ampicillin anion and the respective cations. In the case of [BmIm][Amp] and [C₁₆M₁Im][Amp], a singlet peak was observed with a chemical shift at 9.29 ppm and 9.11 ppm which was attributed to the acidic proton in the C2 position of both imidazolium cations. These peaks are also present in the di-substituted imidazolium halide salts. However, this acidic peak was absent in the spectra for [C₁₆M₂Im][Amp] because of the methyl group substituted on C2. In fact, a singlet at 3.73 ppm is evident of a methyl group substituted on the C2 position of the imidazolium. There was a small upfield shift once the halogen was exchanged for the less electron-donating ampicillin anion (not shown). In addition, the chemical shifts between the hydrogens on the C4 and C5 positions of the imidazolium rings decreased upon successful metathesis. A secondary set of multiplets ranging from 8.27 – 9.19 ppm present in the ¹H-NMR of [CP][Amp] are attributed to the more electron withdrawing nitrogen in the pyridinium ring. The anion exchange from bromide to ampicillin anion was confirmed by examining the multiplet ranging from 7.11 – 7.52 ppm that was directly contributed by the benzyl group in the ampicillin structure. Proton peaks from the substituted methyls on the

quaternary ammonium group in [CTA][Amp] are also evident as a singlet at 1.25 ppm. Lastly, a strong singlet at approximately 1.22 ppm validated the existence of the long alkyl chain in the cation moiety for each Amp-IL.

The surface tension of Amp-ILs and the corresponding surfactant cation groups at different concentrations was measured at 25°C to determine if the micellar properties of the cation were maintained. Figure 3.2 shows a comparison between the critical micelle concentrations (CMCs) between halide-QACs and Amp-ILs. The results show that in each case, the Amp-ILs has lower surface tension than the parent QACs. Critical micelle concentrations were determined from the plot of surface tension and concentration. The tensiometry measurements for [Bmim][Cl] and [Bmim][Amp] demonstrated no discontinuity and that a CMC could not be established. This correlates with previously reported data for [Bmim][Cl].²⁵ Since ampicillin does not have a surfactant-like structure, no enhanced micellization properties were expected for [Bmim][Amp]. Thus, increasing CMCs for Amp-ILs occurs as [CP][Amp] ≤ [C₁₆M₁Im][Amp] < [C₁₆M₂Im][Amp] < [CTA][Amp]. This differs slightly from the order of the halide-QAC CMC values, in which [C₁₆M₁Im][Br] ≤ [C₁₆M₂Im][Br] < [CP][Br] < [CTA][Br]. Substantial reductions in surfactant-like properties for Amp-ILs ranged between 5 – 29 times as compared to halide-QAC, with the least and greatest change observed for [C₁₆M₂Im][Amp] and [CP][Amp], respectively. Since the CMC is dependent upon the nature of the amphiphile, size of the head group, and the length of the alkyl chain, this decrease in CMC is attributed mostly to the larger ampicillin anion that is likely to prevent hydration within the micellar core. This phenomenon was observed in CMC studies containing 1-dodecyl-3-methylimidazolium chloride [DMIM][Cl], in which CMC values were halved once a larger bromide ion replaced the chloride ion.²⁵⁻²⁷ Therefore, the metathesis of anions appears to modify the lipophilic/hydrophilic balance

observed in surfactants. Thereby, it is apparent that Amp-ILs are more hydrophobic than the starting materials used in this study.

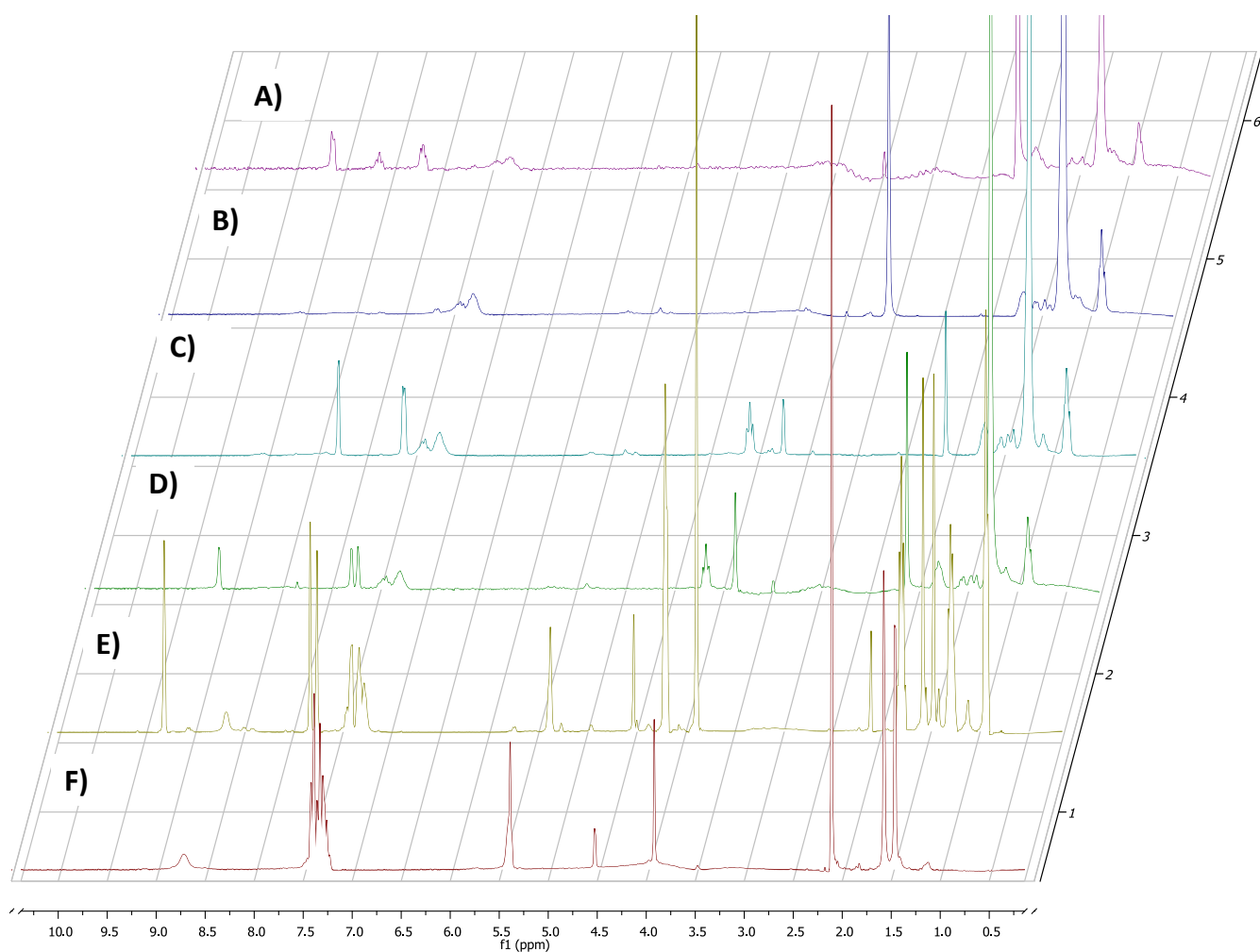


Figure 3.1. Stacked proton nuclear magnetic spectra of various Amp-ILs synthesized in this study, where A=[CP][Amp]; B= [CTA][Amp]; C =[C16M2Im][Amp]; D = [C16M1Im][Amp]; E = [BmIm][Amp]; and F = [Na][Amp].

3.3.1.2.1 Cetylpyridinium Ampicillin ([CP][Amp]),

Yellow solid, yield, 92%. Mp = 56°C [CP][Amp]. CMC= 24 μ M [CP][Amp]; 690 μ M CPB. Water solubility: 348 μ g/mL. 1 H NMR (250 MHz, DMSO) δ 8.73 (tt, 5H), 7.24 (m, 5H),

2.09 (s, 14H), 1.91 (s, 4H), 1.49 (d, 6H), 1.24 (s, 20H), 0.86 (s, 2H). Anal. Calcd for $C_{37}H_{56}N_4O_4S$: C, 68.06; H, 8.64; N, 8.58; S, 4.91. Found: C, 67.97; H, 8.57; N, 8.55; S, 4.84.

3.3.1.2.2 1-Hexadecyl-3-methylimidazolium Ampicillin ($[C_{16}M_1Im][Amp]$)

Off-white solid, yield, 91%. Mp = 55°C $[C_{16}M_1Im][Amp]$. CMC = 24 μ M $[C_{16}M_1Im][Amp]$; 430 μ M $[C_{16}M_1Im][Br]$. Water solubility: 379 μ g/mL. 1H NMR (250 MHz, DMSO) δ 9.11 (s, 1H), 8.31 (s, 1H), 7.72 (d, 2H), 7.59 – 7.12 (m, 5H), 5.36 (s, 2H), 4.14 (t, 2H), 3.85 (s, 2H), 2.09 (s, 3H), 1.77 (t, 2H), 1.47 (dd, 10.0 Hz, 6H), 1.24 (s, 28H), 1.09 (s, 3H), 0.85 (d, 2H). Anal. Calcd for $C_{36}H_{57}N_5O_4S$: C, 65.92; H, 8.76; N, 10.68; S, 4.89. Found: C, 65.79; H, 8.81; N, 10.42; S, 4.87.

3.3.1.2.3 1-Hexadecyl-2,3-dimethylimidazolium Ampicillin ($[C_{16}M_2Im][Amp]$)

Off-white solid, yield, 94%. Mp = 65°C $[C_{16}M_2Im][Amp]$. CMC = 92 μ M $[C_{16}M_2Im][Amp]$; 450 μ M $[C_{16}M_2Im][Br]$. Water solubility: 475 μ g/mL. 1H NMR (250 MHz, DMSO) δ 8.27 (s, 1H), 7.60 (dd, 2H), 7.53 – 6.95 (m, 5H), 5.70 (s, 2H), 5.30 (d, 4H), 4.07 (t, 2H), 3.73 (s, 3H), 2.09 (s, 1H), 1.68 (s, 6H), 1.22 (s, 30H), 0.83 (d, 3H). Anal. Calcd for $C_{37}H_{59}N_5O_4S$: C, 66.33; H, 8.88; N, 10.45; S, 4.79. Found: C, 66.21; H, 8.84; N, 10.44; S, 4.72.

3.3.1.2.4 Cetyltrimethylammonium Ampicillin ($[CTA][Amp]$)

Off-white solid at 90% yield. Mp = 73.89-81.36°C, CMC = 101 μ M $[CTA][Amp]$; 923 μ M $[CTAB]$. Water solubility: not determined. 1H NMR (250 MHz, DMSO) δ 9.03 (s, 1H), 7.80 – 6.99 (m, 5H), 5.69 (s, 2H), 5.31 (d, J = 25.7 Hz, 2H), 3.93 – 3.77 (m, 2H), 3.27 (dd, J = 18.0, 9.8 Hz, 2H), 3.03 (s, 9H), 1.66 (s, 2H), 1.63 – 1.36 (m, 26H), 1.25 (s, 6H), 0.85 (d, J = 6.7 Hz,

3H). Anal. Cald for C₃₅H₆₀N₄O₄S: C, 66.42; H, 9.55; N, 8.85; O, 10.11; S, 5.07. Found: C,66.17; H, 9.53; N, 8.61; O, 10.58; S, 5.11.

3.3.1.2.5 1-Butyl-3-methylimidazolium Ampicillin ([Bmim][Amp])

Yellow viscous liquid in 91% yield. Mp = liquid at room-temperature. CMC= none [Bmim][Amp]; none [Bmim][Cl]. Water solubility: not determined. ¹H NMR (400 MHz, DMSO) δ 9.29 (s, 1H), 8.67 (s, 1H), 7.77 (d, *J* = 27.3 Hz, 2H), 7.52 – 7.11 (m, 3H), 5.35 (d, *J* = 3.8 Hz, 1H), 4.49 (d, *J* = 13.2 Hz, 1H), 4.18 (t, *J* = 7.2 Hz, 2H), 3.92 – 3.74 (m, 4H), 3.47 – 3.09 (m, 2H), 2.55 (d, *J* = 30.0 Hz, 1H), 2.09 (s, 1H), 1.86 – 1.71 (m, 2H), 1.54 (d, *J* = 11.2 Hz, 3H), 1.42 (d, *J* = 20.6 Hz, 3H), 1.32- 1.22 (m, 4H), 0.99 – 0.84 (t, 2H). Anal. Cald for C₂₄H₃₃N₅O₄S: C, 59.12; H, 6.82; N, 14.36; O, 13.12; S, 6.58. Found: C, 59.01; H, 7.08; N, 14.22; O, 13.43; S, 6.26.

3.3.1.3 Solubility

The solubility of Amp-ILs in water was characterized using UV-vis spectroscopy. We determined the solubility for select Amp-ILs are 475, 379, and 348 μg/mL for [C₁₆M₂Im][Amp], [C₁₆M₁Im][Amp], [CP][Amp], respectively. A 100- to 150-fold reduction (*R*²=0.99) in the aqueous solubility of ampicillin was observed once the sodium was replaced with a quaternary ammonium group. Aqueous solubility for [BmIm][Amp] and [CTA][Amp] was not able to be accurately quantified. A positive control consisting of Amp-ILs in isopropanol confirmed that the anionic ampicillin was an intact part of the IL structure as evidenced by absorption bands at 257, 262, and 268 nm.

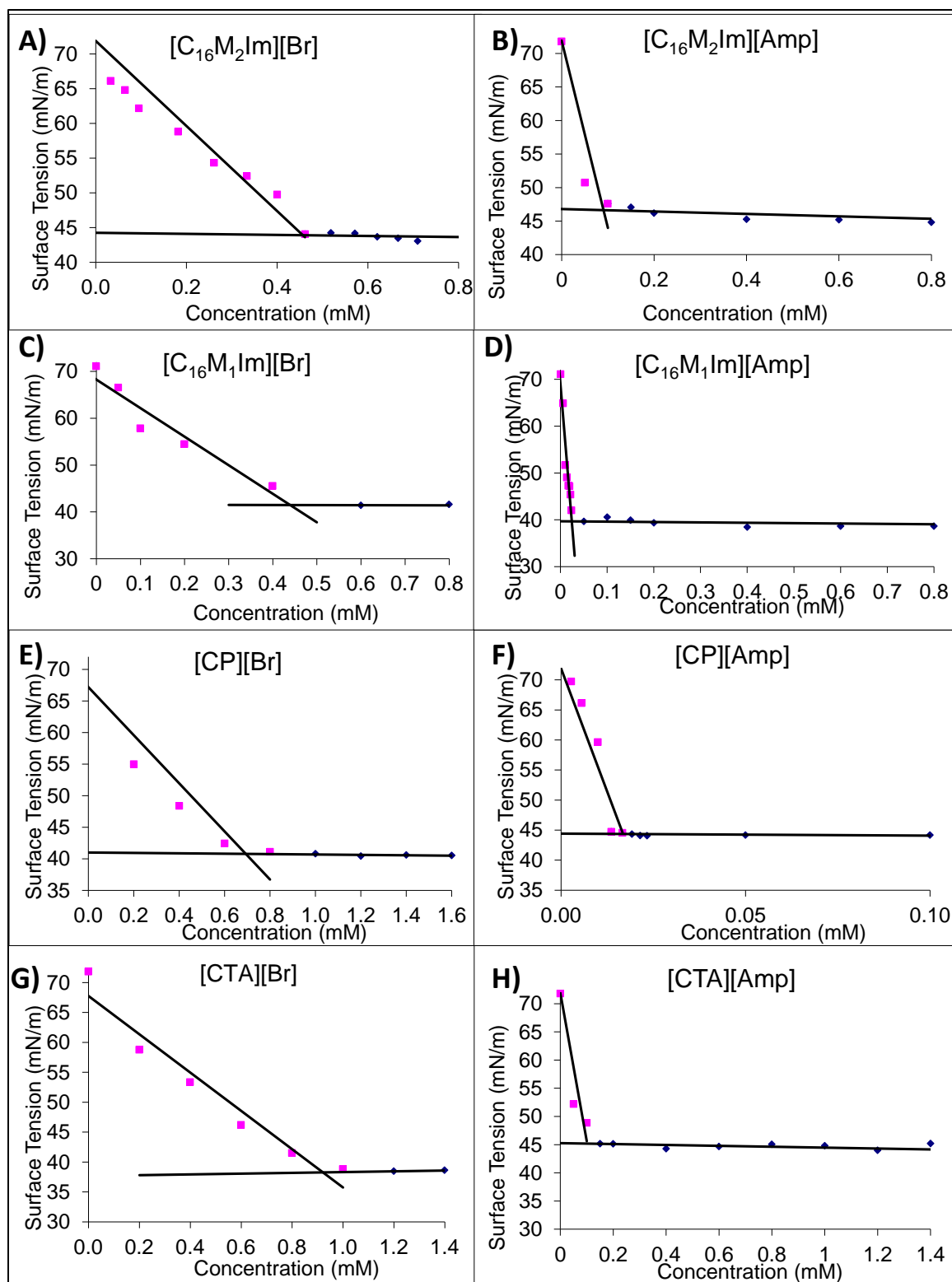
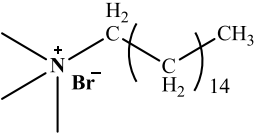
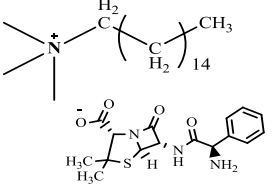
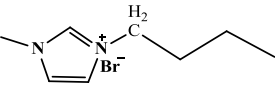
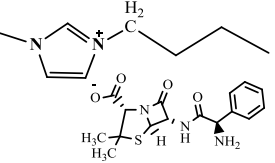
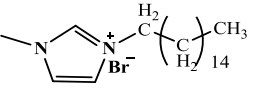
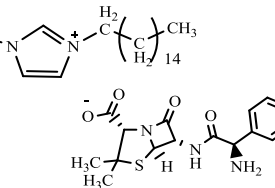
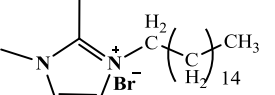
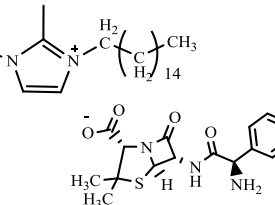
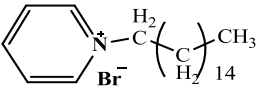
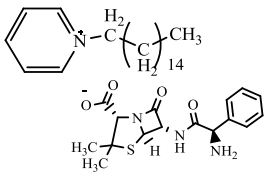


Figure 3.2. Comparison between critical micelle concentrations of imidazolium and pyridinium halides and their corresponding Amp-ILs.

Table 3.1. Synthesis and structures of five ampicillin-based ionic liquids by anion-exchange reactions.

C16-Quaternary Ammonium with Br ⁻ as Anion			Ampicillin – based IL C16-Quaternary Ammonium with Ampicillin as Anion		
Structure	Name and Abbreviation		Structure	Name and Abbreviation	
	Cetyltrimethyl ammonium bromide	[CTA][Br]		Cetyltrimethyl ammonium ampicillin	[CTA][Amp]
	1-butyl-3-methylimidazolium chloride	[BmIm][Br]		1-butyl-3-methylimidazolium ampicillin	[BmIm][Amp]
	1-hexadecyl-3-methylimidazolium bromide	[C ₁₆ M ₁ Im][Br]		1-hexadecyl-3-methylimidazolium ampicillin	[C ₁₆ M ₁ Im][Amp]
	1-hexadecyl-2,3-dimethylimidazolium bromide	[C ₁₆ M ₂ Im][Br]		1-hexadecyl-2,3-dimethylimidazolium ampicillin	[C ₁₆ M ₂ Im][Amp]
	cetylpyridinium bromide	[CP][Br]		cetylpyridinium ampicillin	[CP][Amp]

3.3.2 Antibacterial MIC of ILs

3.3.2.1 Disk-Diffusion Results

The antimicrobial activity of Amp-ILs were qualitatively tested against reference strains of Gram-positive (*L.monocytogenes* 7973 and *S.aureus* 6538) and Gram-negative (*S.typhimurium* 14028. and *E. coli* O157:H7 43895) bacteria. The antimicrobial efficacy of Amp-ILs were qualitatively studied using the Kirby-Bauer Disk Diffusion method (NCCLS M7-A7) against two Gram-positive and two Gram-negative bacteria prior to assessing the minimum inhibitory concentrations (MICs). Zones of inhibition are summarized in Figure 3.3.

The propensity to diffuse and the antibacterial activity of Amp-ILs against select Gram-positive and Gram-negative bacteria were evaluated by the disk-diffusion assay. According to the zone diameter interpretive standard values (NCCLS M2-A4, 1983), the susceptibility zone of *Enterobacteriaceae* and highly sensitive Gram-positive bacteria are above 14 mm and 29 mm for 10 µg ampicillin, respectively (Table 3.2).

Table 3.2. Diffusion zone ranges based on NCCLS diameter criterion for sodium ampicillin disks against Gram-negative and Gram-positive bacteria.

Antibiotic and Bacterial Class	Disk potency	Inhibition zone diameter to nearest mm		
		Resistant	Intermediate	Susceptible
Ampicillin - Gram-negative rods and enterococci	10 µg	11	12 – 13	14
Ampicillin - Staphylococci and highly penicillin-sensitive organisms	10 µg	20	21-28	29

By these zone standards both Amp-ILs and [Na][Amp] are considered ampicillin resistant to Gram-positive bacteria. Therefore, interpretation of the results are based on Gram-negative bacteria susceptibility to these agents. In the case of [Na][Amp], a large diameter indicating Gram-negative susceptibility was observed. *E. coli* O157:H7 did not show susceptibility to any

of the Amp-ILs tested. Interestingly, susceptibility to *S. typhimurium* 14028 was observed for all Amp-ILs, except for the intermediate inhibition zone formed by [C₁₆M₁Im][Amp]. Overall, Amp-ILs diffused poorly as compared to [Na][Amp], While diffusion was not completely inhibited by combining the two salts, none of the Amp-IL compounds diffused as well as [Na][Amp]. We attribute this result to greater hydrophobicity in Amp-IL.; thereby, causing diffusion in aqueous-based agar to be limited. Due to the aforementioned limitation among others caused by the physico-chemical properties of antimicrobial agents, inhibitive zones cannot be used to completely qualify antibacterial activity. Thus, the antibacterial activities of these compounds were tested *in vitro* using the broth-dilution MIC test.

3.3.2.2 Minimum Inhibitory Concentration Results

The antibacterial activity of ampicillin-type ammonium-, pyridinium-, and imidazolium-based ILs were tested against eight bacteria (*i.e.* 4 Gram-positive and 4 Gram-negative). To quantify their antibacterial activities, the minimum inhibitory concentrations (MICs) and minimum bactericidal concentrations (MBC) were determined. As controls, the precursor ions of the Amp-ILs were evaluated for antimicrobial activity to determine the difference in activity between the molecular and IL form of the compounds. The MIC results demonstrate that each Amp-IL exhibited variable activity against both Gram-positive and Gram-negative bacteria (Table 3.3). In sum, the antibacterial activity against Gram-positive bacteria in order of higher MIC value is [CP][Amp] < [CTA][Amp] < [C₁₆M₂Im][Amp] < C₁₆M₁Im][Amp] < [Na][Amp] < [BmIm][Amp]. The antibacterial activity of Amp-ILs against Gram-negative bacteria follow a similar trend as [CP][Amp] < [CTA][Amp] < [C₁₆M₂Im][Amp] < C₁₆M₁Im][Amp] < [Na][Amp] < [BmIm][Amp]. Overall increases in activity ranged from 2-43 times compared to [Na][Amp].

3.3.2.2.1 Ammonium – based Ampicillin Ionic Liquid

The ammonium-type ampicillin IL is composed of four parts: the head ammonium, the C16-alkyl chain, three methyl groups, and the anion (bromide or ampicillin). The MICs of [CTA][Br] against Gram-positive bacteria are comparable to [CTA][Amp], although ranging from 2 – 30 μ M. Considerable differences in antibacterial activity between [CTA][Br] and [CTA][Amp] reveal concentration gaps from 3 to 13 times. Effective antibacterial activities range from 5 to 30 μ M for Gram-negative bacteria. Our results show that [CTA][Amp] was most effective against *E. coli* O157:H7 43895 and *S. mutans* 2502 with equal preferential activity for both classes of bacteria. Mediocre antibacterial activity was observed for remaining isolates with no preference to cell morphology. The antimicrobial mechanism of this Amp-IL is still not known in detail, but is thought to involve a general perturbation of the lipid bilayer in bacterial membranes; however more studies are necessary to validate this hypothesis. Several studies have reported that long alkyl QACs disrupt the outer membrane of Gram-negative bacteria more extensively than shorter chain compounds with subsequent intracellular leakage and cell death.²⁸ Not much literature has explained the roll of QACs on the antimicrobial mechanism of action in Gram-positive systems. However, we attribute this activity to the presence of the cell wall inhibitor, ampicillin.

3.3.2.2.2 Imidazolium – based Ampicillin Ionic Liquids

The antibacterial activity of imidazolium-type ampicillin salts were not only tested but correlated to structure and activity relationships and spectrum of activity. Mainly, the antibacterial activity of the C16-imidazolium ampicillin ILs will be discussed, since [BmIm][Amp] only showed mediocre activity against the organisms tested. Therefore, [C₁₆M₁Im][Amp] and [C₁₆M₂Im][Amp] are composed of three parts: the head imidazole, the

C16-alkyl chain, and the anion (bromide or ampicillin). The MICs of [C₁₆M₁Im][Br] and [C₁₆M₂Im][Br] against *E. coli* O157:H7 43895 and *E. coli* ATCC 25922 showed marginal difference however, the former had greater activity (Table 3.4). In the case of *K. pneumoniae* 4352 and *S. typhimurium* 14028, [C₁₆M₁Im][Br] was more 4 times more effective. The antimicrobial mechanism of these types of long alkyl imidazolium bromides against bacteria is still not known in detail, but is thought to involve a general perturbation of the lipid bilayer in bacterial membranes.²⁹⁻³¹ Similar to ammonium-type QAC, Ahlström *et al.* previously reported that QACs with a C16 hydrophobic chain affected the outer membrane of Gram-negative bacteria more extensively than shorter chain compounds leading to leakage of cytoplasmic material and eventual death of the bacterial cell.²⁸ Previous studies have also demonstrated that imidazolium halides with hydrophobic groups in the C1 and C3 positions of the imidazolium ring demonstrated higher antibacterial activity than 1,2,3-trisubstituted imidazoles.²⁹ This demonstrates that the relative antibacterial activity of these types of compounds can be attributed to the alkyl chain length and head group substitutions, but not the imidazole ring structure.

In the case of the Gram-positive bacterium *E. faecium* 49474, [C₁₆M₁Im][Br] required six fewer moles than [C₁₆M₂Im][Br] to inhibit its growth (Table 3.4). *S. aureus* 6538, *L. monocytogenes* 7973, and *S. mutans* 2502 were equally susceptible to [C₁₆M₁Im][Br] and [C₁₆M₂Im][Br]. This result can be attributed to the lack of a lipopolysaccharide layer. In terms of the cation, Gram-positive bacteria have shown higher susceptibility than Gram-negative bacteria to permeation by the long alkyl chain present on the imidazolium ring. Thus, it is suggested that monoalkyl QACs bind by ionic and hydrophobic interactions to microbial membrane surfaces arranged with the hydrophobic tails inserted into the lipid bilayer, resulting in the rearrangement of the membrane and subsequent leakage of intracellular contents.³⁰ The innocuous bromide

counter-ion does not add any antimicrobial benefit to the halide-QACs, thereby allowing the mechanism of action to be solely attributed to the properties of the cation. It is important to note that the *S. aureus* 6538 used in this study acquired resistance amidst this investigation as determined by high MIC (*e.g.* 40 μ M) and limited disk diffusion zone diameters (Figure 3.3).

After undergoing anion exchange from bromide to the antibiotic, ampicillin, our results demonstrate a reduction in the amount of ampicillin required to inhibit the growth of the challenge pathogens. Since literature has suggested that there are minimal effects on antibacterial activity from the variation of the anion within imidazolium- and pyridinium-type ILs, any changes in antibacterial activity for our Amp-ILs will be attributed to the antibiotic ampicillin.³¹⁻
³³ Similar to the investigation conducted by Docherty *et al.*,³⁴ we also investigated the antibacterial activity of the halide salts, sodium bromide, potassium chloride, and sodium chloride in which no antibacterial activity was observed within the concentration range studied in this investigation (data not shown). When comparing the antibacterial activities of the ampicillin imidazoliums to the halide imidazoliums, improvements in antibacterial activity were evident (data not shown).

Antibacterial activity against Gram-negative bacteria for imidazolium-type Amp-ILs show improved spectrum of activity between di- and tri-substituted imidazolium ampicillins. Minimal changes to the antibacterial activity were observed for both *E. coli* isolates. Nearly 6-fold improvement in MIC values were achieved for *K. pneumoniae* 4352 for [C₁₆M₂Im][Amp]. Equal antibacterial activity was observed among all Gram-negative isolates treated with [C₁₆M₁Im][Amp]. These findings could be explained by the known activities of penicillin and its analogs against Gram-negative bacteria. For example, the β -lactam must be able to penetrate the outer LPS envelope and intrinsically bind to the different target proteins within the bacteria cell

wall.³⁵ However, the LPS barrier protects the cell from large, hydrophobic permeating agents such as certain antibiotics, detergents,³⁶ or in this case Amp-ILs. In addition, the large masses of the Amp-ILs may inhibit the compound from passing through pores located in the LPS layer and actively inhibit transpeptidase activity. Despite being specific to the types of bacteria, the pores located in *E. coli*, for example, do not allow molecules with masses larger than 600Da to enter the cell³⁷ and our Amp-ILs have masses greater than 600 Da on average. Therefore, the antibacterial activity of Amp-ILs against these microorganisms may be result from the cationic portion of the Amp-IL structure. This is further supported in the results outlined in Table 3.3 where it is evident that neither halide nor ampicillin imidazolium produced substantial changes in antibacterial activity compared to [Na][Amp]. When comparing [C₁₆M₁Im][Amp] and [C₁₆M₂Im][Amp] to [Na][Amp], MICs for Gram-negative bacteria were 4-times better for *K. pneumoniae* 4352 but equally or worse treatments for the other microbes.

It is commonly recognized that penicillin and its analogs are more effective on Gram-positive than Gram-negative bacteria due to the absence of the LPS in Gram-positive bacteria and the readily accessible cellular wall.³⁸ In Table 3.3, it can be seen that the antibacterial activities for ampicillin imidazoliums significantly improved requiring between 2 - 30 μ M and 0.8 - 30 μ M for [C₁₆M₁Im][Amp] and [C₁₆M₂Im][Amp], respectively, to inhibit Gram-positive bacteria compared to 8 - 140 μ M required for [Na][Amp]. Similar activity is required to inhibit *S. aureus* for both ampicillin-type imidazoliums. When compared to [Na][Amp], both Amp-ILs required approximately 50% lower concentration to inhibit the growth of resistant *S. aureus* 6538. It is believed that the acquired resistance shown by *S. aureus* 6538 in this study could be due to its development into a mucoid strain which is less susceptible to long-alkyl disinfectants. If this is the case, we attribute the [C₁₆M₂Im][Amp]'s improvement in antibacterial activity to

Amp-IL hydrophobicity and its likelihood to transport through the slime-layer of *S. aureus* 6538. Additionally, 2.25 times fewer moles are required for bacteriostatic activity against *E. faecium* 49474, and equal MIC values are required to inhibit the growth of *L. monocytogenes* 7973 and *S. mutans* 2502. Therefore, imidazolium-based Amp-ILs are equally effective against all candidate Gram-negative pathogens tested in this study with preferential activity to Gram-positive bacteria, namely, *E. faecium* 49474.

3.3.2.2.3 Pyridinium – based Ampicillin Ionic Liquids

The antibacterial activity of the pyridinium-type ampicillin IL was also investigated. These compounds are also composed of three parts: the head pyridinium ring, the C16-alkyl chain, and the anion (bromide or ampicillin). Similar to imidazolium halides, pyridinium halides have been extensively investigated to determine the structural contributions to their disinfecting properties.³⁹ The addition of a long alkyl chain to C1 on the pyridinium ring results in increased IL toxicity against Gram-negative planktonic bacteria.³⁴ It has also been demonstrated that C16-alkyl chains are the most effective portion of the ionic liquid structure when reducing the growth of bacteria.^{29, 40} Therefore, it is suggested that the hydrophobic chain on the pyridinium ring helps to perturb the cell wall. For the Amp-IL [CP][Amp], this cell wall permeation would improve the access of the ampicillin anion to the cell wall.

The MICs of [CP][Amp] against Gram-negative microbes showed improvement in the antibacterial activities when converted into an Amp-IL (Table 3.3). After exchange of the bromide to the ampicillin anion, improvements were observed up to 16 times and 3 times for Gram-negative and Gram-positive bacteria, respectively. These improvements are attributed to a combination of the long-alkyl pyridinium and ampicillin moieties. In comparison to the antibacterial activity of [Na][Amp], the MIC was most notably improved up to 163 times for

Gram-positive bacteria. The greatest difference in antibacterial activity between [CP][Amp] and [Na][Amp] was 7 times for Gram-negative microbes. The most significant improvement was observed when [CP][Amp] was used to inhibit *E. faecium* 49474 and *E. coli* 25922.

As the MIC value was equal to MBC for each Amp-ILs, the antibacterial activities of these compounds were considered to be bactericidal. Therefore, we hypothesize that the antibacterial behavior of the investigated Amp-ILs are due to the combination of a cell wall permeant with a transpeptidase inhibitor. Overall, [CP][Amp] was most effective on *K. pneumoniae* 4352, *E. coli* 25922, *S. aureus* 6538, and *E. faecium* 49474 growth inhibition, with more effective activity on Gram-positive bacteria. This finding may be a result from the synergy between the membrane active cation and cell wall inhibiting anion. This will be further described in Section 3.4.2.

3.3.3 Critical Micelle Concentration and Antibacterial Activity Relationship

Amp-ILs are active well below their CMCs. This could be explained by the fact that below the CMC values, the ILs are free monomers and participate in antibacterial activity; whereas, above the CMC value the ILs are engaged in micelles and unavailable to participate in the disruption of the cell wall. In addition, this bactericidal activity depends upon their ability to adsorb at the water/cell membrane interface, as determined by the CMC value. The CMCs of [CTA][Amp], [C₁₆M₁Im][Amp], [C₁₆M₂Im][Amp], and [CP][Amp] were found to be 101, 24, 92, and 24 μ M, respectively. Average MIC are approximately 1-6 times less than the CMC values, which clearly indicates that these compounds are probably not acting as detergents and are not forming micelles as a mechanism of action. Moreover, the interaction between the QAC and ampicillin as an Amp-IL is due to a change in the physical properties of the cation moiety. Since the CMC values were decreased upon metathesis, it appears that the free monomeric Amp-ILs are able to adsorb at the cell/water interface at dilute concentrations. Cell/wall adsorption can

lead to increases in cell wall solubility and cell membrane permeability by the monomeric Amp-IL and lead to enhanced antimicrobial activity.

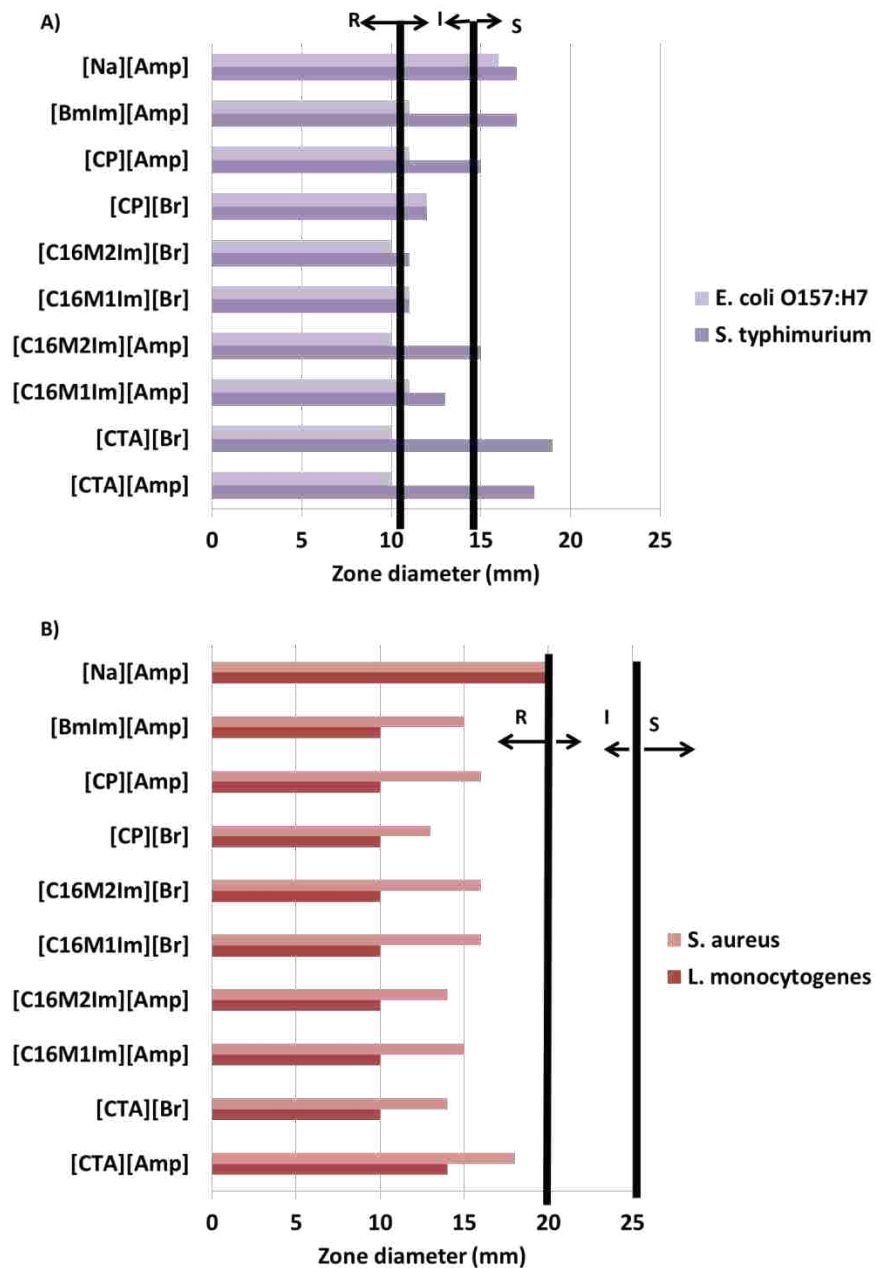


Figure 3.3. Experimental zone diameters obtained using Kirby-Bauer disk diffusion assay. Top panel (A) demonstrate zones of inhibition results, and thresholds for resistance (R), intermediate (I), and susceptible (S) against *E. coli* O157:H7 and *S. typhimurium*. Bottom panel (B) demonstrates experimental inhibition zones acquired for *S. aureus* and *L. monocytogenes*.

Table 3.3. Minimum inhibitory concentrations (MIC, μM) of ammonium-, imidazolium-, and pyridinium-type ampicillin ionic liquids. MIC values and minimum bactericidal concentrations were equivalent in this study.

	<i>E. coli</i> <i>O157:H7</i> 43895	<i>K.</i> <i>pneumoniae</i> 4352	<i>E. coli</i> <i>ATCC</i> 25922	<i>S.</i> <i>typhimurium</i> 14028	<i>S.</i> <i>aureus</i> 6538	<i>E.</i> <i>faecium</i> 49474	<i>S.</i> <i>mutans</i> 2502	<i>L.</i> <i>monocytogenes</i> 7973
[CTA][Amp]	5	30	11	6	25	2	12	30
[C ₁₆ M ₁ Im][Amp]	19	30	20	30	30	1.8	20	30
[C ₁₆ M ₂ Im][Amp]	17	30	18	19	25	0.8	20	30
[CP][Amp]	17	19	6	30	13	0.8	20	30
[BmIm][Amp]	150	200	180	20	200	170	200	50
[Na][Amp]	20	130	10	0.8	40	130	140	8
[CTA][Br]	19	30	30	80	10	11	20	30
[C ₁₆ M ₁ Im][Br]	17	30	30	30	60	30	20	30
[C ₁₆ M ₂ Im][Br]	19	13	30	120	50	18	20	30
[CP][Br]	12	30	100	30	30	2	20	30
[BmIm][Cl]	NA	NA	NA	NA	NA	NA	NA	NA

NA – no activity observed within concentration range tested.

Table 3.4. Interaction indices for ammonium-, imidazolium-, and pyridinium-type ampicillin ionic liquids.*

	<i>E. coli</i> <i>O157:H7</i> 43895	<i>K.</i> <i>pneumoniae</i> 4352	<i>E. coli</i> <i>ATCC</i> 25922	<i>S.</i> <i>typhimurium</i> 14028	<i>S.</i> <i>aureus</i> 6538	<i>E.</i> <i>faecium</i> 49474	<i>S.</i> <i>mutans</i> 2502	<i>L.</i> <i>monocytogenes</i> 7973
[CTA][Amp]	0.13 (S)	0.12 (S)	0.55 (N)	3.75 (N)	0.31 (S)	0.01 (S)	0.04 (S)	1.88 (N)
[C ₁₆ M ₁ Im][Amp]	1.03 (N)	0.62 (N)	1.33 (N)	19.25 (A)	0.63 (N)	0.04 (S)	0.57 (S)	2.38 (N)
[C ₁₆ M ₂ Im][Amp]	0.87 (N)	0.23 (S)	1.20 (N)	11.95 (A)	0.56 (N)	0.03 (S)	0.57 (N)	2.38 (N)
[CP][Amp]	0.50 (S)	0.39 (S)	0.33 (S)	19.25 (A)	0.38 (S)	0.20 (S)	0.57 (N)	2.38 (N)

*: Interaction indices could not be calculated for [BmIm][Amp] because no antimicrobial activity was observed for [BmIm][Cl].

3.3.4 Effect of Ampicillin-content in ILs

The activity of the IL compounds is more clearly described by normalizing the concentrations based on the percentage of ampicillin content within the Amp-ILs and [Na][Amp] (Equation 3.1).

$$\frac{Mw_{\text{ampicillinoate}}}{Mw_{\text{Amp-IL}}} \times \text{MIC} \quad (\text{Eq. 3.1})$$

For all Amp-ILs, it was observed that the reduced concentration of ampicillin anion in Amp-ILs was required to inhibit bacterial growth compared to [Na][Amp] (Figure 3.4). Depending on the bacterial species, the ampicillin content required for inhibition was in the microbe susceptible range for ampicillin activity (*i.e.* 0.1 to 20 $\mu\text{g/mL}$), excluding [BmIm][Amp].¹⁷ The average concentrations of ampicillin, in Amp-ILs, required to kill Gram-negative bacteria were found to be 2.5, 4.5, 3.8, 3.3, and 34.1 $\mu\text{g/mL}$ for [CTA][Amp], [C₁₆M₁Im][Amp], [C₁₆M₂Im][Amp], [CP][Amp], and [BmIm][Amp], respectively. Likewise, 3.3, 3.7, 3.4, 2.9, and 38.4 $\mu\text{g/mL}$ was required for bactericidal activity in Gram-positive bacteria. As previously stated, the average ampicillin content evident in [BmIm][Amp] is higher than the ampicillin-microbe susceptible range. The average MIC in terms of ampicillin content for [Na][Amp] was found to be 13.2 and 26.0 $\mu\text{g/mL}$ for Gram-negative and Gram-positive, respectively. This is a four- to nine-fold improvement in ampicillin content required for antibacterial activity when Amp-ILs are compared to [Na][Amp]. These results demonstrate that lower concentrations of Amp-ILs are capable of bactericidal activity against the tested inoculums. This demonstrates that lower dosage amounts of ampicillin could be implemented if applied in pharmaceutical systems as an Amp-IL.

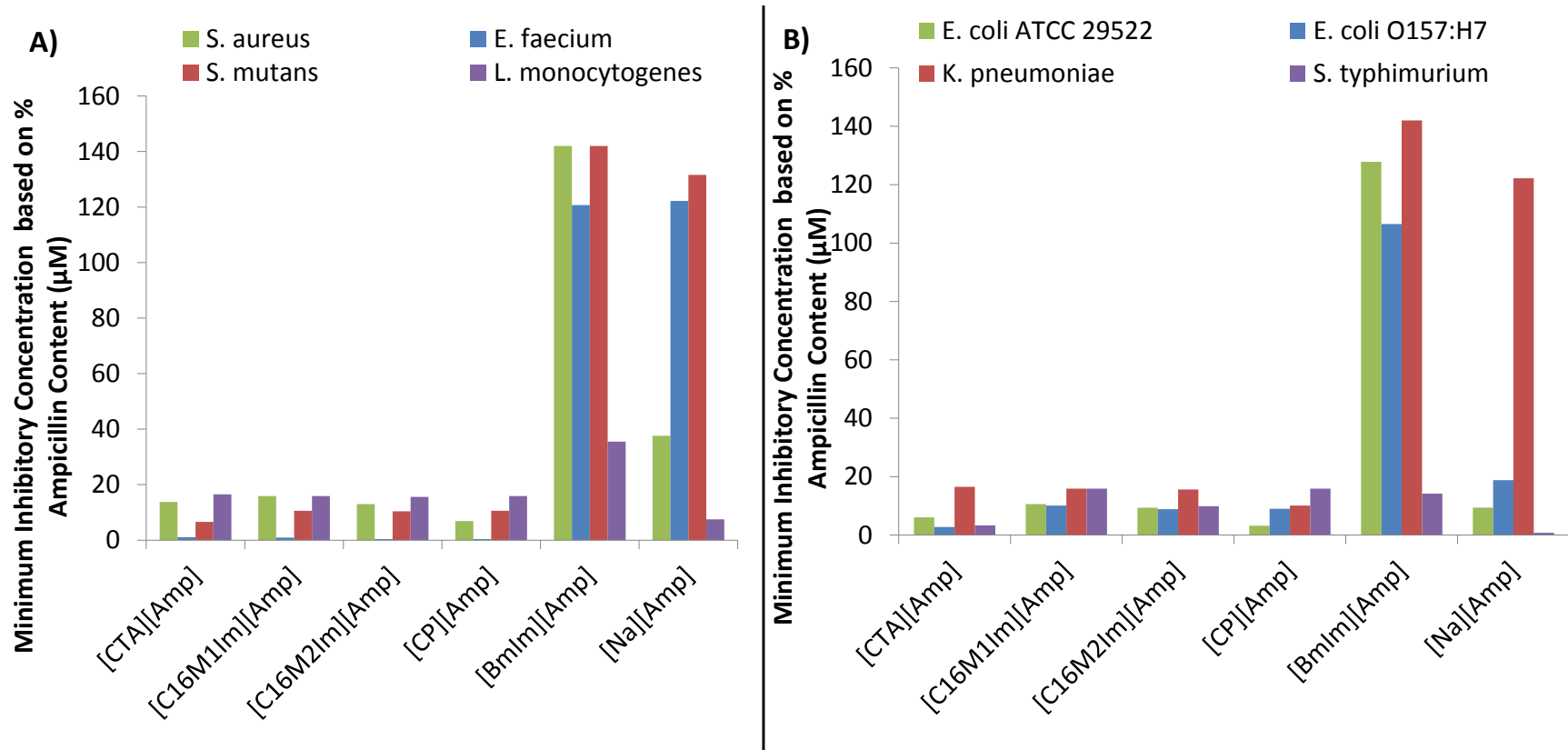


Figure 3.4. Bar graph depicting active concentrations of ampicillin content within Amp-ILs from MIC (μM) for Gram-positive (A) and Gram-negative bacteria (B).

3.3.5 Antibacterial Activity of Combinations

3.3.5.1 Combinatorial Effect of QAC and Sodium Ampicillin Co-Activity

It has been reported that the effect of a pharmaceutical agent on both resistant and sensitive bacterial strains can be enhanced with surfactants. For example, Suling and O'Leary observed that the addition of CTAB increased the activity of penicillin G on *E. coli*, *P. mirabilis*, *K. pneumoniae*, and various *Staphylococci* strains.⁴¹ However, this was not completely evident in our study. We investigated this phenomena using imidazolium- and pyridinium-type Amp-ILs. It was observed that the use of both QAC and [Na][Amp] tested in combination did not outperform the antibacterial activities of the Amp-ILs. For example, in Figure 3.5 the antibacterial activities of [C₁₆M₁Im][Br] + [Na][Amp] and [CP][Br] + [Na][Amp] were 30% less, in comparison to [C₁₆M₁Im][Amp] and [CP][Amp] for *E. coli* O157:H7 43895. Similarly, the antibacterial activity of [C₁₆M₂Im][Br]+[Na][Amp] was reduced by 80%, compared to the IL form, when two components were combined against *E. coli* O157:H7. Our results demonstrate that the use of either QAC, [C₁₆M₁Im][Br] + [Na][Amp], or [C₁₆M₁Im][Amp] could equally inhibit the growth of *E. faecium*; whereas, both [CP][Amp] and [C₁₆M₂Im][Amp] required 73% reduction in concentration compared to the starting materials (Fig. 3.5). As controls [Na][Br] was added to each Amp-IL to understand the effect of the salt as a by-product in these studies, and it was observed that it did not enhance the antibacterial activity of the Amp-ILs. In fact, the antibacterial activities of Amp-IL were reduced with the addition of equal moles of [Na][Br]. It is hypothesized that this result is related to the change in the isotonic environment of the bacteria resulting in a reduction in bacteria size and steric inhibition of the molecule's absorption.

Overall, the Amp-ILs have an increased antibacterial activity for the investigated pathogens. In 83% of the experiments, we demonstrate that Amp-ILs are more effective

antibacterial agents than each salt individually, or in combination, for the tested bacteria. Further investigation of this behavior will be conducted in future studies.

3.3.6 Loewe's Additivity Model

Table 3.4 illustrates the interaction indices of Amp-ILs as calculated according to the Loewe's Additivity Model. This model reveals that Amp-ILs demonstrate independent interaction indices between cation and anion. In 38% of the antibacterial studies using Gram-negative bacteria and 50% using Gram-positive bacteria, synergy was observed by the Amp-ILs. Additivity was observed in 44% and 50% of the Gram-negative and Gram-positive isolates. However, antagonism was only observed in 19% of the Amp-IL treatments on Gram-negative and none on Gram-positive microbes. These results show that [CP][Amp] and [CTA][Amp] are the better Amp-ILs to obtain synergetic interactions in Gram-negative bacteria. Although minimal, the probability of observing antagonism in Gram-negative bacteria in test systems is 20% likely. Systems containing Gram-positive bacteria show that in the worse instance, additivity could be observed. Nonetheless, synergy is still equally as probable when considering the use of the Amp-ILs alternative.

A closer look at a comparison study between the interaction indices between Amp-ILs and the mixture of stoichiometric mixture reveal the benefit of using this approach. For instance, the interaction indices determined for [CP][Amp] and its precursors in combination (red bars) reveal that synergy was favorable for the Amp-IL against both Gram-positive and Gram-negative strains. Contrary to the previous result, the stoichiometric mixture revealed additivity and antagonism for *E. coli* O157:H7 and *E. faecium*, respectively. Upon comparing the differences in interaction indices between Amp-ILs and the precursor ion combination, a 2- and 33-fold favorable improvement was observed when treating *E. coli* O157:H7 and *E. faecium*,

respectively with [CP][Amp]. Likewise, an unclean Amp-IL containing equimolar [Na][Br] demonstrated that the presence of by-product antagonizes the activity of [CP][Amp] causing results to become additive and antagonistic.

In a similar system containing an Amp-IL consisting of a C16-imidazolium cation, it is apparent that the combination and presence of [Na][Br] also attenuates the synergetic behavior. Although [C₁₆M₁Im][Amp] is marginally more synergetic than the precursor and unclean combinations, each system is considered to be additive according to established interaction index thresholds. Thus, additivity was observed for [C₁₆M₁Im][Amp], [C₁₆M₁Im][Br]+[Na][Amp], and [C₁₆M₁Im][Amp]+[Na][Br] (blue bars) against *E. coli* O157:H7. When treating *E. faecium*, [C₁₆M₁Im][Amp] demonstrated antagonism. We conclude that these results show that the co-administration of sodium ampicillin and 1-hexamethyl-3-methylimidazolium bromide ([C₁₆M₁Im][Br]+[Na][Amp]) are neutral and do not improve the activity of the other and the presence of [Na][Br] interferes with the synergetic activity of the Amp-IL.

We also investigated the change in interaction index upon the addition of a methyl group to C-2 of the imidazolium structure and increase in hydrophobicity. Similar to the other Amp-ILs, [C₁₆M₂Im][Amp] (green bars) was a more synergetic ion pair than the combinations against *E. coli* O157:H7 in spite of its moderate additive index. However, [C₁₆M₂Im][Amp] was 42 times more synergetic than the mixtures when treating *E. faecium*. Likewise, the combination and presence of [Na][Br] with the Amp-IL antagonizes its activity causing a additive effect. In sum, the interaction indices ranging in order of increasing synergy is [C₁₆M₁Im][Br] > [C₁₆M₂Im][Amp] > [CP][Amp].

In each study, the differences in interaction indices are apparent. For *E. coli* O157:H7, all Amp-ILs were more synergetic than either combination. Similarly, the more hydrophobic Amp-ILs (*i.e.* [CP][Amp] and [C₁₆M₂Im][Amp]) showed substantial improvements in synergy. Another common feature among the interaction indices calculated for systems containing Amp-ILs and [Na][Br] is the attenuated observed synergy. We attribute this reduction in synergy to the relative hydrophilicity of the Amp-ILs. As the aqueous solubility is increased, there is a greater probability of the ions to dissociate and re-associate with the precursor counter-ions. Thus, the relative interaction indices obtained for the Amp-ILs demonstrates an apparent increase in synergy with increasing hydrophobicity.

3.4 Conclusion

We have successfully demonstrated the synthesis and antibacterial application of a novel class of antibiotic-based ILs composed of either ammonium, imidazolium, or pyridinium cations. Improvements in the bactericidal activity of the ampicillin anion were obtained when the anion was combined with a QAC as the cation. The results indicate that Amp-ILs may be effective alternatives as antibacterial agents in lieu of the use of either individual ionic parent compounds (*i.e.* [QAC] or [Na][Amp]) or the combination in solution (*i.e.* [QAC] + [Na][Amp]).

The advantages by use of antibiotic-based ILs are numerous. Aside from the possibility of extending the clinical usage of antibacterial agents that are associated with bacterial resistance, there is potential to improve the half-life, reduce dosage rates, tailor the bioavailability of the drug, reduce costs associated with new drug testing and formulation, and expand the therapeutic activity of the antibiotic by pairing it with other biological ions. Although, these specific types of ampicillin ionic liquids may be considered toxic and not cleared for systemic use, the potential to apply these antibacterial materials to biomedical

sterilization, food processing, and wound care therapy is promising. Thus, Chapter 4 highlights an extension of this work in which a potent antiseptic and various β -lactam antibiotics are integrated for their potential use against pathogenic bacteria in disease prevention and eradication of *E. coli* O157:H7 from the terminal recta of cattle.

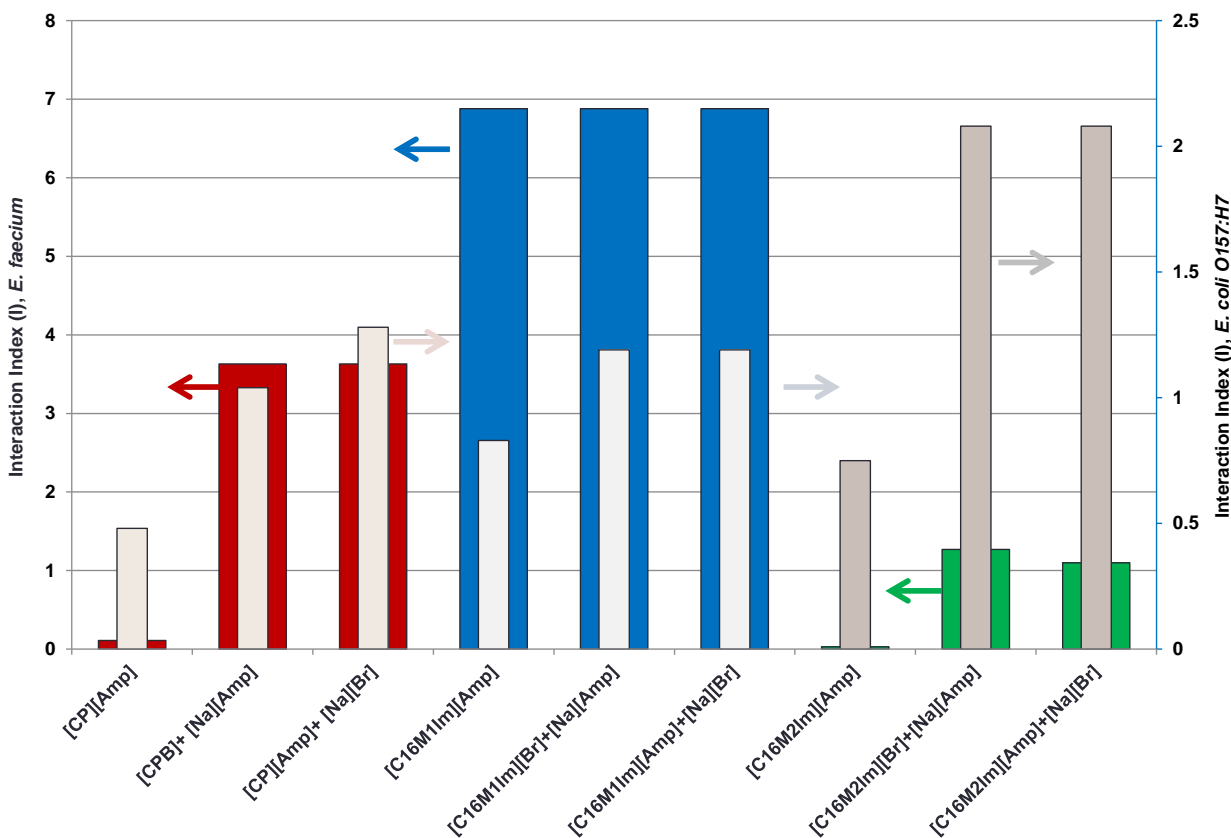


Figure 3.5. Interaction indices calculated for ampicillin-based ionic liquids. Each color correlates to a specific Amp-IL, where red = [CP][Amp] and its combinations, blue = [C₁₆M₁Im][Amp] and its combinations, and green = [C₁₆M₂Im][Amp] and its combinations. Darker colors are measured by the left axis indicative of *E. faecium* results and the right axis describes the interaction indices against *E. coli* O157:H7.

3.5 References

1. Maheshwari, R.; *Indian Journal of Microbiology*, **2007**, *47*, 181-183.
2. Crowley, P.J.; Martini, L.G.; *Drug Discovery Today: Therapeutic Strategies*, **2004**, *1*, (4), 537-542.
3. Nelson, R.; *Lancet*, **2003**, *362*, 1726-1727.
4. U.S. Congress Office of Technology Assessment, Impacts of Antibiotic Resistant Bacteria. Ed.; U.S. Government Printing Office: Washington, D.C., **September 1995**, Report # OTA-H-629.
5. Cole, E.C.; Addison, R.M.; Rubino, J.R.; Leese, K.E.; Dulaney, P.D.; Newell, M.S.; Wilkins, J.; Gaber, D.J.; Wineinger, T.; Criger, D.A.; *Journal of Applied Microbiology*, **2003**, *95*, (4), 664-676.
6. Lancini, G.C.; Parenti, F.; Gallo, G.G.; *Antibiotics: A Multidisciplinary Approach*. 2nd ed. Plenum Press: New York, **1995**.
7. Hsueh, P.-R.; Chenc, W.-H.; Teng, L.-J.; Luha, K.-T., *International Journal of Antimicrobial Agents* **2005**, (26), 43-49.
8. Qiu, L.; Bae, Y.; *Pharmaceutical Research*, **2006**, *23*, (1), 1-30.
9. Torchilin, V.; *Pharmaceutical Research*, **2007**, *24*, (1), 1-16.
10. Peppas, N.A.; *Current Opinion in Colloid & Interface Science*, **1997**, *2*, (5), 531-537.
11. Said, S.; Mahrous, H.; Kassem, A.; *Infection*, **1976**, *4*, 49-50.
12. Bodor, N.; Venkatraghavan, V.; Winwood, D.; Estes, K.; Brewster, M.E.; *Int. J. Pharm.*, **1989**, *53*, 195-208.
13. Yousef, R.T.; Ghobashy, A. A.; *Acta Pharmaceutica Suecica*, **1968**, *5*, (4), 385-392.
14. Pop, E.; *Advanced Drug Delivery Reviews*, **1994**, *14*, 211-226.
15. Krande, P.; Mitragotri, S., *Pharmaceutical Research*, **2002**, *19*, 655-660.
16. Müllertz, A.; Ogbonna, A.; Ren, S.; Rades, T., *Journal of Pharmacy and Pharmacology*, **2010**, *62*, (11), 1622-1636.
17. NCCLS. In *M2-A6*; National Committee on Clinical Laboratory Standards: Wayne, PA, USA, **2003**.
18. Davidson, A.G.; Stenlake, J.B.; *Analyst*, **1974**, *99*, 476-481.
19. Samanta, A.; *The Journal of Physical Chemistry B*, **2006**, *110*, (28), 13704-13716.

20. Paul, A.; Samanta, A.; *Journal of Chemical Sciences*, **2006**, *118*, (4), 335-340.
21. Mandal, P.K.; Paul, A.; Samanta, A.; *Journal of Photochemistry and Photobiology A: Chemistry*, **2006**, *182*, (2), 113-120.
22. NCCLS. In *M2-A8*; National Committee on Clinical Laboratory Standards: Villanova, PA, **2006**.
23. Stevens, M.G.; Olsen, S.C.; *Journal of Immunological Methods*, **1993**, *157*, (1-2), 225-231.
24. Stowe, R.P.; Koenig, D.W.; Mishra, S.K.; Pierson, D.L.; *Journal of Microbiological Methods*, **1995**, *22*, (3), 283-292.
25. Jungnickel, C.; Luczak, J.; Ranke, J.; Fernandez, J.; Muller, A.; Thoming, J.; *Colloids and Surfaces A: Physicochem. Eng. Aspects*, **2008**, (316), 278-284.
26. Dong, B.; Li, N.; Zheng, L.; Yu, L.; Inoue, T.; *Langmuir*, **2007**, *23*, 4178-4182.
27. Modaressi, A.; Sifaoui, H.; Mielcarz, M.; Domanska, U.; Rogalski, M.; *Colloids and Surfaces A: Physicochemical and Engineering Aspects*, **2007**, *302*, 181-185.
28. Ahlstrom, B.; Thompson, R.A.; Edebo, L.; *Acta Pathologica, Microbiologica, et Immunologica Scandinavica*, **1999**, *107*, 318-324.
29. Dembereinyamba, D.; Seung, P.; Huen, L.; Chang, K.; Ick-Dong, Y.; *Bioorganic Medicinal Chemistry*, **2004**, *12*, 853-857.
30. Ioannou, C.J.; Hanlon, G.W.; Denyer, S.P.; *Antimicrobial Agents and Chemotherapy*, **2007**, *51*, (1), 296-306.
31. Docherty, K.M.; Kulpa, C.F.; *Green Chemistry*, **2005**, *7*, 185-189.
32. Luis, P.; Ortiz, I.; Aldaco, R.; Irabien, A.; *Ecotoxicology and Environmental Safety*, **2007**, *67*, 423-429.
33. Ranke, J., Molter, K., Stock, F., Bottin-Weber, U., Poczobutt, J., Hoffmann, J., Ondruschka, B.; *Ecotoxicology and Environmental Safety*, **2004**, *58*, (396).
34. Couling, D.J.; Bernot, R.J.; Docherty, K.M.; Dixon, J.K.; Maginn, E.J.; *Green Chemistry*, **2006**, *8*, 82-90.
35. Scholar, E.M.; Pratt, W.B.; *The Antimicrobial Drugs*. Second ed. Oxford: New York, **2000**.
36. Maloy, S.R.; Cronan, J.E.; Freifelder, D.; *Microbial Genetics*. Second ed. Jones and Bartlett Publishers: Sudbury, **1994**.
37. *Jawetz, Melnick, & Adelberg's Medical Microbiology*. 23 ed. McGraw-Hill, **2004**.

38. Tipper, D.J.; Strominger, J.L.; *Proceedings of the National Academy of Sciences*, **1965**, *54*, 1133-1141.
39. Krysinski, J.; *Pharmazie*, **1995**, *50*, (9), 593-597.
40. Pernak, J.; Sobaszkiewicz, K.; Mirska, I.; *Green Chemistry*, **2003**, *5*, (1), 52-56.
41. Suling, W.J.; O'Leary, W.M.; *Antimicrobial Agents and Chemotherapy*, **1975**, *8*, (3), 334-343.

CHAPTER 4 SYNTHESIS, CHARACTERIZATION, AND BIOLOGICAL EVALUATION OF BETA (β)-LACTAM BASED CHLORHEXIDINE GUMBOS AGAINST ENTEROHEMORRHAGIC ESCHERICHIA COLI

4.1 Introduction

Enterohemorrhagic *Escherichia coli* (EHEC) infections are associated with bloody diarrhea, thrombotic thrombocytopenic purpura, hemorrhagic colitis, and hemolytic uremic syndrome.^{1, 2} Although strains of EHEC are represented by several serotypes, the majority of severe infections are caused by serotype O157.^{1, 3} Cattle and other ruminants are reservoirs of infection and sources for fecal contamination in food and beverages; therefore, they are associated with large outbreaks of disease caused by EHEC.^{4, 5} Aside from enforcing good hygienic practices with all aspects of food handling, from harvest to preparation, EHEC transmission might be better controlled by reducing fecal shedding from food-producing animals.² Several methods tested in attempts to control the colonization of pathogenic microbes in food-producing animals included regulating the animal's diet and with vaccination. Studies of such control measures to reduce or eliminate fecal shedding of EHEC in cattle have been inconclusive.^{4, 6-8}

One current approach to reduce EHEC fecal shedding in a food-producing animal is the use of antiseptics. Various compounds have demonstrated some efficacy in the reduction of EHEC in a food-producing animal's feces; however, many of these compounds are inherently toxic and not approved for this use in animals. One such compound is the di-cationic biguanide, chlorhexidine. Low *et al.* reported that chlorhexidine enemas eliminated high-level fecal shedding and reduced low-level shedding by killing *E. coli* O157:H7 at the terminal rectum.⁸ However, the effective concentrations used for eliminating or reducing EHEC fecal shedding are cytotoxic.⁹⁻¹² Many antibiotics commonly used in animal feedlots selectively reduce fecal

shedding of EHEC in ruminants.⁵ One such antibiotic used in cattle feedlots is ampicillin. However, the rapid rise of antimicrobial resistance in Gram-negative bacteria, particularly in those with extended spectrum β -lactamases (ESBL), severely curtails the widespread use of antibiotics in the control of microbe colonization in food-producing animals.¹³ Other methods of reducing EHEC fecal shedding have been explored using FDA approved ionophores as feed additives. However, ionophores such as monensin, lasalocid, laidlomycin propionate, and bambarmycin are ineffective in reducing EHEC shedding in fecal samples, particularly those isolated from sheep.^{14, 15}

With the goal of developing a safe and effective compound that could be administered to food-producing ruminants such as cattle, goats, and sheep to reduce fecal shedding of EHEC, chlorhexidine and ampicillin were combined to form a unique GUMBOS, chlorhexidine di-ampicillin. These two compounds were chosen based primarily on their history of use in veterinary practice. Other β -lactam antibiotics were also included to see if their differing degrees in antibacterial potency and spectrum of activity would positively or negatively affect EHEC eradication. Integrating pharmaceutically active cations and anions into entities known as Active Pharmaceutical Ingredient – based Ionic Liquids (API-ILs) is an innovative approach to resolving issues associated with single or combination therapy using individual cationic or anionic agents. For example, API-ILs can be synthesized using antibiotics, analgesics, and anti-inflammatory drugs.¹⁶⁻²⁰

ILs are arbitrarily defined as salts that melt below 100°C but there are many ion combinations that form salts with melting points less than 250°C with interesting and useful properties.²¹ These ILs belong to a new category of applied low melting salts called Group of Uniform Material Based on Organic Salts (GUMBOS).²² Beta (β)-lactam chlorhexidine salts are

API-ILs that can be considered as GUMBOS. The purpose of this study was to synthesize and characterize GUMBOS composed of the antiseptic, chlorhexidine, and four β -lactam antibiotics (*i.e.* ampicillin, carbenicillin, oxacillin, and cephalothin) and investigate their antibacterial activities and mechanisms of action on several strains of EHEC. Cytotoxicity studies and predictive intestinal permeabilities were studied *in vitro* to assess the GUMBOS feasibility in removing EHEC from the terminal recta of ruminants.

4.2 Materials and Methods

4.2.1 Synthesis of Chlorhexidine di-ampicillin GUMBOS

An excess of sodium antibiotic was added to a chlorhexidine methanolic solution in stoichiometric amounts to a round-bottom flask. The mixture was stirred for two days at room temperature to ensure the complete formation of chlorhexidine di-ampicillin, chlorhexidine carbenicillin, chlorhexidine di-oxacillin, and chlorhexidine di-cephalothin. After removing methanol using rotary evaporation, the un-reacted and by-products were removed by washing several times with deionized water. The products were finally dried under high vacuum overnight. Identity and purity of the GUMBOS were confirmed by ^1H and ^{13}C NMR spectroscopy and mass spectrometry. The structural components of the β -lactam based chlorhexidine GUMBOS are shown in Figure 4.1.

4.2.2 Dissolution Profile Measurement

The dissolution rates for β -lactam based chlorhexidine GUMBOS were measured using UV spectrophotometry at 260 nm in 18.2 m Ω deionized water. Here, 20 mg samples were placed in a stirred, 100 ml Erlenmeyer flask containing 50 ml of 18.2 m Ω deionized water. Over time, one milliliter aliquots were collected and filtered through a 0.1 μm pore size syringe filter (Whatman). Dissolution profiles were measured in triplicate at room temperature until absorbance plateau.

4.2.3 *In Vivo* Prediction of Intestinal Permeability and Absorption

Intestinal permeability was approximated using the BD Gentest Pre-coated PAMPA Plate System (BD Biosciences, MA, USA). The procedure required that 300 μL of 200 μM compound solutions in PBS buffer (100mM, pH 7.4) be added to the wells in a donor plate while 200 μL of PBS buffer were added to corresponding wells in an acceptor plate. After the acceptor plate was coupled to the donor plate, the assembly was incubated for 5 hours at 20°C. The last 100 μL of wells from the donor and acceptor plates were added to a UV transparent 96-well plate for quantification using a plate reader. The final concentrations in each plate were determined using calibration curves at 260 nm. Membrane permeability was calculated using formulas provided in the assay and resultant predictive intestinal absorption values were determined using a $\text{Log } P_e \geq -6$ threshold that indicates $\geq 75\%$ intestinal absorption.

4.2.4 Antimicrobial Activity

Seven strains of *E. coli* O157:H7 were used in this study (Table 4.3). Each isolate was grown individually on MacConkey Agar with sorbitol for 24 hours at 37°C. *E. coli* (ATCC 25922) was used as a non-pathogenic strain. All bacteria were obtained from the collection maintained in the Food Safety/ Food Microbiology laboratory, Louisiana State University.

Minimal inhibitory concentrations (MIC) were determined in triplicate by micro-broth dilution essentially as described by Motyl et al.²³ Test inocula were prepared with colonies suspended in saline (0.85% NaCl) to a 0.5 McFarland standard. Cation-adjusted Mueller-Hinton broth (Difco, Detroit, MI) with 2% DMSO was used to serially dilute (1:1) GUMBOS, sodium antibiotic, chlorhexidine diacetate, or the stoichiometric combination of the antibiotic and chlorhexidine diacetate [2:1 v/v for chlorhexidine di-ampicillin, chlorhexidine di-cephalothin, and chlorhexidine di-oxacillin or 1:1 v/v] for chlorhexidine carbenicillin). After inoculation, plates were incubated 24 h at 37°C. Minimum bactericidal concentrations of GUMBOS were

determined by plating the clear MIC wells from microtiter plates onto trypticase soy agar and looking for colonies after 24 h incubation. Antibacterial activity was statistically analyzed using SAS 9.2 (SAS Institute Inc., Cary, NC), $p < 0.05$.

4.2.5 GUMBOS Interaction Indices

Loewe's additivity model²⁴⁻²⁶ was used to evaluate the interaction index (I) of chlorhexidine diacetate and sodium antibiotic used in combination compared to I calculated for GUMBOS. An I value of < 0.5 denotes synergy; the combined effects of two agents are greater than the sum of their individual effects. If I is ≥ 0.5 but ≤ 4 , the effect of two agents is said to be additive (*i.e.*, the combined effect is equal to individual activities). If $I > 4$ then the two agents are considered antagonistic, meaning the effect of the combined agents is smaller than one of the agents alone.

Equation 4.1 (Eq.4.1) shows the Loewe's additivity mathematical model used to calculate I values for drug combinations, where X refers to a specific inhibition level (*i.e.* 99.9%), C_a and C_b are the concentrations of drug A and B when used in combination, and C_A and C_B are the concentrations of drug A and B administered separately and have the same level of inhibition²⁶.

$$I = \frac{C_a}{C_A} + \frac{C_b}{C_B} \quad (\text{Eq. 4.1})$$

The model used to represent the mixture of chlorhexidine diacetate (CHXAc) and sodium antibiotic (Na β L) in the stoichiometric equivalent concentrations for the β -lactam based chlorhexidine GUMBOS is shown in Equation 4.2:

$$I_{\text{combo}} = \frac{[\text{CHXAc}]_{\text{COMBO}}}{[\text{CHXAc}]_{100\%}} + \frac{[\text{Na}\beta\text{L}]_{\text{COMBO}}}{[\text{Na}\beta\text{L}]_{100\%}} \quad (\text{Eq. 4.2})$$

Models for the β -lactam based chlorhexidine GUMBOS are shown in Equations 4.3 and 4.4.

$$I_{\text{GUMBOS}} = \frac{0.33 \times [\text{CHX} - \beta\text{L}_2]}{[\text{CHX}][\text{Ac}]_{100\%}} + \frac{0.66 \times [\text{CHX} - \beta\text{L}_2]}{[\text{Na}][\beta\text{L}]_{100\%}} \quad (\text{Eq. 4.3})$$

Equation 4.3 was used to calculate interaction indices for GUMBOS (*i.e.* chlorhexidine di-ampicillin, chlorhexidine di-cephalothin, and chlorhexidine di-oxacillin) which consists of a 1 chlorhexidine diacetate: 2 sodium antibiotic stoichiometric ratio.

$$I_{GUMBOS} = \frac{0.5 \times [CHX - \beta L]}{[CHX][Ac]_{100\%}} + \frac{0.5 \times [CHX - \beta L]}{[Na_2][\beta L]_{100\%}} \quad (\text{Eq. 4.4})$$

Equation 4.4 was used to calculate interaction indices for chlorhexidine carbenicillin GUMBOS which consists of a 1 chlorhexidine diacetate: 1 disodium antibiotic stoichiometric ratio.

4.2.6 Time-Kill Kinetics of Chlorhexidine di-ampicillin

Since chlorhexidine di-ampicillin required the lowest concentration to kill EHEC isolates, its time-kill kinetics were performed as a model in reference to the antiseptic chlorhexidine diacetate. Time-kill kinetics of chlorhexidine di-ampicillin was assessed using the BacLight Live/Dead Assay (Molecular Probes, Carlsbad, CA) as outlined in the protocol. More specifically, *E. coli* O157:H7 strain 43895 suspensions were adjusted to 1×10^8 CFU/mL (~0.3 OD₆₇₀) and treated with 7.3 μM (MBC of chlorhexidine di-ampicillin) antimicrobial agent. At different times, bacteria aliquots were stained with fluorescent probe mixture (SYTO 9 and Propidium Iodide) and mixed thoroughly. Samples were incubated in the dark for 15 minutes prior to fluorescence detection.

4.2.7 Mechanism of Action Studies

4.2.7.1 Membrane Perturbating Activity of GUMBOS on *E. coli*

Outer membrane permeation was evaluated using the 1-N-phenyl-naphthylamine (NPN) fluorescent probe as described previously by Hugo and Denyer and Helander *et al.*^{27, 28} Briefly, *E. coli* O157:H7 strain 43895 grown into log-phase ($\lambda_{630\text{nm}} = 0.5 \pm 0.5$) was centrifuged (1,000 x g, 15 mins, 25°C) and resuspended in half volume of HEPES buffer (5mM, pH 7.2). The hydrophobic probe, NPN (final concentration of 20 μM), was added to bacteria and dispensed

100 μL /well to black 96-well microtiter plates containing 100 μL of serially diluted GUMBOS or chlorhexidine diacetate ranging from 3 – 500 μM , buffer (negative control), or 500 μM EDTA (positive control). To test the impact divalent cations (*i.e.* Mg^{+2}) have on the membrane permeating ability of GUMBOS as compared to known membrane permeating properties of chlorhexidine diacetate, a separate microtiter plate containing 5mM MgCl_2 was used to assess the role divalent cations have on the membrane permeation of these compounds. Increases in fluorescence (λ_{ex} 355nm, λ_{em} 405nm) were monitored within 3 mins from three parallel wells per sample and concentration, in triplicate.

4.2.7.2 Membrane Potential Effect of Chlorhexidine di-ampicillin on *E. coli*

BacLight™ Bacterial Membrane Potential assay (Molecular Probes, Carlsbad, CA) was used as outlined in the protocol to determine if GUMBOS depolarizes EHEC bacterial membranes. Here, 100 μL aliquots of log-phase growth 10^6 CFU/ml *E. coli* O157:H7 strain 43895 was treated with 100 μL of 3 – 250 μM chlorhexidine diacetate or GUMBOS. Extents of depolarization were quantified according to a 5 μM valinomycin-potassium calibration curve (1 – 50 mM KCl). The proton ionophore, carbonyl cyanide 3-chlorophenylhydrazone (CCCP), which destroys membrane potential by eliminating the proton gradient, was used as a positive control. After 30 minutes of antimicrobial treatment, bacteria were stained with 30 μM DIOC₂ (3, 3'-diethyloxacarbocyanine iodide). Fluorescence measurements (λ_{ex} 488nm, λ_{emGreen} 538nm, and λ_{emRed} 612nm) were obtained in a black 96-well fluorescence microtiter plate. Endpoint fluorescence red/green ratiometric values were used to quantify intracellular cytosolic potassium concentrations, its leakage, and corresponding changes in Nernst membrane potential. The red – to – green fluorescence ratio identifies the portion of bacteria with intact membranes (red fluorescence) and depolarized membranes (green fluorescence) since the DIOC₂ dye shifts from red – to – green emission upon changes in membrane potential and membrane integrity.

Fluorescence measurements were performed in triplicate using a FluoStar 0403 microplate reader (BMG Lab Tech GmbH, Ortenburg, Germany) within 10 minutes, from three parallel wells per sample concentration).

4.2.7.3 Membrane Activity of Chlorhexidine di-ampicillin on *E. coli*

Membrane effects of chlorhexidine di-ampicillin as compared to the parent salts individually were evaluated on log-phase cultures of EHEC isolates using SEM. EHEC cultures were prepared from the logarithmic growth phase to a 10^8 CFU/ml starting concentration. Mueller-Hinton broth containing EHEC inocula of 10^8 CFU/ml were treated with supra-MICs of sodium ampicillin, chlorhexidine diacetate, chlorhexidine di-ampicillin, or the stoichiometric mixture of parent ions for 1 hour at 37°C. Untreated controls were prepared in cation-adjusted Mueller-Hinton growth medium. Samples were fixed on a 0.2 µm pore polycarbonate filter in 2.5% glutaraldehyde in 0.2 M cacodylate buffer pH 7.2 for 1h, then rinsed 5 times in 0.1 M cacodylate buffer containing 0.02M glycine over 12 h period. Then the materials were rinsed in water twice, dehydrated in ethanol series, dried with chemical hexamethyldisilazane (HMDS) series, mounted on aluminum SEM stubs, coated with platinum in an EMS550X sputter coater, and imaged with JSM-6610 High vacuum mode SEM (Peabody, MA).

4.2.8 HeLa, NIH/3T3, and EOMA Cell Viability Tests

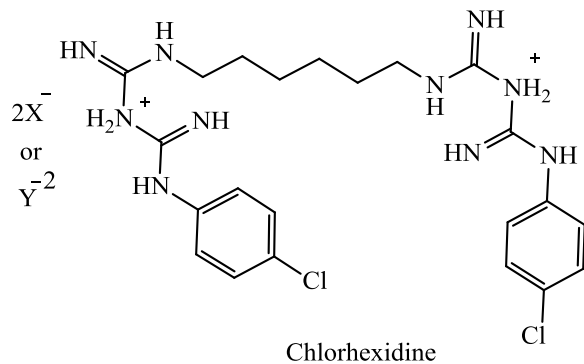
To determine cell viability, the colorimetric MTS dye (CellTiter 96 ® Aqueous One Solution Cell Proliferation Assay, Promega, Madison, WI) assay was used as an indicator of cell viability. HeLa (ATCC CCL-2), NIH/3T3 (ATCC CRL-1658), and EOMA (ATCC CRL-2586) were cells grown in Dulbecco's Modified Eagle Medium – Reduced Serum (DMEM-RS) supplemented with 3% FBS were plated at a density of 1×10^4 cells/well into 96-well culture plates (Falcon, Franklin Lakes, NJ). Varying concentrations (3 µM to 350 µM) of GUMBOS, chlorhexidine diacetate, and sodium antibiotic were used to treat cells for 24 h at 37°C + 5%

CO₂. Cells treated with medium only served as a negative control. After 24 h incubation, 40 μ L of MTS solution was added to each well and incubated for an additional 1 hour. The absorbance intensity was measured using a Perkin Elmer Wallac Victor2 V Fluorescence/Luminescence Plate Reader (Boston, MA) at 490 nm. All experiments were performed in quadruplicate and the relative cell viability (%) was expressed as a percentage relative to the untreated control cells. Cytotoxicity was statistically analyzed using SAS 9.2 (SAS Institute Inc., Cary, NC), $p < 0.05$.

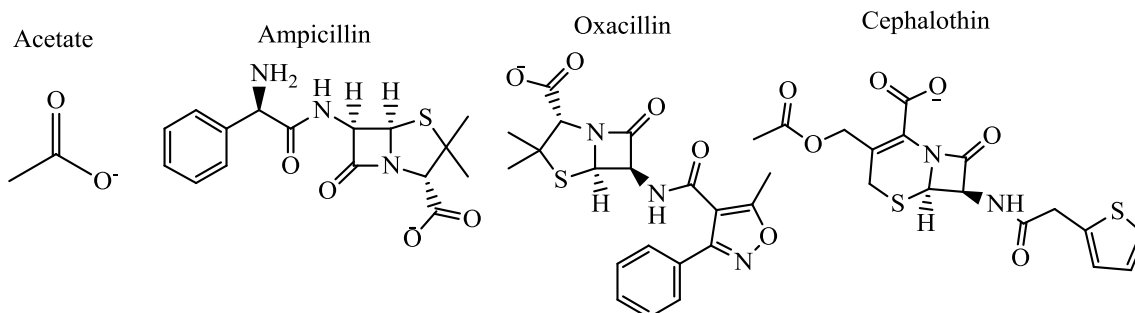
4.3 Results

4.3.1 Representative GUMBOS Structural Analysis: Chlorhexidine di-Ampicillin

The structural components for all β -lactam chlorhexidine based GUMBOS are illustrated in Figure 4.1. Using chlorhexidine di-ampicillin as a representative, inspection of its spectroscopic properties indicates that both chlorhexidine and ampicillin are present in the GUMBOS structure. More specifically, characteristic shifts in the ¹H-NMR and ¹³C-NMR demonstrate changes in the chemical microenvironments of the ionic pairs, while particular photo-physical properties of respective ions were still observed using absorbance spectroscopies. Representative ¹H-NMR and ¹³C-NMR obtained for chlorhexidine di-ampicillin are shown in Figures 4.2 and 4.3. Since all GUMBOS in this class contain chlorhexidine as the cation and various β -lactam antibiotic analogs as the anions, only the details regarding chlorhexidine di-ampicillin will be discussed. However, structural assignments for all β -lactam based chlorhexidine GUMBOS are provided in Sections 4.3.1.1 – 4.3.1.4.



Where X =



Where Y =

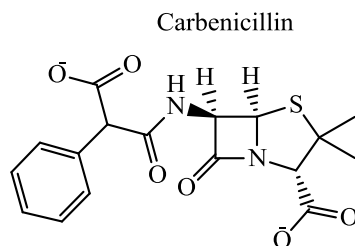


Figure 4.1 Molecular structures of dicationic chlorhexidine (top) and X counterions (from left to right) acetate, ampicillin, oxacillin, and cephalothin and Y counterion carbenicillin. GUMBOS consisting of chlorhexidine X consists of two anionic molecules electrostatically tethered to one chlorhexidine molecule, whereas chlorhexidine Y consist of one carbenicillin molecule ionically bound to chlorhexidine.

Proton NMR of the ampicillin structure reveals that H-2 and H-3 β are in the same plane; whereas H-5 and H-3 α are in close proximity (Figure 4.2). Upon ion exchange, ampicillin's H-3 α and H-3 β protons experience isolated changes in their respective microenvironments which caused a 0.28 ppm shift upfield from 1.45 to 1.18 ppm for H-3 β protons. We attribute this change to the close proximity of H-3 β to either aromatic regions of chlorhexidine and secondary ampicillin in its new conformation. In addition to the downfield shifts observed for the aromatic

protons in ampicillin, the NH_2^+ groups in the guanidine structure shifted downfield from 7.51 to 8.54 ppm after exchanging the acetate anions for ampicillin.

The ^{13}C -NMR spectra for chlorhexidine di-ampicillin also shows the presence of both cation and anion constituents (Figure 4.3). Beginning with the ampicillin molecule, three peaks (*i.e.* 173.4, 167.5 and 167.3 ppm) correspond to the carbonyl groups (*i.e.* C-2 α , C-7, and C-9) in the anionic structure. Additionally, several peaks ranging between 122 – 139 ppm correlate to the phenyl groups within both cation and anion. Tertiary carbons in the thiazolidine ring of ampicillin (C-2) were confirmed by two peaks at 76 and 184 ppm. Contributions from the carbons adjacent to the secondary amine-functionalized carbamimidoyl group (C-11 and C-12) in the chlorhexidine cation and the primary and tertiary amines (*i.e.* C-10 and C-5) in the ampicillin anion were evident by peaks shown at 60, 61, 59 and 68 ppm, respectively. Lastly, the carbon peaks near 27 ppm are indicative of ampicillin's C-3 α and C-3 β methyl groups and C-10 in the hexamethyl linker in the chlorhexidine di-ampicillin structure, respectively.

The molecular mass of chlorhexidine di-ampicillin was determined using ESI-TOF in the positive-ion mode (Figure 4.4). The spectra gave a base peak at m/z 1203.4, which is assigned $[\text{M} + \text{H}]^+$ of $\text{C}_{54}\text{H}_{66}\text{Cl}_2\text{N}_{16}\text{O}_8\text{S}_2$ (calc. 1202.24). This molecular formula corresponds to one chlorhexidine and two ampicillin molecules. Table 4.1 lists other m/z peaks which were found to correspond to monomer or $[\text{ampicillin} - \text{Na}]^+$, dimer or $2 [\text{ampicillin} - \text{Na}]^+$, and 1:1 chlorhexidine hydride: ampicillin. These results suggest that the reaction between one molecule of chlorhexidine and two molecules of ampicillin were successful.

The optical profile of chlorhexidine di-ampicillin was evaluated using CD and UV-vis spectrophotometry (Figure 4.5 and 4.6). The analyte absorbed strongly in the UV range of the spectrum which is typical of aromatic chromophores. Therefore, this analytical technique was

used to qualify the presence of each parent ion in chlorhexidine di-ampicillin. Three characteristic bands were evident in the absorption profile. The strong bands with a maximum at 208 and 259 nm are due to $n - \sigma^*$ and $\pi - \pi^*$ transitions from the chlorhexidine cation; whereas, the weak absorbance band at 208 nm and 230 nm is attributed to the $\pi - \pi^*$ and $n - \pi^*$ transitions in the ampicillin anion, respectively.²⁹⁻³¹ Therefore, the optical rotation of chlorhexidine di-ampicillin was monitored between 200 and 300 nm.

The molar ellipticity profile of sodium ampicillin consists of a strong Cotton band maximizing at about 232 nm, which suggests the intact β -lactam ring in the anionic structure.^{32, 33} This agrees with Rasmussen and Higuchi,⁴² who proved that losses in β -lactam drug activity can be observed by monitoring the distinct optical rotary differences for intact and open β -lactam rings. As such, the optical rotation was investigated for combinations of chlorhexidine diacetate and sodium ampicillin and the chlorhexidine di-ampicillin GUMBOS. The molar ellipticities of two ratios (*e.g.* 1:1 and 1:2 cation:anion) of chlorhexidine diacetate and sodium ampicillin were investigated. In terms of the 1:1 combination of precursor ions, the ampicillin component rotated optically at 232 nm. This shows that the presence of chlorhexidine diacetate does not disturb the structural integrity of the ampicillin β -lactam ring. Since ampicillin is known to readily form dimers causing its molar ellipticity to shift towards lower energies, the stoichiometric mixture of chlorhexidine diacetate and sodium ampicillin were investigated.³⁴ Similarly, a five nanometer bathochromic shift was observed for the 1:2 ratio of chlorhexidine diacetate: sodium ampicillin with a Cotton band at 237 nm. When investigating the molar ellipticity of chlorhexidine di-ampicillin, a similar positive peak was observed at 222 nm which confirms that the anionic component was intact and that ampicillin did not form a dimeric species while exchanged with chlorhexidine. This ten nanometer hypsochromic shift suggests that a higher energy is required

to rotate the ampicillin molecules in the GUMBOS structure. We hypothesize the observed hypsochromatism to have occurred due to intermolecular hydrogen bonding and electrostatic attractive forces that restrict the molecular rotation of the ampicillin molecules within the GUMBOS structure. Supported by the Franck-Condon Principle, molecular vibrations observed by interactions with noninterfering concomitant molecules or adjacent molecules and a chromophore are known to modify its nuclear coordinates of a chromophore analogous to the solvation coordinate concept. Thus, the presence of both chlorhexidine and β -lactam antibiotics (*e.g.* ampicillin, carbenicillin, oxacillin, or cephalothin) were confirmed using spectroscopy.

4.3.1.1 Chlorhexidine di-Ampicillin [CHX][Amp]

Off-white solid, yield 98%. Water solubility: 126 $\mu\text{g/mL}$. Ksp: 4.63×10^{-12} M³. ¹H NMR (400 MHz, DMSO-d₆) δ 8.56 - 8.36 (m, 2 H), 7.21 - 7.50 (m, 18 H), 5.08 (d, J=2.74 Hz, 2 H), 4.96 (s, 4 H), 3.69 (d, J=3.13 Hz, 2 H), 3.26 (br. s., 2 H), 3.07 (dt, J=7.04, 6.65 Hz, 4 H), 1.85 (s, 4 H), 1.57 (s, 6 H), 1.49 (br. s., 4 H), 1.46 (br. quin., 4 H), 1.44 (br. s., 4 H), 1.27 (br. quin., 4 H), 1.17 (s, 6 H), 1.15 (br. s., 2 H) ¹³C NMR (101 MHz, DMSO) δ 180.88, 172.88, 172.36, 166.94, 166.76, 139.07, 128.24, 127.01 - 128.43, 121.90, 76.07, 68.38, 60.80, 60.01, 58.64, 27.38, 26.76, 25.97. Anal. Calcd for C₅₄H₆₈C₁₂N₁₆O₈S₂: C, 53.86; H, 5.69; Cl, 5.89; N, 18.61; O, 10.63; S, 5.33. Found: C, 53.22; H, 5.81; Cl, 5.56; N, 18.37; S, 5.16. HRMS (ESI) m/z calcd for C₅₄H₆₈C₁₂N₁₆O₈S₂, [M+H⁺], 1203.4424; found, 1203.4136.

4.3.1.2 Chlorhexidine Carbenicillin [CHX][Carb]

Colorless solid, yield 93%. Mp = 178°C decomp. Water solubility: 52 $\mu\text{g/mL}$. Ksp: 3.53×10^{-9} M². ¹H NMR (400 MHz, DMSO-d₆) δ 0.69 - 0.76 (m, 1 H) 0.96 (s, 1 H) 1.06 (br. s., 2 H) 1.15 (br. s., 4 H) 1.34 (br. s., 4 H) 1.40 - 1.54 (m, 5 H) 1.61 (s, 2 H) 2.96 (br. s., 4 H) 3.07 (s, 1 H) 3.16 - 3.34 (m, 3 H) 3.43 (d, J=5.14 Hz, 1 H) 3.47 - 3.51 (m, 1 H) 3.52 - 3.56 (m, 1 H) 3.92 -

3.99 (m, 1 H) 4.18 - 4.27 (m, 1 H) 4.82 (br. s., 1 H) 6.96 - 7.20 (m, 9 H) 7.28 (br. s., 3 H) 7.36 - 7.68 (m, 2 H) 8.24 - 8.35 (m, 1 H). ^{13}C NMR (101 MHz, DMSO) δ 128.71, 122.65, 108.20, 40.40, 40.19, 26.42. Anal. Calcd for $\text{C}_{39}\text{H}_{48}\text{Cl}_2\text{N}_{12}\text{O}_6\text{S}$: C, 53.00; H, 5.47; Cl, 8.02; N, 19.02; O, 10.86; S, 3.63. Found: C, 51.12; H, 5.68; Cl, 7.74; N, 18.34; S, 3.50. HRMS (ESI) m/z calcd for $\text{C}_{39}\text{H}_{48}\text{Cl}_2\text{N}_{12}\text{O}_6\text{S}$, $[\text{M}^+]$, 883.8462; found, 883.8457.

4.3.1.3 Chlorhexidine di-Cephalothin [CHX][Ceph]

Orange solid, yield 83%. Water solubility: 218 $\mu\text{g}/\text{mL}$. K_{sp} : $1.89 \times 10^{-11} \text{ M}^3$. ^1H NMR (400 MHz, DMSO- d_6) δ 1.27 (br. s., 5 H) 1.45 (br. s., 6 H) 1.79 (d, $J=3.42$ Hz, 1 H) 2.01 (s, 6 H) 3.07 (br. s., 5 H) 3.17 (s, 3 H) 3.27(d, $J=17.61$ Hz, 3 H) 3.33 (br. s., 4 H) 3.50 (d, $J=17.36$ Hz, 3 H) 3.77 (d, $J=2.93$ Hz, 4 H) 4.79 (d, $J=11.98$ Hz, 2 H) 5.00 (d, $J=4.65$ Hz, 3 H) 5.03(s, 1 H) 5.53 (dd, $J=8.31, 4.89$ Hz, 2 H) 6.89 - 6.98 (m, 5 H) 7.29 (d, $J=8.80$ Hz, 6 H) 7.33 - 7.38 (m, 2 H) 7.44 (d, $J=8.31$ Hz, 13 H) 9.03 (d, $J=8.31$ Hz, 2 H) ^{13}C NMR (101 MHz, DMSO) δ 170.97, 170.41, 165.77, 163.59, 137.47, 134.44, 128.71, 127.04, 126.69, 125.39, 122.47, 113.60, 64.77, 59.12, 57.67, 40.63, 40.42, 36.23, 26.42, 25.64, 21.17. Anal. Calcd for $\text{C}_{54}\text{H}_{62}\text{Cl}_2\text{N}_{14}\text{O}_{12}\text{S}_4$: C, 49.96; H, 4.81; Cl, 5.46; N, 15.10; O, 14.79; S, 9.88. Found: C, 48.61; H, 4.99; Cl, 5.31; N, 14.70; S, 9.61. HRMS (ESI) m/z calcd for $\text{C}_{54}\text{H}_{62}\text{Cl}_2\text{N}_{14}\text{O}_{12}\text{S}_4$, $[\text{M}^+]$, 1298.3227; found, 1298.3199.

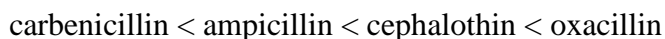
4.3.1.4 Chlorhexidine di-Oxacillin [CHX][Oxa]

Colorless solid, yield 85%. Water solubility: 167 $\mu\text{g}/\text{mL}$. K_{sp} : $8.38 \times 10^{-12} \text{ M}^3$. ^1H NMR (400 MHz, DMSO- d_6) δ 8.99 (d, $J = 9.0$ Hz, 4H), 7.90 – 7.85 (br. m, 2H), 7.76 (d, $J=7.6$ Hz, 4H), 7.71 – 7.64 (br. S, 1H), 7.60 – 7.52 (br. m, 2 H). 7.52 - 7.43 (m, 15H), 7.38 (t, $J = 7.4$ Hz, 2H), 7.28 (d, $J = 8.4$ Hz), 4.96 (d, $J=8.0$ Hz, 2 H), 4.61 (t, $J = 8.4$ Hz, 2H), 3.67 (s, 8 H), 3.40 (s., 1 H), 3.27 (br. s., 2H), 3.05 (s, 4 H), 1.55 (s, 6H), 1.43 (br. m., 4H), 1.25(br. m., 4H),

1.19 (s, 6H), ¹³C NMR (101 MHz, DMSO) δ 173.07, 1708.51, 169.46, 161.59, 159.98, 138.94, 129.85, 128.77, 128.22, 127.87, 121.84, 112.43, 75.22, 65.84, 59.67, 57.77, 52.01, 27.83, 26.02, 11.81. Anal. Calcd for C₆₀H₆₈Cl₂N₁₆O₁₀S₂: C, 55.08; H, 5.24; Cl, 5.42; N, 17.13; O, 12.23; S, 4.90. Found: C, 53.61; H, 5.40; Cl, 5.27; N, 16.67; S, 4.77. HRMS (ESI) m/z calcd for C₆₀H₆₈Cl₂N₁₆O₁₀S₂, [M⁺], 1308.3191; found, 1308.3062.

4.3.2 Pharmacokinetic Properties and Bioavailability of β -lactam-based Chlorhexidine GUMBOS

Pharmacokinetic properties of β -lactam-based chlorhexidine GUMBOS reveal an increase in hydrophobicity and a reduction in first-order dissolution rates when the anion is changed from acetate to an antibiotic (Figure 4.7). Dissolution rates were found to be 0.133 min⁻¹, 0.109 min⁻¹, 0.044 min⁻¹, and 0.038 min⁻¹ for chlorhexidine di-ampicillin, chlorhexidine carbenicillin, chlorhexidine di-cephalothin, and chlorhexidine di-oxacillin GUMBOS, respectively. It was also observed that aqueous solubility increases with molecular weight and chlorhexidine-anion stoichiometry in which the anions rank in this order:



This suggests that tuning molecular weight and ionic stoichiometry can affect the relative hydrophobicity and dissolution rates of the GUMBOS.

Table 4.1. Diffusion rates and predicted intestinal permeability acquired using PAMPA GenTest assay.

	Pe (cm/s)	Log Pe
Sodium ampicillin	1.81 x 10⁻⁵	-4.93
Chlorhexidine diacetate	9.39 x 10⁻⁷	-6.02
Chlorhexidine di-ampicillin	4.03 x 10⁻⁶	-5.39

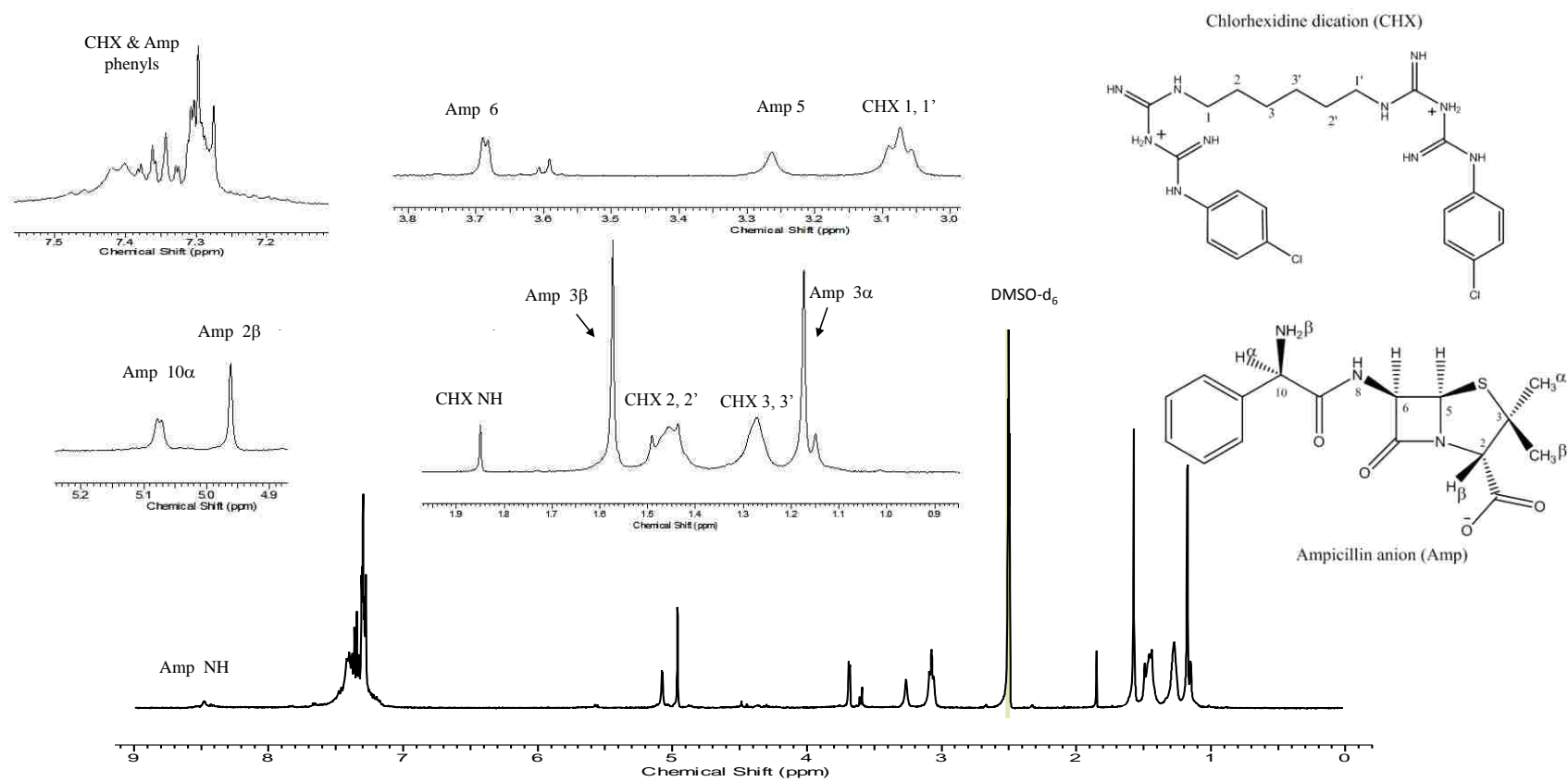


Figure 4.2. Proton (^1H)-NMR of chlorhexidine di-ampicillin.

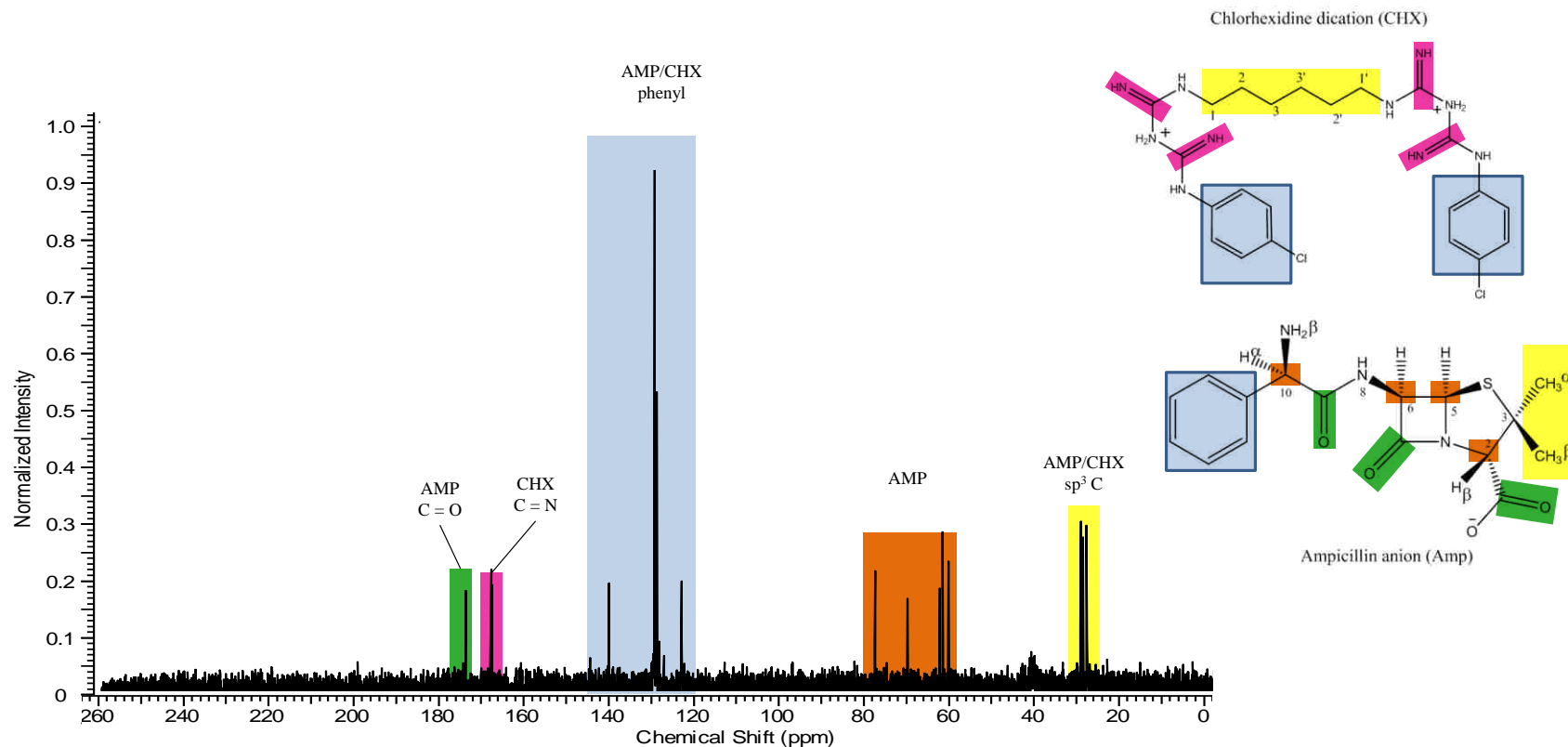


Figure 4.3. Carbon (^{13}C)-NMR of chlorhexidine di-ampicillin. The peaks indicative of either ion are labeled as CHX (chlorhexidine) and AMP (ampicillin) in addition to their color coated structural assignments in the embedded picture.

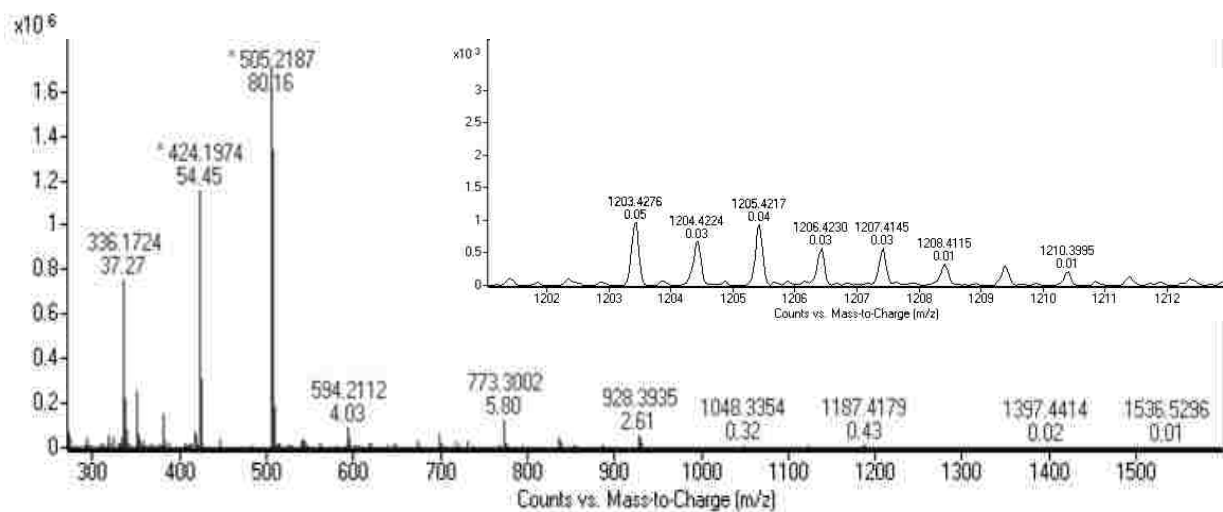
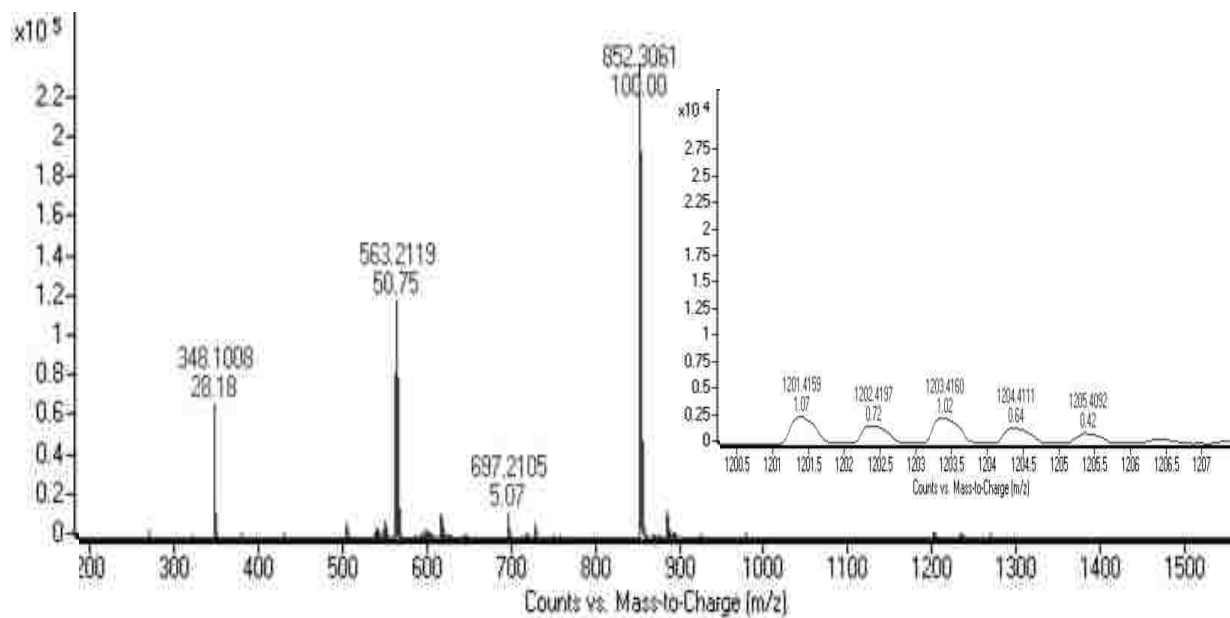


Figure 4.4. Mass spectra of chlorhexidine di-ampicillin GUMBOS in both negative-ion mode (top) and positive-ion mode (bottom).

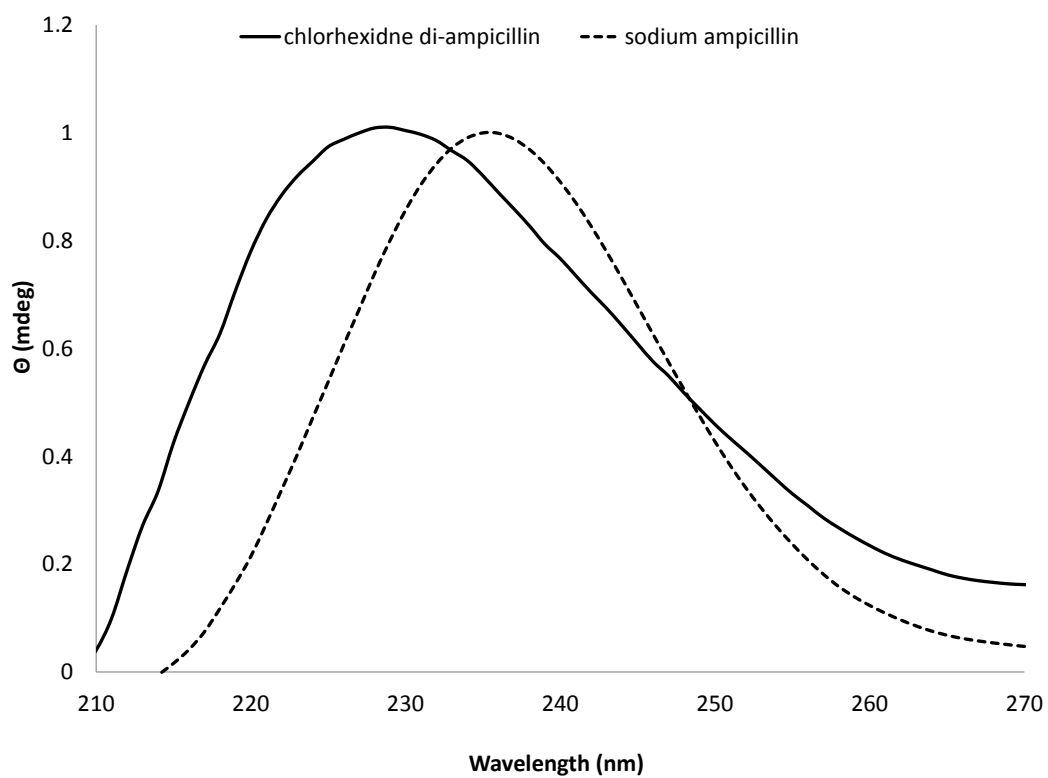


Figure 4.5. Optical ellipticities of chlorhexidine di-ampicillin (solid) and sodium ampicillin (dashed) in PBS (100mM, pH 7.4).

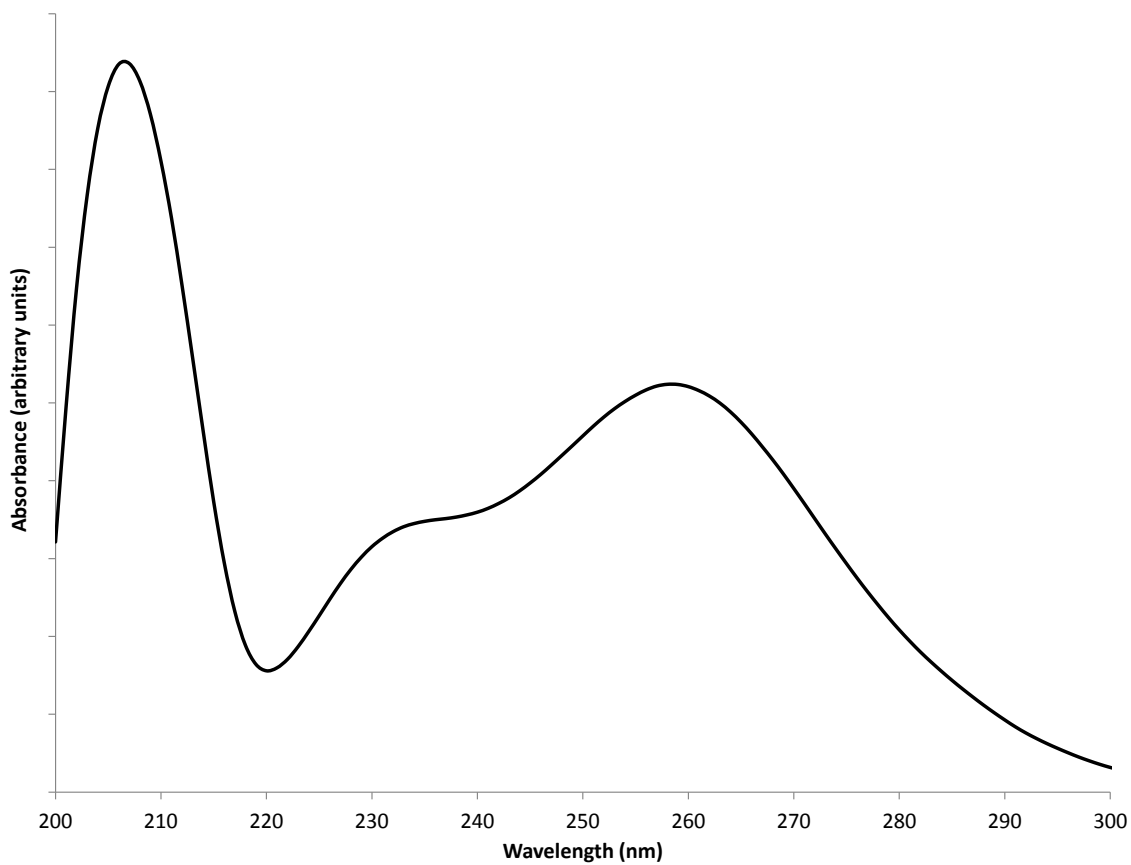


Figure 4.6. Absorbance spectra of chlorhexidine di-ampicillin in methanol.

Table 4.2. List of ions with structures detected in positive-ion and negative-ion mode.

Name	Structure	Theoretical Mass -to-Charge	Experimental Mass -to-Charge	
			[M + H] ⁺	[M - H] ⁻
Chlorhexidine di-ampicillin		1202.4235	1203.4276	1201.4159
Chlorhexidine ampicillin hydride		853.3128		852.3061
Ampicillin dimer		698.2193		697.2105
Chlorhexidine acetate hydride		564.2243		563.2119
Chlorhexidine base		505.4466	505.2187	
Chlorhexidine fragment		423.9457	424.1974	
Chlorhexidine fragment		335.8351	336.1724	
Ampicillin monomer		349.1046		348.1008

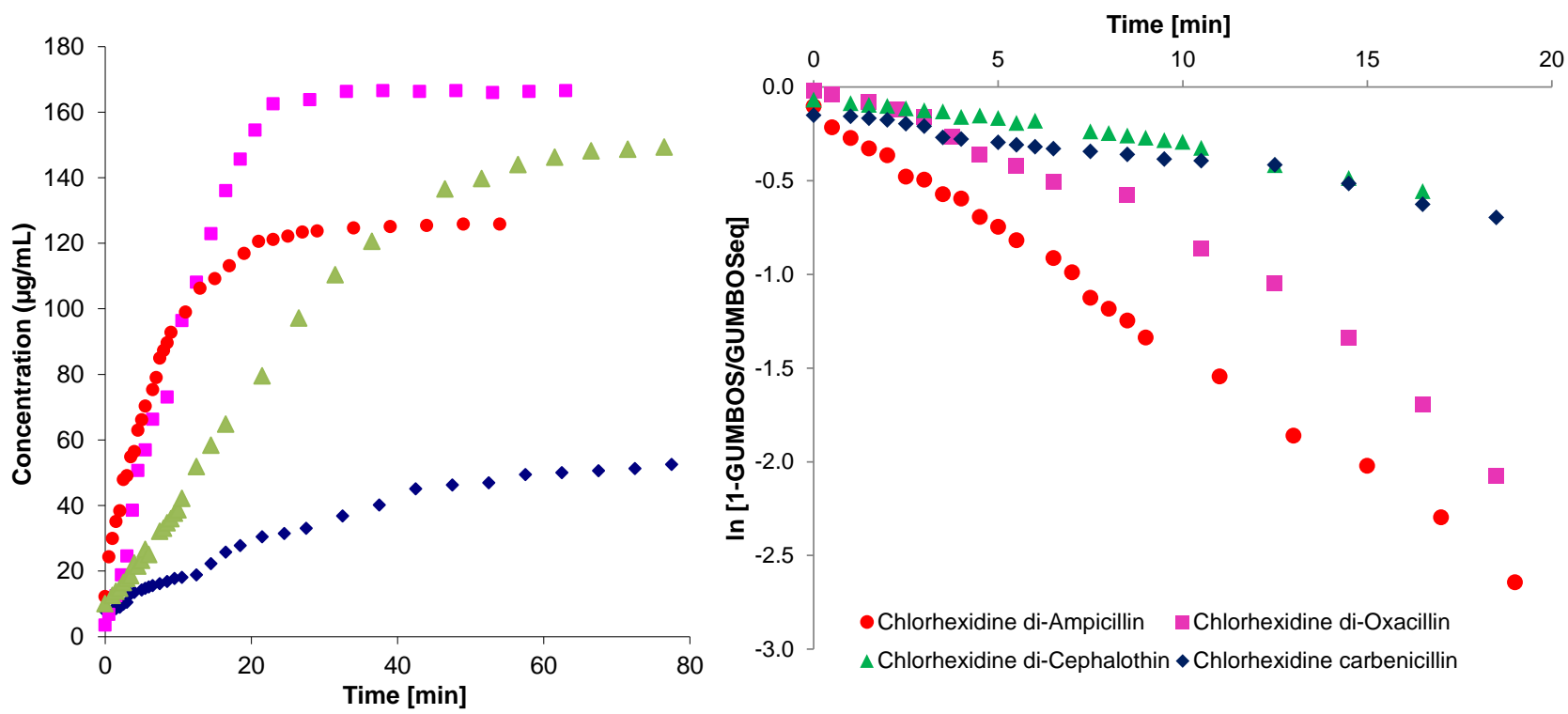


Figure 4.7. Release and first-order dissolution profiles of β -lactam based chlorhexidine GUMBOS in deionized water at 298 K.

Bioavailabilities of β -lactam-based chlorhexidine GUMBOS show that antibiotic-chlorhexidine ionic pairs have better intestinal permeability than the acetate form (Table 4.2). Human intestinal absorption (HIA) was found to range between 86 – 95% for β -lactam-based chlorhexidine GUMBOS which is 20% better absorption over the use of chlorhexidine diacetate. The mean effective permeability coefficients (Pe) for β -lactam-based chlorhexidine GUMBOS in 200 μ M PBS were found to be $9.39 (+/- 0.87) \times 10^{-7}$ cm/s, $4.03 (+/- 1.03) \times 10^{-6}$ cm/s, $3.67 (+/- 0.74) \times 10^{-6}$ cm/s, $4.98 (+/- 0.087) \times 10^{-6}$ cm/s, and $4.91 (+/- 0.17) \times 10^{-6}$ cm/s for chlorhexidine diacetate, chlorhexidine di-ampicillin, chlorhexidine carbenicillin, chlorhexidine di-cephalothin, and chlorhexidine di-oxacillin, respectively. Statistical analysis showed that the intestinal permeability of chlorhexidine diacetate was significantly increased by the use of antibiotics as anions ($p < 0.05$). However, there was no significant difference between Pe values for the GUMBOS, indicating that the intestinal permeation was independent of the cationic moiety.

4.3.3 Anti-EHEC Activity

4.3.3.1 Representative Combination Antibacterial Activity with Chlorhexidine Diacetate and Sodium Ampicillin

Different ratios of sodium ampicillin and chlorhexidine diacetate were found to have varying antibacterial activities against 6 EHEC isolates and *E. coli* 25922 (Figure 4.8). The most susceptible strain to either chlorhexidine diacetate, sodium ampicillin, or the various mixtures was found to be *E. coli* O157:H7 strain 43895. Additionally, EHEC isolates from chicken 301 and human 43890 showed the greatest susceptibility to chlorhexidine diacetate alone. Chlorhexidine diacetate antibacterial activity was less effective on EHEC pork 204P and beef 933 isolates and *E. coli* 25922. Sodium ampicillin was preferentially more active on two out of the seven *E. coli* strains investigated although all MIC values were less than 10 μ M (4 μ g/mL) as shown in Figure 4.8. All isolates tested were susceptible to both chlorhexidine diacetate and sodium ampicillin.

Table 4.3. Sources of *Escherichia coli* Strains

<i>Strain</i>	Characteristics
<i>Escherichia coli</i> 25922*	Quality control strain, Clinical isolate (stx1-, stx2-)
<i>Escherichia coli</i> O157:H7 43895*	Hamburger isolate(stx1+, stx2+)
<i>Escherichia coli</i> O157:H7 43889*	Human isolate (stx1-, stx2+)
<i>Escherichia coli</i> O157:H7 43890*	Human isolate (stx1+, stx2-)
<i>Escherichia coli</i> O157:H7 301C**	Chicken isolate (stx1+, stx2+)
<i>Escherichia coli</i> O157:H7 204P**	Pork isolate (stx1+, stx2+)
<i>Escherichia coli</i> O157:H7 933 **	Beef isolate (stx1+, stx2+)
<i>Escherichia coli</i> O157:H7 C7929**	Apple cider isolate (stx1+, stx2+)
* American Type Culture Collection, Manassas, VA	
** Michael P. Doyle, University of Georgia, GA	

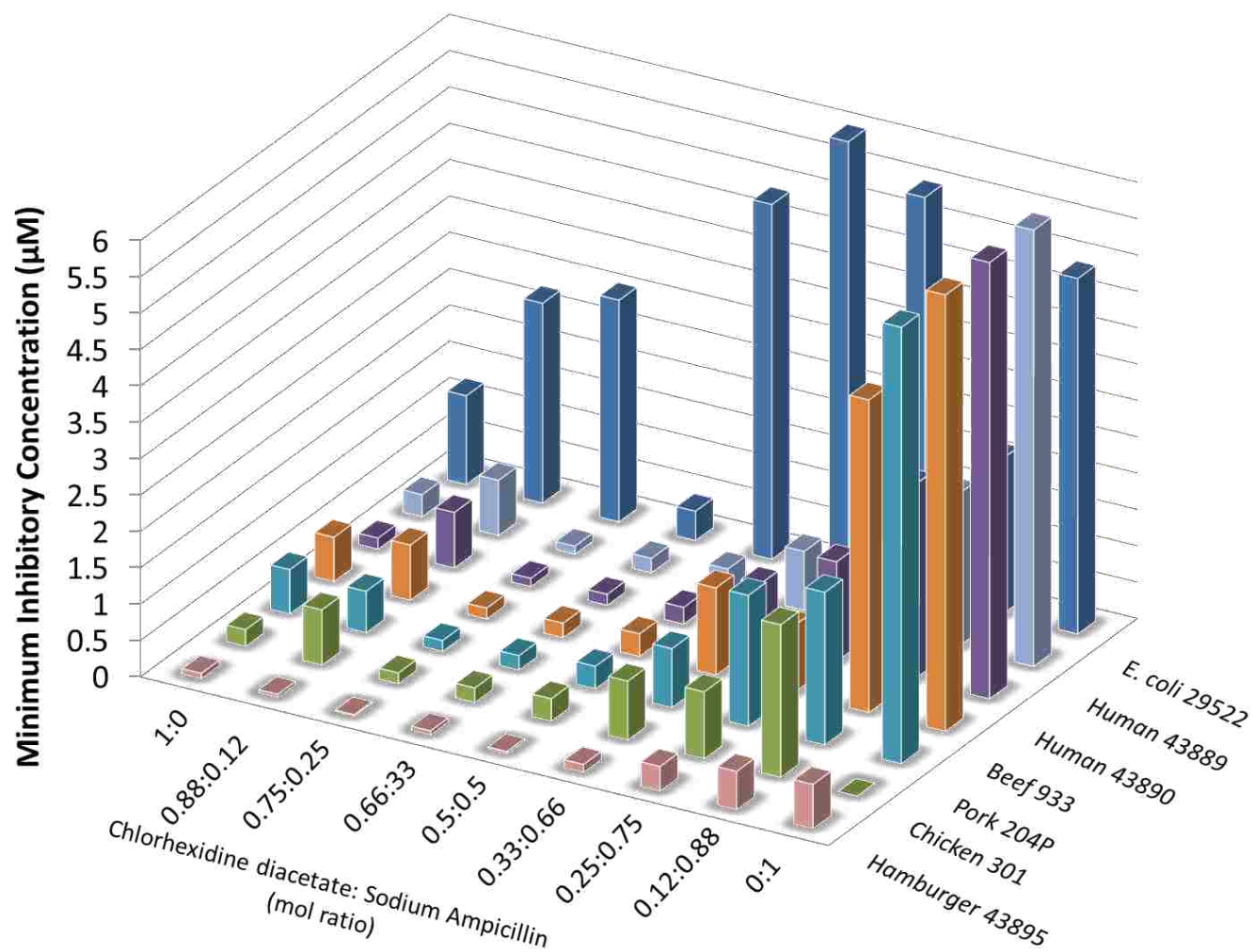


Figure 4.8. Antibacterial activities of chlorhexidine diacetate and sodium ampicillin in combination against *E. coli* 25922 and *E. coli* O157:H7 strains isolated from different sources.

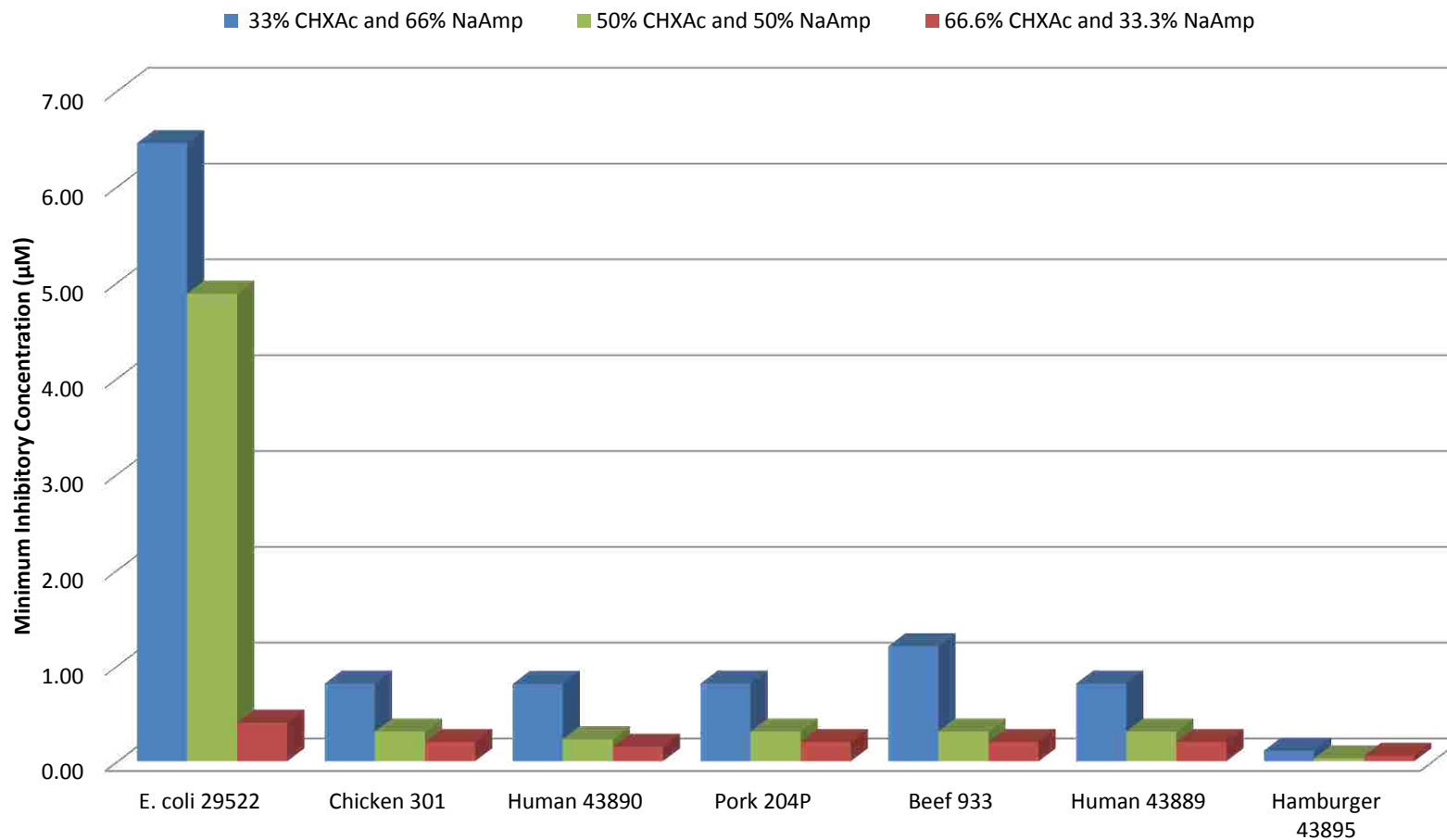


Figure 4.9. Antibacterial activities of three mixtures of chlorhexidine diacetate and sodium ampicillin against *E. coli* 25922 and *E. coli* O157:H7 strains isolated from different sources.

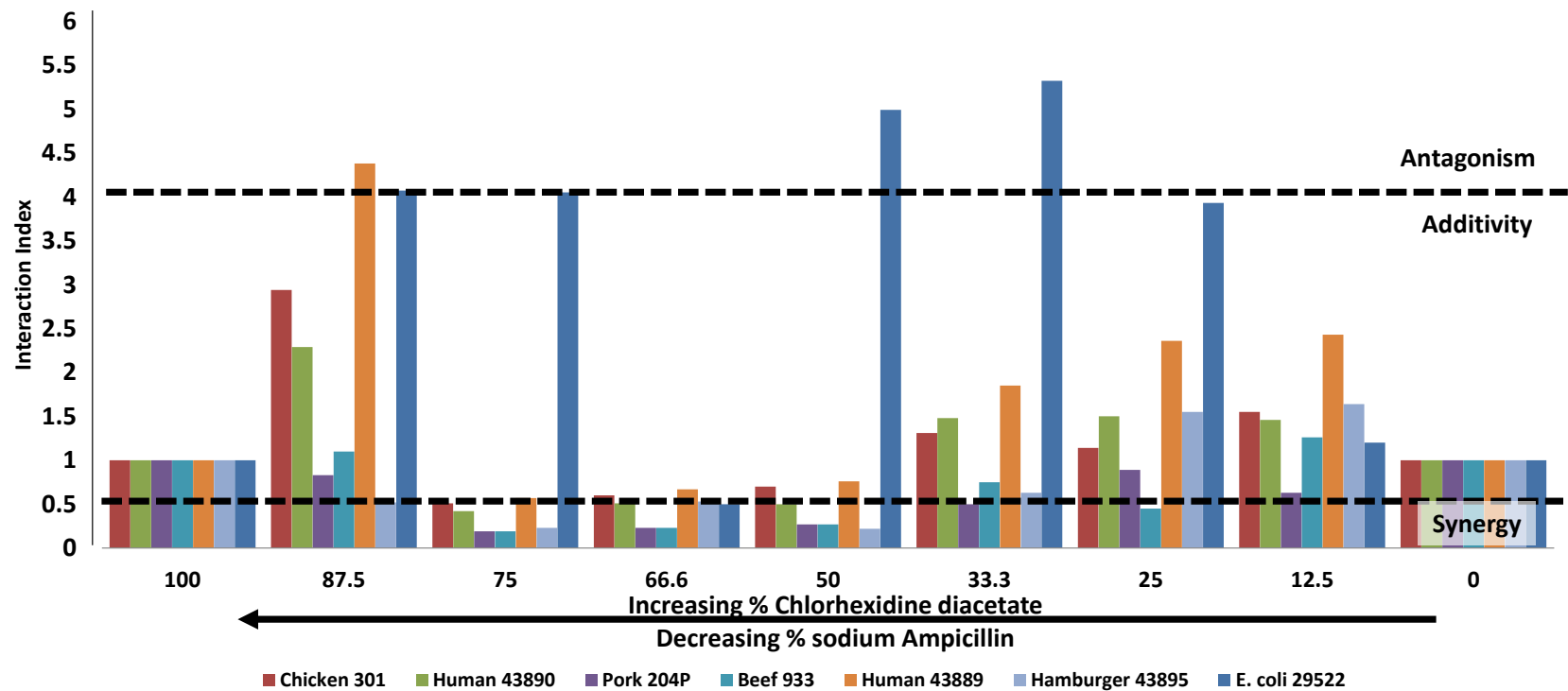


Figure 4.10. Interaction indices for mixtures of chlorhexidine diacetate and sodium ampicillin against *E. coli* 25922 and *E. coli* O157:H7 strains isolated from different sources.

When investigating the antibacterial activities of chlorhexidine diacetate and sodium ampicillin in mixtures, it is apparent that EHEC inhibition varies among strains. Overall, MIC values worsened as the abundance of sodium ampicillin increased to more than 50%, with greatest antagonism observed in *E. coli* 25922. When specifically examining the stoichiometric equivalent to the chlorhexidine di-ampicillin GUMBOS, the mixture is more effective against EHEC isolates than *E. coli* 25922 (Figure 4.9). The most effective antibacterial combination consisted of 66.6% chlorhexidine diacetate and 33.3% sodium ampicillin. Therefore, the effective combinations of chlorhexidine diacetate and sodium ampicillin required a larger abundance of chlorhexidine diacetate than sodium ampicillin.

Figure 4.10 reveals the interaction indices obtained for combinations of chlorhexidine diacetate and sodium ampicillin in which majority of them were neutral. Increasing concentrations of sodium ampicillin resulted in increasing antagonism within mixtures. Synergetic responses are evident in concentrations greater than 50% chlorhexidine diacetate. As percentages of chlorhexidine diacetate exceeded 75%, interactions with sodium ampicillin led to antagonism and additivity.

4.3.3.2 Chlorhexidine di-Ampicillin

The antibacterial activities of the reacted chlorhexidine di-ampicillin GUMBOS were compared to chlorhexidine diacetate and sodium ampicillin and the stoichiometric combination of parent salts against EHEC (Table 4.4). Chlorhexidine di-ampicillin inhibited EHEC growth at a concentration ranging from 0.05 to 0.10 μM with an average inhibition observed at 0.07 μM . The average MICs for chlorhexidine diacetate and sodium ampicillin were 0.3 μM and 6.5 μM , respectively. Average inhibitory concentrations for the mixed salts (1:2 chlorhexidine diacetate and sodium ampicillin, v/v%) was determined to be 2.1 μM . Thus, chlorhexidine di-ampicillin required 28 – 154 and 8 – 49 times lower concentration to inhibit the growth of EHEC isolates

than sodium ampicillin and the combination of parent salts, respectively. Although comparable, chlorhexidine di-ampicillin was 2-10 times more effective than chlorhexidine diacetate, with an average 4-fold improvement in MIC. Growth observed 24h after plating non-turbid MIC wells demonstrated that chlorhexidine di-ampicillin is bacteriostatic at lower concentrations, but bactericidal at concentrations greater than 7.3 μM (103x chlorhexidine di-ampicillin MIC).

4.3.3.3 Chlorhexidine Carbenicillin

The antibacterial activities of the reacted chlorhexidine carbenicillin GUMBOS were compared to chlorhexidine diacetate and disodium carbenicillin (Table 4.5). Chlorhexidine carbenicillin inhibited EHEC strain 43895 growth with 0.11 μM . The average MICs for chlorhexidine diacetate and disodium carbenicillin were 0.3 μM and 93.75 μM , respectively. Chlorhexidine carbenicillin required 3 and 852 times lower concentration to inhibit the growth of EHEC isolates than chlorhexidine diacetate and disodium carbenicillin, respectively. Similar to chlorhexidine di-ampicillin, comparable antibacterial activity to chlorhexidine diacetate was observed for chlorhexidine carbenicillin. Additionally, chlorhexidine carbenicillin is considered to be bacteriostatic since its MBC (*i.e.* 3.3 μM) is greater than its MIC by nearly 30x.

4.3.3.4 Chlorhexidine di-Cephalothin

The antibacterial activity of chlorhexidine di-cephalothin was compared to chlorhexidine diacetate and sodium cephalothin (Table 4.5). Chlorhexidine di-cephalothin inhibited EHEC strain 43895 growth with 0.10 μM . The average MICs for chlorhexidine diacetate was 0.3 μM . The antibacterial activity of sodium cephalothin was found to be 104 μM . Thus, chlorhexidine di-cephalothin required 3 and 1040 times lower concentration to inhibit the growth of EHEC isolates than chlorhexidine diacetate and sodium cephalothin, respectively. The MBC obtained for chlorhexidine di-cephalothin was also 3.3 μM which exceeds its MIC by 33-fold.

4.3.3.5 Chlorhexidine di-Oxacillin

The antibacterial activity of chlorhexidine di-oxacillin was compared to chlorhexidine diacetate and sodium oxacillin (Table 4.5). Chlorhexidine di-cephalothin inhibited EHEC strain 43895 growth with 0.13 μM . The average MICs for chlorhexidine diacetate was 0.3 μM . The antibacterial activity of sodium cephalothin was found to be 98 μM . Thus, chlorhexidine di-cephalothin required 3 and 753 times lower concentration to inhibit the growth of EHEC isolates than chlorhexidine diacetate and sodium oxacillin, respectively. The MBC obtained for chlorhexidine di-cephalothin was also 3.3 μM which exceeds its MIC by 26-fold.

4.3.4 Interaction Indices

Interaction indices tabulated for GUMBOS were compared to the mixture of precursor salts in Table 4.6. Synergy was observed for chlorhexidine di-ampicillin in all EHEC isolates ($I_{\text{avg}} = 0.28$), whereas, both antagonism and additivity ($I_{\text{avg}} = 3.3$) were seen for the stoichiometric mixture in 71% and 29% of the test organisms, respectively. Additivity was observed for chlorhexidine di-ampicillin and the mixture against *E. coli* 25922.

Table 4.7 lists the interaction indices obtained for GUMBOS against *E. coli* O157:H7 strain 43895 and *E. coli* ATCC 25922. The results reveal that all β -lactam based chlorhexidine GUMBOS were synergetic against *E. coli* O157:H7 strain 43895 with increased synergy by anion type in the following order:

$$\text{Ampicillin} < \text{Carbenicillin} < \text{Cephalothin} < \text{Oxacillin}$$

Interaction indices for the GUMBOS follow a similar trend, despite chlorhexidine di-ampicillin additivity, against *E. coli* ATCC 25922.

Table 4.4. Minimum inhibitory concentrations (μM) of antibacterial agents against *E. coli* O157:H7 strains isolated from different sources. Standard deviations are from three measurements.

	<i>E. coli</i> 25922	Chicken 301C	Pork 204P	Beef 933	Apple Cider C7929	Hamburger 43895	Human 43889	Human 43890
Chlorhexidine diacetate	0.3 ± 0.1	0.6 ± 0.05	0.1 ± 0.02	0.4 ± 0.06	0.3 ± 0.07	0.2 ± 0.03	0.3 ± 0.05	0.2 ± 0.03
Sodium ampicillin	7 ± 1	4 ± 0.5	5 ± 0.1	7 ± 0.1	10 ± 0.3	2 ± 0.2	10 ± 0.1	7 ± 0.3
Combination 1 Chlorhexidine diacetate:2 Sodium Ampicillin	0.8 ± 0.1	2 ± 0.3	0.4 ± 0.1	1 ± 0.3	7 ± 1	0.7 ± 0.1	2 ± 0.03	2 ± 0.06
Chlorhexidine di-ampicillin	0.3 ± 0.1	0.06 ± 0.02	0.05 ± 0.01	0.08 ± 0.04	0.1 ± 0.04	0.08 ± 0.02	0.06 ± 0.02	0.07 ± 0.02

Table 4.5. Average minimum inhibitory concentrations (μM) of β -lactam-based chlorhexidine GUMBOS against *E. coli* ATCC 25922 and *E. coli* O157:H7 ATCC 43895. Standard deviations are from six measurements.

	<i>E. coli</i> 25922	<i>E. coli</i> 43895
Chlorhexidine diacetate	0.28 ± 0.03	0.23 ± 0.02
Chlorhexidine di-ampicillin	0.26 ± 0.10	0.08 ± 0.04
Chlorhexidine carbenicillin	0.22 ± 0.06	0.11 ± 0.03
Chlorhexidine di-cephalothin	0.20 ± 0.07	0.10 ± 0.03
Chlorhexidine di-oxacillin	0.20 ± 0.06	0.13 ± 0.04

Table 4.6. Calculated interaction indices (classification denoted in parentheses, where A = Antagonism, N = Neutral, and S = Synergy) for chlorhexidine di-ampicillin GUMBOS and the combined parent salts according a modified Loewe's Additivity Model.

	<i>E. coli</i>	Chicken	Pork	Beef	Apple Cider C7929	Hamburger	Human	Human
	25922	301 C	204 P	933		43895	43889	43890
Stoichiometric Combination								
1 Chlorhexidine diacetate:2 Sodium Ampicillin	2.8 (N)	1.4 (N)	1.9 (N)	1.2 (N)	10.1 (A)	1.5 (N)	2.0 (N)	5.1 (A)
GUMBOS								
Chlorhexidine di-Ampicillin	0.9 (N)	0.1 (S)	0.5 (S)	0.1 (S)	0.5 (S)	0.3 (S)	0.2 (S)	0.3 (S)

Table 4.7. Calculated interaction indices (classification denoted in parentheses, where A = Antagonism, N = Neutral, and S = Synergy) for β -lactam based chlorhexidine GUMBOS according a modified Loewe's Additivity Model.

	<i>E. coli</i>	<i>E. coli</i>
	25922	43895
Chlorhexidine di-ampicillin	0.88 (A)	0.28 (S)
Chlorhexidine carbenicillin	0.47 (S)	0.23 (S)
Chlorhexidine di-cephalothin	0.33 (S)	0.22 (S)
Chlorhexidine di-oxacillin	0.21 (S)	0.19 (S)

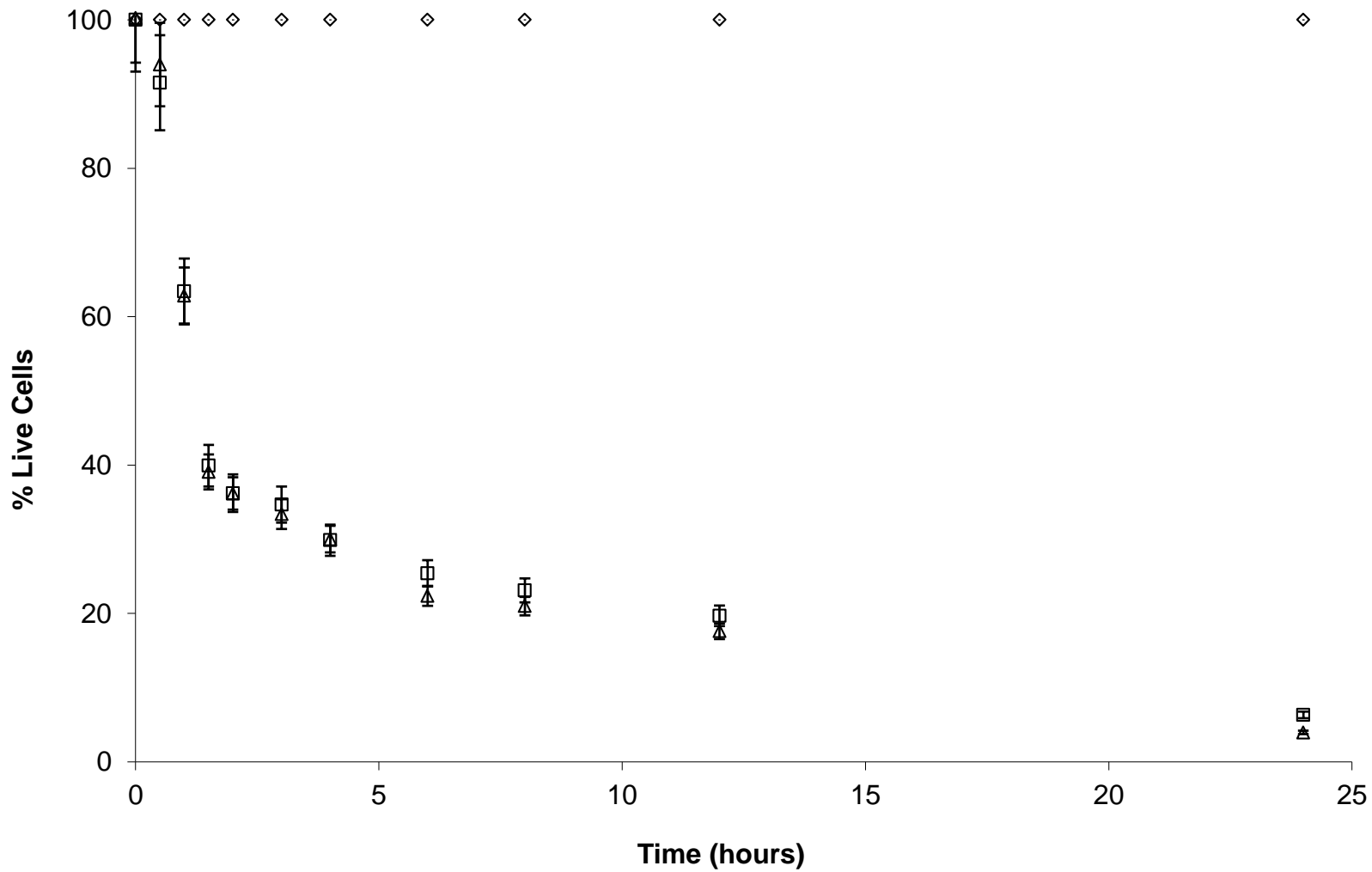


Figure 4.11. Killing kinetics of *E. coli* O157:H7 ATCC 43895 at 7.3 μ M chlorhexidine di-ampicillin (Δ) and chlorhexidine diacetate (\square) as compared to the control (\diamond). Error bars represent standard deviations from three measurements.

4.3.5 Time-kill Activity of Chlorhexidine di-ampicillin on *E. coli* O157:H7 43895

Bactericidal rates for chlorhexidine di-ampicillin and chlorhexidine diacetate were monitored at the MBC for chlorhexidine di-ampicillin against 10^6 CFU/ml, (Figure 4.11). A minimum of five hours minimal was required to kill 10^6 CFU/mL bacteria at $7.3 \mu\text{M}$ for both chlorhexidine salts.

4.3.6 Mechanism of Action Studies

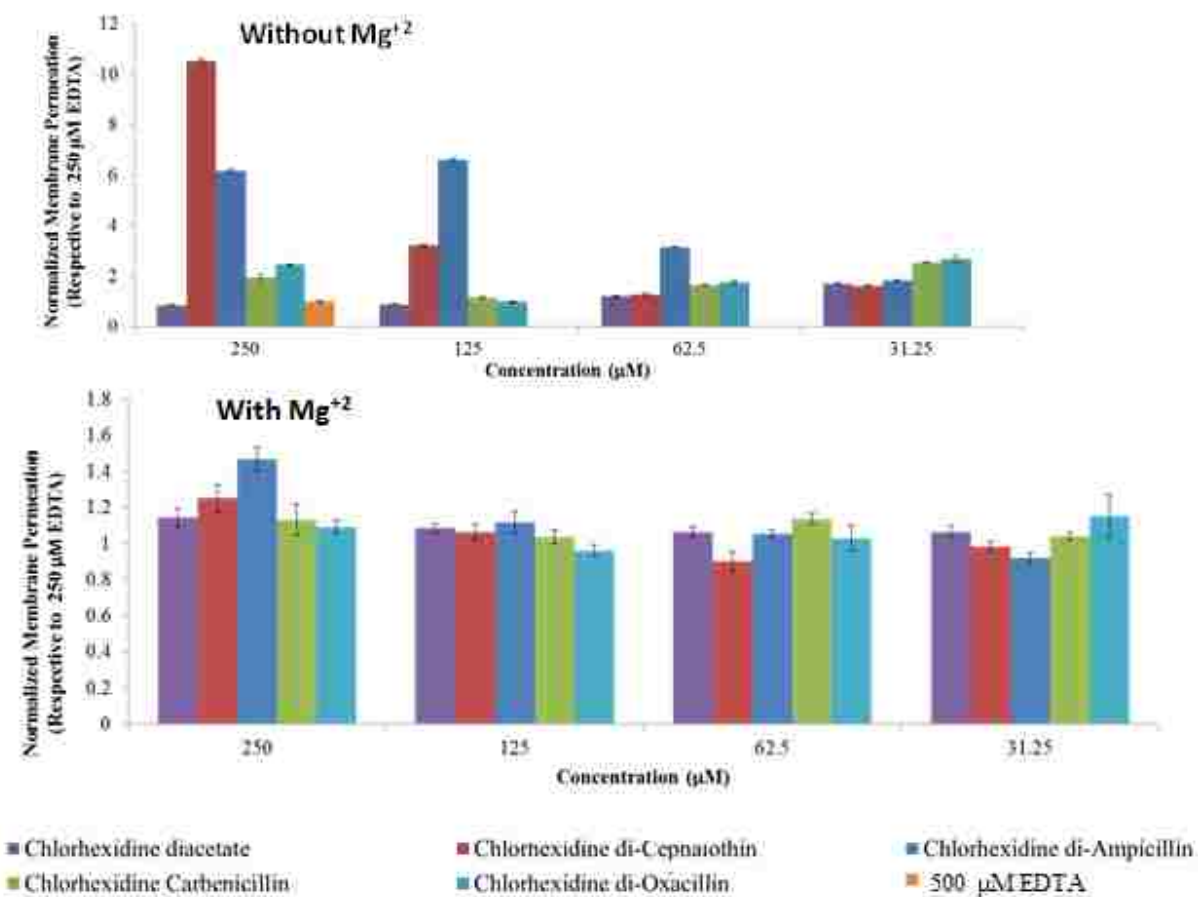


Figure 4.12. Effect of GUMBOS on *E. coli* O157:H7 ATCC 43895 outer membranes in absence (top) and presence (bottom) of 5mM magnesium ions. Results normalized to NPN membrane fluorescence obtained by EDTA as negative control.

4.3.6.1 Effects of Divalent Cations on EHEC Susceptibility to GUMBOS

The effects of divalent cations on the antibacterial susceptibility of chlorhexidine salts to *E. coli* O157:H7 strain 43895 was evaluated. The addition of $200 \mu\text{M}$ Ca^{2+} or Mg^{2+} antagonized

the antibacterial activity of all β -lactam based chlorhexidine GUMBOS equally to chlorhexidine diacetate (data not shown). This attenuation in antibacterial activity suggests that excess divalent cations interfere with the membrane activity of these agents and that the ions play a vital role in the GUMBOS mechanisms of action.

4.3.6.2 Effects of GUMBOS on Permeability of *E. coli* O157:H7 strain 43895 Outer Membrane

To determine whether GUMBOS targeted the outer membranes of EHEC, we performed the NPN assay. No fluorescence accumulation was evident when GUMBOS or starting materials were added to the buffer containing NPN absent of cells. The addition of GUMBOS to EHEC cells in the presence of NPN caused a time-dependent increase in fluorescence with fluorescence stability occurring at 3 minutes. Equal membrane permeation for all salts at concentrations below 30 μ M was observed (data not shown). At higher concentrations, the greatest damage in membrane integrity was observed by chlorhexidine di-ampicillin in the absence of extraneous magnesium ions (Figure 4.12). Enhanced membrane permeation, with respect to EDTA, decreases in the following order: chlorhexidine di-cephalothin > chlorhexidine carbenicillin > chlorhexidine di-oxacillin > chlorhexidine diacetate. As expected, EDTA also caused increases in fluorescence intensity without subsequent cell death. At the largest concentration, chlorhexidine di-cephalothin causes 10.5x more membrane damage than EDTA. Chlorhexidine di-ampicillin permeates the outer membrane 6x more effectively than EDTA. Chlorhexidine di-oxacillin, chlorhexidine carbenicillin, and chlorhexidine diacetate detrimentally impacts the membrane 2.5, 2, and 0.8 times better than EDTA. At lower concentrations, the extent of damage is attenuated and the GUMBOS membrane activity are equally 2 times better than EDTA. Normalized results demonstrate that six times less concentration of GUMBOS can permeate bacteria cells more efficiently than 250 μ M EDTA. To confirm disrupted action on the outer

membrane via replacement of divalent cations with β -lactam based chlorhexidine GUMBOS, we investigated whether the divalent cations inhibited the increase in NPN fluorescence. Similar to EDTA, we found that the addition of either Ca^{2+} or Mg^{2+} inhibited the increase in NPN fluorescence induced by all chlorhexidine salts. Thus, the membrane activities of GUMBOS and chlorhexidine diacetate to the cellular outer membrane are antagonized by the presence of excess magnesium or calcium (Figure 4.12B). This indicates that displacement of divalent ions is an important feature for activity.

4.3.6.3 Effects of GUMBOS on *E. coli* O157:H7 strain 43895 Membrane Potential

Beta-lactam based chlorhexidine GUMBOS caused different extents of membrane depolarization at concentrations above 4 μM . More specifically, greater depolarization was achieved using chlorhexidine di-ampicillin as compared to the other chlorhexidine salts. Even more so, all GUMBOS outperformed chlorhexidine diacetate (Figure 4.13). The GUMBOS' ability to depolarize *E. coli* outer membranes decrease in the following order: chlorhexidine di-ampicillin, chlorhexidine di-cephalothin, chlorhexidine di-oxacillin, and chlorhexidine carbenicillin. Our results show that chlorhexidine diacetate is unable to depolarize EHEC cellular outer membranes as efficiently as GUMBOS.

4.3.6.4 GUMBOS Activity on LPS-Rich and Deficient *E. coli*

Antibacterial activity against wild-type and increased membrane permeable *E. coli* strains show that chlorhexidine di-ampicillin GUMBOS were 17x more effective in inhibiting *E. coli imp4213* than wild-type *E. coli* (Figure 4.14). Likewise, chlorhexidine carbenicillin and chlorhexidine di-oxacillin preferentially inhibited *E. coli imp4213* by 9x and 8x, respectively. This implies that β -lactam based chlorhexidine GUMBOS are able to cross the LPS-deficient outer membrane of *imp4213* more readily than the LPS-rich membrane that is present in wild-type *E. coli*. The MICs for chlorhexidine diacetate and GUMBOS were comparable in *imp4213*

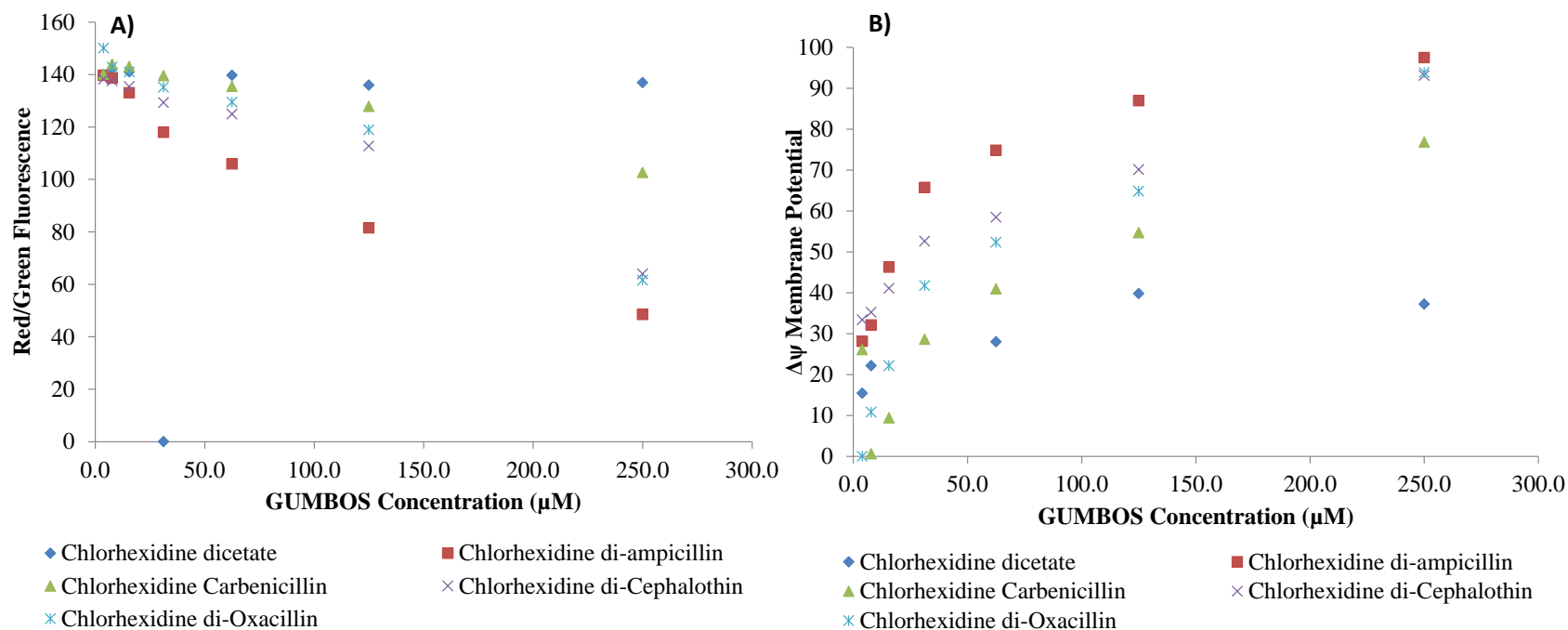


Figure 4.13. Changes in *Escherichia coli* O157:H7 ATCC 43895 membrane potentials using DIOC₂ stained cells treated with increasing concentrations of GUMBOS. The Panel (A) show the red/green ratiometric fluorescence obtained for different concentration of GUMBOS. Using the Nernst equation, results in Panel (A) are converted to membrane potential values as shown in Panel (B). GUMBOS Error bars represent standard deviations from nine measurements.

inhibition; whereas, variable differences in antibacterial activity were observed with GUMBOS treatment on wild-type *E. coli*.

Antibacterial activity on wild-type *E. coli* occurred in the following order: chlorhexidine di-ampicillin > chlorhexidine diacetate = chlorhexidine carbenicillin > chlorhexidine di-oxacillin. We attribute this order to the already established mechanism of action for chlorhexidine salts that contain a bio-inactive counter-ion (*i.e.* dihydrochloride, diacetate, or digluconate).^{9-11, 35-39} Regardless of the anion, GUMBOS still interact with the outer membrane of Gram-negative bacteria at divalent-cation-binding sites on LPS, displaces stabilizing divalent cations, and causes outer membrane permeation similarly to other polycationic antibiotics. Furthermore, β -lactam antibiotics do not interfere with the membrane activity when chlorhexidine is used in the form of GUMBOS.

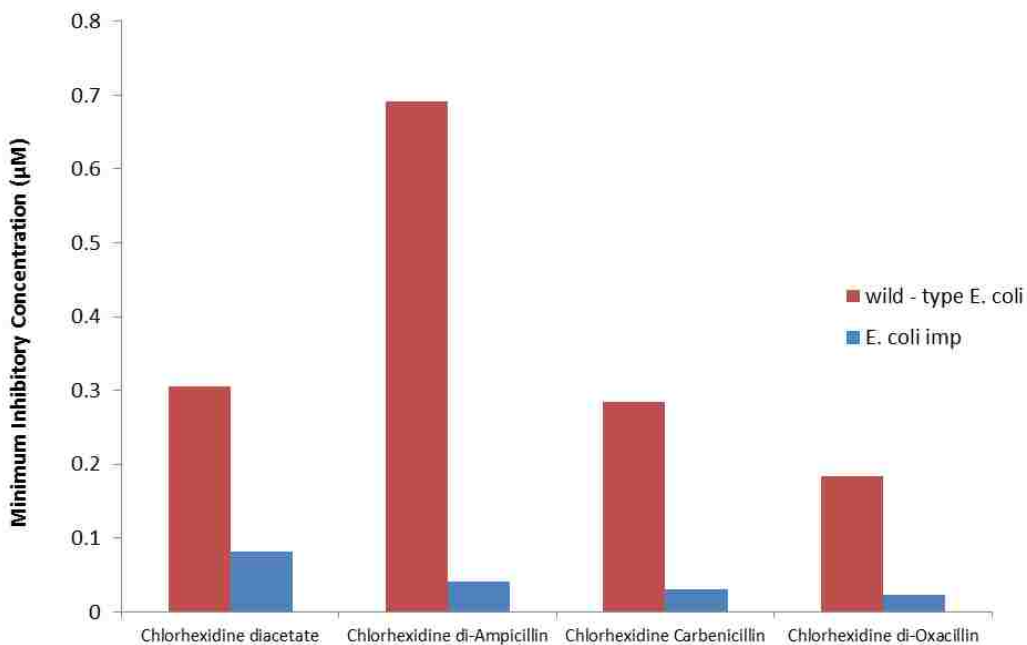


Figure 4.14. Antibacterial activity of β -lactam based chlorhexidine GUMBOS against wild-type and imp4213 *E. coli* strains.

4.3.6.5 Effects of GUMBOS on membrane integrity of *E. coli* O157:H7 strain 43895.

Scanning electron micrographs of post-treated EHEC revealed elongated cells following exposure to sodium ampicillin (Figure 4.15B). The cell surface for both untreated (Figure 4.15A) and sodium ampicillin treated EHEC present a smooth cell surface. Evaluation of imaged cells showed that untreated and sodium ampicillin treated cells maintained ultra-structural integrity of the outer membrane. Figures 4.15C and 4.15E illustrated that chlorhexidine diacetate and the mixture of salts disrupted the outer membrane of EHEC, as indicated by the ruffled surface of the cells. In addition to the ruffled cellular surface similar to chlorhexidine diacetate, there was long, undivided cells which is a feature of ampicillin treatment (Figure 4.15E). Our results demonstrate that > 90% of chlorhexidine di-ampicillin-exposed cells suffered from inner and outer membrane perturbation, which caused the intracellular materials to leak (Figure 4.15D).

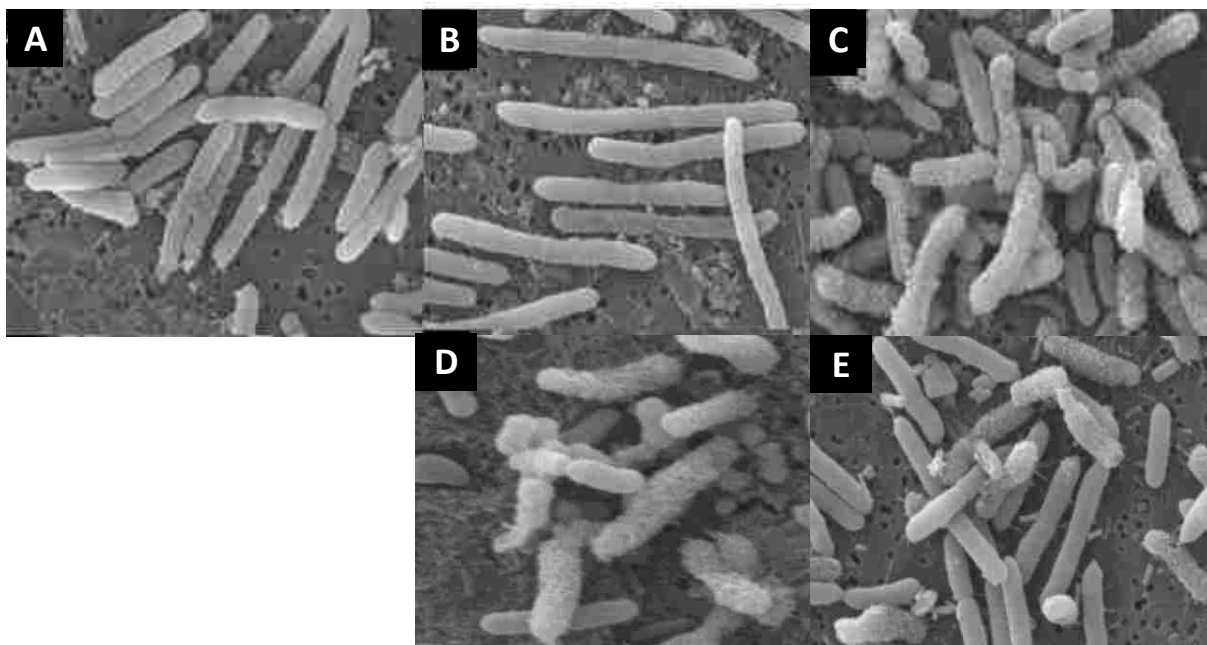


Figure 4.15. SEM images of A) untreated and antibacterial treated *E. coli* O157:H7 ATCC 43895 with B) 50 μ M sodium ampicillin, C) 50 μ M chlorhexidine diacetate, D) 50 μ M chlorhexidine di-ampicillin, and E) 50 μ M stoichiometric mixture of parent salts.

4.3.7 Cytotoxicity

Potential routes of administration were evaluated by monitoring acute mammalian cytotoxicity using HeLa cervical cells, NIH/3T3 fibroblasts, and EOMA endothelial cellular lines (Table 4.8). Overall, cytotoxicity of the investigated chlorhexidine salts and stoichiometric molar drug combinations increases in this order, ampicillin < oxacillin < cephalothin < acetate \leq carbenicillin. Differences observed between cellular lines may indicate tunable therapeutic indices amongst chlorhexidine salts and potential expansion in administration routes. The impacts GUMBOS have on each cellular line tested are described in more detail in the subsequent sections.

4.3.7.1 Cytotoxicity to HeLa Cervical Cells

Cytotoxicity using HeLa cells is shown in Table 4.8. The acute toxicities (LD_{50}) of GUMBOS were determined to range between 44 to 149 μM . More specifically, the toxicity of chlorhexidine diacetate, sodium ampicillin, and combined chlorhexidine diacetate and sodium ampicillin was 43, and >400, and 76 μM , respectively. Chlorhexidine di-ampicillin is less toxic to cervical cells than starting materials and combined precursor ions with a LD_{50} of 149 μM . This GUMBOS is able to attenuate cytotoxicity nearly 2 – 3.5 times in comparison to chlorhexidine diacetate and the stoichiometrically combined chlorhexidine diacetate and sodium ampicillin salts, respectively. Although not as statistically significant from the mixture of chlorhexidine and antibiotic, both chlorhexidine di-cephalothin and chlorhexidine di-oxacillin had improved LD_{50} values from chlorhexidine diacetate. Chlorhexidine carbenicillin is the only GUMBOS that had a LD_{50} value similar to chlorhexidine diacetate and worse than stoichiometric mixture of chlorhexidine diacetate and disodium carbenicillin. Reduced toxicity to cervical cells validates the use of some chlorhexidine salts systemically.

4.3.7.2 Cytotoxicity to NIH/3T3 Fibroblast Cells

Cytotoxicity results to NIH/3T3 fibroblasts reveal that β -lactam based chlorhexidine GUMBOS are as equally nontoxic as chlorhexidine diacetate. As expected, β -lactam antibiotics were not toxic within the concentration range tested and cell viability did not significantly vary between chlorhexidine diacetate, mixtures, and GUMBOS when investigating acute toxicity against NIH/3T3 fibroblast cells. However, polytherapeutic mixtures containing chlorhexidine and antibiotic are more cytotoxic than β -lactam based chlorhexidine GUMBOS. Since chlorhexidine diacetate is commonly used non-systemically, or as a topical disinfectant, this shows that the novel chlorhexidine salts can continually be used topically without inflicting additional toxicity.

4.3.7.3 Cytotoxicity to EOMA Endothelial Cells

Similar to HeLa cells, GUMBOS treatment on EOMA endothelial cells show variable cytotoxicity. For instance, chlorhexidine carbenicillin and chlorhexidine di-oxacillin are more toxic to endothelial cells than chlorhexidine diacetate. On the other hand, chlorhexidine di-ampicillin and chlorhexidine di-cephalothin are less toxic, with the latter by nearly 2x chlorhexidine diacetate. These differences in cytotoxicity show that some GUMBOS are safe to use systemically when large concentrations are considered. However, the antibacterial activities of these salts against EHEC are more than 1000x less than their respective EOMA LD₅₀ values which suggests their safe use systemically.

Acute toxicity for chlorhexidine diacetate, antibiotic, and GUMBOS was determined *in vitro* using HeLa, NIH/3T3, and EOMA cells. The LD₅₀ values against all cells were about 43 μ M or 2.7% w/v for chlorhexidine diacetate which agrees with previously published values. Such concentrations of chlorhexidine have caused mild to severe inflammatory responses as well as induced apoptosis, necrosis, and over-expression of cellular stress indicators when used

systemically.⁴⁰⁻⁴³ Reports indicate that cytotoxicity results in mild to severe discomfort when increasing quantities of chlorhexidine are ingested, although it is poorly absorbed. Additionally, its use intravenously has caused hypotonic-induced hemolysis.⁹ Since literatures supports that a 2% concentration of chlorhexidine may detrimentally affect host tissues, reducing the apparent toxicity associated with chlorhexidine in the GUMBOS structure is priority. At the LD₅₀ for chlorhexidine diacetate, mammalian cells treated with GUMBOS resulted in better cell viability. Thus, our results suggest that these cells were more sensitive to the toxic effects of chlorhexidine diacetate and its use with antibiotics in stoichiometric combination at concentrations above 3 μ M. Interestingly, the addition of antibiotic molecules to the chlorhexidine structure as a mixture or GUMBOS was able to reduce the cytotoxic effects of chlorhexidine on mammalian cells. This approach demonstrates that the reacted GUMBOS have potential to extend the antibacterial efficacy of antibiotics while reducing toxicities associated with chlorhexidine diacetate.

In summary, GUMBOS toxicity to fibroblasts was similar as each salt but different with HeLa and EOMA cells. Both HeLa and EOMA viabilities are similar in β -lactam based chlorhexidine GUMBOS where ampicillin is the least toxic anion used and carbenicillin is the most. We attribute this to the cation-anion stoichiometry and anion size among GUMBOS. More specifically, a 3-fold increase in chlorhexidine carbenicillin toxicity to HeLa cells was observed when compared to chlorhexidine di-ampicillin. We attribute this difference in toxicity to the structural difference between the two antibiotics. It is apparent that modifying C-8 to a carboxylate (*i.e.* carbenicillin) forms a dianionic species that has a 1:1 cation-anion stoichiometry with chlorhexidine. This differs from the 1:2 stoichiometry of chlorhexidine di-ampicillin that has a primary amine on C-8 instead of a carboxylate like in carbenicillin. When comparing all GUMBOS to chlorhexidine carbenicillin, it is apparent that this molecular change most

negatively affected the cell viability of mammalian cells. Furthermore, the differences in acute toxicity infer that chlorhexidine di-ampicillin, chlorhexidine di-cephalothin, and chlorhexidine di-oxacillin would be better GUMBOS to use during the treatment of a systemic infection since they are less cytotoxic than the other chlorhexidine salts investigated. These results indicate that β -lactam based chlorhexidine GUMBOS are safer alternatives to antibiotic-chlorhexidine drug mixtures when used either topically or systemically.

Table 4.8. Acute cytotoxicity (LD_{50}) of chlorhexidine di-ampicillin, chlorhexidine diacetate, sodium ampicillin, and the stoichiometric equivalent on HeLa cells. Standard deviations from four measurements.

Antimicrobial Agent	HeLa	NIH/3T3	EOMA
Chlorhexidine diacetate	43 \pm 6	47 \pm 2	80 \pm 3
Chlorhexidine di-Ampicillin	149 \pm 4	48 \pm 3	109 \pm 6
Chlorhexidine diacetate + Sodium Ampicillin	76 \pm 9	43 \pm 2	67 \pm 11
Chlorhexidine Carbenicillin	44 \pm 7	48 \pm 7	73 \pm 10
Chlorhexidine diacetate + Disodium Carbenicillin	58 \pm 13	51 \pm 4	59 \pm 4
Chlorhexidine di-Cephalothin	79 \pm 12	52 \pm 5	150 \pm 13
Chlorhexidine diacetate + Sodium Cephalothin	64 \pm 9	52 \pm 6	103 \pm 14
Chlorhexidine di-Oxacillin	139 \pm 6	48 \pm 4	97 \pm 16
Chlorhexidine diacetate + Sodium Oxacillin	102 \pm 21	44 \pm 4	92 \pm 7

4.4 Discussion

The broth dilution technique indicated that GUMBOS were effective in inhibiting bacterial growth at 24 h when challenged with several EHEC isolates with MIC ranging between 0.05 – 0.15 μM . These concentrations were significantly better than the MIC values obtained for mixtures of commercial chlorhexidine diacetate and antibiotic. This observation demonstrates that the GUMBOS would be a more effective antibacterial agent than simply using the two parent agents in combination on *E. coli* O157:H7. Likewise, interaction indices classify GUMBOS to be a synergetic ionic pair in comparison to the additive nature of the parent salts in mixture. Thus, our results indicate that the co-administration of antibiotic and chlorhexidine diacetate will not achieve similar synergy as observed by the reacted GUMBOS. Additionally, minimum bactericidal concentrations obtained for GUMBOS were comparable to the effective concentration used to eradicate EHEC from cattle in a study by Naylor *et al.*⁸ Time-kill results also show that GUMBOS are rapidly bactericidal as chlorhexidine diacetate. Such a quick reduction in cell number has been previously reported for chlorhexidine salts.^{44, 45} Overall, GUMBOS are bacteriostatic at lower concentrations and bactericidal at higher concentrations. This type of antibacterial activity is similar to chlorhexidine diacetate. At low concentrations, chlorhexidine is bacteriostatic primarily disrupting the bacterium's osmotic equilibrium and causing the internal contents to leak; however, at higher concentrations of chlorhexidine, the contents of the bacterial cell begins to precipitate out.⁴⁶

Since β -lactam chlorhexidine GUMBOS is composed of two separate and distinct antimicrobial agents, it is important to understand the underlying mechanism of their synergetic behavior and how it differs from the mixture of the two parent salts as combination drug therapy. Keeping the principle of combination antibiotic design in mind, investigating novel ion-pairs

with desirable synergistic combinations can allow lower concentrations of drugs within combinations to be implemented.⁴⁷ Thus, integrating the membrane active chlorhexidine cation and cell wall targeting β -lactam antibiotic into a GUMBOS is hypothesized to deliver a lethal impact with a novel mechanism to decontaminate *E. coli* O157:H7 from infected cattle. Within this mechanism of action, we believe a hybridization of the independent activities and physical and chemical properties are governing the enhanced membrane activity at a localized site on the bacterial cell. Our results support that the mechanism of action for chlorhexidine is conserved within the β -lactam based chlorhexidine GUMBOS and that the antibiotic compliments this activity by modifying the physical and chemical properties of the antiseptic-antibiotic conjugate. To achieve equal membrane disruption, the mixture of salts would require the unlikely probability of antibiotic molecules and a chlorhexidine molecule arriving at the cell in a localized lethal dose and it reacting to subsequently change the physico-chemical properties of chlorhexidine. With this, the mechanism of action for GUMBOS must use attractive forces between the cation (chlorhexidine) and anion (antibiotic) to contain the ionic pair and remain as one unit while it inflicts antibacterial activity.

Supported by an approach commonly known as ion pair transport, reacting counter-ions with active pharmaceutical agents has successfully been used to increase the lipophilicity, physiological compatibility, and poor bioavailability of certain hydrophilic drugs.^{48, 49} Thus, this method has shown effective in improving cellular uptake of hydrophilic drugs and to increase its overall molecular lipophilicity at the site where activity is to take place.⁵⁰ Neubert and Dittrich reported that the incorporation of various lipophilic counter-ions on ampicillin improved its transport across cellular membranes.⁵¹ Therefore, the increased hydrophobicity of chlorhexidine as a counter-ion was expected to improve the membrane transport of antibiotic and

simultaneously maintain its antibacterial activity.⁵² Our results support that β -lactam based chlorhexidine GUMBOS as ion-pair are more hydrophobic than the more soluble antibiotic and chlorhexidine diacetate salts and can traverse membranes more efficiently. Lengsfeld *et al.* also found that hydrophobic ion pairs cross cell membranes easier than hydrophilic ionizable drugs, and the associated antibiotics show better minimum inhibitory concentrations than their parent salts.⁵⁰ Therefore, the greater lipophilicity of the GUMBOS is a more efficient membrane permeant than other chlorhexidine salts (*i.e.* dihydrochloride, diacetate, or digluconate) with biologically inactive counter-ions.^{9-11, 36, 37, 39} Therefore, improved MICs and enhanced membrane permeation behavior observed in the GUMBOS system as compared to the free ionizable mixture of salts or individual parent ions is attributed to the hydrophobic nature of the novel GUMBOS.

More importantly, we see that the membrane activity of the chlorhexidine moiety is apparent and enhanced in spite of the presence of the antibiotic in the GUMBOS form. This contradicts previous findings that suggest the presence of other anionic salts and detergents antagonize the antibacterial activity of chlorhexidine salt.⁵³ The antibacterial activity of stoichiometric mixtures containing chlorhexidine diacetate and sodium antibiotic demonstrates that β -lactams do not interfere with chlorhexidine activity when unreacted.^{44, 54} However, this is not the case with reacted β -lactam based chlorhexidine GUMBOS since synergistic and increased antimicrobial activity over the mixture was observed. Antibacterial activities observed in this study show that β -lactam antibiotics do not interfere with chlorhexidine when reacted and suggest that the two ions must be functional without inhibiting the activity of the other.

Since polycationic molecules are reported to preferentially interact with the outer membranes of Gram-negative bacteria by acting to competitively displace divalent cations that

cross-bridge adjacent lipopolysaccharide ((LPS) molecules, we sought to investigate if this was true for β -lactam chlorhexidine GUMBOS. As such, the antibacterial activity of the novel GUMBOS, a dicationic antiseptic containing two β -lactam antibiotics, was further investigated using EHEC in the presence and absence of Ca^{2+} or Mg^{2+} , wild-type *E. coli*, *E. coli imp4213*, and *E. coli DH5a* (pAMP) in pursuit of understanding its mechanism of action. It was found that EHEC susceptibility to all chlorhexidine salts were attenuated by Ca^{2+} and Mg^{2+} . These findings suggest that the antibacterial mechanism of action involves the displacement of divalent cations. Authors have shown that chlorhexidine salts (*i.e.* dihydrochloride, digluconate, and diacetate) are capable of permeating the outer membrane of *E. coli* and that this action was antagonized by divalent cations such as Mg^{2+} and Ca^{2+} .⁴⁵ Upon addition of increasing concentrations of EDTA, which disrupts divalent-cation cross-bridges by chelation, the bactericidal activity against EHEC was restored in MIC studies containing Ca^{2+} . Even more so, high concentrations of EDTA improved the GUMBOS antibacterial activity although it was not effective against EHEC alone. Harper and Epis also found that chlorhexidine antibacterial activity was improved *in vitro* when EDTA or EDTA/Tris systems were implemented against Gram-negative bacteria.⁵⁵ We hypothesize that the presence of excess divalent cations may repel GUMBOS by inhibiting its interaction with LPS disallowing effective cation displacement. Therefore, improvements in MIC values with increasing EDTA show that the removal of divalent cations enables effective bactericidal activity.

An enhancement of NPN fluorescence in intact EHEC cells upon exposure to increasing GUMBOS concentration supports that the GUMBOS permeabilized the outer membrane of EHEC cells. As expected, the addition of divalent cations inhibited their membrane activities, as observed by equal NPN fluorescence quenching. This could also be explained by competition

between GUMBOS and the divalent cations for a divalent-cation-binding site on the outer membrane since excess divalent cations reduce the likelihood of the GUMBOS effectively destabilizing the membrane. Both chlorhexidine diacetate and GUMBOS are sensitive to divalent cations and are similarly inhibited by their presence. Membrane potential studies also reveal that chlorhexidine di-ampicillin caused greater membrane damage to *E. coli* O157:H7 strain ATCC 43895, than parent ion or mixture, resulting in superior depolarization of membrane potentials.^{10, 35, 37, 39} In addition, our results further demonstrate that neither combination nor precursor ion resulted in comparable disruption of bacteria cell outer membranes or potentials.

Antibacterial activities of chlorhexidine di-ampicillin (MIC = 0.16 μ M) as a representative agent against ampicillin resistant strain of *Escherichia coli* DH5a (pAMP plasmid) shows that its antibacterial activity is 2.5x better than the combination (MIC = 0.36 μ M), but equal to chlorhexidine diacetate (MIC = 0.16 μ M). This implies that the presence of free ampicillin within the drug combination acts as an antagonist to the antibacterial activity of chlorhexidine against ampicillin resistant strains. Since the MIC values of chlorhexidine di-ampicillin are not equal to the drug mixture, ampicillin resistant *E. coli* DH5a cannot effectively deactivate the GUMBOS in the same way as the antiseptic/antibiotic combination. Thus, we are not certain if the antibiotic is degraded by penicillinase as a GUMBOS and future studies are underway to confirm this. However, our results suggest that neither the presence nor absence of ampicillin interferes with chlorhexidine antibacterial activity when reacted.

4.5 Conclusions

The results of this study suggest that β -lactam based chlorhexidine GUMBOS may be a viable alternative to antiseptics and antibiotics in the prevention of *E. coli* O157:H7 colonization from ruminant reservoirs of infection. More importantly, the levels of potency, reduced toxicity,

and improved synergy observed in GUMBOS were not exceeded by the equivalent combination of chlorhexidine diacetate and antibiotic. Examination of our data also indicates that GUMBOS have bactericidal activity against EHEC by directly disrupting the outer membrane. This activity is premised on the displacement of divalent cations from their binding sites on LPS on the outer membrane. The direct action of GUMBOS may contribute to its bactericidal activity against Gram-negative bacteria. Other applications beyond reducing fecal shedding of EHEC in cattle might be found wherever chlorhexidine might be used; for example, in the prevention of meningitis in neonates by the eradication of group B streptococci in the vaginas of pregnant women or in the reduction of resistant infections associated with catheter-induced bacteremia. Ultimately, the GUMBOS approach represents an alternative to traditional pharmaceutical drug design and conventional combination drug therapy.

4.6 Acknowledgements

The authors thank Ying Xiao from the LSU Socolofsky Microscopy Center for bacterial cell imaging, Thomas Silhavy for providing *E. coli imp4213* and wild-type *E. coli* used in the mechanism of action studies, Karen MacDonough for assistance in cytotoxicity studies, and Marilyn Dietrich of the LSU Flow Cytometry Facility for facilitating the membrane potential and Live/Dead studies. Marsha Cole thanks the United Negro College Fund Special Programs Harriet Jenkins Pre-doctoral Fellowship for financial support. This research was supported in part by a grant from the United States Department of Agriculture Cooperative State Research, Education, and Extension Service, National Institutes of Health Grant # R01 GM79670, and the National Science Foundation Grant # CHE - 0911118. Dr. Hobden and Dr. Hayes are members of the LSU Musculoskeletal Scientific Research Consortium.

4.7 References

1. Farina, C.; Goglio, A.; Conedera, G.; Minelli, F.; Caprioli, A.; *European Journal of Clinical Microbiology and Infection Disease Letters*, **1996**, *15*, 351-353.
2. Karmali, M.A.; Gannon, V.; Sargeant, J.M.; *Veterinary Microbiology*, **2010**, *140*, 360-370.
3. Baljer, G.; Wieler, L.H.; *Lohmann Information*, **1999**, (22), 21-26.
4. Callaway, T.R.; Carr, M.A.; Edrington, T.S.; Anderson, R.C.; Nisbet, D.J.; *Current Issues in Molecular Biology*, **2009**, *11*, 67-80.
5. Galland, J.C.; Hyatt, D., R.; Crupper, S.S.; Acheson, D.W.; *Applied and Environmental Microbiology*, **2001**, *67*, (4), 1619-1627.
6. Stevens, M.P.; van Diemen, P.M.; Dziva, F.; Jones, P.W.; Wallis, T.S.; *Microbiology*, **2002**, *148*, 3767-3778.
7. Hughes, D.T.; Terekhova, D.A.; Liou, L.; Hovde, C.J.; Sahl, J.W.; Patankar, A.V.; Gonzalez, J.E.; Edrington, T.S.; Rasko, D.A.; Sperandio, V.; *Proceedings of the National Academy of Sciences*, **2010**, *107*, (21), 9831-9836.
8. Naylor, S.W.; Nart, P.; Sales, J.; Flockhart, A.; Gally, D.L.; Low, J.C.; *Applied and Environmental Microbiology*, **2007**, *73*, (5), 1493-1500.
9. Foulkes, D.M.; *Journal of Periodontal Research*, **1973**, *8*, (Suppl. 12), 55-57.
10. Gjermo, P.; *Journal of Dental Research*, **1989**, *68* ((Special Issue)), 1602-1608.
11. Zeng, P.; Rao, A.; Wiedmann, T.S.; Bowles, W.; *Drug Development and Industry Pharmacy*, **2009**, *35*, 172-176.
12. Stoimenovski, J.; MacFarlane, D.R.; *Chemical Communications*, *47*, (41), 11429-11431.
13. von Baum, H.; Marre, R.; *Journal of Medical Microbiology*, **2005**, *295*, 503-511.
14. Edrington, T.S.; Callaway, T.R.; Varey, P.D.; Jung, Y.S.; Bischoff, K.M.; Elder, R.O.; Anderson, R.C.; Brabban, A.D.; Nisbet, D.J.; *Journal of Applied Microbiology*, **2003**, *94*, 207-213.
15. Edrington, T.S.; Callaway, T.R.; Bischoff, K.M.; Genovese, K.J.; Elder, R.O.; Anderson, R.C.; Nisbet, D.J.; *Journal of Animal Science*, **2003**, *81*, 553-560.
16. Bica, K.; Rijksen, C.; Nieuwenhuyzen, M.; Rogers, R.D.; *Physical Chemistry Chemical Physics*, **2010**, *12*, 2011-2017.

17. Hough, W.L.; Smiglak, M.; Rodríguez, H.; Swatloski, R.P.; Spear, S.K.; Daly, D.T.; Pernak, J.; Grisel, J.E.; Carliss, R.D.; Soutullo, M.D.; Davis, J.H.J.; Rogers, R.D.; *New Journal of Chemistry*, **2007**, *31*, 1429-1436.
18. Kumar, V.; Malhotra, S.V.; Eds. *Ionic Liquid as Pharmaceutical Salts: A Historical Perspective*. American Chemical Society: Washington D.C., **2010**.
19. Rodríguez, H.; Bica, K.; Rogers, R.D.; *Tropical Journal of Pharmaceutical Industry*, **2008**, *7*, (3), 1011-1012.
20. Cole, M.R.; Li, M.; El-Zahab, B.; Janes, M.E.; Hayes, D.; Warner, I.M.; *Chemical Biology & Drug Design*, **2011**, *78*, (1), 33-41.
21. Del Sesto, R.E.; McCleskey, T.M.; Burrell, A.K.; Baker, G.A.; Thompson, J.D.; Scott, B.L.; Wilkes, J.S.; Williams, P.; *Chemical Communications*, **2008**, (4), 447-449.
22. Bwambok, D.K.; El-Zahab, B.; Challa, S.K.; Li, M.; Chandler, L.; Baker, G.A.; Warner, I.M.; *ACS Nano*, **2009**, *3*, (12), 3854-3860.
23. Motyl, M.; Dorso, K.; Barrett, J.; Giacobbe, R.; *Basic Microbiological Techniques Used in Antibacterial Drug Discovery*. UNIT 13A.3 ed. John Wiley & Sons, Inc., **2006**.
24. Tallarida, R.J.; *Journal of Pharmacology and Experimental Therapeutics*, **2001** *298*, (3), 865-872.
25. Lee, J.J.; Kong, M.; Ayers, G.D.; Lotan, R.; *Journal of Biopharmaceutical Statistics*, **2007**, *17*, (3), 461-480.
26. Straetemans, R.; O'Brien, T.; Wouters, L.; Van Dun, J.; Janicot, M.; Bijmens, L.; Burzykowski, T.; Aerts, M.; *Biometrical Journal*, **2005**, *47*, 299-308.
27. Denyer, S.P.; Hugo, W.B.; Eds. *Mechanisms of Action of Chemical Biocides: Their Study and Exploitation*. Blackwell Scientific Publications: Boston, **1991**.
28. Helander, I.M.; Matilla-Sandholm, T.; *Journal of Applied Microbiology*, **2000**, *88*, 213-219.
29. Zhou, Y.; Wu, S.; Contcello, V.P.; *Biomacromolecules*, **2001**, *2*, 111-125.
30. Calinescu, M.; Negreanu-Pirjol, T.; Georgescu, R.; Calinescu, O.; *Central European Journal of Chemistry*, **2010**, *8*, (3), 543-549.
31. Riehl, J.P.; Richardson, F.S.; *Tetrahedron*, **1979**, *35*, 1499-1508.
32. Rasmussen, C.E.; Higuchi, T.; *Journal of Pharmaceutical Sciences*, **1971**, *60*, (11), 1608-1616.
33. Purdie, N.; Swallows, K.A.; *Analytical Chemistry*, **1987**, *59*, (9), 1349-1351.

34. Aki, H.; Sawai, N.; Yamamoto, K.; Yamamoto, M.; *Pharmaceutical Research*, **1991**, 8, (1), 119-122.
35. Barrett-Bee, K.; Newbould, L.; Edwards, S.; *FEMS Microbiology Letters*, **1994**, 119, (1-2), 249-253.
36. Chawner, J.A.; Gilbert, P.; *Journal of Applied Microbiology*, **1989**, 66, (3), 253-258.
37. Chawner, J.A.; Gilbert, P.; *International Journal of Pharmaceutics*, **1989**, 55, (2-3), 209-215.
38. Ivana, K.; Drew, M.; Thad, A.H.; Edward, S.; *Chemistry and Physics of Lipids*, **2010**, 163, (6), 480-487.
39. Kuyyakanond, T.; Quesnel, L.B.; *FEMS Microbiology Letters*, **1992**, 100, (1-3), 211-215.
40. Block, S.S., Ed. *Disinfection, Sterilization, and Preservation*. 5th ed. Lippincott, Williams, and Wilkins: Philadelphia, **2001**.
41. Kolahi, J.; Ghalayani, P.; Varshosaz, J.; *Journal of International Academy of Periodontology*, **2006**, 8, (2), 45-46.
42. Chow, A.Y.K.; Hirsch, G.H.; Buttar, H.S.; *Toxicology and Applied Pharmacology*, **1977**, 42, (1), 1-10.
43. Tanomaru Filho, M.; Leonardo, M.R.; Silva, L.A.B.; Aníbal, F.F.; Faccioli, L.H.; *International Endodontic Journal*, **2002**, 35, (9), 735-739.
44. McDonnell, G.; Russell, A.D.; *Clinical Microbiology Reviews*, **1999**, 12, (1), 147-179.
45. Gilbert, P.; Moore, L.E.; *Journal of Applied Microbiology*, **2005**, 99, (4), 703-715.
46. Katzung, B.G.; *Basic & Clinical Pharmacology* Eleventh ed. McGraw-Hill New York, NY, **2001**.
47. Moellering, R.C.; *American Journal of Medicine*, **1983**, 75, (2A), 4-8.
48. Neubert, R.; *Pharmaceutical Research*, **1989**, 6, (9), 743-747.
49. Reynolds, D.P.; Lanevskij, K.; Japertas, P.; Didziapertris, R.; Petrauskas, A.; *Journal of Pharmaceutical Sciences*, **2009**, 98, (11), 4039- 4054.
50. Lengsfeld, C.S.; Pitera, D.; Manning, M.; Randolph, T.W.; *Pharmaceutical Research*, **2002**, 19, (10), 1572-1576.
51. Neubert, R.; Dittrich, T.; *Pharmazie*, **1989**, 44, (1), 67-68.
52. Potts, R.O.; Guy, R.H.; *Pharmaceutical Research*, **1992**, 9, (5), 663-669.

53. Beeuwkes, H.; *Antonie van Leeuwenhoek*, **1958**, *24*, (1), 49-62.
54. Kawamura-Sato, K.; Wachino, J.-i.; Kondo, T.; Ito, H.; Arakawa, Y.; *Journal of Antimicrobial Chemotherapy*, **2008**, *61*, (3), 568-576.
55. Harper, W.E.; Epis, J.A.; *Microbios*, **1987**, *51*, 107-112.

CHAPTER 5 ANTIBACTERIAL EFFECTS OF BETA (β)-LACTAM ANTIBIOTIC-CHLORHEXIDINE HYBRID SALTS ON ANTIBIOTIC RESISTANT MICROORGANISMS

5.1 Introduction

Multi-drug resistant (MDR) bacterial infections comprise more than 30% of nosocomial infections in the United States.¹ Particularly, the associated morbidities from Gram-negative opportunistic bacteria (GNB) account for nearly 80% of intensive care unit infections including those specifically causing pneumonia, or infecting the urinary tract, blood stream, and surgical sites.^{2,3} Of the ten most common pathogens responsible for 84% of nosocomial infections, thirty-three percent is contributed by GNB, in which 8% result from MDR-GNB.⁴ These pathogens include ESBL producing *Escherichia coli*, ampicillin-resistant *Klebsiella species*, *Acinetobacter baumannii*, and *Salmonella species*, and fluoroquinolone- or carbapenem-resistant *Enterobacteriaceae*, *Serratia marcescens* and *Pseudomonas aeruginosa*.⁵⁻¹⁰ Infections arising from MDR-GNB primarily come from the microorganisms' highly efficient innate drug resistance; however the lack of host resistant mechanisms, resulting from compromised immune systems, allows for infection to set more readily. Those elements (*i.e.* AmpC – β -lactamases, MBLs, ESBLs, oxacillinases, and KPC enzymes) combined with the lack of novel antibiotic development has created a platform in which infections due to antibiotic resistant bacteria have become superior.¹¹ Therefore, prompt and appropriate pragmatic antimicrobial therapy is necessary to improve clinical prognosis in the treatment of severe resistant infections.¹¹

Although the antibiotic arsenal is limited, very few effective treatment options for infections caused by MDR bacteria still remain. Primarily, combination drug therapy has become the principal approach used to treat skin and soft tissue infections caused by MDR-

GNB and DR-Gram-positive bacteria (GPB).⁹ The use of multiple drugs in tandem is gaining momentum as a systematic approach to treat complex disease. This has led to a number of combination drug therapies that have become staples in treating such infections, while several pharmaceutical companies seek to discover improved dual-mode-of-action compounds. Common antibacterial combination drugs consists of β -lactam drugs approved in the U.S. are Co-Amoxiclav (Amoxicillin + Clavulanate), Timentin (Ticarcillin + Clavulanate), Unasyn (Ampicillin + Sulbactam), and Zosyn (Piperacillin + Tazobactam). Since these drug combinations are losing drug efficacy, other combinations such as mixtures of polymyxin B and tigecycline, meropenem, cefepime, or amikacin or β -lactams with aminoglycosides are being investigated.^{12, 13} Likewise, mixtures of antibiotics with nonantibiotics are beginning to be considered as a useful approach to extend therapy against MDR bacteria.¹⁴

Although the use of drugs in tandem might allow a patient the convenience of fewer dose regimens with potent antimicrobial activity, several problems associated with polytherapy exist. Aside from higher costs and uncontrollable drug responses with narrow therapeutic windows, each aforementioned combination drug formulation is limited to the serendipitous chance that each drug will arrive and deactivate a bacterial cell at the same time without causing adverse or idiosyncratic reactions to the host. However, neither of these treatment options is considered to be dual-mode-of-action and has yet to address the potential to cause lipopolysaccharide (LPS) endotoxin blood poisoning. Therefore, extending drug mixtures to multi-modal ionic pairs that allow potent antimicrobials to be used in formulation with controlled pharmacokinetic properties and nontoxicity may be a viable alternative to combating MDR bacterial infections.

Recently, we reported the improved antibacterial activities of β -lactam based chlorhexidine GUMBOS on several isolates of *E. coli* O157:H7 with the intent to control and

prevent the transmission of disease resulting from EHEC contamination from cattle ruminants. Since the GUMBOS display unparalleled antibacterial synergism, nontoxicity, and tunable pharmacokinetic properties it is interesting to investigate these materials as applied to other systems treated with combination drug therapy. Herein, we use β -lactam based chlorhexidine GUMBOS as a modern approach to treat MDR infections caused by GNB and GPB in addition to preventing subsequent blood poisoning. The major objectives of this study were to investigate the antibacterial activity of β -lactam-based chlorhexidine GUMBOS against drug-susceptible (DS) and MDR bacteria and to exploit chlorhexidine's abilities to sequester LPS endotoxin *in vitro* as a novel modern reacted ionic drug therapeutic treatment option.

5.2 Materials and Methods

5.2.1 Antimicrobial Activity

Table 5.1 lists the clinical isolates that were used in this study. The minimum inhibitory concentration (MIC) values of the starting materials and GUMBOS and the fractional inhibitory concentrations (FIC) of the stoichiometric mixture were determined in triplicate by broth dilution method in 96-well micro-titer plates.¹⁵ Test inoculums were adjusted using saline (0.85% NaCl) according to a 0.5 McFarland standard using colonies grown individually on tryptic soy agar plates. Cation-adjusted Mueller-Hinton broth with 5% DMSO was used to serially dilute (1:1) antibacterial agents from 0.012 μ M to 200 μ M and to adjust bacteria inoculums to 10^5 - 10^6 CFU/mL. Isolates were treated with GUMBOS, sodium antibiotic salt, chlorhexidine diacetate, or combinations of sodium antibiotic salt and chlorhexidine diacetate in a checkerboard dilution format. The MIC or FIC for each antimicrobial agent was recorded as the lowest concentration that did not show visual turbidity after 24 h incubation at 37°C. Antibacterial activity was statistically analyzed using SAS 9.2.2 (SAS Institute Inc., Cary, NC, USA), $p < 0.05$.

Table 5.1. Sources and characteristics of drug-susceptible and drug-resistant bacterial strains

Strain	Characteristic
<i>Escherichia coli</i> 25922 ⁺	Clinical isolate, Quality control organism
<i>Escherichia coli</i> O157:H7 43895 ⁺	EHEC, hamburger isolate (<i>stx1+</i> , <i>stx2+</i>)
<i>Salmonella typhi</i> ⁺⁺	Fluoroquinolone resistant
<i>Acinetobacter baumannii</i> 225T2 ⁺⁺	Respiratory isolate, MDR*
<i>Acinetobacter baumannii</i> 250 ⁺⁺	Skin isolate, MDR
<i>Acinetobacter baumannii</i> 252 ⁺⁺	Catheter isolate, MDR
<i>Acinetobacter baumannii</i> 254 ⁺⁺	Wound drain isolate, MDR
<i>Enterbacter cloacae</i> 210T2 ⁺⁺	Pleural fluid isolate, MDR
<i>Enterbacter aerogenes</i> 221T2 ⁺⁺	Sputum, MDR
<i>Klebsiella pneumoniae</i> 10031 ⁺	Quality control organism
<i>Klebsiella pneumoniae</i> 50T2 ⁺⁺	Urine isolate, MDR
<i>Klebsiella pneumoniae</i> 86T2 ⁺⁺	Pleural fluid isolate, MDR
<i>Pseudomonas aeruginosa</i> 124T2 ⁺⁺	Respiratory: Sputum isolate, β -lactam drug resistant
<i>Pseudomonas aeruginosa</i> 27853 ⁺	Blood isolate, Quality control organism
<i>Pseudomonas aeruginosa</i> PSA3 ⁺⁺	Urine Isolate, β -lactam drug resistant
<i>Pseudomonas aeruginosa</i> PSA4 ⁺⁺	Sputum isolate, β -lactam, fluoroquinolone, carbapenem drug resistant
<i>Serratia marscescens</i> ⁺⁺	Wound isolate, MDR
<i>Staphylococcus aureus</i> 25923 ⁺	Clinical isolate
<i>Streptococcus mutans</i> 35668 ⁺	Quality control organism
<i>Streptococcus faecalis</i> 19433 ⁺	Quality control organism
<i>Micrococcus luteus</i> 4698 ⁺	Quality control organism
<i>Streptococcus faecalis</i> 9790 ⁺	Quality control organism
<i>Bacillus cereus</i> 1178 ⁺	Quality control organism
<i>Methicillin-resistant Staphylococcus aureus</i> 449 ⁺⁺	Wound isolate, vancomycin susceptible
<i>Methicillin-resistant Staphylococcus aureus</i> KHRI ⁺⁺	Prosthetic joint infection isolate, vancomycin susceptible

*MDR= β -lactam, fluoroquinolone, carbapenem, aminoglycoside-resistant
⁺ Obtained from American Type Culture Collection, Manassas, VA
⁺⁺ Obtained from Jeffrey A. Hobden, Louisiana State University Health Science Center, LA

5.2.2 Lipopolysaccharide (LPS) Sequestration

Lipopolysaccharide (*E. coli* O111:B4) of the highest purity was obtained commercially from Sigma Aldrich (St. Louis, MO, USA). (LPS) sequestration was investigated by competitively displacing BODIPY-cadaverine (BC, Molecular Probes, Inc. Eugene, OR, USA) that is bound to LPS using increasing concentrations of the chlorhexidine containing salts. More specifically, the BC-LPS conjugate was prepared by mixing 1 μM BC solution (Tris-buffer, pH 7.4, 50 mM) with 5 mg/L of LPS. Then, small aliquots of chlorhexidine diacetate or GUMBOS were titrated into 3 mL of BC-LPS solution contained into a quartz cuvette. Changes in fluorescence ($\lambda_{\text{ex}} = 580 \text{ nm}$, $\lambda_{\text{em}} = 620 \text{ nm}$) was monitored with a 1 cm pathlength quartz cuvette (Starna Cells) using a Spex Fluorolog – 3 spectrofluorimeter Model FL3-22TAU3 (Jobin Yvon, Edison, NJ, USA) at room-temperature. The percent BC displacement upon increasing concentration of chlorhexidine salts was determined by comparing the fluorescence of LPS with and without BC, where BC solution without LPS is the 100% displaced control sample.

5.3 Results and Discussion

5.3.1 Representative Antibacterial activities of Chlorhexidine diacetate and β -lactam Antibiotics against *S. aureus* 29523 and *K. pneumoniae* 10031

Table 5.2 shows the MIC results for the starting material against representative Gram-positive and Gram-negative bacteria. Effective MIC values for chlorhexidine diacetate treatment on *S. aureus* 29523 and *K. pneumoniae* 10031 are $0.8 \pm 0.6 \mu\text{M}$ and $15.6 \pm 6.3 \mu\text{M}$, respectively. The MIC values obtained for chlorhexidine diacetate match the values obtained in other studies conducted on the *S. aureus* 29523. However, a three-fold decrease in MIC values was observed when *K. pneumoniae* 10031 were treated with chlorhexidine diacetate. Beta-lactam antibiotics showed variable antibacterial activity on both Gram-positive and Gram-negative strains investigated. *Staphylococcus aureus* 29523 were increasingly susceptible to antibiotics in this order: sodium ampicillin < disodium carbenicillin < sodium cephalothin = sodium oxacillin. However,

disodium carbenicillin and sodium cephalothin were equally efficient in preventing *K. pneumoniae* 10031 growth. Lack of antimicrobial activity was seen for sodium oxacillin and sodium ampicillin.

Table 5.2. Antibacterial activities (MIC, μM) of chlorhexidine diacetate, sodium ampicillin, disodium carbenicillin, sodium cephalothin, and sodium oxacillin against representative microorganisms *S. aureus* 29523 and *K. pneumoniae* 10031.

	<i>S. aureus</i> 29523	<i>K. pneumoniae</i> 10031
Chlorhexidine diacetate	0.8 \pm 0.6	15.6 \pm 6.3
Sodium Ampicillin	25	>50
Disodium Carbenicillin	12.5 \pm 3.3	12.5 \pm 1.5
Sodium Cephalothin	1.6 \pm 0.4	12.5 \pm 5.8
Sodium Oxacillin	1.6 \pm 0.2	>50

5.3.2 Comparative Antibacterial Activities of Chlorhexidine and β -lactam Antibiotics in Combination and as GUMBOS

Using the checkerboard technique, the combined effects of chlorhexidine diacetate and various β -lactam antibiotics against representative organisms *S. aureus* and *K. pneumoniae* are presented in Figures 5.1 and 5.2. *Staphylococcus aureus* 29523 was variably susceptible to combinations of chlorhexidine diacetate and β -lactam antibiotics. Carbenicillin was the most synergetic antibiotic used with chlorhexidine diacetate to inhibit *S. aureus* 29523 growth. The most synergetic FIC ratio observed against the Gram-positive isolate consisted of 0.39 μM chlorhexidine diacetate and 1.56 μM carbenicillin disodium. Similarly, 1.56 μM sodium cephalothin compliments 0.20 μM chlorhexidine diacetate antibacterial activities against *S. aureus* 29523. Fewer synergetic ratios between chlorhexidine diacetate and sodium ampicillin or sodium oxacillin were seen in *S. aureus* 29523 growth inhibition studies. Predominantly, FIC ratios consisting of chlorhexidine diacetate and either sodium ampicillin or sodium oxacillin reveal that 66% combinations tested were additive for both.

In the FIC studies against *K. pneumoniae* 10031, fewer synergetic combinations were observed. Interaction indices ranked from 0.5 – 5 for each antiseptic and antibiotic combination tested. More specifically, interaction indices suggest that the presence of antibiotic greatly antagonizes the activity of chlorhexidine diacetate. However, *K. pneumoniae* 10031 was the most

susceptible to combinations of chlorhexidine diacetate and disodium carbenicillin. In this case, 6.25 μM chlorhexidine diacetate and 12.5 μM disodium carbenicillin efficiently inhibited *K. pneumoniae* 10031 growth. Lower concentrations of chlorhexidine diacetate and disodium carbenicillin drastically become antagonistic and susceptibility to *K. pneumoniae* 10031 are substantially reduced. The remaining antibiotics, sodium ampicillin, sodium cephalothin, and sodium oxacillin, showed increasing antagonism with the latter being the worst in combination with chlorhexidine diacetate. Despite the increasing antagonism in concentrations less than 12.5 μM chlorhexidine diacetate and 12.5 μM sodium ampicillin or sodium cephalothin, additivity is maintained in 80% of the FIC values tested.

5.3.3 Antibacterial Activities of β -lactam-based Chlorhexidine GUMBOS

5.3.3.1 Drug Susceptible and Drug Resistant Gram-positive

The antibacterial activities of β -lactam based chlorhexidine GUMBOS were investigated against 6 drug-susceptible GPB and two *Methicillin-resistant S. aureus* strains. Figure 5.3 shows the results obtained for this study. Overall, it required less than 1.5 μM of the antibacterial agents to inhibit the growth of both DS-GPB and *MRSA*. For each GPB, chlorhexidine diacetate performs equally or worse than the GUMBOS. The antibacterial activities for the GUMBOS increase proportionately with molecular weight. More specifically, one or more GUMBOS are better inhibitors of GPB bacteria than chlorhexidine diacetate in 88% of isolates tested. It required 0.8 $\mu\text{M} \pm 0.6 \mu\text{M}$ chlorhexidine diacetate to inhibit both DS-GPB and *MRSA*. Chlorhexidine diacetate was least effective against *MRSA* 449. When evaluating the activity of chlorhexidine di-ampicillin, *B. cereus* 1178, *S. mutans* 35668, and *S. faecalis* 19433 were the most susceptible. *Staphylococcus aureus* 25923 was least susceptible to chlorhexidine di-ampicillin. Both *MRSA* strains required 0.7 $\mu\text{M} \pm 0.1 \mu\text{M}$ chlorhexidine di-ampicillin for growth inhibition. The average MICs of GPB required by chlorhexidine carbenicillin and chlorhexidine di-cephalothin were determined to be 0.5 $\mu\text{M} \pm 0.3\mu\text{M}$. The most effective β -lactam chlorhexidine GUMBOS used to treat GPB was found to be

chlorhexidine di-oxacillin. More specifically, the concentration required to inhibit GPB ranges from 0.1 to 0.8 μM , with the latter the concentration to inhibit *S. faecalis* 9790. Likewise, both *MRSA* strains required 0.1 μM for growth inhibition. In summary, antibacterial potency for the novel β -lactam based chlorhexidine GUMBOS increases in the following order: chlorhexidine diacetate < chlorhexidine di-ampicillin < chlorhexidine carbenicillin < chlorhexidine di-cephalothin < chlorhexidine di-oxacillin.

5.3.3.2 β -lactam antibiotic Susceptible Gram-Negative Bacteria

The antibacterial activities of β -lactam based chlorhexidine GUMBOS were investigated against antibiotic susceptible GNB. Figure 5.4 shows the results obtained for this study. Overall, less than 0.3 μM of the antibacterial agents were required to inhibit the growth of DS-GNB. For each DS-GNB, chlorhexidine diacetate was outperformed by the GUMBOS. *Escherichia coli* 25922 required 0.25 $\mu\text{M} \pm 0.05 \mu\text{M}$ antibacterial agents to inhibit its growth. Therefore, *E. coli* 25922 is equally susceptible to all chlorhexidine salts tested in this study. However, preferential antibacterial activities toward *Escherichia coli* (EHEC) 43895 and ampicillin-resistant *S. typhi* were seen when comparing the GUMBOS efficacy to quality control strain *E. coli* 25922. *Escherichia coli* 43895 required 0.11 $\mu\text{M} \pm 0.3 \mu\text{M}$ GUMBOS to inhibit its growth. This concentration is half the concentration of chlorhexidine diacetate necessary to equally inhibit the growth of *E. coli* 25922. Hence, either type of GUMBOS is sufficient to inhibit the growth of EHEC 43895. It was observed that *S. typhi* was the most susceptible to GUMBOS investigated in this study. Interestingly, antibacterial activity increases proportionately with increasing molecular weight. Chlorhexidine di-ampicillin was least effective in inhibiting *S. typhi* growth. The efficacy of the GUMBOS against *S. typhi* increases in this order: chlorhexidine di-ampicillin < chlorhexidine carbenicillin < chlorhexidine di-cephalothin < chlorhexidine di-oxacillin. Although worse, the antibacterial activity of chlorhexidine di-ampicillin against *S. typhi* is not statistically different from chlorhexidine diacetate.

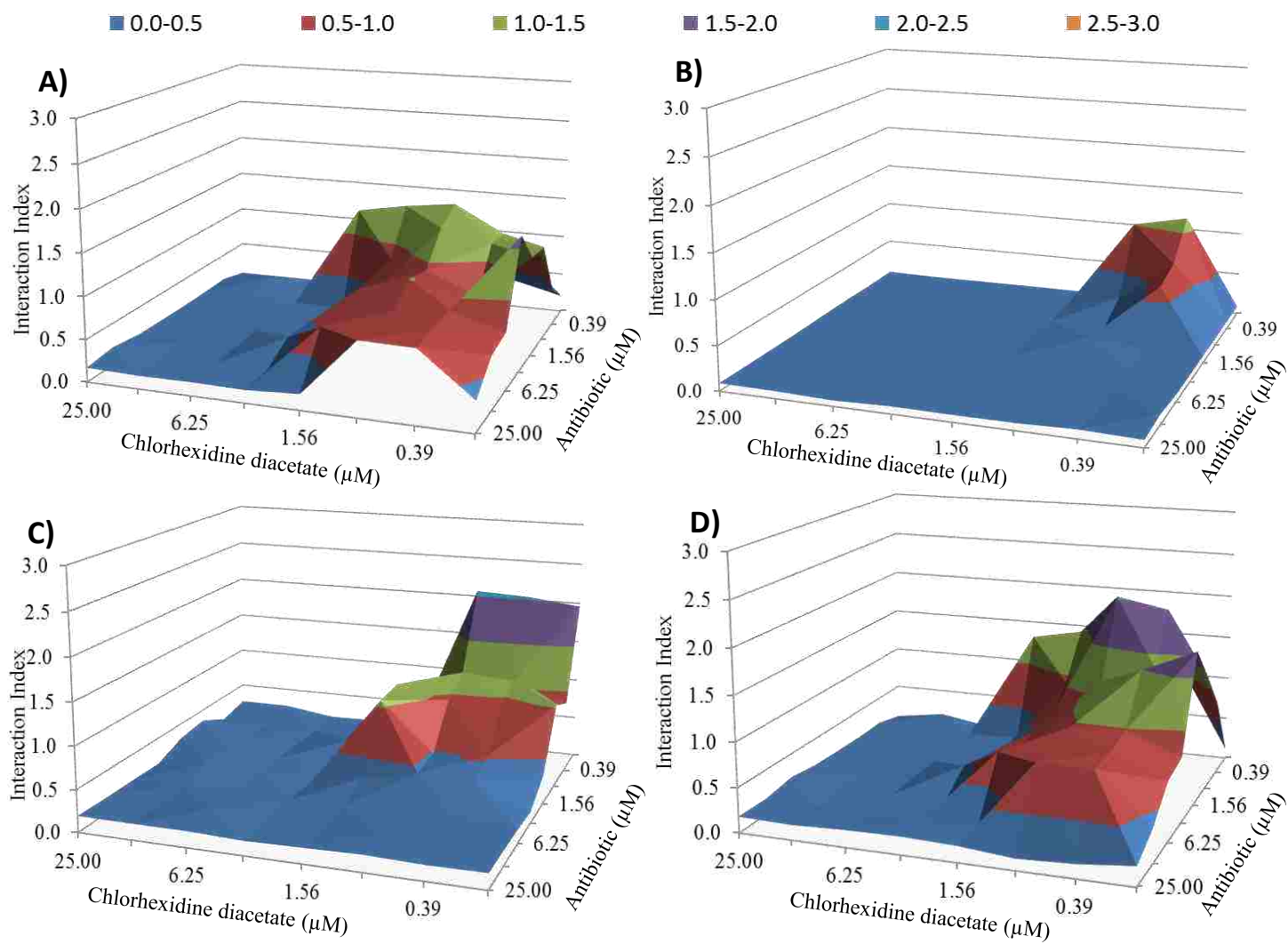


Figure 5.1. Interaction indices determined by fractional inhibitory concentrations (μM) of chlorhexidine diacetate and A) sodium ampicillin, B) disodium carbenicillin, C) sodium cephalothin, or D) sodium oxacillin against *S. aureus* 25923.

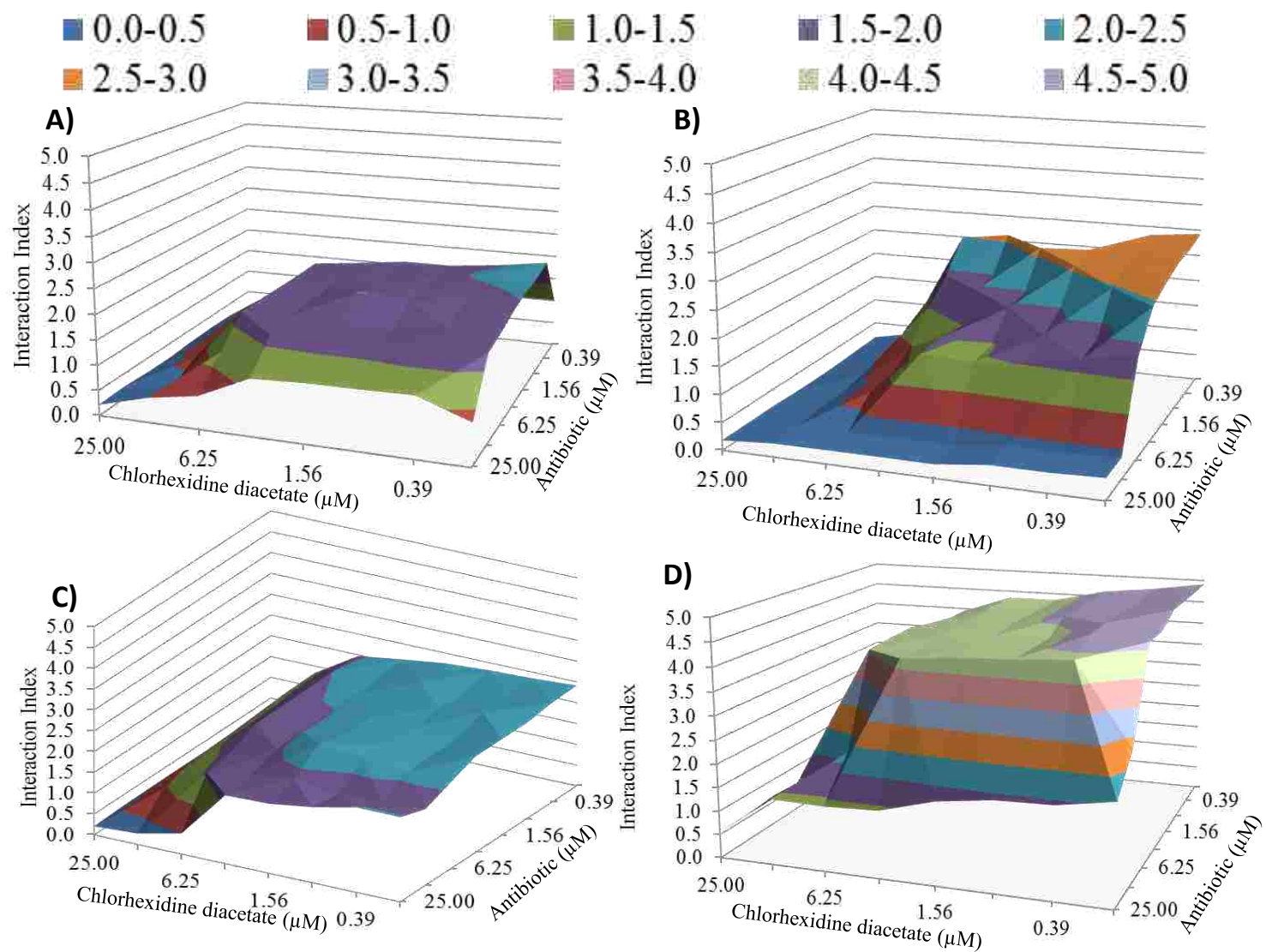


Figure 5.2. Interaction indices determined by fractional inhibitory concentrations (μM) of chlorhexidine diacetate and A) sodium ampicillin, B) disodium carbenicillin, C) sodium cephalothin, or D) sodium oxacillin against *K. pneumoniae* 10031.

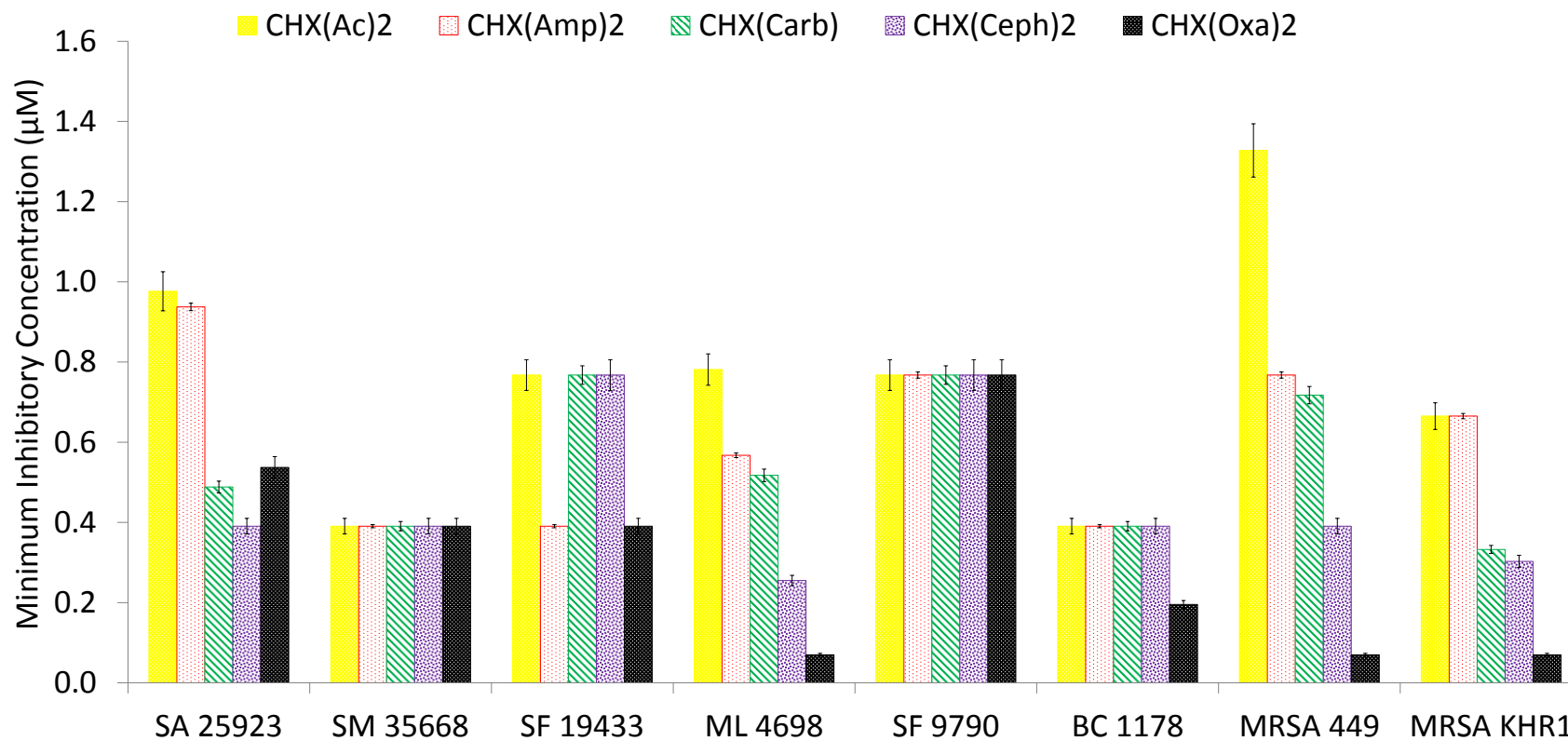


Figure 5.3. Antibacterial activity of β -lactam-based chlorhexidine GUMBOS on drug-susceptible and drug-resistant Gram-positive bacteria.

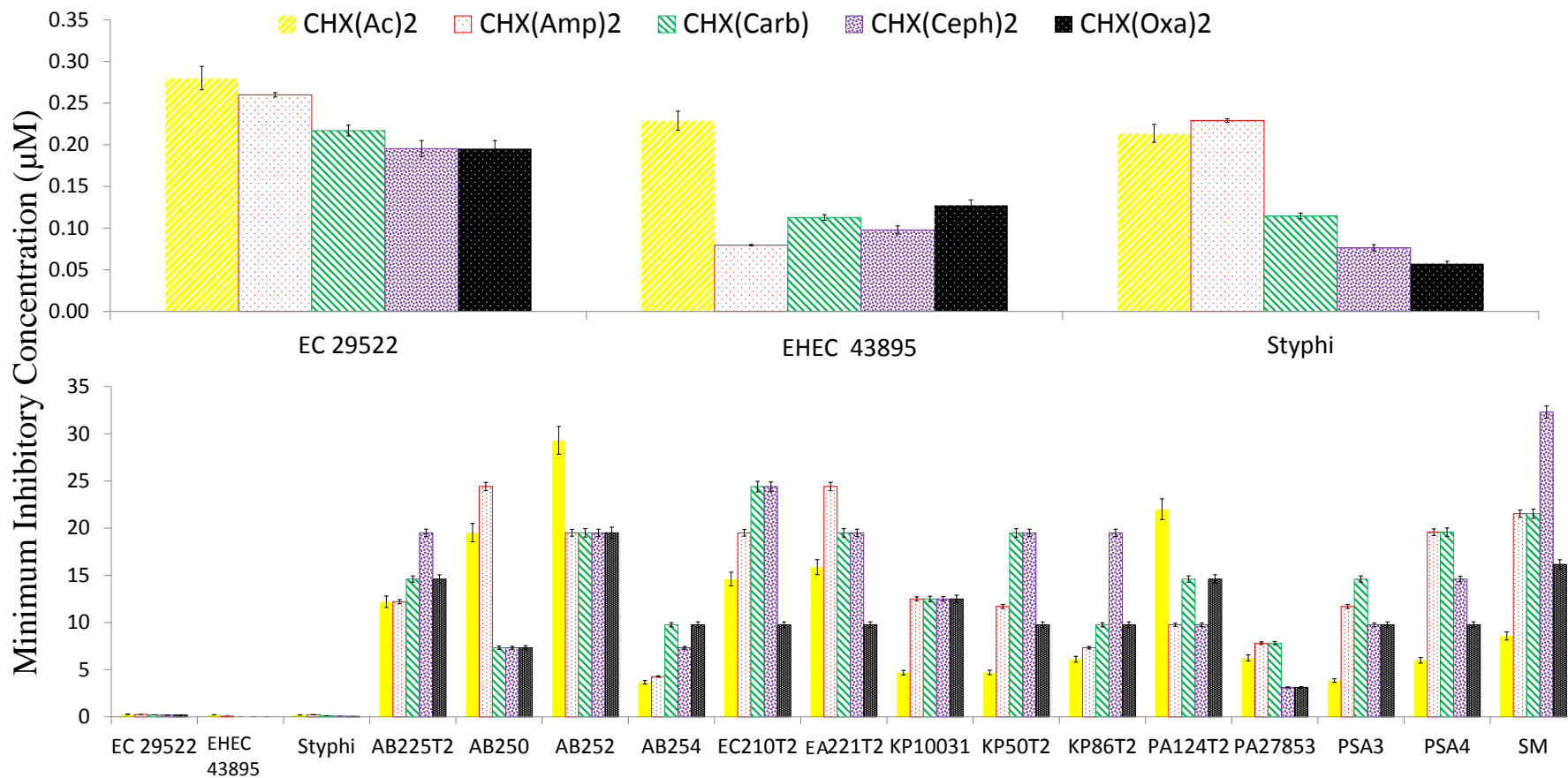


Figure 5.4. Antibacterial activity of β -lactam-based Chlorhexidine GUMBOS on drug-susceptible and drug-resistant Gram-negative bacteria.

5.3.3.3 Multi-Drug Resistant Gram-Negative Bacteria

The antibacterial drug susceptibility of 14 ampicillin-resistant GNB was assayed by the 5 chlorhexidine salts. Twelve of the fourteen ampicillin-resistant GNB are considered MDR, in which 6 major bacterial genera responsible for MDR infections are represented. Overall, less than 35 μM antibacterial agents were required to inhibit MDR-GNB growth. Chlorhexidine susceptibility for the clinical isolates of *A. baumannii* ranked with chlorhexidine di-oxacillin = chlorhexidine carbenicillin > chlorhexidine di-cephalothin > chlorhexidine di-ampicillin > chlorhexidine diacetate. Similar to other classes of bacteria investigated, *A. baumannii* increases with increasing molecular weight. However, it appears that this organism might be more susceptible to the decreased ionic stoichiometry or the unique structural configuration of the chlorhexidine carbenicillin GUMBOS. Both *Enterobacter* species were equally susceptible to the chlorhexidine salts. The most effective growth inhibitor of both *E. aerogenes* 221T2 and *E. cloacae* 210T2 was found to be chlorhexidine di-oxacillin; whereas, the least effective agent was chlorhexidine di-ampicillin. It required 10 – 20 μM of β -lactam based chlorhexidine GUMBOS to inhibit *K. pneumoniae* isolates. Although *K. pneumoniae* 10031 is not a MDR-GNB, greater antimicrobial susceptibility was only observed to chlorhexidine carbenicillin, chlorhexidine di-cephalothin, and chlorhexidine di-oxacillin. Chlorhexidine diacetate was able to efficiently inhibit both ampicillin-resistant and MDR-*K. pneumoniae* growth with approximately 5 μM . Ampicillin-resistant *P. aeruginosa* 27853 was more susceptible to the hydrophobic chlorhexidine di-oxacillin and chlorhexidine di-cephalothin GUMBOS only requiring 3 μM for growth inhibition. Minimum inhibitory concentrations between 10 – 16 μM were effective against MDR-*P. aeruginosa*. Chlorhexidine carbenicillin was found to be least effective on MDR-*P. aeruginosa*. Overall, mean antibacterial activities were found to be 11.2 μM , 14.7 μM , 15.4 μM , 15.6 μM , and 11.1 μM for chlorhexidine diacetate, chlorhexidine di-ampicillin, chlorhexidine carbenicillin, chlorhexidine di-cephalothin, and chlorhexidine di-oxacillin, respectively.

5.3.4 Interaction Indices

Figure 5.5 shows all interaction indices acquired for β -lactam-based chlorhexidine GUMBOS. It is apparent that different extents of synergy are observed for the GUMBOS for MRSA, DS-GPB, DS-GNB, and MDR-GNB. Although FIC indices of the antibiotic and chlorhexidine mixtures show ranges of additivity for all combinations against *S. aureus* 25923 and *K. pneumoniae* 10031, synergy was observed in each case that the β -lactam-based chlorhexidine GUMBOS was used. Interaction indices (I) was found to range between 0.3 and 1.5 for GUMBOS. More specifically, decreasing synergy was observed for all isolates in this order: chlorhexidine di-cephalothin > chlorhexidine di-ampicillin = chlorhexidine carbenicillin > chlorhexidine di-oxacillin. Likewise, all GUMBOS were synergetic against GPB, *E. coli* 43890, and *E. coli* 25922. Interaction indices obtained for *S. typhi* and *K. pneumoniae* 10031 reveal the GUMBOS to be additive and that neither chlorhexidine nor antibiotic are more effective than the other in the form of GUMBOS. For all of the GUMBOS, synergy was solely found for 14% of the MDR-GNB isolates. When considering synergy by type of GUMBOS, the combination of chlorhexidine and oxacillin in the form of chlorhexidine di-oxacillin proved to be a successful combination for 57% of the MDR-GNB isolates. In conclusion, GUMBOS were able to synergistically inhibit % of the bacteria tested in this study. Thus, the use of β -lactam antibiotics reacted with chlorhexidine yield better synergetic salt pairs (*i.e.* β -lactam-based chlorhexidine GUMBOS) that show better interaction indices than the combination of precursor salts on the same microorganisms.

5.3.5 Antibacterial activity in 10% Human Serum Albumin

The antibacterial activity of β -lactam based chlorhexidine GUMBOS were also assayed in the presence of 10% Human Serum Albumin (HSA, Sigma Aldrich, St. Louis, MO, USA). It was found that the antibacterial activities worsened variably for each chlorhexidine salt. Table 5.3 reveals the MIC values obtained for each GUMBOS in the presence of 10% HSA. Using *EHEC* 43895 as a representative microbe, it was observed that nearly 50-fold more chlorhexidine diacetate

was needed to inhibit its growth. Likewise, the GUMBOS required 90 – 300 times more material to inhibit the growth of *E. coli* O157:H7 43895, which was extremely susceptible to the GUMBOS in the absence of HSA. This suggests that systemic administration of these GUMBOS may be problematic in that the agents might interact strongly with albumin proteins causing their antibacterial activity to be limited. Future studies will be required to investigate the *in vivo* potential of these agents.

Table 5.3. Antibacterial activities (MIC, μM) of chlorhexidine diacetate, chlorhexidine di-ampicillin, chlorhexidine carbenicillin, chlorhexidine di-cephalothin, and chlorhexidine di-oxacillin against representative microorganism *E. coli* O157:H7 43895 in the presence of 10% human serum albumin.

	<i>E. coli</i> O157:H7 43895
Chlorhexidine diacetate	11.7 \pm 5.5
Chlorhexidine di-ampicillin	15.6 \pm 4.3
Chlorhexidine carbenicillin	23.4 \pm 11
Chlorhexidine di-cephalothin	31.3 \pm 8.2
Chlorhexidine di-oxacillin	11.7 \pm 5.5

5.3.6 Therapeutic Indices Chlorhexidine and Antibiotics in Combination and as GUMBOS

The therapeutic index (TI) is widely used to calculate the flexible dosing concentrations between the effective antibacterial activities and lethal concentrations of antibacterial drugs. Therefore, larger therapeutic indices indicate greater flexibility in the strength of concentrations used to treat systemic infections. As mentioned before in Chapter 4, chlorhexidine diacetate is an effective antimicrobial with poor intestinal bioavailability and higher systemic cytotoxicity; hence its therapeutic index is lower. Changing the antibiotic component in the GUMBOS has greatly expanded the therapeutic index of chlorhexidine when considering the different mammalian cell lines (Figure 5.6).

Ranges for GUMBOS TI (*i.e.* $100 < \text{TI} < 300$) obtained by *MRSA* and DS-GPB. More specifically, TI varied among GPB in the following order: chlorhexidine di-ampicillin > chlorhexidine di-oxacillin > chlorhexidine di-cephalothin > chlorhexidine carbenicillin > chlorhexidine diacetate for HeLa cells. The TI obtained for NIH/3T3 fibroblasts show indifference among chlorhexidine salts. Endothelial cells also have variable TI; in which, the greatest and least TI was found for chlorhexidine di-cephalothin and chlorhexidine carbenicillin, respectively. Drug susceptible GNB consistently have the largest therapeutic index (*i.e.* $300 < \text{TI} < 900$) for HeLa, NIH/3T3 and EOMA cells. Of the three cellular lines, NIH/3T3 fibroblasts had the lowest therapeutic index which suggests a discrete margin of GUMBOS treatment concentrations would be available for wounds. However, the narrowest TI (*i.e.* $2 < \text{TI} < 10$) was approximated for MDR-GNB. Therapeutic ranges for treating MDR-GNB systemic infections were improved 10-fold for β -lactam-based chlorhexidine GUMBOS compared to the 3-fold therapeutic index observed for chlorhexidine diacetate.

5.3.7 Lipopolysaccharide (LPS) Sequestration

The dose-dependent displacement of BODIPY-cadaverine from LPS endotoxin shows that each β -lactam GUMBOS can sequester LPS with differing affinities. Figure 5.7 illustrates that equal LPS sequestration can be achieved by concentrations of chlorhexidine diacetate and chlorhexidine di-ampicillin below 30 μM . However, greater concentrations of chlorhexidine di-ampicillin have 16% better sequestration from 30 to 62 μM . The ability to sequester LPS by the remaining GUMBOS occurs slowly until 13 μM is reached. In which concentrations above 13 μM significantly discriminates the LPS sequestering abilities of chlorhexidine di-cephalothin and chlorhexidine di-oxacillin. At the maximum concentration of GUMBOS, 78 and 97% LPS was able to be bound by chlorhexidine di-cephalothin and chlorhexidine di-oxacillin, respectively. However, chlorhexidine carbenicillin was the worst LPS sequestering agent used in this study. Chlorhexidine

▨ Chlorhexidine di-ampicillin
 ▨ Chlorhexidine carbenicillin
 ▨ Chlorhexidine di-cephalothin
 ■ Chlorhexidine di-oxacillin

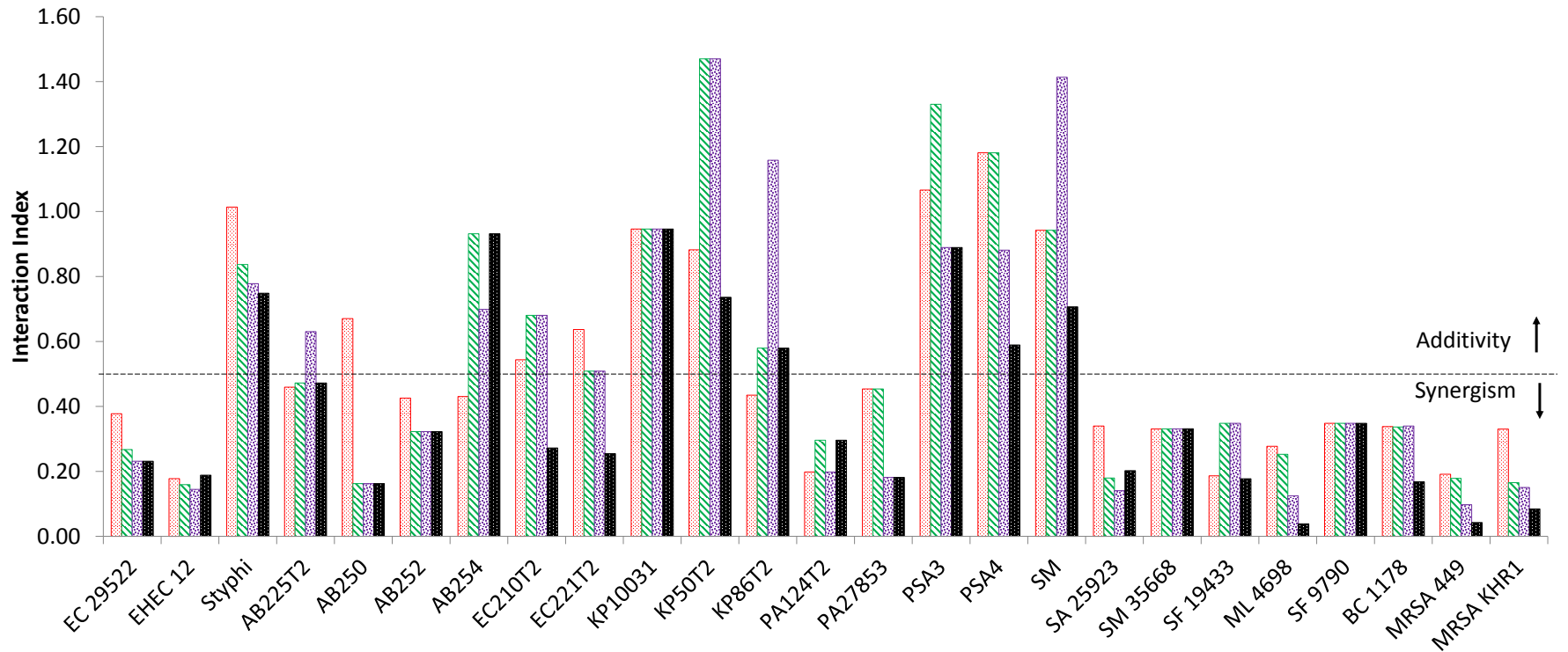


Figure 5.5. Interaction indices on MDR- and MDS bacteria for chlorhexidine di-ampicillin, chlorhexidine carbenicillin, chlorhexidine di-cephalothin, and chlorhexidine di-oxacillin.

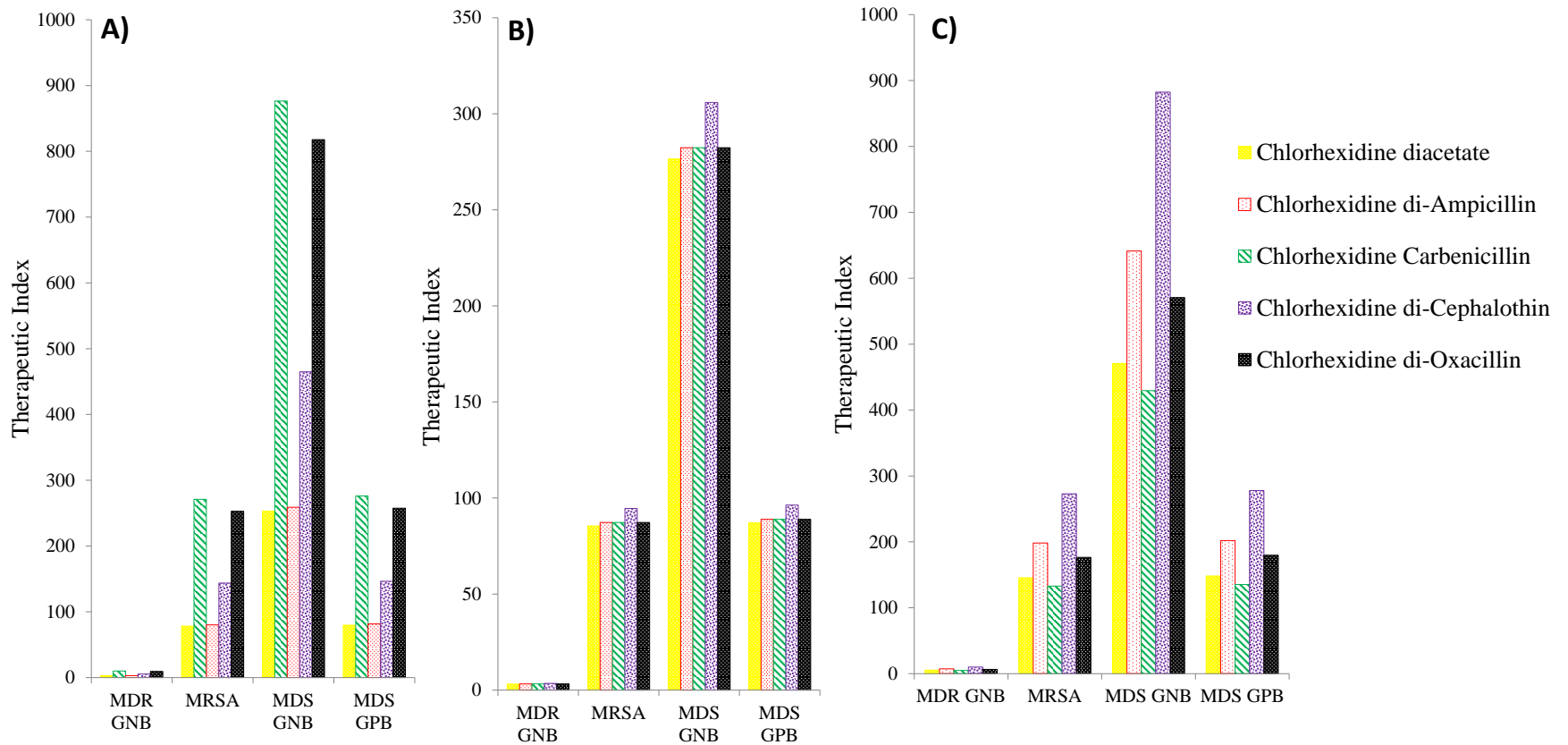


Figure 5.6. Therapeutic Indices using mean inhibitory concentrations per bacteria drug susceptibilities for β -lactam-based chlorhexidine GUMBOS, where A = HeLa, B = NIH/3T3, and C = EOMA.

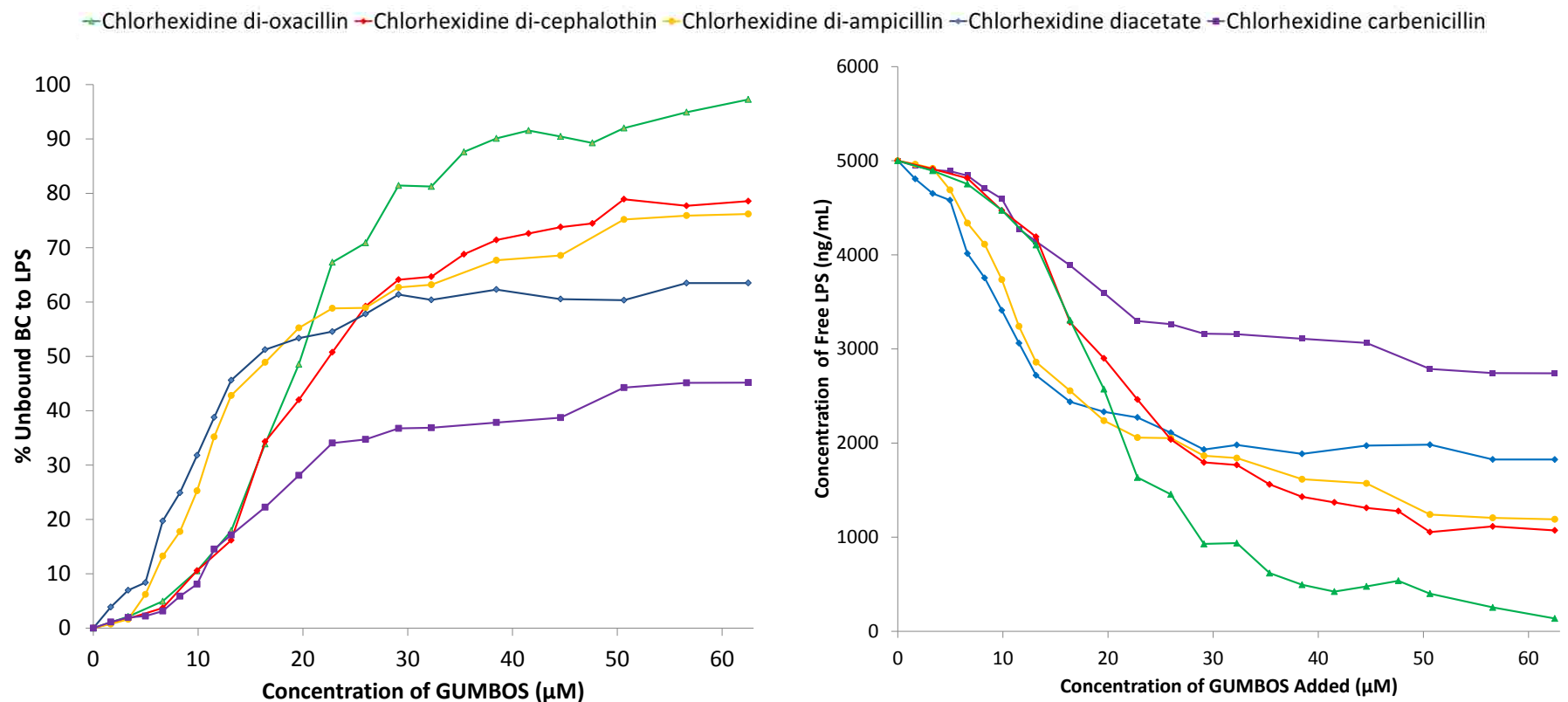


Figure 5.7. Determination of BODIPY-cadaverine (BC) displacement from LPS (left) and remaining LPS concentration (right) by chlorhexidine diacetate, chlorhexidine di-ampicillin, chlorhexidine di-cephalothin, chlorhexidine di-oxacillin, and chlorhexidine carbenicillin. BODIPY-cadaverine was mixed with LPS and various concentrations of GUMBOS added. Displacement of BODIPY-cadaverine from LPS was calculated as $[1 - (F - F_0)/(F_{\max} - F_0)] * 100\%$, where F_0 is the fluorescence intensity at LPS saturation with BODIPY-cadaverine and F_{\max} is the fluorescence intensity without LPS.

carbenicillin was only able to sequester 44% LPS. Further processing of this data using a Scatchard interpretation reveals further details about the binding affinities between GUMBOS and LPS. We found that the GUMBOS have very strong binding affinities to LPS. More specifically, increasing binding affinities occur in the following order: chlorhexidine carbenicillin < chlorhexidine di-cephalothin < chlorhexidine di-ampicillin < chlorhexidine diacetate < chlorhexidine di-oxacillin.

Although not yet understood, the different abilities for GUMBOS to sequester LPS are hypothesized to be driven by the GUMBOS hydrophobicity and unique structural configuration. Our data shows that LPS sequestration increases with increasing hydrophobicity, where chlorhexidine diacetate is the least and chlorhexidine di-oxacillin is the greatest, within the GUMBOS consisting of two antibiotics. Therefore, this physical property is believed to facilitate the GUMBOS adsorption into the hydrophobic alkyl appendages of the lipid A moiety of LPS. This agrees with the findings of David et al. who have, to date, investigated the interaction of several lipopolyamines with the lipid A moiety of LPS.¹⁶⁻²⁰ Although chlorhexidine carbenicillin is more hydrophobic than chlorhexidine diacetate, we believe that hydrophobicity alone is not capable of successfully removing LPS *in vitro*. When comparing chlorhexidine carbenicillin and chlorhexidine diacetate, the increased hydrophobicity of the GUMBOS has led to better antibacterial activity. However, the difference in stoichiometry or structural configuration may also contribute to the variances in LPS sequestering ability. Therefore, the intermolecular forces that contain the LPS-binding GUMBOS are believed to promote a favorable conformation that facilitates direct binding to the phosphate sites on the lipid A moiety of LPS. Since each phosphate group is approximately 16 Å apart,¹⁹ it is believed that these GUMBOS have a structural conformation that that allows the dicationic biguanidinium residues on the

chlorhexidine backbone to bind favorably to the LPS phosphate groups. The one-to-one stoichiometry between chlorhexidine and carbenicillin is thought to create a structural conformation that is too acute to successfully bind to the phosphates. This electrostatically driven process is hypothesized to occur in spite of the antibiotics since there are several hydrogen bonding donor and acceptor groups between the two ions that are able to maintain the ionic pair without the use of their charges. Further studies are required to confirm the hypotheses premised on the unique LPS-GUMBOS interactions and their ability to sequester LPS endotoxin better than chlorhexidine diacetate alone. However, this study suggests that the efficiency of these compounds may be a result of the culmination of the ability to suppress cell activation in addition to the antibacterial activities.

5.4 Michaelis-Menten Kinetics using CENTA as a Substrate against Type I Penicillinase

5.4.1 CENTA and Chlorhexidine

Kinetic studies demonstrate that each component of the GUMBOS structure impacts the activity of penicillinase on CENTA degradation. Active ampicillin moieties within the GUMBOS structure is believed to specifically promote binding of chlorhexidine di-ampicillin to penicillin binding proteins (*e.g.* transpeptidase) as well as identify the GUMBOS role in enzymatic degradation by Type 1 penicillinases to be understood. If ionic dissociation of the GUMBOS occurs, then it is expected that the kinetics of CENTA with either mixture or GUMBOS would be similar. Table 5.4 summarizes the kinetic results obtained for sodium ampicillin, chlorhexidine diacetate, and chlorhexidine di-ampicillin in the presence of CENTA.

Using CENTA in combination with chlorhexidine diacetate suggests how the stoichiometric mixture containing unreacted 1:2 chlorhexidine diacetate: sodium ampicillin (v/v %) is impacted by enzyme hydrolysis. More importantly, the addition of chlorhexidine diacetate

Table 5.4. Average kinetic parameters between Type 1 penicillinase and CENTA substrate in the presence of sodium ampicillin, chlorhexidine diacetate, and chlorhexidine di-ampicillin secondary substrates. The Michaelis-Menten constants were calculated using linear regions from the different rate saturation curves. Apparent values are an average with standard deviations from all kinetic parameters acquired for each inhibitor concentration from four measurements.

Substrate	K _m (μM)	K _{m, app} (μM)	V _{max} (mM/min)	V _{max app} (mM/min)	K _{cat}	K _{cat} /K _m (10 ⁸)	K _i (μM)
Chlorhexidine diacetate	-	3.33 ± 0.76	-	0.38 ± 0.09	641 ± 158	2.09 ± 0.99	na
Chlorhexidine di-ampicillin	-	42.3 ± 19.1	-	2.65 ± 0.87	4993 ± 1478	1.07 ± 0.22	59.3 ± 38.8
Sodium ampicillin	-	25.1 ± 13.5	-	1.60 ± 0.93	2715 ± 1571	1.26 ± 0.39	25.0 ± 15.5
CENTA	28.3 ± 4.4	-	2.77 ± 0.36	-	4707 ± 261	1.66 ± 0.74	-

na: Inhibitor dissociation constant for chlorhexidine diacetate could not be calculated

to increasing concentrations of CENTA revealed an uncompetitive-like inhibitive effect on the substrate although resembling a rare inhibition type known as induced- substrate inhibition (Figure 5.8). Since chlorhexidine diacetate does not structurally resemble the inhibitor it will not interfere with the penicillinase active binding site.

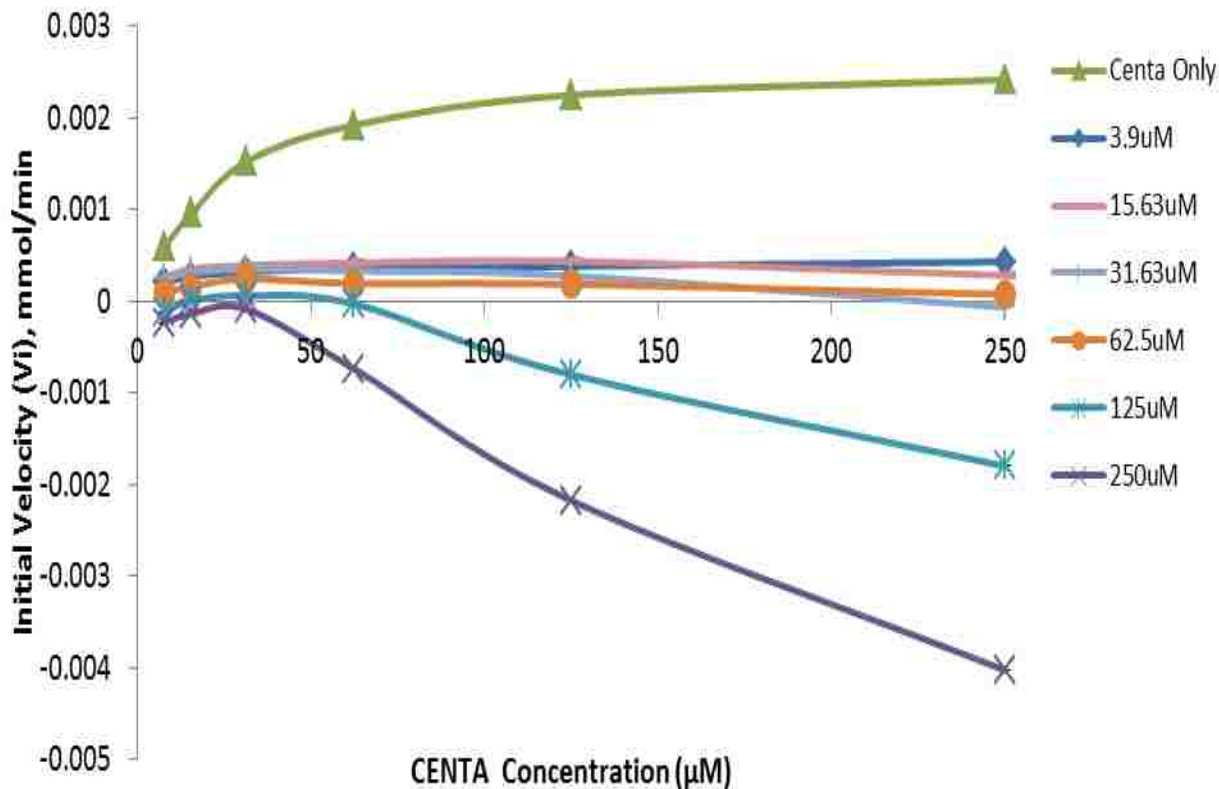


Figure 5.8. Saturation curve with 0.5 units Type 1 penicillinase showing the relationship between CENTA (substrate) concentration and its degradation rates in the presence of increasing concentrations of chlorhexidine diacetate at 37°C.

In fact, it is electrostatically attracted to CENTA's anionic carboxylate groups within the enzyme-substrate complex, since penicillinase degradation would not compromise the charge-distribution of this molecule.^{21, 22} It was observed that even at low concentrations of chlorhexidine diacetate, the degradative rate of CENTA ($v_{max_{app}} = 0.38 \mu\text{M}$) was decreased suggesting that the conversion of enzyme-inhibitor-substrate complex to product is reduced.

Increasing CENTA concentrations were not able to overcome this inhibitive effect, so it is concluded that the presence of CENTA is required to provide a site for chlorhexidine diacetate to interfere with binding. Since this data does not follow conventional Michaelis-Menten kinetics, the inhibitor dissociation constant (K_i) could not be calculated. In summary, the mixture of precursor ions may prevent the degradation of ampicillin if the chlorhexidine diacetate and sodium ampicillin arrive synchronously to the active site of penicillinase. However, the unlikely probability of this occurring may not allow chlorhexidine to work synergistically with ampicillin.

5.4.2 CENTA and Chlorhexidine di-Ampicillin

As for chlorhexidine di-ampicillin, CENTA hydrolysis deviated substantially from standard Michaelis-Menten kinetics, demonstrating induced-substrate inhibition at higher substrate concentrations (Figure 5.9). This irreversible process behaves similarly to the system consisting of the stoichiometric mixture. Since ampicillin is structurally similar to CENTA and is electrostatically bound to the chlorhexidine molecule, initial competitive inhibition is observed at low concentration of GUMBOS. In this case, the GUMBOS compete with CENTA to bind to the free enzyme at the active site. At insufficient inhibitive concentrations, increasing the amount of CENTA allows it to overcome inhibition since penicillinase is consumed in the enzyme-substrate complex. However, if the individual rate saturation plots are evaluated in the presence of increasing chlorhexidine di-ampicillin, it appears that an induced-substrate inhibitive effect occurs upon increasing concentrations of CENTA substrate. Increasing the CENTA concentration enables penicillinase to bind additional molecules at other inactive sites which, in this case, may cause the chlorhexidine di-ampicillin's physical and chemical properties to inflict protein distortion disabling penicillinase hydrolytic activity.²³ Subsequent binding of the second substrate, chlorhexidine di-ampicillin, seems not to be productive and therefore reduces the

catalytic activity at the first step. In addition, binding chlorhexidine di-ampicillin drastically decreases the nucleophilic activity of water causing the deacylation step (*i.e.* conversion from enzyme-substrate complex to product) to be inhibited. On average, adding the chlorhexidine di-ampicillin molecules had no effect on the overall substrate recognition and penicillinase active processes, since it is clear that the inhibition of activity is largely, if not entirely, due to the formation of the enzyme - GUMBOS complex. Although more studies are ongoing to investigate the influence GUMBOS has on penicillinase activity, we believe that chlorhexidine di-ampicillin will retain the binding affinity of the ampicillin moiety to the serine active site in the penicillin binding protein, transpeptidase. Additionally, our preliminary results suggest chlorhexidine di-ampicillin irreversibly binds to these proteins detrimentally impacting the sequence of events required to degrade the β -lactam drug.

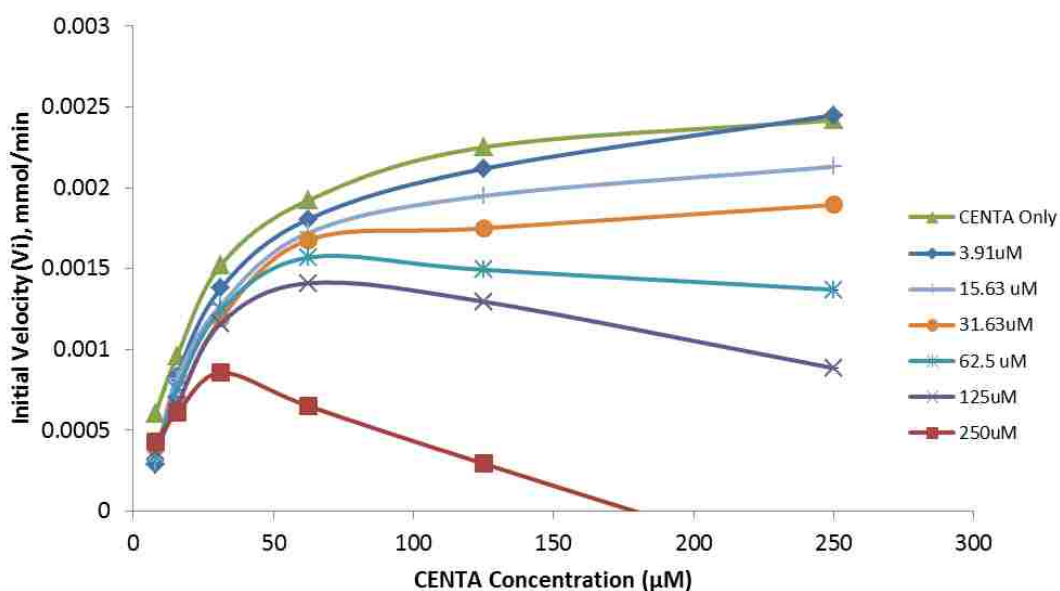


Figure 5.9. Saturation curves with 0.5 units Type 1 penicillinase showing the relationship between CENTA (substrate) concentration and its degradation rates in the presence of increasing concentrations of chlorhexidine di-ampicillin at 37°C.

Thus, chlorhexidine di-ampicillin shows potential to resist enzymatic hydrolysis by Type 1 penicillinase containing microorganisms as well as remain effective against ampicillin resistant microorganisms. However innate resistance mechanisms to β -lactam drugs present in non-penicillinase Gram-negative bacteria may require the antibacterial activity to rely solely on the chlorhexidine molecule.

5.5 Conclusion

A trend among GUMBOS and their antibacterial activities, increasing molecular weights, and relative hydrophobicities were found to gauge drug susceptibility. In general, GUMBOS antibacterial activity was selective for drug-susceptible GNB over GPB, with both having better drug susceptibilities than MDR-GNB. Overall, the growth inhibitive activity of antibiotic-based GUMBOS on MDR-GNB occurred in this order: *S. marscescens* < *E. cloacae* < *E. aerogenes* < *A. baumannii* < *K. pneumonia* < *P. aeruginosa*, in which the least antibacterial activity was observed on *S. marscescens*. In summary, $0.5 \pm 0.2 \mu\text{M}$, $0.2 \pm 0.07 \mu\text{M}$, $14 \pm 6 \mu\text{M}$ is required to inhibit GPB, DS-GNB, and MDR-GNB, respectively. Since the MIC of GUMBOS ($14 \pm 6 \mu\text{M}$) is insignificantly different from the MIC of chlorhexidine diacetate ($11 \pm 8 \mu\text{M}$), it is assumed that the choice of antibiotic has a negligible impact on these particular microorganisms. Thus, incorporating chlorhexidine and β -lactam antibiotics into salts appears to only alter the physical properties of chlorhexidine resulting in better bacterial susceptibility. However, the abundance of protein *in vivo* may limit the systemic use of the materials as anti-infective agents.

To date, the ability to sequester LPS endotoxin as observed using fluorescence spectroscopic studies reveals an added, yet unexpected benefit from the inclusion of the chlorhexidine molecule into the GUMBOS structure. This work shows that the GUMBOS are able to neutralize the immunostimulatory endotoxins of GNB that are released from bacteria once treated with different bactericides. As implied by Zorko *et al.* the incorporation of bisbiguanides in combination with antibiotics does not result in lower concentrations of antibiotics.²⁴ In fact, additivity is observed between the two components. However, improved antibacterial activities of the GUMBOS and large therapeutic index suggest that they would be useful to treat topical infections that result from DR- bacteria. In this case, the role of the chlorhexidine molecule in the GUMBOS would be to neutralize the pro-inflammatory endotoxin constituents that are released upon subsequent cell death at the same time as killing the microbe. Therefore, the LPS study preliminarily shows that these GUMBOS are dual-mode-of-action compounds and that in addition to eradicating an infection, at least 20% LPS endotoxin can be sequestered using the lowest MDR-GNB inhibitory concentration of GUMBOS. Preliminary findings suggest that the presence of the β -lactam anion in the GUMBOS still enables penicillin binding protein recognition; however, an irreversible substrate-induced inhibitive activity was found on Type I penicillinase suggesting the β -lactam drugs within the GUMBOS have an ability resist enzymatic degradation. These results show that the GUMBOS are able to retain antibacterial activity against drug-resistant bacteria that use penicillinase as its primary resistance mechanism. Future work would be required to investigate the roles GUMBOS have on other types of bacterial resistance mechanisms and its antibacterial activity. Ultimately, the broad spectrum anti-inflammatory/ antibacterial activity observed by the β -lactam based chlorhexidine GUMBOS shows that the properties of both ions are conserved as an ion-pair and that tunable therapeutic

treatments against drug-susceptible and drug-resistant bacteria are available by implementing this modular, ionic approach.

5.6 References

1. Peleg, A.Y.; Hooper, D.C.; *New England Journal of Medicine*, **362**, (19), 1804-1813.
2. Bouza, E.; Cercenad, E.; *Seminars in Respiratory Infections*, **2002**, *17*, 215-230.
3. Paterson, D.L.; *American Journal of Medicine*, **2006**, *119*, (6 Suppl 1), S20-28; discussion S62-70.
4. Hidron, A.I.; Edwards, J.R.; Patel, J.; Horan, T.C.; Sievert, D.M.; Pollock, D.A.; Fridkin, S.K.; *Infection Control and Hospital Epidemiology*, **2008**, *29*, (11), 996-1011.
5. Sleigh, J.D.; *British Medical Journal*, **1983**, *287*, 1651-1653.
6. Mohamudha, P.R.; Srinivas, A.N.; Rahul, D.; Harish, B.N.; Parija, S.C.; *International Journal of Collaborative Research on Internal Medicine & Public Health*, **2010**, *2*, (7), 226-237.
7. Pessoa-Silva, C.L.; Meurer Moreira, B.; Câmara Almeida, V.; Flannery, B.; Almeida Lins, M.C.; Mello Sampaio, J.L.; Martins Teixeira, L.; Vaz Miranda, L.E.; Riley, L.W.; Gerberding, J.L.; *Journal of Hospital Infection*, **2003**, *53*, (3), 198-206.
8. Arpin, C.; Dubois, V.; Coulange, L.; Andre, C.; Fischer, I.; Noury, P.; Grobost, F.; Brochet, J.-P.; Jullin, J.; Dutilh, B.; Larribet, G.; Lagrange, I.; Quentin, C.; *Antimicrobial Agents and Chemotherapy*, **2003**, *47*, (11), 3506-3514.
9. Patterson, D.L.; *American Journal of Infection Control*, **2006**, *34*, (5, Supplement 1), S20-S28.
10. Rahal, J.J.; *Clinical Infectious Diseases*, **2009**, *49*, (Supplement 1), S4-S10.
11. Paterson, D.L.; Bonomo, R.A.; *Clinical Microbiology Reviews*, **2005**, *18*, (4), 657-686.
12. Clock, S.A.; Whittier, S.; Weisenberg, S.A.; Kubin, C.J.; Schuetz, A.N.; Tabibi, S.; Alba, L.; Jenkins, S.; Saiman, L.; In *48th Annual Meeting of the Infectious Disease Society of America*: Vancouver, British Columbia, Canada, **2010**.
13. Bouza, E.; Cercenado, E.; *Seminars in Respiratory Infections*, **2002**, *17*, (3), 215-230.
14. Ejim, L.; Farha, M.A.; Falconer, S.B.; Wildenhain, J.; Coombes, B.K.; Tyers, M.; Brown, E.D.; Wright, G.D.; *Nature Chemical Biology*, **2011**, *7*, (6), 348-350.

15. Motyl, M.; Dorso, K.; Barrett, J.; Giacobbe, R.; *Basic Microbiological Techniques Used in Antibacterial Drug Discovery*. UNIT 13A.3 ed. John Wiley & Sons, Inc., **2006**.
16. David, S.A.; Sil, D.; Wang, X.; Quinn, P.J. Harris, J.R.; Biswas, B.B.; Quinn, P., Eds.; Springer Netherlands; Vol. 53, pp 255-283.
17. David, S.A.; Silverstein, R.; Amura, C.R.; Kielian, T.; Morrison, D.C.; *Antimicrobial Agents and Chemotherapy*, **1999**, 43, (4), 912-919.
18. David, S.A.; John Wiley & Sons, Ltd., **2001**; Vol. 14, pp 370-387.
19. Burns, M.R.; Jenkins, S.A.; Wood, S.J.; Miller, K.; David, S.A.; *Journal of Combinatorial Chemistry*, **2005**, 8, (1), 32-43.
20. Wood, S.J.; Miller, K.; David, S.A.; *Combinatorial Chemistry & High Throughput Screening*, **2006**, 7, (3), 239-249.
21. Bebrone, C.; Moali, C.; Mahy, F.; Rival, S.; Docquier, J.D.; Rossolini, G.M.; Fastrez, J.; Pratt, R.F.; Frere, J.-M.; Galleni, M.; *Antimicrobial Agents and Chemotherapy*, **2001**, 45, (6), 1868-1871.
22. Grenier, D.; *Journal of Dental Research*, **1993**, 72, (3), 630-633.
23. Hjeljord, L.G.; Rølla, G.; Bonesvoll, P.; *Journal of Periodontal Research*, **1973**, 8, 11-16.
24. Zorko, M.; Jerala, R.; *Journal of Antimicrobial Chemotherapy*, **2008**, 62, 4, 730-737

CHAPTER 6 CONCLUSIONS AND FUTURE STUDIES

6.1 Concluding Remarks

Adequate antibiotic therapy and antiseptic use are the cornerstones of appropriately managing all infectious disease. However, infections resulting from pathogenic bacteria, with drug resistant bacteria of a higher concern, have become paradoxical due to the contraindications surrounding the use of antibiotic therapy. Primarily, the fear of liberating endotoxins and the emergence of multi-drug resistant organisms have limited clinicians to the number of effective anti-infective agents available for treatment. Therefore, the synthesis and characterization of novel antibiotic- and antiseptic- hybrid salts derived from API-ILs and GUMBOS as discussed in this dissertation have shown to offer multiple advantages that allow for some antibiotics to be reconsidered for infection treatment.

In Chapter 3, the development of ampicillin-based ILs using various antiseptic surfactants as cations, have revealed a reduction in the antibiotic content required to inhibit the growth of Gram-positive and Gram-negative bacteria. Although yielding additive interaction indices, their efficacies against *E. coli* O157:H7, *K. pneumoniae*, *S. aureus*, and *E. faecium* revealed that ampicillin-based ILs have outperformed the antibacterial activities of both quaternary ammonium halide and sodium ampicillin.

In Chapter 4, the synergy found among four antibiotics and chlorhexidine combinations in the form of GUMBOS have shown to possibly expand the armamentarium available for combination antibiotic therapy. Larger therapeutic indices, improved bioavailability, and enhanced pharmacokinetic properties of these materials exploit the plausibility for these GUMBOS to be considered as modern forms of combinatorial drugs. Likewise, the reduction in

chlorhexidine toxicity observed in this study was also discussed. Potential for these novel nontoxic anti-infective agents lies in their abilities to remove pathogenic *E. coli* O157:H7 from the terminal recta of ruminants with unparalleled antibacterial activity and damage to the bacterium. Thus, mechanism studies exposed the potentiated membrane active properties of chlorhexidine upon the addition of β -lactam antibiotics as counter-ions.

In Chapter 5, the application of antibiotic-based chlorhexidine GUMBOS was discussed for the prevention, control, and treatment of drug-resistant bacterial infections. Preliminary results show that these hybrid salts more effectively killed both drug-susceptible and drug-resistant bacteria as compared to the mixture of precursor salts. Exploring the ability to remove lipopolysaccharide components *in vitro* using GUMBOS, revealed tunable endotoxin sequestration with potential to reduce the onset of endotoxemia, bacteremia, and sepsis. Penicillinase kinetics investigations revealed unusual GUMBOS-enzyme binding between chlorhexidine di-ampicillin and penicillinase suggesting the potential to use chlorhexidine as an inhibitor of β -lactam drug degradation when administered as a GUMBOS form. Developing multi-modal therapeutic GUMBOS by means of anti-infective agents derived from hybridizing antibiotics with antiseptics, as shown in this dissertation, show the ability potential to positively reduce the emergence of multi-drug resistant infections and subsequent endotoxin septicemia.

6.2 Future Studies

Until now, various approaches have been used to treat pathogenic infections and prevent transmission of disease such as, but not limited to, antibiotic development, vaccine administration, antiseptic use, and combined antibiotics. However, the emergence and re-emergence of resistant infectious disease implicates the paramount importance to continue the pursuit of anti-infective agents. As such, the use of multi-functional anti-infective agents derived

from GUMBOS offer ways to modernize the therapeutic approaches required to detect, identify, and treat resistant infections. Incorporating other technologies into antimicrobial GUMBOS can potentially serve as localized markers of disease and as vesicles for antimicrobial drug-delivery.

The need to rapidly treat surface- and deep-wounds often caused by, but not limited to, methicillin-resistant *Staphylococcus aureus* or *Acinetobacter baumannii* makes these types of multimodal GUMBOS developed in this research desirable. As such the development of nanoparticles derived from GUMBOS, or nanoGUMBOS, may provide a more bioavailable, nontoxic, and potent approach to treat disease systemically as compared to the bulk parent material. Exploiting the properties often associated with the high surface area of nanoparticles may find conceivable use in anti-infective therapy. For example, anti-infective nanoGUMBOS can provide concentrated, localized therapy in a more bioavailable form.

To remedy the contraindications associated with endotoxemia induced by antibiotic therapy, further studies investigating the anti-inflammatory properties of β -lactam based chlorhexidine GUMBOS via endotoxin sequestration *in vitro* have arisen. Endotoxemia, or the presence of lipopolysaccharide (LPS) endotoxins circulating in the blood, often occurs post-antibiotic treatment and is therefore, contraindicated for Gram-negative bacterial infections. The presence of endotoxin in the blood can induce a systemic inflammatory cascade of responses leading to severe morbidity or even mortality. This problem necessitates advancements in prevention or treatment for systemic inflammatory response to endotoxin that is separate from targeting individual cellular mediators. Therefore, nontoxic systemic endotoxin sequestrants derived from anti-infective GUMBOS would be suitable for this effort. In this way, bacteria vitality can be inhibited and bacteria toxic wastes can be removed *in vivo*. Moreover, LPS consists of different glycoforms that vary in activity. Thus, the affinities of GUMBOS to each

endotoxin glycoform may predicate their potential to be used as inhibitors of antibiotic-induced inflammation specific to a particular form of endotoxin.

The development of multimodal gel-based GUMBOS is also plausible from this research using the modular concept. More specifically, GUMBOS can be synthesized to be species selective sensing agents that offer rapid and sensitive detection and antimicrobial therapy in tandem. In this effort, the tunable properties of GUMBOS can be exploited by using antiseptic and antibiotic GUMBOS reacted with a species-selective chromogen that can allow for the simultaneous treatment and detection of multi-drug resistant bacteria, topically.

This research also provides the groundwork to apply this technology to other vectors of infectious disease. In addition to targeting drug-resistant or pathogenic bacteria, the consideration of GUMBOS as anti-parasitic and antiviral agents can be segmented from this research. Incorporating functional groups onto charged drug scaffolds that are sensitive and active to a particular vector of disease is an ideal extension of this work. Likewise, this may serve useful in designing potent agents effective against some sporulating bacteria. The facile and rapid synthesis of GUMBOS from active pharmaceuticals approved by the U.S. Food and Drug Administration allow this modular, pragmatic approach to lead to the next generation of combination drug therapy equipped for disease control, detection, prevention, and eradication.

APPENDIX: LETTERS OF PERMISSION

TigerMail Mail - Thank you for your RightsLink / John Wiley and Sons transaction

Page 1 of 2



Marsha Cole <mcole3@tigers.lsu.edu>

Thank you for your RightsLink / John Wiley and Sons transaction

2 messages

Copyright Clearance Center <rightslink@marketing.copyright.com> Thu, Jan 12, 2012 at 2:52 PM
Reply-To: Copyright Clearance Center <reply-fe53107276630d7a7312-14153369_HTML-636562549-114453-29420@info.copyright.com>
To: mcole3@tigers.lsu.edu

To view this email as a web page, go [here](#).

Do Not Reply Directly to This Email

To ensure that you continue to receive our emails, please add rightslink@marketing.copyright.com to your [address book](#).



Thank You For Your Order!

Dear Ms. Marsha Cole,

Thank you for placing your order through Copyright Clearance Center's RightsLink service. John Wiley and Sons has partnered with RightsLink to license its content. This notice is a confirmation that your order was successful.

Your order details and publisher terms and conditions are available by clicking the link below:
http://s100.copyright.com/CustomerAdmin/PLF.jsp?IID=2012010_1326401430340

Order Details

Licensee: Marsha R Cole
License Date: Jan 12, 2012
License Number: 2826660438340
Publication: Journal of Applied Microbiology
Title: Cationic antiseptics: diversity of action under a common epithet
Type Of Use: Dissertation/Thesis
Order Reference: Thesis
Total: 0.00 USD

To access your account, please visit <https://myaccount.copyright.com>.

Please note: Online payments are charged immediately after order confirmation; invoices are issued daily and are payable immediately upon receipt.

To ensure we are continuously improving our services, please take a moment to complete our [customer satisfaction survey](#).

Create PDF files without this message by purchasing novaPDF printer (<http://www.novapdf.com>) ition%20I... 3/11/2012

B.1:v4.2

[+1-877-622-5543](tel:+1-877-622-5543) / Tel: [+1-978-646-2777](tel:+1-978-646-2777)
customercare@copyright.com
<http://www.copyright.com>



This email was sent to: mcole3@tigers.lsu.edu

Please visit [Copyright Clearance Center](#) for more information.

This email was sent by Copyright Clearance Center
222 Rosewood Drive Danvers, MA 01923 USA

To view the privacy policy, please [go here](#).

Copyright Clearance Center <rightslink@marketing.copyright.com> Thu, Jan 12, 2012 at 2:57 PM
Reply-To: Copyright Clearance Center <reply-fe53107276630d7a7312-14153369_HTML-636562549-114453-29425@info.copyright.com>
To: mcole3@tigers.lsu.edu

[Quoted text hidden]



Marsha Cole <mcole3@tigers.lsu.edu>

Thank you for your RightsLink / American Society for Microbiology transaction

1 message

Copyright Clearance Center <rightslink@marketing.copyright.com>

Sat, Dec 3, 2011 at 9:12 PM

Reply-To: Copyright Clearance Center <reply-fe621d7277650677e1c-14153369_HTML-636562549-114463-

27393@info.copyright.com>

To: mcole3@tigers.lsu.edu

To view this email as a web page, go [here](#).

Do Not Reply Directly to This Email

To ensure that you continue to receive our emails, please visit myaccount.copyright.com to your address book.

RightsLink



Thank You For Your Order!

Dear Ms. Marsha Cole,

Thank you for placing your order through Copyright Clearance Center's RightsLink service. American Society for Microbiology has partnered with RightsLink to license its content. This notice is a confirmation that your order was successful.

Your order details and publisher terms and conditions are available by clicking the link below:

<http://rightslink.copyright.com/CustomAdmin/PLF.jsp?ID=20111201522968263646>

Order Details

Licensee: Marsha R Cole

License Date: Dec 3, 2011

License Number: 2601670179646

Publisher: Clinical Microbiology Reviews

Title: Antiseptics and Disinfectants: Activity, Action, and Resistance

Type Of Use: Dissertation/Thesis

Order Reference: Antiseptics Chapter

Total: \$0.00 USD

To access your account, please visit <https://myaccount.copyright.com>.

Please note: Online payments are charged immediately after order confirmation; invoices are issued daily and are payable immediately upon receipt.

To ensure we are continuously improving our services, please take a moment to complete our [customer satisfaction survey](#).

B.1:442

[+1-877-622-5543](tel:+18776225543) / Tel: [+1-378-545-3777](tel:+13785453777)
customercare@copyright.com
<http://www.copyright.com>



This email was sent to: ajc@ms3081pdx.nsl.edu

Please visit www.copyright.com for more information.

This email was sent by Copyright Clearance Center,
222 Rosewood Drive, Danvers, MA 01923 USA

To view this privacy policy, please [click here](#)



Marsha Cole <mcole3@tigers.lsu.edu>

Thank you for your RightsLink / John Wiley and Sons order

1 message

Copyright Clearance Center <rightslink@marketing.copyright.com> Mon, Jun 13, 2011 at 10:52 AM
Reply-To: Copyright Clearance Center <reply-fe6d10717665067c7411-14153369_HTML-636562549-114453-1503@info.copyright.com>
To: mcole3@tigers.lsu.edu

To view this email as a web page, go [here](#).

To ensure that you continue to receive our emails, please add rightslink@marketing.copyright.com to your [address book](#).

RightsLink



Thank You For Your Order!

Dear Ms. Marsha Cole,

Thank you for placing your order through Copyright Clearance Center's RightsLink service. John Wiley and Sons has partnered with RightsLink to license its content.

Your order details and publisher terms and conditions are available by clicking the link below:

http://s100.copyright.com/CustomerAdmin/PLF.jsp?IID=2011060_1307980272912

Order Details

Licensee: Marsha R Cole

License Date: Jun 13, 2011

License Number: 2687131418912

Publication: Chemical Biology & Drug Design

Title: Design, Synthesis, and Biological Evaluation of β -Lactam Antibiotic-Based Imidazolium- and Pyridinium-Type Ionic Liquids

Type Of Use: Dissertation/Thesis

Total: 0.00 USD

To access your account, please visit <https://myaccount.copyright.com>.

Please note: Credit cards are charged immediately after order confirmation; invoices are issued daily and are payable immediately upon receipt.

To ensure we are continuously improving our services, please take a moment to complete our [customer satisfaction survey](#).

B.1.v4.2

[+1-877-622-6543](tel:+1-877-622-6543) / Tel: [+1-978-646-2777](tel:+1-978-646-2777)
customercare@copyright.com
<http://www.copyright.com>



This email was sent to: mcole3@tigers.lsu.edu

Please visit [Copyright Clearance Center](#) for more information.

This email was sent by Copyright Clearance Center
222 Rosewood Drive Danvers, MA 01923 USA

To view the privacy policy, please [go here](#).

VITA

Marsha Cole was born in Dallas, Texas, to Mark and Patti Cole. She completed her elementary education at Golden Meadows Elementary School prior to attending the Jackson Math, Science, and Technology Magnet Middle School of Garland, Texas. Despite her disadvantaged background, she graduated with honors from North Garland Math, Science, and Technology Magnet High School in 3.5 years (May 2003). She graduated in four years from Grambling State University's Department of Chemistry with the highest GPA (May 2007). Marsha began cultivating her career as a researcher under Dr. Danny Hubbard through the National Institute of Health – Research in Scientific Enhancement Program, which is program that encourages minorities to complement their academic learning with hands-on research. While there, she was one of the first recipients of the Siemen's Foundation Teacher Scholarship and MTVU Scholarship, in which only 5 women scholars in STEM were awarded. She is also a recipient of the American Chemical Society Scholarship and Thurgood Marshall Scholarship Funds. In August 2007, Marsha began her graduate studies as an analytical chemist and received several honors during her graduate career including the *Louis Stokes-Louisiana Alliance for Minority Participation (LS-LAMP) Bridge-to-Doctorate Fellowship*, *Graduate Alliance for Education in Louisiana Dissertation Writing Fellowship (GAELA)*, *National Aeronautics and Space Administration/United Negro College Fund Special Programs Corporation (NASA/UNCFSP) Harriet Jenkins Pre-Doctoral Fellowship*, *Alpha Kappa Alpha Academic Enhancement Fellowship Award*, and *Ford Foundation Fellowship Honorable Mention*. She has also acquired the LSU Departmental Best Graduate Student Literature Presentation in Analytical Chemistry in Spring 2009 and Departmental James Traynham Award for Outstanding Chemistry

Graduate Student in Teaching and Research. Marsha Cole is also a NASA appointed Student Ambassador.

Marsha Cole is also a member of Alpha Kappa Alpha Sorority, Incorporated, Iota Sigma Pi, National Organization for the Professional Advancement of Black Chemists and Chemical Engineers, American Society of Microbiologists, and the American Chemical Society. In addition to tutoring general chemistry to undergraduate and high school students, she has served as a mentor through the Integration of Education and Mentoring Programs at LSU by mentoring the scientific development of middle and high school minority students that attend Baton Rouge Magnet High School and the Mentorship Academy.

She has also participated in a number of research experiences, with the most recent at the Jet Propulsion Laboratory via receipt of the Center Based Research Award (formerly known as Harriet G. Jenkins Mini-Research Award). She also was selected to represent the Department of Chemistry and present her dissertation research at the esteemed LSU College of Science Dean Circle Dinner. Marsha is now pursuing opportunities for the next phase of her young career and has recently been awarded a two-year Intramural Research Opportunity (INRO) from the Office of Training and Diversity at the National Institute of Allergy and Infectious Diseases, National Institutes of Health. Marsha will graduate with the degree of Doctor of Philosophy in chemistry from Louisiana State University in August 2012. Her publications and conference presentations during her graduate career include:

β -lactam based Chlorhexidine GUMBOS as Inhibitors of Penicillinase Activity. **Marsha R. Cole**, Grover Waldrop, and Isiah M. Warner. *Manuscript in preparation*. (2012)

β -lactam based Chlorhexidine GUMBOS as Anti-inflammatory Lipopolysaccharide Endotoxin Sequestering Agents. **Marsha R. Cole**, Adaku Lucious, Cristina Murphy, Vivian Ferdinand, and Isiah M. Warner. *Manuscript in preparation*. (2012)

Therapeutic and Antibacterial Effects of Antibiotic-based Chlorhexidine salts on Wound and Blood Infections caused by Gram-Negative Resistant Pathogens. **Marsha R. Cole**, Brian Harrington, Jeffrey Hobden, and Isiah M. Warner. *Manuscript in preparation*. (2012)

Synthesis of Chlorhexidine di-Ampicillin and Its Activity against Enterohemorrhagic *Escherichia coli*. **Marsha R. Cole**, Min Li, Ammar Qureshi, Ravirajsinh Jadeja, Daniel Hayes, Jeffrey Hobden, Marlene Janes, and Isiah M. Warner. *Manuscript in revision to Antimicrobial Agents and Chemotherapy*. (2012)

Synthesis and Antibacterial Potentiation of β -lactam Antibiotic-based Ionic Liquids.” **Marsha R. Cole**, Min Li, Bilal El-Zahab, Marlene E. Janes, Daniel Hayes, and Isiah M. Warner. *Chemical Biology and Drug Design*. 78:1, 33-41 (2011)

Combinatorial Approach to Enantiomeric Discrimination: Synthesis and 19F NMR Screening of a Chiral Ionic Liquid-Modified Silane Library. Min Li, Jerry Gardella, David K. Bwambok, Bilal El-Zahab, Sergio de Rooy, **Marsha Cole**, Mark Lowry, Isiah M. Warner. *Journal of Combinatorial Chemistry*. (2009) 11:6, 1105-1114

Integrating Fundamental and Conventional Response Measurements to Create a Surfactant Database for Light Duty Liquids (LDLs). Sharon Kennedy, **Marsha Cole**, John Rouse, Greg Szewczyk, *Colgate Palmolive Internal Publication*. Report #4804. (2006)

PROFESSIONAL PRESENTATIONS

(Presentations, in reverse chronological order)

Cole, Marsha R.; Nicholas Speller; Harrington, Brian; Hobden, Jeffrey; and Warner, Isiah M., “Characterization of Bi-functional β -lactam-based Chlorhexidine GUMBOS”, 2012 Broadening Participation Research NSF Joint Annual Meeting, Washington, DC, June 12 - 15, 2012 (poster).

Cole, Marsha R.; Nicholas Speller; Harrington, Brian; Hobden, Jeffrey; and Warner, Isiah M., “Characterization of Bi-functional β -lactam-based Chlorhexidine GUMBOS, Franco-American Colloque, Minatoc, Grenoble, France, June 7 -8, 2012 (poster).

Cole, Marsha R., “Feminine Forces in Aerospace: A Life Without Limits”, NASA Woman’s History Month and Leadership Conference, NASA Headquarters, Washington, DC, March 8, 2012, *invited*.

Hobden, Jeffrey; **Cole, Marsha R.**; and Warner, Isiah M., “Medicinal GUMBOS – The Future of Anti-Infective Agents”, 2012 Department of Microbiology, Immunology, and Parasitology Seminar Series, LSU Health Sciences Center, New Orleans, LA, February 1, 201, *invited*.

Cole, Marsha R., “From Statistic to Scientist”, NASA Fostering Education for the Underrepresented in STEM, NASA OSSI Symposium, Chantilly, VA, November, 29, 2011, *invited*.

Cole, Marsha R.; Harrington, Brian; Hobden, Jeffrey; and Warner, Isiah M., “Characterization of Bi-functional β -lactam-based Chlorhexidine GUMBOS”, 2011 NASA AMES STEM Symposium, San Jose, CA, July 25 -27, 2011 (poster).

Cole, Marsha R.; Li, Min; Qureshi, Ammar; Hayes, Daniel; James, Marlene; and Warner, Isiah M., “Antibacterial Activities and Synergy Evaluation of Ampicillin – based GUMBOS as a Combination Drug Therapeutic Agent”, 38th Annual Conference of the National Organization for the Professional Advancement of Black Chemists and Chemical Engineers (NOBCChE), Houston, TX, April 19 -22, 2011, *invited*.

Cole, Marsha R. and Warner, Isiah M., “Antibacterial Activities and Synergy Evaluation of Chlorhexidine Ampicillin GUMBOS as a Combination Drug Therapeutic Agent on Pathogenic Bacteria”, Analytical Division of Chemistry Resesarch Seminar, Louisiana State University, Baton Rouge, LA, February 28, 2011, *invited*.

Cole, Marsha R.; Harrington, Brian; Hobden, Jeffrey; and Warner, Isiah M., “Antibacterial Activities and Synergy Evaluation of Chlorhexidine Ampicillin GUMBOS as a Combination Drug Therapeutic Agent on Pathogenic Bacteria”, Grambling State University, Grambling, LA, February 26, 2011, *invited*.

Cole, Marsha R., “money, Money, MONEY!!! Guide Successful Scholarship Applications for Undergraduate and Graduate Students”, LSU NOBCChE Chapter Annual Graduate and Professional Symposium, Baton Rouge, LA, October 12, 2010, *invited*.

Cole, Marsha R.; Li, Min; El-Zahab, Bilal; Janes, Marlene E.; Hayes, Daniel; and Warner, Isiah M. “Design, Synthesis, and Biological Evaluation of β -Lactam Antibiotic-Based Imidazolium- and Pyridinium-Type Ionic Liquids”, American Chemical Society Southeastern/ Southwestern Regional Meeting, New Orleans, LA, December 3, 2010, *invited*.

Cole, Marsha R.; Yang, Wanwan; and Ponce, Adrian, “Inhibitory Study of Spore Germination for *Clostridium* and *Bacillus* species”, Caltech-Jet Propulsion Laboratory, Pasadena, CA, July 16, 2010, *invited*.

Cole, Marsha R.; Li, Min; El-Zahab, Bilal; Janes, Marlene E.; Hayes, Daniel; and Warner, Isiah M., “Synthesis and Antibacterial Potentiation of β -lactam Antibiotic-based Ionic Liquids”, 37th Annual Conference of the National Organization for the Professional Advancement of Black Chemists and Chemical Engineers (NOBCChE), Atlanta, Georgia 2010, (poster).

Cole, Marsha R.; Janes, Marlene E.; and Warner, Isiah M “Selective Inhibition of EHEC from nonpathogenic *E. coli* using GUMBOS as a Combination Drug Therapeutic Agent”, National Aeronautics and Space Administration-Jet Propulsion Laboratory, Pasadena, CA, August 3, 2010, *invited*.

Cole, Marsha R., “New HPLC Method for the Sensitive Determination of Pheomelanin in Biological Materials using pre-Column Fluorescence Derivatization with Naphthalene-2,3-dicarboxaldehyde”, Analytical Division of Chemistry Literature Seminar, Louisiana State University, Baton Rouge, LA, February 9, 2009, *invited*.

Cole, Marsha R.; Li, Min; El-Zahab, Bilal; and Warner, Isiah M. “Synthesis and Characterization of Antibiotic-Based Ionic Liquids”, 2009 Sustaining Diverse Environments NSF Joint Annual Meeting, Washington, DC, June 6 - 10, 2009 (poster).

Cole, Marsha R.; Li, Min; El-Zahab, Bilal; and Warner, Isiah M. “Synthesis and Characterization of Antibiotic-Based Ionic Liquids”, 2008 Transforming STEM NSF Joint Annual Meeting, Washington, DC, June 16 - 19, 2008 (poster).

Cole, Marsha R., “Why Science Saved my Life”, Grambling State University, Grambling, LA, October 14, 2006, *invited*.

Cole, Marsha R. and Hines, Michelle; “Beauty Beyond Skin Deep: Integrating Science and Beauty for the Formulation of Successful Skin Care Products”, Mary Kay Company, Dallas, TX, August 10, 2007, *invited*.

Cole, Marsha R.; Thomas, Isaac; and Smith, Melanie; “Motion of the Lotion: Inside Stokes Law and Brownian Theory”, MGE/MSA LAMP Conference, Tempe, AZ, April 21, 2007, (poster).

Cole, Marsha R.; Thomas, Isaac; and Smith, Melanie; “Motion of the Lotion: Inside Stokes Law and Brownian Theory”, Mary Kay Company, Dallas, TX, August 4, 2006, *invited*.

Cole, Marsha R.; “Green Lights: How the TMSF is Helping to Drive Me Toward a Brighter Future”, Thurgood Marshall Scholarship Fund 6th Annual HBCU Leadership Recruitment Conference & Exhibition, New York, NY, November 5, 2005, *invited*.

Conference/Meeting/Workshops, in reverse chronological order

Judge, Mentorship Academy 2012 Science Fair, Baton Rouge, LA, May 2012.

Panelist, Triple Ex (Excite, Explore, Experiment) Raising Researchers Workshop for Undergraduate Research, Integration of Education and Mentoring, Baton Rouge, LA, March 2012.

Judge, Baton Rouge High School Science Fair, Baton Rouge, LA, January 2012.

Judge, Triple Ex (Excite, Explore, Experiment) Annual Conference for Undergraduate Research, Integration of Education and Mentoring, Baton Rouge, LA, November 2011.

Selection Committee Member, Dynamic Assessment Process, Posse Foundation, New Orleans, Louisiana, September 2011.